NASA/CR—2004-212881 MTD211A5

RQL Integrated Module Rig Test

Frederick S. Koopman, John T. Ols, Frederick C. Padget IV, and Kenneth S. Siskind
Pratt & Whitney, West Palm Beach, Florida

February 2004

The NASA STI Program Office . . . in Profile

Since its founding, NASA has been dedicated to the advancement of aeronautics and space science. The NASA Scientific and Technical Information (STI) Program Office plays a key part in helping NASA maintain this important role.

The NASA STI Program Office is operated by Langley Research Center, the Lead Center for NASA's scientific and technical information. The NASA STI Program Office provides access to the NASA STI Database, the largest collection of aeronautical and space science STI in the world. The Program Office is also NASA's institutional mechanism for disseminating the results of its research and development activities. These results are published by NASA in the NASA STI Report Series, which includes the following report types:

- TECHNICAL PUBLICATION. Reports of completed research or a major significant phase of research that present the results of NASA programs and include extensive data or theoretical analysis. Includes compilations of significant scientific and technical data and information deemed to be of continuing reference value. NASA's counterpart of peer-reviewed formal professional papers but has less stringent limitations on manuscript length and extent of graphic presentations.

- TECHNICAL MEMORANDUM. Scientific and technical findings that are preliminary or of specialized interest, e.g., quick release reports, working papers, and bibliographies that contain minimal annotation. Does not contain extensive analysis.

- CONTRACTOR REPORT. Scientific and technical findings by NASA-sponsored contractors and grantees.

- CONFERENCE PUBLICATION. Collected papers from scientific and technical conferences, symposia, seminars, or other meetings sponsored or cosponsored by NASA.

- SPECIAL PUBLICATION. Scientific, technical, or historical information from NASA programs, projects, and missions, often concerned with subjects having substantial public interest.

- TECHNICAL TRANSLATION. English-language translations of foreign scientific and technical material pertinent to NASA's mission.

Specialized services that complement the STI Program Office's diverse offerings include creating custom thesauri, building customized databases, organizing and publishing research results . . . even providing videos.

For more information about the NASA STI Program Office, see the following:

- Access the NASA STI Program Home Page at ***http://www.sti.nasa.gov***

- E-mail your question via the Internet to help@sti.nasa.gov

- Fax your question to the NASA Access Help Desk at 301–621–0134

- Telephone the NASA Access Help Desk at 301–621–0390

- Write to:
  NASA Access Help Desk
  NASA Center for AeroSpace Information
  7121 Standard Drive
  Hanover, MD 21076

NASA/CR—2004-212881 MTD211A5

RQL Integrated Module Rig Test

Frederick S. Koopman, John T. Ols, Frederick C. Padget IV, and Kenneth S. Siskind
Pratt & Whitney, West Palm Beach, Florida

Prepared under Contract NAS3–27235

National Aeronautics and
Space Administration

Glenn Research Center

February 2004

Note that at the time of research, the NASA Lewis Research Center was undergoing a name change to the NASA John H. Glenn Research Center at Lewis Field. Both names may appear in this report.

Available from

NASA Center for Aerospace Information
7121 Standard Drive
Hanover, MD 21076

National Technical Information Service
5285 Port Royal Road
Springfield, VA 22100

Available electronically at http://gltrs.grc.nasa.gov

RQL Integrated Module Rig Test

Frederick S. Koopman, John T. Ols, Frederick C. Padget IV,
and Kenneth S. Siskind
Pratt & Whitney
West Palm Beach, Florida 33410

Foreword

This report documents the activities conducted under Work Breakdown Structure (WBS) 1.0.2.7 of the NASA Critical Propulsion Components (CPC) Program under Contract NAS3-27235 to evaluate the low emissions potential of a Rich-Quench-Lean (RQL) combustor for use in the High Speed Civil Transport (HSCT) application. The specific intent was to demonstrate a Rich-Quench-Lean combustor capable of achieving the program goal of emissions of nitrogen oxides (NO_X EI) less than 5 gm/Kg fuel at the supersonic flight condition while maintaining combustion efficiencies in excess of 99.9%. The chosen combustor module would then be tested in the subscale annular rig test prior to testing in the subscale core engine demonstrator, if the RQL concept were to be chosen at the Combustor Downselect.

The NASA Subelement Task Manager for this task was Mr. David J. Anderson of NASA Lewis Research Center, Cleveland, Ohio. Dr. Robert P. Lohmann was the Pratt & Whitney IPT Team Leader. Mr. Kenneth Siskind and Mr. John Ols were responsible for the design and analysis of the experimental combustor hardware while Mr. Frederick Padget (UTRC) and Mr. Frederick Koopman (UTRC) were principal investigators for the experimental assessment of the combustor at United Technologies Research Center. Combustion tests were conducted at the Jet Burner Test Stand of United Technologies Research Center, with particular acknowledgement of the support of Mr. Jimmey L. Grimes.

Table of Contents

List of Tables

List of Figures

Section I - Summary

The low emissions potential of a Rich-Quench-Lean (RQL) combustor for use in the High Speed Civil Transport (HSCT) application was evaluated as part of Work Breakdown Structure (WBS) 1.0.2.7 of the NASA Critical Propulsion Components (CPC) Program under Contract NAS3-27235. Combustion testing was conducted in cell 1E of the Jet Burner Test Stand at United Technologies Research Center.

Specifically, a Rich-Quench-Lean combustor, utilizing reduced scale quench technology implemented in a convoluted liner/quench plate configuration, demonstrated the capability of achieving an emissions index of nitrogen oxides (NO_X EI) of 9.2 gm/Kg fuel at the supersonic flight condition (relative to the program goal of 5 gm/Kg fuel). This Rich-Quench-Lean combustor, with reduced scale quench technology, also demonstrated exceptional efficiency, 99.98%, relative to the program goal of 99.9% efficiency at supersonic cruise conditions.

A Rich-Quench-Lean combustor, utilizing the more conventional wall-jet technology, demonstrated the capability of achieving an emissions index of nitrogen oxides (NO_X EI) of 13.6 gm/Kg fuel at the supersonic flight condition (relative to the program goal of 5 gm/Kg fuel). This Rich-Quench-Lean combustor, with wall-jet technology, also demonstrated the capability of achieving the program goal of 99.9% efficiency at supersonic cruise conditions. However, this wall-jet RQL combustor was operated at an elevated combustor pressure drop, approximately 8.5% (relative to a design target combustor pressure drop of 5%), to achieve this NOx and CO emissions performance.

Section II - Introduction

Environmental impacts will dictate substantial constraints on the High Speed Civil Transport (HSCT) aircraft that will in turn establish its economic viability. Emissions output, and in particular the oxides of nitrogen generated during supersonic flight in the stratosphere, is especially significant because of their potential for participating in the destruction of ozone at these high altitudes. These concerns lead to the need to severely constrain the output of NO_x from the engines for this aircraft. Comprehensive studies of the dynamics of the upper atmosphere as it influences ozone concentrations are being conducted under the NASA sponsored Atmospheric Effects of Stratospheric Aircraft program (Ref. 1). The initial results from these studies have led to a goal of an emissions index of 5 gm of NO_x/kg fuel at the supersonic cruise flight condition. Since this level is five to eight times lower than that achievable with current engine combustor technology only the most aggressive and advanced low emissions technology can be considered for the power plants for this aircraft. Pratt & Whitney and General Electric are studying two combustor concepts in the NASA-sponsored High Speed Research program to define a burner that achieves this NO_x emissions goal at the supersonic cruise operating condition. Such a burner must also preserve high efficiency, broad operability, and low emissions at all other operating conditions as well as being durable and economically competitive.

The effort at Pratt & Whitney has focused on the Rich-Quench-Lean (RQL) combustor. A conceptual embodiment of this combustor is shown in Figure II - 1 and Figure II - 2. This combustor concept incorporates separated zones of combustion to preserve combustor stability while achieving emission control. The combustion process is initiated in a fuel-rich combustion zone and completed in a fuel-lean combustion zone, with a rapid transition between them. All of the fuel is introduced in the rich zone but with only a fraction of the air required for complete combustion. The rich combustion process provides the combustor stability and, being deficient in oxygen, completes a significant portion of the overall energy release without forming oxides of nitrogen. The combustion products proceed to a quench section where the remainder of the combustion air is introduced in a rapid, intense mixing process. The downstream lean zone is used to complete CO and soot burn-off. Low NO_x emissions will be achieved only if the quench or transition process between the zones is sufficiently vigorous to avoid significant flow residence time near stoichiometric mixture proportions. Sub-scale testing of a single injector or modular version of the RQL combustor at the HSCT engine supersonic cruise operating conditions has demonstrated the low emissions potential of this concept and generated a significant design data base. This effort has been conducted at United Technologies Research Center (UTRC) and was performed as Task 3, HSR Low NO_x Combustor, of NASA Lewis Research Center contract NAS3-25952, Aero-Propulsion Technology Research Program, with Pratt & Whitney of the United Technologies Corporation (Ref. 2).

For the High Speed Civil Transport engine application the aerothermal design point of the Rich-Quench-Lean combustor is the supersonic cruise condition. The results of the evaluations performed in Ref. 2 indicate that the equivalence ratio in the rich zone should be about 1.8 - 2.0. This equivalence ratio is sufficiently high to preclude NO_x emissions at the exit of the rich zone while minimizing the proclivity for smoke formation. To minimize NO_x production in the quench and lean zones, liner cooling airflow to the lean zone is minimized and the remainder of the combustor air enters through the quench air system. This air serves a dual function in that it provides convective cooling of the rich zone liner while being directed to the quench section by an enclosing hood. Based on an overall fuel/air ratio of 0.030 at nominal supersonic cruise, these considerations lead to a combustor airflow distribution of about 22-24% in the rich zone, 71-73% through the quench system and 5% for lean zone liner cooling. Figure II - 3 shows the rich zone operating characteristics, on a stoichiometry diagram, for a fixed geometry combustor that incorporates this airflow distribution. It is evident that the characteristic of any combustor with a fixed rich zone airflow fraction is a line that must pass through the origin of the graph. For the particular engine cycle under consideration, both the high-power, supersonic cruise operating point and the low-power, ground-idle point are shown on the characteristic line. This range of "rich zone" equivalence ratios, from 0.6 to 2.0, is similar to many gas turbine combustors typically used for subsonic aircraft,

implying that a fixed geometry combustor with 22% combustor airflow in the "rich" zone might satisfy the operational requirements of this engine.

However, while this airflow distribution is optimized from the point of view of supersonic cruise operation, as the engine is operated at fuel/air ratios less than supersonic cruise, the mixture strength in the rich zone would approach and eventually pass through stoichiometric proportions. Since the highest gas temperatures occur in the products of stoichiometric or near-stoichiometric combustion, steady state operation at points in this regime could have adverse effects on durability of the rich zone liner and on the emissions output at some intermediate power levels. This effect is demonstrated graphically on Figure II - 3, where a regime of prohibited steady state operation, labeled "Durability", is indicated around stoichiometric proportions.

While not immediately relevant to the fixed geometry 22% rich zone airflow configuration, Figure II - 3 also indicates another area of prohibited steady state operation. This second prohibited region occurs at low, overall engine fuel/air ratios and high rich zone equivalence ratios. This regime indicates the operation of the rich zone at above stoichiometric conditions that will generate large quantities of CO and smoke but for which there is inadequate temperature levels in the quench and lean zones to oxidize these products. Consequently, the so-called "rich" zone (at high power) can only be operated at lean, or below stoichiometric proportions at low power to avoid large quantities of CO and smoke in the exhaust. With the constraints of avoiding steady state operation in the prohibited zones of the rich zone stoichiometry diagram while still achieving the operational capability of a flight engine, variable geometry approaches to manipulate combustor airflow distribution were considered an enabling technology. An effort to specifically address the design issues associated with a variable geometry combustor was performed as Task 22, Variable Geometry Concepts for Rich-Quench-Lean Combustors, of NASA Lewis Research Center contract NAS3-26618, Large Engine Technology Program, with Pratt & Whitney of the United Technologies Corporation (Ref. 3). The findings from that effort were applied in the development of this integrated module rig which extensively utilized a variable geometry fuel injector during this combustor development activity. A representative stoichiometry diagram for a variable geometry RQL combustor and a fuel-shifted RQL combustor are shown in Figure II - 4. Fuel shifting was investigated further in Ref. 4.

Objectives

The objective of the task reported herein, which was conducted as Work Breakdown Structure (WBS) 1.0.2.7 of the NASA Critical Propulsion Components (CPC) Program under Contract NAS3-27235, was to evaluate the low emissions potential of a Rich-Quench-Lean (RQL) combustor for use in the High Speed Civil Transport (HSCT) application. The specific intent was to demonstrate a Rich-Quench-Lean combustor, utilizing either conventional wall-jet technology or reduced scale quench technology implemented in a convoluted liner/quench plate configuration, for the process of quench air introduction, capable of achieving the program goal of emissions of nitrogen oxides (NO_X EI) less than 5 gm/Kg fuel at the supersonic flight condition while maintaining combustion efficiencies in excess of 99.9%. Emphasis was also placed on robust designs that could be introduced with minimal additional development and refinement because of the rapid-paced High Speed Research program requirements. Specific objectives of the task were to:

- Design and fabricate various quench vane configurations, that implement wall-jet quench technology, as initially developed in the Single Module Rig Tests, parametrically varying key geometric and flow variables and evaluate their performance in this Integrated Module Rig combustor.
- Design and fabricate various convoluted liner/quench plate configurations, that implement reduced scale quench technology, parametrically varying key geometric and flow variables and evaluate their performance in this Integrated Module Rig combustor.

- Perform combustion tests with each configuration at supersonic cruise condition and at other critical conditions in the flight envelope, including airport vicinity and subsonic cruise conditions, to determine performance, emissions and operability of these concepts.
- Select a combustor module configuration, that represents one of the twelve modules of the subscale RQL annular rig, for subsequent development effort in that subscale annular rig and ultimately for incorporation into the subscale core engine demonstrator, if the RQL combustor concept is chosen at the Combustor Downselect.

The activities performed in this program were consistent with the above objectives. The design activities for the parametric quench vane series and for the convoluted liner/quench plate configuration series were conducted by Pratt & Whitney. The design of the facility and the emissions system were conducted by United Technologies Research Center. The design activities of the variable geometry fuel injection system were conducted as a joint activity between Pratt & Whitney and United Technologies Research Center. Combustion tests of the Integrated Module Rig were conducted in dedicated facilities at the United Technologies Research Center. This facility was located in Cell 1E of the Jet Burner Test Stand at United Technologies Research Center. The facility is capable of testing at combustor pressures up to 200 psia and combustor inlet air temperatures of 1400°F. The Integrated Module Rig combustor contained a modular, 5-inch diameter RQL combustor that allowed evaluation of quench section geometry components in a size scale consistent with the next major test vehicles in the High Speed Research program. The Integrated Module Rig combustor hardware, including rich zone liners and quench section hardware were designed and fabricated specifically for this task and were representative of the modules under design consideration for the subscale annular rig. The Integrated Module Rig combustor was designed to accept either a wall-jet configuration or a convoluted liner/quench plate configuration. Each of these combustor configurations was designed utilizing a modular construction technique to allow parametric changes to key combustor hardware. The rig and combustors were designed to provide easy access to the quench section hardware in particular, since that region would be the focus of emissions reduction technology. A diagnostic emissions probe system, capable of axial translation and rotational motion with individual port and ganged sampling, was developed to provide insight into the emissions performance characteristics of the RQL combustor. The facility and combustors were designed to facilitate a rapid change-over between the wall-jet and convoluted liner/quench plate combustor configurations making efficient use of the existing test facility and to support the rapid development process in support of the forthcoming combustor downselect in the High Speed Research Critical Propulsion Components Program.

This report details the activities and results of the evaluation of the rich-quench-lean combustor technology development in a single, integrated module, towards a subscale annular combustor rig demonstration. Section I provides a Program Summary, while Section II includes introductory and background information. Section III provides a description of the test facility and Section IV provides a description of the combustor hardware, including the wall-jet combustor configuration and the convoluted liner/quench plate combustor configuration. Section V describes the instrumentation and emissions systems used in the evaluation of the performance of the combustor concepts while the results of the combustion test programs are discussed in Section VI and Section VII. Conclusions are presented in Section VIII.

Section III - Combustor Test Facility

Layout

The rich-quench-lean (RQL) combustor test facility included a high-temperature airflow distribution and control system, a variable geometry fuel injector and control system, the RQL combustor, an emissions system and an exhaust system as shown in Figure III - 1 and Figure III - 2.

The total combustor airflow (WAT) was supplied to the test facility installed in Cell 1E of the Jet Burner Test Stand at United Technologies Research Center by continuous-flow compressors. This flow was metered by a venturi and heated by a series of two non-vitiated air heaters. In the Integrated Module Rig configuration, the total combustor airflow traveled through a 6 inch pipe to the combustor and the rich zone and quench zone airflows were set by the combustor hardware and determined by the relative effective flow areas of the passages leading into each zone of the combustor. The variable geometry fuel, as its name implies, provide a controllable, variable effective flow area for air introduced into the rich zone of the combustor and hence the split of air into the rich zone or quench zone could be manipulated as a key parametric variable for exploration of emissions reduction potential as well as for operability and durability benefits as discussed previously in the Section II - Introduction.

A water-cooled emissions probe support section was located at the exit of the combustor. The emissions sampling system is described in Section V - Instrumentation. Downstream of the probe support section, the combustor exhaust passed through a diffuser and transition section located upstream of the combustor back-pressure control valve. The transition section diverted the flow through two 90-deg. turns prior to the introduction of high-pressure water sprays to cool the flow before entering the back-pressure valve. An axially-traversing, circumferentially-rotating emissions sampling probe was mounted in the transition section along the combustor centerline, for a majority of the tests. A fixed location emissions sampling probe system was used for some of the combustion tests. A small window was also mounted in the OD wall of the transition section to provide indication of a combustor flame when the traversing emissions system was installed. When the fixed location emissions system was utilized, the proof-of-light window was located at the aft end of the transition section..

Airflow Delivery and Heating

Four centrifugal air compressors, capable of delivering airflow rates up to 20 lb/s at pressures of 400 psia, supplied the high-pressure airflow required for the RQL combustor tests. These airflow rates were established by using a large capacity regulator to provide a fixed pressure to a total airflow metering venturi. A secondary system, also supplying airflow at 400 psi, delivered un-metered cooling air to the proof-of-light viewing window.

Combustor inlet air temperature (T3) of 1200F was achieved with multiple, non-vitiated heating systems. An indirect, natural gas-fired heater and an electrical resistance heater were plumbed in series to obtain the 1200F inlet temperatures. The first heater, rated at 15.1 BTU/hr, was capable of raising the airflow temperature from ambient to approximately 850F delivered temperature to the test cell. The second unit, a 480 Volt, 3 phase, 650 KW system provided the additional energy required to boost the air temperature from 850F to 1200F.

The variable geometry fuel injection system was designed to control the airflow split via manipulation of the effective area of the fuel injector/bulkhead assembly in combination with the fixed geometry of the rich zone liner cooling/quench air flow passages. The variable geometry injector was designed to provide the desired rich zone flow in the range of 10% - 40% of the total combustor air flow.

Fuel Flow

Jet-A fuel was supplied to the test cell from above ground storage tanks using a 1200 psi positive displacement pump capable of flow rates of 4800 lb/hr. The fuel was delivered to the test combustor by independently controlled primary and secondary systems. The primary system delivered flow rates of 200 to 550 lb/hr and the secondary system delivered flow rates to 200 lb/hr. Fuel flows for each system were controlled with a pressure-reducing regulator in series with an appropriately sized orifice and metered with a turbine flow meter.

Water Flows

The lean zone of the Integrated Module Rig RQL combustor was cooled by low pressure water. The internal, cast ceramic liner reduced the heat loss from the combustor and maintained a hot combustor wall. However, the cast ceramic was not a sufficient insulator to restrict metal temperatures of the pressure vessel spool sections to acceptable limits. The required water flow rate was minimal and was set to a conservative level of nominally 10 GPM for this combustor section. High pressure water was injected upstream of the back-pressure valve. This flow reduced the combustor exhaust gas temperature and suppressed noise. It was supplied from the facility closed loop cooling system by a high pressure, centrifugal water pump capable of flows up to 350 GPM at pressures of 700 psi.

Nitrogen Flow

High pressure gaseous nitrogen, used for fuel injector purge and sampling probe purge, was supplied from a 15000 SCF storage tank that was charged to 2400 psi by a liquid nitrogen vaporizer-compressor system. The nitrogen was regulated to provide adequate pressures and flows for purge.

Section IV - Combustor Hardware Design

Test Section Spool and Fuel Preparation Devices

In the Integrated Module Rig, the combustor airflow was delivered to the test section spool that housed the fuel injector as well as the combustor module including the rich zone and quench sections, as shown in Figure IV - 1 through Figure IV - 4. The test section spool was constructed of a 6 inch, 300-lb class flange on the inlet with a 6 inch diameter schedule 40 pipe extending for approximately 12.7" from the face of the inlet flange to the end of the 6 inch pipe. A boss was welded on to the cylindrical pipe section to allow the variable geometry actuation mechanism to egress from the test section to enable external control of the variable geometry injector. Welded to the downstream end of the 6 inch pipe was an 8 inch OD, 6.9" ID cylinder with and an 8 inch, 400-lb class flange on the exit. Eight flats with through slots were machined on this 8-inch OD region to allow for the mount blocks to attach to the test section spool. These eight mount blocks provided axial constraint and radial spline positioning of the tabs protruding off of the rich zone liner. The total length of the test spool section was 20.5 inches. The material for the spool was Type 304H Stainless Steel.

Variable Geometry Fuel Injector

This axial flow aerated injector combines a small airflow two-passage injector with a variable geometry airflow component located co-axially with the core two passage injector. The two passage aerating injector was sized consistent with minimum rich zone air loading and was surrounded by a variable geometry annular swirler that can open to meet the entire range of airflow demand. This design approach offers the decided advantage of divorcing the fuel atomization process from the modulated airflow feature and was the preferred mechanical approach for the aerating injector.

Figure IV - 5 shows a cross-section of the variable geometry tri-swirler aerating injector design. The design is built on a baseline axial flow swirler, aerating or airblast injector geometry. Air was introduced through three airflow passages, each of which was equipped with independent vane swirlers (co-swirled). Fuel was introduced in a thin annular film in between the inner air stream and the intermediate air stream. High-speed airflows impinging onto and shearing the low-speed fuel sheet enabled a high level of atomization. In this concept, only the outer air passage flow area was modulated. The swirl angle in the inner passage was 60 degrees. The inner swirler passage has about 0.35 in^2 of effective flow area. The intermediate swirler air-path provides two functions: 1) to be the "outer", radially-positioned air-stream relative to the fuel filmer to shear and atomize the fuel (similar in function to the outer swirler of a two passage injector) and; 2) to introduce the remainder (or nearly so) of the minimum airflow for the rich zone. The intermediate passage was consequently sized for about 0.20 in^2 of effective area at a 60-degree swirl angle. The outer air swirler and aircap were designed with 45-degree swirl vanes and sized to provide, in combination with the other two passages the total ACd of 2.20 in^2 required at the maximum flow position. This resulted in an air cap outside diameter of 4.3 inches. When installed in a combustor with a nominal bulkhead height of five inches it was evident the face of the aircap represented a substantial fraction of the cooled bulkhead surface. Figure IV - 6 shows a photograph of the assembled tri-swirler injector including the non-flight type actuation system.

Two different valving arrangements were originally considered to control the outer air passage flow. One used a sliding dam to change the area feeding the air swirler. The other used a series of axially aligned sliding ribs, one for each swirl vane, which, when inserted to different degrees between swirl vanes, blocked off parts of each swirl passage. Based on the findings of the Ref. 3, the sliding dam valve was utilized in this variable geometry injector design.

Cold flow testing of this injector showed that the maximum effective area achieved by this design was 2.21 in^2 versus the required ACd of 2.20 in^2. The minimum effective flow area achieved by the injector when the variable passage was completely blocked off was 0.52 in^2.

Airblast Fuel Injector

The fuel injector employed for some of the Integrated Module Rig tests was an axial-flow swirler with an airblast fuel nozzle that passed all of the rich zone airflow. This fuel injector had been designed and fabricated under a prior contract (NAS3-25952) (Ref. 2) and was tested in the Modular RQL combustor rig as part of the baseline testing of the variable geometry concepts testing under a prior contract (NAS3-26618) (Ref. 3). The technology base of this airblast injector is well established in commercial engine application including PW2000 and PW4000 models. The fuel injector, shown in Figure IV - 7, was attached to a water-cooled bulkhead. Air was introduced through two concentric annular passages, each of which was equipped with independent, vane swirlers. The outer swirler contained 20 curved vanes, with a final turning angle of 60 deg. These outer vanes were located in a flow annulus with a 2.50 inch OD and a 1.89 inch ID. The central swirler contained 5 straight vanes, inclined to a turning angle of 50 deg., in a flow annulus with a 1.25 inch OD and a 0.75 inch ID. The two swirl passages induced co-rotating flow in the rich zone.

Fuel was supplied through a single 0.25 inch OD by 0.035 inch thick wall tube welded to an internal plenum that fed fifteen 0.020 inch diameter holes angled at 45 deg. and equally spaced on a 1.525 inch diameter. The fuel was introduced to the combustor in a thin annular film between the central air stream and the outer air stream. High speed airflows impinging onto and shearing the low speed fuel sheet enabled a high level of atomization.

Wall-Jet Combustor Configuration

The Integrated Module Rig Wall-Jet combustor configuration consisted of a fuel injection device (described above), a rich zone liner, quench vanes, a quench extension or lean transition section and a lean zone as shown in Figure IV - 1. Details of each section are described below.

Rich Zone Liner

The rich zone liner was constructed from PWA1422, a directionally solidified nickel alloy. The liners were fabricated using the quickcast process that utilizes a stereolithography model as the pattern in the investment casting process. The liner was approximately 6.3 inches long and was cylindrical in shape with approximately a 5 inch inner diameter. The leading edge of the liner necked down to 4.4 inches in diameter to accept the variable geometry fuel injector or the bulkhead for the fixed geometry injector. The fuel injector engaged approximately 0.7 inches axially into the liner providing a net axial flow field length from bulkhead to quench holes of approximately 5.6 inches. As the rich zone flow field progresses towards the quench plane, the liner shape is curved radially inward to create the quench throat diameter, a key parametric variable assessed during the combustion tests. Two quench throat diameters (and hence rich zone liner exit diameters), 3.9 inches and 3.4 inches, were evaluated. The liner was held in position by eight tabs spaced uniformly about the circumference of the outer surface of the liner. These tabs were engaged by a tab holder mechanism that protruded from the test section spool to grab the tabs on the liner. The surfaces of the rich zone liner exposed to the combusting gases were coated with a thermal barrier coating (TBC) applied with a plasma spray process. The rich zone liner was convectively cooled with the quench air which flowed through an outer shroud annulus of approximately 0.32 inches in annular height. The use of convection enhancement turbulation mechanisms cast onto the outer surface of the rich zone liner was evaluated during this program as well. The convection cooling annulus was created by the outer surface of the rich zone liner and a Hastelloy-X tubular shroud. The Hastelloy-X tubular shroud served also as a mount flange for the quench vanes as well as providing the proper shroud annular height to maintain adequate convection cooling on the backside of the rich zone liner. This Hastelloy-X shroud also served as a radiation shield to prevent the hot rich zone combustor liner from radiating to the test section spool and provided a flame shield for safety in case of a rich zone liner burn through.

Quench Vanes

The objective of the quench vane design was to achieve rapid mixing of the rich-zone flow with the quench air, so that minimal nitric oxides (NO_X) are formed as the local conditions in the quench zone pass through an equivalence ratio of 1 and regions of high, mixed-gas temperatures.

To assess the impact of the many design variables associated with quench air introduction many quench vane designs were committed to fabrication prior to the initiation of the Integrated Module Rig testing so that rapid changes in hardware could be accomplished to facilitate efficient use of the combustion test facility. Therefore, there was not extensive feedback of test results to affect the evolution of the design, but a broader range of parameters was assessed. Nevertheless, several considerations can be described which were important in the design of a quench vane.

The quench vanes were constructed from PWA1480, a single crystal nickel alloy. The vanes were fabricated using the quickcast process that utilizes a stereolithography model as the pattern in the investment casting process. A stereolithography pattern and the resulting quench vanes are shown in Figure IV - 8 and Figure IV - 9, respectively. The quench vanes were designed to take the rich zone liner convective cooling air and turn it 90 degrees and divide it into discrete quench jets. To minimize pressure losses associate with this process, the air passage was designed to be continuously convergent as the vane transitioned the flow from the cooling annulus into the quench jet. A mount flange was added to the quench vanes and they were individually bolted on the Hastelloy-X shroud mount flange. Individual quench vanes were designed and fabricated to avoid the thermal stresses associated with a full hoop structure. To allow the quench vanes to be thermally isolated from the rich zone liner, a gap existed at the leading surface of the quench vane The extent of this gap was investigated in this program as shown in Figure IV - 18.

A number of quench vane geometries were designed, fabricated and tested in this program to assess key quench jet orifice parameters and their effect on NO_X emissions. (Table IV - 1 and Figure IV - 10 through Figure IV - 15)

Number of Vanes per Set	Quench Zone Diameter (inches)	Quench Jet Orientation	Total Quench Zone Crossflow Area, A_Q (in^2)	Total Jet Area, A_J (in^2)	A_Q/A_J
8	3.9	Radial	11.946	3.765	3.173
8	3.9	10 deg swirl	11.946	3.765	3.173
8	3.9	20 deg swirl	11.946	3.765	3.173
12	3.9	Radial	11.946	3.765	3.173
16	3.9	Radial	11.946	3.765	3.173
24	3.9	Radial	11.946	3.765	3.173
8	3.4	Radial	9.079	3.765	2.411
12	3.4	Radial	9.079	3.765	2.411
24	3.4	Radial	9.079	3.765	2.411

Table IV - 1 Summary of Quench Vane Geometries Investigated in Integrated Module Rig Configuration

The shape of the orifices for these vanes were rectangular, characterized by a width crosswise to the flow and a length. (see Table IV - 2)

Number of Vanes per Set	Width, W (in)	Length, L (in)
8	0.686	0.686
12	0.457	0.686
16	0.343	0.686
24	0.229	0.686

Table IV - 2 Quench Vane Orifice Parameters for Integrated Module Rig

Quench Extension or Lean Transition Section

The quench extension section consisted of a water-cooled spool piece with a diameter that matched the quench throat diameter and extended for an axial distance to allow a confined region for the quench mixing process to occur prior to expansion or dump of the flow into the lean zone. Various quench extension lengths were evaluated in this program, including 1.1 inches, 1.6 inches, 2.7 inches and 3.2 inches. The inner surface of the quench extension or lean transition section exposed to the combusting gases was either coated with a thermal barrier coating (TBC) applied with a plasma spray process or protected with a castable ceramic liner insert to isolate the combusting gas from artificial cooling induced by water-cooling the spool section.

Quench Conical Transitions

The geometrical shape of the entrance and exit of the quench zone was assessed in the wall-jet combustor configuration to determine its impact on emissions performance. Since the shape of these inlet and exit regions had changed from previous Single Module Rig tests, particularly on the inlet side to enable incorporation of the quench vane geometry, an evaluation was performed in the Integrated Module Rig to determine if a conical shaped inlet or exit was essential to the low emissions performance of the RQL combustor. A conical transition at the inlet to the quench region was formed by the use of the castable ceramic to create an insert at the aft end of the rich zone liner as shown in Figure IV - 16. A conical transition exitting from the quench region, downstream from the quench extension region was created by casting the desired shape into the lean zone Plicast liners as shown in Figure IV - 17.

Lean Zone

The lean zone section was cylindrical in shape, 5 inches diameter, and had a total spool section length of 9 inches. The exit plane fo the combustor was defined by the location of the probe tips of the axially-traversable, emissions probe system. In the furthest downstream position, the probe tips penetrated 3 inches into the lean zone cylindrical section. Thus, the maximum effective axial length of the lean zone was 6 inches. However, this length could be shortened by traversing the probe system forward, hence making lean zone residence time a primary focus in the combustion test program.

The lean zone combustor section was fabricated as a double-wall spool with 8 inch, 300 psi flanges. The section was specified to use commercially available carbon steel pipe or tube and achieve a 0.125 inch high annular gap to pass an axially-flowing water coolant. Spacer wires were used during fabrication to preserve the gap uniformity of the water cooling passage. The active water cooling enabled a usable test section pressure rating of 200 psia. Typically, the spool was fed by four, 0.5 inch water coolant delivery lines and four lines were also used for the water coolant exhaust. A nominal water cooling flow rate of 10 GPM was utilized.

The lean combustor section contained a castable ceramic liner to provide thermal insulation and achieve the internal dimensions mentioned above. The insulating liners were cast from Plibrico Plicast 40, a commercially available ceramic consisting of mostly alumina. This material was selected because of its favorable thermal shock properties and its ability to withstand combustor temperatures up to 3400F.

Reduced Scale Quench Convoluted Liner/Quench Plate Configuration

The Integrated Module Rig Reduced Scale Quench Convoluted Liner/Quench Plate combustor configuration consisted of a fuel injection device (described previously), a convoluted rich zone liner, an insert "nose piece" to guide the convective cooling air around the convoluted liner, a quench plate and a lean zone as shown in Figure IV - 19 and Figure IV - 20. Details of each section are described below.

Rich Zone Convoluted Liner and Insert

The rich-quench module consisted of a rich zone liner, shown in Figure IV - 21, constructed from PWA1422, a directionally solidified nickel alloy. The liners were fabricated using the quickcast process that utilizes a stereolithography model as the pattern in the investment casting process. The liner was 6.715 inches long and was cylindrical in shape with a 5 inch inner diameter towards the front end of the rich zone. The leading edge of the liner necked down to 4.33 inches in diameter to accept the fuel injector/bulkhead. The bulkhead/swirler/fuel injector sub-assembly engaged approximately 0.7 inches axially into the liner providing a net axial flow field length from bulkhead to quench holes of approximately 6 inches. As the rich zone flow field progresses towards the quench plane, the liner shape is convoluted to channel the rich zone flow into four channels, as shown in Figure IV - 22 and Figure IV - 23 in preparation for the injection of the quench air. All four channels are 0.5 inches in channel height. The two outermost channels extended 2.85 inches in vertical length while the inner two channels extended 5.15 inches in vertical length. These channels resulted in a flow area of 9.573 in^2 for the Gen I liner or 8.86 in^2 for the Gen II liner approaching the quench air introduction plane. The liner was held in position by eight tabs spaced uniformly about the circumference of the outer surface of the liner. These tabs were engaged by a tab holder mechanism that protruded from the test section spool to grab the tabs on the liner. The surfaces of the rich zone bulkhead and the convoluted liner exposed to the combusting gases were coated with a thermal barrier coating (TBC) applied with a plasma spray process. The rich zone liner was convectively cooled with quench air. Towards the aft end of the rich zone section, the convective cooling air was guided, such that the air maintained contact with the rich zone liner, through the use of an insert "nose-piece" which acts as an aerodynamic guide so that the convective air maintains its velocity and, hence, cooling effectiveness as it is channeled into the convoluted regions. The liner/nose piece assemblies were suspended inside a Hastelloy-X tubular shroud that forced the quench air across the upstream cylindrical surface of the rich liner for convective cooling of that region.

Quench Plate

Beyond directing the cooling/quench air along the backside surface of the convoluted liner, the insert "nose-piece" also distributed the quench air to the downstream edge of the liner. There it was injected into the rich zone gas from small orifices in a toothed quench plate to produce the reduced-scale-quench (RSQ) mixing. This quench plate was the main focus of the development and optimization efforts of this program.

The quench plate geometries designed, fabricated and tested in this combustion rig are shown in Figure IV - 24 through Figure IV - 30. The quench orifices were sized to control the pressure drop and, in combination with the rich zone swirler effective flow area, provide the appropriate quantity of quench air to maintain the desired split of approximately 23% air into the front end of the combustor. The quench orifices were slots of 0.300 or 0.325 inches in axial length. The width of each slot varied throughout the channel lengths and was determined to provide optimum mixing for minimizing NO_X emissions. The quench channels in the quench plate were designed to the same dimensions as the exhaust of the convoluted rich zone liner, 0.5 inches in channel height. These quench plates were also fabricated from PWA1422 utilizing the quickcast process. Additionally, a small fraction of the quench air (4% of total combustor air) was bled through small effusion holes, 274 holes of 0.030 inches in diameter, on the downstream face of the plate as cooling air for the aft face of the quench plate. This aft face and the

convoluted surface extending just downstream of the quench orifices were coated with the plasma sprayed TBC for thermal protection as well.

Lean Zone

The lean zone section was cylindrical in shape and had a total spool section length of 9 inches. The inlet region of the lean zone section, as defined by the hot surface of the castable ceramic liner exposed to the combustion gases, was 6 inches in diameter so that none of the quench channels would be blocked. This flow area was quickly converged, over a 1 inch length, to a 5 inch diameter for the remaining 8 inches of the spool section. The exit plane of the combustor was defined by the location of the probe tips of the axially-traversable, emissions probe system. In the furthest downstream position, the probe tips penetrated 3 inches into the lean zone cylindrical section. Thus, the maximum effective axial length of the lean zone was 6 inches. However, this length could be shortened by traversing the probe system forward, hence making lean zone residence time a primary focus in the combustion test program.

The lean zone combustor section was fabricated as a double-wall spool with 8 inch, 300 psi flanges. The section was specified to use commercially available carbon steel pipe or tube and achieve a 0.125 inch high annular gap to pass an axially-flowing water coolant. Spacer wires were used during fabrication to preserve the gap uniformity of the water cooling passage. The active water cooling enabled a usable test section pressure rating of 200 psia. Typically, the spool was fed by four, 0.5 inch water coolant delivery lines and four lines were also used for the water coolant exhaust. A nominal water cooling flow rate of 10 GPM was utilized.

The lean combustor section contained a castable ceramic liner to provide thermal insulation and achieve the internal dimensions mentioned above. The insulating liners were cast from Plibrico Plicast 40, a commercially available ceramic consisting of mostly alumina. This material was selected because of its favorable thermal shock properties and its ability to withstand combustor temperatures up to 3400F.

Section V - Instrumentation

Wall-Jet Configuration

Static Pressures

The pressure instrumentation for the Integrated Module Rig Wall-Jet Combustor configuration is shown in Figure V - 1 and Figure V - 2. Pressures were recorded via a combination of individual transducers and scanners. Combustor inlet static pressure (P3) was measured in the plenum just upstream of the fuel injector. The rich zone static pressure (PRICH) was measured just downstream of the fuel injector bulkhead and the lean zone static pressure (PLEAN) was measured approximately 4.5 inches downstream of the lean zone entrance. The difference between P3 and PRICH, along the effective area of the variable geometry fuel injector, was used to calculate the rich zone airflow and, hence, the airflow split. (A calibration curve from cold flow testing had previously been generated for the variable geometry injector, as effective flow area as a function of variable geometry position and the control system was calibrated and provided on-line position and feedback of the variable geometry system.) Dual measurements of inlet pressure, rich zone pressure and lean zone pressure were made for redundancy. Static pressure measurements were recorded in the convection cooling shroud region of the rich zone liner. Measurement locations included various axial and circumferential locations. This pressure instrumentation had originally been used to assess pressure losses in this shroud region in earlier programs but because the predominant focus of this program was emissions, that instrumentation and the resulting measurements were not significantly evaluated for this effort.

For all locations where redundant measurements were acquired (e.g. combustor inlet, rich zone etc...), the readings were assessed and analyzed for validity. All readings determined to be valid were averaged to obtain the measurement value for that location.

Temperatures

The temperature instrumentation for the Integrated Module Rig Wall-Jet Combustor configuration is also shown in Figure V - 1 and Figure V - 2. Temperatures were recorded via a combination of individual thermocouples and scanners. Combustor inlet stagnation temperature (T3) was measured in the plenum just upstream of the fuel injector. Dual measurements of inlet temperature were made for redundancy.

Surface thermocouples were welded to the backside surface of the rich combustor liner to measure the backside metal temperature of the rich zone liner. The thermocouples were located along the liner as shown in Figure V - 2 and Figure V - 5 through Figure V - 8.

For all locations where redundant measurements were acquired, the readings were assessed and analyzed for validity. All readings determined to be valid were averaged to obtain the measurement value for that location.

Reduced Scale Quench Convoluted Liner/Quench Plate Configuration

Static Pressures

The pressure instrumentation for the Integrated Module Rig Reduced Scale Quench Convoluted Liner/Quench Plate Combustor configuration is shown in Figure V - 3. Pressures were recorded via a combination of individual transducers and scanners. Combustor inlet static pressure (P3) was measured in the plenum just upstream of the fuel injector. The rich zone static pressure (PRICH) was measured just downstream of the fuel injector bulkhead and the lean zone static pressure (PLEAN) was measured

approximately 4.5 inches downstream of the lean zone entrance. The difference between P3 and PRICH, along the effective area of the variable geometry fuel injector, was used to calculate the rich zone airflow and, hence, the airflow split. (A calibration curve from cold flow testing had previously been generated for the variable geometry injector, as effective flow area as a function of variable geometry position and the control system was calibrated and provided on-line position and feedback of the variable geometry system.) Dual measurements of inlet pressure, rich zone pressure and lean zone pressure were made for redundancy.

For all locations where redundant measurements were acquired (e.g. combustor inlet, rich zone etc...), the readings were assessed and analyzed for validity. All readings determined to be valid were averaged to obtain the measurement value for that location.

Temperatures

The temperature instrumentation for the Integrated Module Rig Reduced Scale Quench Convoluted Liner/Quench Plate Combustor configuration is also shown in Figure V - 3 and Figure V - 4. Temperatures were recorded via a combination of individual thermocouples and scanners. Combustor inlet stagnation temperature (T3) was measured in the plenum just upstream of the fuel injector. Dual measurements of inlet temperature were made for redundancy.

Surface thermocouples were welded to the backside surface of the rich combustor liner to measure the backside metal temperature of the rich zone liner. The thermocouples were located along the liner as shown in Figure V - 4.

For all locations where redundant measurements were acquired, the readings were assessed and analyzed for validity. All readings determined to be valid were averaged to obtain the measurement value for that location.

Emissions Sampling and Analysis

Traversing Emissions Sampling System

The principle focus of the combustion test program was to document combustor emissions levels achieved at operating conditions, primarily the supersonic cruise condition, representative of an HSCT aircraft engine. Emissions samples were acquired in the lean zone at multiple radial, circumferential and axial locations.

The lean zone sampling probe (Figure V - 9 through Figure V - 11) consisted of an array of five emissions sampling ports attached to a common housing and cooling supply tube. The emissions system was designed and configured to allow each of the five ports to be sampled individually or, through control system valving, any number of ports, up to and including all five ports, could be ganged together to obtain a representative ganged sample along a diametral line across the combustor gas path.

Four of the probe tips were positioned at radii of 0.562", 1.125", 1.687" and 2.000" and a fifth was placed on the centerline. The ports at the 0.562" and 1.687" radial locations were positioned on one side of the centerline port while the ports at the 1.125" and 2.000" radial locations were placed diametrically across the centerline port on the other side. These port locations were not positioned at centers of equal areas, as might be found in more traditional emissions systems. Instead, the position of these ports was designed to provide the capability of performing detailed diagnostic evaluation and mapping at planes close to the quench air injection location.

Driven by a motorized Velmex Unislide axial positioning system and rotary table, the probe was axially traversable over a 6 inch length. The zero position was defined as beginning at the leading edge of the lean zone spool section and increasing values of probe axial position indicate that the probe system was moved aft of its zero position. This feature allowed emissions levels to be obtained at various lean zone residence times for a given operating condition or permitted emissions to be acquired at a constant

residence time while conditions were varied. The probe was also capable of rotating ±180 deg. Combining this flexibility with the individual port sampling capability provided the capability to obtain a detailed point-by-point profile of the emissions concentration at a plane defined by the probe's axial position.

Each probe tip was designed to provide an aerodynamic quenching of the gas sample. The probe system was operated to maintain a choked inlet at the sampling port orifice during acquisition of gas samples for emissions analysis. The quenching process was accomplished by a rapid expansion of the gas sample to supersonic conditions, reducing the static temperature of the gas sample and thereby freezing its composition. Energy was extracted from the sample by convective heat transfer to the probe's water coolant flow which further reduced the gas sample total temperature. The sample flow was then shocked to a subsonic condition at a stabilization step. The probe tip was design to remove sufficient energy from the sample such that the sample's static temperature after the shock would be low enough to inhibit further chemical reactions. The aerodynamic-quenching probe concept is described in more detail in Ref. 5.

Fixed Location Emissions Sampling System

The probe tip (Figure V - 11), designed to minimize NO_X formation and CO oxidation, included a 0.030 inch diameter sample inlet, a supersonic expansion area ratio of 4.27 and a supersonic quenching length of 1.97 inches. Each probe tip consisted of three concentric, 304 Stainless Steel tubes: 1) an outer tube having a 0.375 inch OD x 0.028 inch wall; 2) a mid-tube having a 0.25 inch OD x 0.016 inch wall; and 3) an inner tube having a 0.094 inch OD x 0.016 inch wall. Water cooling, necessary to insure durable and reliable probe operation in the combusting flow, especially in the near stoichiometric mixture regions at locations close to the quench air addition plane, and for heat extraction from the sample as described above, was supplied to the entire probe at a nominal flow rate of 10 GPM, with the tips receiving approximately 2 GPM each.

A fixed location emissions probe system was also utilized for some of the Integrated Module Rig tests. This probe system was previously documented in Ref. 2 and is shown in Figure V - 12 and Figure V - 13. The emissions probe tips were positioned 6 inches downstream from the leading edge of the lean zone spool section.

Emissions Analysis Procedures and Performance Parameters

The UTRC emissions sampling and analysis system is maintained and operated in accordance with ARP 1256A specifications. The emissions cart employed is capable of continuous monitoring of emissions of carbon monoxide (CO), oxygen (O_2), carbon dioxide (CO_2), unburned hydrocarbons (UHC) and oxides of nitrogen (NO_x) as shown in Figure V - 14. CO and CO_2 levels are determined from individual Milton Roy Model 3300 non-dispersive infrared analyzers. A Thermo Environmental Model 10 chemiluminescence analyzer is used to measure NO_X composition. A Rosemount Model 755 paramagnetic device is used for oxygen analysis and a Beckman Model 402 flame ionization detector is used to monitor unburned hydrocarbons.

Emissions samples were routed from the probe through electrically heated lines to a valving system, where the samples could either be combined or extracted individually, and then delivered to the gas analyzers. The samples were then transferred from the valving system to the emissions cart through an externally insulated 304 Stainless Steel line that was maintained at 350F. The transfer line had a 0.18 inch ID and was approximately 75 feet long. At the cart the sample was divided for distribution to the five analyzers. The NO_X and UHC samples were plumbed directly to the corresponding analyzers and measured as wet samples. The CO_2, CO and O_2 samples passed through a capillary dryer which was used to remove the moisture before those samples were analyzed. The composition of NO_X, CO, UHC, CO_2 and O_2 were determined from the appropriate analyzer reading and a corresponding calibration curve.

The results from analyses of the emission sample were used to calculate the primary performance parameters for a combustion test. These parameters included the fuel/air ratio, emissions indices, flame

temperature and combustion efficiency. Since each of these parameters was based on the sample analysis, the parameter reflected either a local value when individual probe samples were analyzed, or a global value, (along a diametral line across the combustor gas path for the traversing probe system), when all probes were ganged together.

Fuel/Air Ratio

The fuel/air ratio calculated from the emissions analysis followed the technique outlined by Spindt (Ref. 6). This procedure has been used by UTRC for analysis of emissions-based fuel/air ratio because it is based on ratios of the component concentrations and is, therefore, not sensitive to small errors in gas sample analysis. Furthermore, no correction for condensed water is necessary, as long as all components are treated the same. This method can be applied to exhaust gas analysis without regard to the degree of combustion encountered, which is appropriate for the detailed diagnostic evaluations conducted when sampling the potentially near-stoichiometric mixture regions at locations near the quench plane air addition. The fuel/air ratio (f/a) was calculated as:

$$f/a = \left\{ F_b \left(11.492\, F_c \cdot \frac{1 + R/2 + Q}{1 + R} + \frac{120(1 - F_c)}{3.5 + R} \right) \right\}^{-1}$$

where:

$$F_b = \frac{PPM_{CO} + PPM_{CO_2}}{PPM_{CO} + PPM_{CO_2} + PPM_{UHC}}$$

$$F_c = \frac{12.01}{12.01 + 1.008\left(\frac{H}{C}\right)}$$

$$R = \frac{PPM_{CO}}{PPM_{CO_2}}$$

$$Q = \frac{PPM_{O_2}}{PPM_{CO_2}}$$

and:

PPM_i = parts per million molar concentration of species i
C, H = number of carbon and hydrogen atoms, respectively, contained in the fuel.

The Spindt technique combined CO, UHC, CO_2, and O_2 emissions to determine the fuel/air ratio, but as for any similar procedure, the result was largely influenced by the CO_2 and O_2 concentrations.

Emissions Index

An emissions index of specie i (EI_i) was calculated for NO_x, CO, UHC, CO_2 and O_2 according to:

$$EI_i = \frac{PPM_i}{1000} \cdot \frac{\left(1 + f/a\right)}{f/a} \cdot \frac{MW_i}{MW_{comb}}$$

where:

PPM_i = parts per million molar concentration of specie i
MW_i = molecular weight of specie i
f/a = fuel/air ratio based on the sample analysis
MW_{comb} = molecular weight of the combustor composition

For the Integrated Module Rig Wall-Jet combustor configuration tests, the CO, CO_2 and O_2 emissions indices are reported in an as measured state, i.e. semi-dry (sample passed through a capillary dryer). This was deemed acceptable for parametric testing where only back-to-back comparisons are made for configurations tested in the same facility. For the Integrated Module Rig Reduced Scale Quench Convoluted Liner/Quench Plate combustor configuration tests with quench plates #3, #4, #11 and #14, the CO, CO_2 and O_2 emissions indices are reported in an as measured state, i.e. semi-dry (sample passed through a capillary dryer). This was deemed acceptable for parametric testing where only back-to-back comparisons are made for configurations tested in the same facility. For the Integrated Module Rig Reduced Scale Quench Convoluted Liner/Quench Plate combustor configuration tests with quench plate #15, all emissions are reported, consistent with ICAO Annex 16 procedures, in an in-situ state, i.e. wet (accounting for water vapor in the combustion products). This was consistent with the procedures used in evaluation of the emissions from the same configuration in the Fuel Shifting Sector Rig. The correction for water vapor for CO, CO_2 and O_2 essentially amounts to approximately a 5% correction to the emissions indices.

Combustion Efficiency

The combustion efficiency (η_{comb}, with units of percent) was calculated from the sample analysis, where inefficiencies were represented by emissions indices of the incompletely oxidized species, CO and UHC:

$$\eta_{comb} = 100 - 0.1\left(0.235\,EI_{CO} + EI_{UHC}\right)$$

The efficiency calculation assumed that the unburned hydrocarbons had the same heat of combustion as the Jet-A fuel, 18500 BTU/lb.

Section VI – Wall-Jet Combustor Test Evaluation Results

Wall-Jet Test Chronology

The series of parametric tests in support of the wall-jet combustor design were conducted in Cell 1E of the Jet Burner Test Stand at United Technologies Research Center. The test series was initiated on January 11, 1996 and progressed through March 12, 1997. During this period, a series of ~~44~~ tests were conducted and are documented in Table VI - 1.

Run	Date	Injector	Quench Throat Diameter (in)	# of Quench Orifices	Quench Jet Orientation	Quench Extension Length (in)	Quench Conical Transition	Rich Zone Liner	Convection Augmentation	Liner - Quench Vane Gap (in)	Emissions Probe System
1	1/11/96	VG	3.9	8	radial	1.1	none	Hastelloy-X	smooth	**0.090**	fixed
2	2/9/96	VG	3.9	8	radial	1.1	none	Hastelloy-X	smooth	**0.090**	fixed
3	2/15/96	VG	3.9	8	radial	1.1	none	Hastelloy-X	smooth	**0.090**	fixed
4	2/19/96	VG	3.9	8	radial	1.1	none	Hastelloy-X	smooth	**0.090**	fixed
5	2/27/96	VG	3.9	8	radial	1.1	none	Hastelloy-X	smooth	0.030	fixed
6	3/1/96	VG	3.9	8	radial	1.1	none	Hastelloy-X	smooth	0.030	fixed
7	3/5/96	VG	3.9	8	radial	1.1	none	Hastelloy-X	smooth	0.030	fixed
8	3/7/96	VG	3.9	8	10 deg. swirl	1.1	none	Hastelloy-X	smooth	0.030	fixed
9	5/17/96	VG	3.9	**24**	radial	1.1	none	Hastelloy-X	smooth	0.030	traversing
10	5/22/96	VG	3.9	**24**	radial	1.1	none	Hastelloy-X	smooth	0.030	traversing
11	5/24/96	VG	3.9	**24**	radial	1.1	none	Hastelloy-X	smooth	0.030	traversing
12	5/28/96	VG	3.9	**24**	radial	1.1	none	DS	turbulated	0.030	traversing
13	6/3/96	VG	3.9	**24**	radial	1.1	none	DS	turbulated	0.030	traversing
15	6/12/96	VG	3.9	**16**	radial	1.1	none	DS	turbulated	0.030	traversing
16	6/14/96	VG	3.9	**16**	radial	1.1	none	DS	turbulated	0.030	traversing
17	6/21/96	VG	3.9	**12**	radial	1.1	none	DS	turbulated	0.030	traversing
18	6/26/96	VG	3.9	8	radial	1.1	none	DS	turbulated	0.030	traversing
19	6/19/96	VG	3.9	8	radial	1.1	none	Hastelloy-X	smooth	0.030	traversing
20	7/8/96	VG	3.9	8	radial	1.1	**inlet**	Hastelloy-X	smooth	0.030	traversing
21	7/9/96	VG	3.9	8	radial	1.1	none	DS	turbulated	0.030	traversing
22	7/16/96	VG	3.9	8	radial	1.1	**inlet**	Hastelloy-X	smooth	0.030	fixed
23	7/18/96	VG	3.9	8	radial	1.1	**inlet**	Hastelloy-X	smooth	0.030	fixed
24	7/22/96	VG	3.9	8	radial	1.1	none	DS	turbulated	0.030	fixed
25	8/1/96	VG	3.9	8	radial	**1.6**	**exit**	DS	turbulated	0.030	fixed
26	8/7/96	VG	3.9	8	radial	**1.6**	none	DS	turbulated	0.030	fixed
27	8/14/96	VG	3.9	8	radial	1.1	**exit**	DS	turbulated	0.030	fixed
28	8/21/96	VG	3.9	8	radial	1.1	none	DS	smooth	0.030	fixed
29	9/4/96	VG	3.9	8	radial	1.1	none	DS	smooth	0.030	traversing
30	9/6/96	VG	3.9	8	20 deg. swirl	1.1	none	DS	smooth	0.030	traversing
31	9/12/96	VG	3.9	8	radial	1.1	none	DS	smooth	0.030	**Rich Zone**
32	10/1/96	VG	**3.4**	**12**	radial	**3.2**	none	DS	smooth	0.030	traversing
33	10/3/96	VG	**3.4**	**12**	radial	**3.2**	none	DS	smooth	0.030	traversing
34	10/8/96	VG	**3.4**	**12**	radial	**1.6**	none	DS	smooth	0.030	traversing
35	10/22/96	VG	**3.4**	8	radial	**1.6**	none	DS	smooth	0.030	traversing
44	12/6/96	VG	**3.4**	8	radial	1.1	none	DS	smooth	0.030	traversing
45	12/10/96	VG	**3.4**	8	radial	**2.7**	none	DS	smooth	0.030	traversing
46	1/29/97	**FG**	**3.4**	8	radial	**2.7**	none	DS	smooth	0.030	traversing
47	2/7/97	**FG**	**3.4**	**24**	radial	**2.7**	none	DS	turbulated	0.030	traversing
48	2/18/97	**FG**	**3.4**	8	radial	**2.7**	none	DS	turbulated	0.030	traversing
49	2/21/97	**FG**	**3.4**	8	radial	**2.7**	none	DS	turbulated	0.030	traversing
50	2/24/97	**FG**	**3.4**	8	radial	**2.7**	none	DS	turbulated	0.030	traversing
51	2/27/97	**FG**	**3.4**	8	radial	**2.7**	none	DS	turbulated	0.030	traversing
52	3/3/97	**FG**	**3.4**	8	radial	**2.7**	none	DS	turbulated	0.030	traversing
54	3/12/97	VG	**3.4**	8	radial	**2.7**	none	DS	turbulated	0.030	traversing

Table VI - 1 Integrated Module Rig Wall-Jet Combustor Run Log and Configuration Summary

Discussion of Wall-Jet Emissions Results

Combustion tests were performed with the quench vane geometries to assess the performance of the various designs with respect to NO_X and CO emissions at the supersonic cruise and other conditions. The quench vane designs, previously described, were tested using aerodynamic and diagnostic parameter variations. These variations included:

- combustor pressure drop (Figure VI - 98 through Figure VI - 101)
- fuel/air ratio (Figure VI - 102 through Figure VI - 106)
- combustor inlet pressure (Figure VI - 107 through Figure VI - 110)
- combustor inlet temperature (Figure VI - 111 through Figure VI - 114)
- lean zone residence time (Figure VI - 115 through Figure VI - 126)
- rich zone equivalence ratio (Figure VI - 127 through Figure VI - 128)
- individual port sampling providing radial profiles of emissions (Figure VI - 129 through Figure VI - 140)

In addition to these parametric variations, detailed maps of emissions were acquired (Figure VI - 163 through Figure VI - 169) during run 20 at an inlet temperature of 870F, inlet pressure of 120 psia, an overall fuel/air ratio of 0.028 and a rich zone equivalence ratio of 2.8. These maps were obtained by sequentially rotating the sampling probe and collecting emissions from each of the individual sampling orifices at 0, 11.5, 22.5, 33.75 and 45 degree probe orientations. In this manner a detailed map was developed and used to assess the quality of mixing. While the data acquired during this detailed sampling only spanned a 45 degree sector, the graphics shown in the figures have the contour map replicated to create a full 360 degree contour picture for visualization purposes.

Run 31 was dedicated to acquiring emissions in the rich zone of the wall-jet combustor. For this configuration, the fixed location emission probe system was positioned immediately downstream of the quench extension section so that the probe tips extended upstream into the rich zone. Two probes were utilized during this test, one residing on the centerline and the other residing at a radial position of 1.62 inches from the combustor centerline. Emissions acquired from these probe positions at various rich front end conditions including supersonic cruise showed minimal NOx in the rich zone, measured values were less than 1 ppm, as would be expected from a rich combusting environment.

Geometric & Configuration Effects on Emissions

Effect of Number of Quench Orifices

The effect that the number of quench orifices had on emissions performance can be assessed by comparing the results of the runs shown in Table VI - 2 through Table VI - 4.

Run	Date	Injector	Quench Throat Diameter (in)	# of Quench Orifices	Quench Jet Orientation	Quench Extension Length (in)	Quench Conical Transition	Rich Zone Liner	Convection Augmentation	Liner - Quench Vane Gap (in)	Emissions Probe System
12	5/28/96	VG	3.9	**24**	radial	1.1	none	DS	turbulated	0.030	traversing
13	6/3/96	VG	3.9	**24**	radial	1.1	none	DS	turbulated	0.030	traversing
16	6/14/96	VG	3.9	**16**	radial	1.1	none	DS	turbulated	0.030	traversing
17	6/21/96	VG	3.9	**12**	radial	1.1	none	DS	turbulated	0.030	traversing
18	6/26/96	VG	3.9	**8**	radial	1.1	none	DS	turbulated	0.030	traversing

Table VI - 2 Combustion Tests Evaluating the Influence of the Number of Quench Orifices (8, 12, 16, 24)

The emissions performance comparison from the runs described above is shown in Figure VI - 1 through Figure VI - 4. The first two figures show the behavior as a function of actuation of the variable geometry injector, causing a variation in rich zone equivalence ratio as the combustor inlet conditions are held constant. From this parametric comparison, it may appear that the 24 quench orifice configuration has slightly lower NOx and CO emissions relative to the other configurations with 8, 12 or 16 quench orifices. The second two figures show the behavior as a function of lean zone residence time, as measured by axially traversing the emissions probe system downstream during the combustion test. From this comparison, it appears that all configurations yielded similar behavior. These comparisons did not conclusively show a benefit of any particular number of quench jets.

Run	Date	Injector	Quench Throat Diameter (in)	# of Quench Orifices	Quench Jet Orientation	Quench Extension Length (in)	Quench Conical Transition	Rich Zone Liner	Convection Augmentation	Liner - Quench Vane Gap (in)	Emissions Probe System
34	10/8/96	VG	3.4	**12**	radial	1.6	none	DS	smooth	0.030	traversing
35	10/22/96	VG	3.4	**8**	radial	1.6	none	DS	smooth	0.030	traversing

Table VI - 3 Combustion Tests Evaluating the Influence of the Number of Quench Orifices (8 vs 12)

The emissions performance comparison from these runs comparing 8 vs 12 quench orifices is shown in Figure VI - 5 through Figure VI - 12. The first two figures show the behavior as plotted against inlet temperature. These inlet temperature parametrics were conducted by varying inlet temperature, pressure and overall fuel/air ratio simultaneously in order to hold the combustor reference velocity constant as documented in the procedures described in Ref. 2. While the trend as a function of inlet temperature is similar for the 8 and 12 orifice configuration, the 8 orifice configuration has slightly lower NOx emissions at the final 1200F condition. However, the CO emission performance in this parametric clearly shows that the 12 orifice configuration had lower CO emissions. The lean zone residence time excursions show that the 12 orifice configuration exits the quench zone with a high NOx emissions but remained flat while the 8 orifice configuration displayed the behavior of increasing NOx emissions as the flow progresses downstream from the quench region. The CO performance as a function of lean zone residence time clearly shows that the 12 orifice configuration was significantly lower in CO emissions as a function of lean zone residence time. This is similar for the unburned hydrocarbon behavior and hence the combustor efficiency. The performance as a function of rich zone equivalence ratio, via variable geometry actuation, shows the 8 orifice configuration with lower NOx but higher CO as well.

Run	Date	Injector	Quench Throat Diameter (in)	# of Quench Orifices	Quench Jet Orientation	Quench Extension Length (in)	Quench Conical Transition	Rich Zone Liner	Convection Augmentation	Liner - Quench Vane Gap (in)	Emissions Probe System
10	5/22/96	VG	3.9	**24**	radial	1.1	none	Hastelloy-X	smooth	0.030	traversing
19	6/19/96	VG	3.9	**8**	radial	1.1	none	Hastelloy-X	smooth	0.030	traversing
29	9/4/96	VG	3.9	**8**	radial	1.1	none	DS	smooth	0.030	traversing
47	2/7/97	FG	3.4	**24**	radial	2.7	none	DS	turbulated	0.030	traversing
48	2/18/97	FG	3.4	**8**	radial	2.7	none	DS	turbulated	0.030	traversing
49	2/21/97	FG	3.4	**8**	radial	2.7	none	DS	turbulated	0.030	traversing
50	2/24/97	FG	3.4	**8**	radial	2.7	none	DS	turbulated	0.030	traversing
51	2/27/97	FG	3.4	**8**	radial	2.7	none	DS	turbulated	0.030	traversing
52	3/3/97	FG	3.4	**8**	radial	2.7	none	DS	turbulated	0.030	traversing

Table VI - 4 Combustion Tests Evaluating the Influence of the Number of Quench Orifices (8 vs 24)

The emissions performance comparison from these runs comparing 8 vs 24 quench orifices is shown in Figure VI - 13 through Figure VI - 20. The rich zone equivalence ratio parametric excursion did not show a clear benefit between 8 or 24 quench orifices. The fuel/air ratio excursion showed that the 8 orifice configuration was lower in NOx and CO emissions relative to the 24 orifice configuration at the conditions documented in the figures, as did the excursion in combustor inlet pressure.

Effect of Conical Transition at Inlet to Quench Region

The effect that the conical transition at the inlet to the quench region had on emissions performance can be assessed by comparing the results of the runs shown in Table VI - 5.

Run	Date	Injector	Quench Throat Diameter (in)	# of Quench Orifices	Quench Jet Orientation	Quench Extension Length (in)	Quench Conical Transition	Rich Zone Liner	Convection Augmentation	Liner - Quench Vane Gap (in)	Emissions Probe System
19	6/19/96	VG	3.9	8	radial	1.1	**none**	Hastelloy-X	smooth	0.030	traversing
20	7/8/96	VG	3.9	8	radial	1.1	**inlet**	Hastelloy-X	smooth	0.030	traversing

Table VI - 5 Combustion Tests Evaluating the Influence of a Conical Transition at the Inlet to the Quench Region

The impact of this geometric configuration was assessed by comparing the individual probe emissions samples plotted as a function of radial position of the emissions probe tips as shown in Figure VI - 21 and Figure VI - 22. From this comparison, it was apparent that the inlet conical geometric feature was not significant to the emissions performance of this RQL combustor.

Effect of Conical Transition at Exit from Quench Region

The effect that the conical transition at the exit from the quench region had on emissions performance can be assessed by comparing the results of the runs shown in Table VI - 6.

Run	Date	Injector	Quench Throat Diameter (in)	# of Quench Orifices	Quench Jet Orientation	Quench Extension Length (in)	Quench Conical Transition	Rich Zone Liner	Convection Augmentation	Liner - Quench Vane Gap (in)	Emissions Probe System
25	8/1/96	VG	3.9	8	radial	1.6	**exit**	DS	turbulated	0.030	fixed
26	8/7/96	VG	3.9	8	radial	1.6	**none**	DS	turbulated	0.030	fixed

Table VI - 6 Combustion Tests Evaluating the Influence of a Conical Transition at the Exit from the Quench Region

The impact of this geometric configuration is shown in Figure VI - 23 through Figure VI - 30. The comparison of the emissions performance from these parametrics show that the exit conical geometric feature was not significant to the emissions performance of this RQL combustor.

Effect of Gap Between Rich Zone Liner and Quench Vane

The effect that the gap between the rich zone liner and the quench vane had on emissions performance can be assessed by comparing the results of the runs shown in Table VI - 7.

Run	Date	Injector	Quench Throat Diameter (in)	# of Quench Orifices	Quench Jet Orientation	Quench Extension Length (in)	Quench Conical Transition	Rich Zone Liner	Convection Augmentation	Liner - Quench Vane Gap (in)	Emissions Probe System
2	2/9/96	VG	3.9	8	radial	1.1	none	Hastelloy-X	smooth	**0.090**	fixed
4	2/19/96	VG	3.9	8	radial	1.1	none	Hastelloy-X	smooth	**0.090**	fixed
5	2/27/96	VG	3.9	8	radial	1.1	none	Hastelloy-X	smooth	**0.030**	fixed
6	3/1/96	VG	3.9	8	radial	1.1	none	Hastelloy-X	smooth	**0.030**	fixed
7	3/5/96	VG	3.9	8	radial	1.1	none	Hastelloy-X	smooth	**0.030**	fixed
28	8/21/96	VG	3.9	8	radial	1.1	none	DS	smooth	**0.030**	fixed

Table VI - 7 Combustion Tests Evaluating the Influence of a Gap Between the Rich Zone Liner and the Quench Vane

Figure VI - 31 through Figure VI - 38 show the impact of varying the gap between the rich zone liner and the quench vane. For this parametric evaluation, the fixed location emissions probe system was utilized. The local emissions sample measurements shown in the first four figures, show that there is minimal impact on NOx and CO emissions from a change in this gap dimension. However, the unburned

hydrocarbon emissions appeared to benefit from the smaller gap distance and, therefore, the efficiency for the configuration with the larger gap distance was slightly lower. The rich zone equivalence ratio parametric showed similar behavior.

Effect of Emissions Probe System

The effect that the emissions probe system had on emissions performance can be assessed by comparing the results of the runs shown in Table VI - 8.

Run	Date	Injector	Quench Throat Diameter (in)	# of Quench Orifices	Quench Jet Orientation	Quench Extension Length (in)	Quench Conical Transition	Rich Zone Liner	Convection Augmentation	Liner - Quench Vane Gap (in)	Emissions Probe System
24	7/22/96	VG	3.9	8	radial	1.1	none	DS	turbulated	0.030	**fixed**
18	6/26/96	VG	3.9	8	radial	1.1	none	DS	turbulated	0.030	**traversing**
5	2/27/96	VG	3.9	8	radial	1.1	none	Hastelloy-X	smooth	0.030	**fixed**
6	3/1/96	VG	3.9	8	radial	1.1	none	Hastelloy-X	smooth	0.030	**fixed**
7	3/5/96	VG	3.9	8	radial	1.1	none	Hastelloy-X	smooth	0.030	**fixed**
28	8/21/96	VG	3.9	8	radial	1.1	none	DS	smooth	0.030	**fixed**
19	6/19/96	VG	3.9	8	radial	1.1	none	Hastelloy-X	smooth	0.030	**traversing**
29	9/4/96	VG	3.9	8	radial	1.1	none	DS	smooth	0.030	**traversing**

Table VI - 8 Combustion Tests Evaluating the Influence of Emissions Probe Systems

Figure VI - 39 though Figure VI - 46 document the differences observed in emissions performance as a function of the probe system utilized. The NOx emissions are shown to be insensitive to the particular emissions probe system utilized. However, the traversing probe system seemed to measure higher CO emissions than the fixed probe system for the conditions documented in the figures. Given the similarity of the two probe tip designs following the recommend procedures for aerodynamic quench (Ref. 5), it is not apparent why this behavior was observed for the CO emissions.

Effect of Quench Extension Length

The effect that the length of the extended confined region immediately downstream of the quench air addition plane had on emissions performance can be assessed by comparing the results of the runs shown in Table VI - 9.

Run	Date	Injector	Quench Throat Diameter (in)	# of Quench Orifices	Quench Jet Orientation	Quench Extension Length (in)	Quench Conical Transition	Rich Zone Liner	Convection Augmentation	Liner - Quench Vane Gap (in)	Emissions Probe System
44	12/6/96	VG	3.4	8	radial	**1.1**	none	DS	smooth	0.030	traversing
35	10/22/96	VG	3.4	8	radial	**1.6**	none	DS	smooth	0.030	traversing
45	12/10/96	VG	3.4	8	radial	**2.7**	none	DS	smooth	0.030	traversing
34	10/8/96	VG	3.4	12	radial	**1.6**	none	DS	smooth	0.030	traversing
32	10/1/96	VG	3.4	12	radial	**3.2**	none	DS	smooth	0.030	traversing
33	10/3/96	VG	3.4	12	radial	**3.2**	none	DS	smooth	0.030	traversing

Table VI - 9 Combustion Tests Evaluating the Influence of Quench Extension length

The series of figures describing the effect that the quench extension length has on the emission performance are shown in Figure VI - 47 through Figure VI - 58. The first group, comparing extension lengths of 1.1, 1.6 and 2.7 inches, is shown in the first 6 figures. The CO and unburned hydrocarbon emissions benefitted from an increase in the length of this quench extension region while the NOx emissions remained relatively un-affected. The detailed individual emissions probe samples show a flatter NOx profile with the longer extension length and no central CO peak as was observed with the shorter 1.1

inch quench extension length. The second group of figures compares the 1.6 inch quench extension with the 3.2 inch quench extension. For the inlet temperature and rich zone equivalence ratio excursions, the NOx and CO emissions are similar for these two quench extension lengths. The lean zone residence time excursion shows lower CO emissions for the shorter quench extension length configuration. The explanation for this inconsistency with the above comparison group is not apparent.

Effect of Quench Throat Diameter

The effect that the diameter of the quench throat at the quench air addition plane had on emissions performance can be assessed by comparing the results of the runs shown in Table VI - 10.

Run	Date	Injector	Quench Throat Diameter (in)	# of Quench Orifices	Quench Jet Orientation	Quench Extension Length (in)	Quench Conical Transition	Rich Zone Liner	Convection Augmentation	Liner - Quench Vane Gap (in)	Emissions Probe System
19	6/19/96	VG	**3.9**	8	radial	1.1	none	Hastelloy-X	smooth	0.030	traversing
29	9/4/96	VG	**3.9**	8	radial	1.1	none	DS	smooth	0.030	traversing
44	12/6/96	VG	**3.4**	8	radial	1.1	none	DS	smooth	0.030	traversing

Table VI - 10 Combustion Tests Evaluating the Influence of Quench Throat Diameter

The emissions performance comparison from these runs investigating quench throat diamter is shown in Figure VI - 59 through Figure VI - 64. The individual emissions probe samples and the lean zone residence time excursion show lower NOx emissions for the smaller quench throat diameter while the CO emission remained relatively un-affected by the change in quench throat diameter. These comparisons were performed for a given constant airflow in the combustor. However, the smaller quench throat diameter resulted in the combustor operating at a higher overall pressure drop. It is not apparent whether the lower NOx emissions was a result of the improved mixing with the smaller quench throat diameter or a function of the increase in pressure drop. Unfortunately, a pressure drop excursion had not been conducted during these particular combustor configuration tests to be able to provide insight into this phenomenon.

Effect of Swirled Quench Jets

The effect that swirling the quench jets had on emissions performance can be assessed by comparing the results of the runs shown in Table VI - 11.

Run	Date	Injector	Quench Throat Diameter (in)	# of Quench Orifices	Quench Jet Orientation	Quench Extension Length (in)	Quench Conical Transition	Rich Zone Liner	Convection Augmentation	Liner - Quench Vane Gap (in)	Emissions Probe System
5	2/27/96	VG	3.9	8	**radial**	1.1	none	Hastelloy-X	smooth	0.030	fixed
6	3/1/96	VG	3.9	8	**radial**	1.1	none	Hastelloy-X	smooth	0.030	fixed
7	3/5/96	VG	3.9	8	**radial**	1.1	none	Hastelloy-X	smooth	0.030	fixed
28	8/21/96	VG	3.9	8	**radial**	1.1	none	DS	smooth	0.030	fixed
8	3/7/96	VG	3.9	8	**10 deg. swirl**	1.1	none	Hastelloy-X	smooth	0.030	fixed
19	6/19/96	VG	3.9	8	**radial**	1.1	none	Hastelloy-X	smooth	0.030	traversing
29	9/4/96	VG	3.9	8	**radial**	1.1	none	DS	smooth	0.030	traversing
30	9/6/96	VG	3.9	8	**20 deg. swirl**	1.1	none	DS	smooth	0.030	traversing

Table VI - 11 Combustion Tests Evaluating the Influence of Swirled Quench Jet Orientation

The results from these series of tests are shown in Figure VI - 65 through Figure VI - 85. The 10 degree swirl configuration did not significantly impact emissions as shown in the figures. However, the 20 degree swirl configuration had a significant effect on the CO emissions performance. The detailed

individual probe sample emissions measurements show a very large CO peak in the center of the 20 degree swirl configuration. In addition, The emissions based fuel/air ratio at the central region shows very high fuel air ratios as the quench jets did not penetrate into the central region of the quench cylindrical flow field, as would be expected when the quench jet air is highly swirled. The lean zone residence time excursion also shows the inability of this configuration to oxidize the CO from the rich combustion zone, as large CO emissions persist well downstream into the lean zone. Similar behavior occurs for the unburned hydrocarbons for the 20 degree swirl configuration.

Effect of Rich Zone Liner Backside Cooling Convection Augmentation

The effect that this convection augmentation had on emissions performance can be assessed by comparing the results of the runs shown in Table VI - 12.

Run	Date	Injector	Quench Throat Diameter (in)	# of Quench Orifices	Quench Jet Orientation	Quench Extension Length (in)	Quench Conical Transition	Rich Zone Liner	Convection Augmentation	Liner - Quench Vane Gap (in)	Emissions Probe System
18	6/26/96	VG	3.9	8	radial	1.1	none	DS	**turbulated**	0.030	traversing
19	6/19/96	VG	3.9	8	radial	1.1	none	Hastelloy-X	**smooth**	0.030	traversing
29	9/4/96	VG	3.9	8	radial	1.1	none	DS	**smooth**	0.030	traversing

Table VI - 12 Combustion Tests Evaluating the Influence of Liner Backside Cooling Augmentation

While the main emphasis on convection augmentation is obviously its impact on liner temperatures, the impact on emissions was also of interest. The emissions performance shown in Figure VI - 86 and Figure VI - 87 show that the augmentation adversely impacted the CO emissions from this inlet pressure excursion series of test conditions. It is hypothesized that the augmentation added significant turbulence to the liner convection cooling flow (hence its improvement in heat transfer capability), causing the quench jet penetration to decrease and therefore, result in higher CO emissions.

Effect of Fuel Injector

The effect that the fuel injector had on emissions performance can be assessed by comparing the results of the runs with the variable geometry fuel injector and the fixed geometry fuel injector as shown in Table VI - 13.

Run	Date	Injector	Quench Throat Diameter (in)	# of Quench Orifices	Quench Jet Orientation	Quench Extension Length (in)	Quench Conical Transition	Rich Zone Liner	Convection Augmentation	Liner - Quench Vane Gap (in)	Emissions Probe System
48	2/18/97	**FG**	3.4	8	radial	2.7	none	DS	turbulated	0.030	traversing
49	2/21/97	**FG**	3.4	8	radial	2.7	none	DS	turbulated	0.030	traversing
50	2/24/97	**FG**	3.4	8	radial	2.7	none	DS	turbulated	0.030	traversing
51	2/27/97	**FG**	3.4	8	radial	2.7	none	DS	turbulated	0.030	traversing
52	3/3/97	**FG**	3.4	8	radial	2.7	none	DS	turbulated	0.030	traversing
54	3/12/97	**VG**	3.4	8	radial	2.7	none	DS	turbulated	0.030	traversing

Table VI - 13 Combustion Tests Evaluating the Influence of Fuel Injector

The back-to-back tests with only a fuel injector change are shown in Figure VI - 88 through Figure VI - 97. Lean operation in the front end attempts to isolate the injector performance from the interactions with the other features of the RQL combustor. The figures show that the NOx emissions performance of the fixed geometry injector was lower than the variable geometry injector while CO emissions performance was similar for both injectors. Surprisingly, the unburned hydrocarbons were significantly worse for the fixed geometry injector at these conditions. Detailed diagnostics of the injector flow fields would provide further insight into this observed behavior.

Runs 48 through 52 were also used to make a preliminary assessment of how a fuel-shifted wall-jet RQL combustor might perform throughout the flight envelope and especially in its airport vicinity emissions. Tests were conducted to simulate a variety of airport vicinity conditions. Fuel/air ratio excursions were performed and emissions acquired as a function of these conditions for both a module operating with a rich front end and a module operating with a lean front. This data was then combined using the method of superposition, accounting for an airflow distribution of approximately 60% for an OD bank of modules and 40% for an ID bank of modules, to estimate an integrated value of emissions at the exit of a fuel-shifted RQL combustor. The acquired data for both the lean and rich front end conditions and the airport vicinity emissions estimates are shown in Figure VI - 154 through Figure VI - 162. A more comprehensive evaluation of fuel shifting for a reduced scale quench RQL combusor in a multiple module sector rig, including rich module - lean module interaction effects, was investigated in Ref. 4.

Configuration CPC032/CPC033

Evaluation of all of the results obtained during the wall-jet combustor configuration showed that the best emissions performing configuration was the configuration tested in runs 32 & 33 which combined the long quench extension length with the small quench throat diameter, summarized in Table VI - 14.

Run	Date	Injector	Quench Throat Diameter (in)	# of Quench Orifices	Quench Jet Orientation	Quench Extension Length (in)	Quench Conical Transition	Rich Zone Liner	Convection Augmentation	Liner - Quench Vane Gap (in)	Emissions Probe System
32	10/1/96	VG	3.4	12	radial	3.2	none	DS	smooth	0.030	traversing
33	10/3/96	VG	3.4	12	radial	3.2	none	DS	smooth	0.030	traversing

Table VI - 14 Wall-Jet Combustor Configuration of Runs 32 & 33

The comprehensive results from this configuration are documented in Figure VI - 141 through Figure VI - 153.

Section VII – Reduced Scale Quench Convoluted Liner/Quench Plate Combustor Test Evaluation Results

Reduced Scale Quench Convoluted Liner/Quench Plate Test Chronology

The series of parametric tests in support of the reduced scale quench convoluted liner/quench plate combustor design were conducted in Cell 1E of the Jet Burner Test Stand at United Technologies Research Center. The test series was initiated on November 5, 1996 and progressed through March 22, 1997. During this period, a series of 18 tests were conducted and are documented in Table VII - 1.

Run	Date	Injector	Liner	Insert	Quench Plate	Quench Extension	Liner-Quench Plate Gap	Emissions System
38	11/05/96	VG	ver 2	ver 2	ver 3	none	yes	traversing
39	11/06/96	VG	ver 2	ver 2	ver 3	none	yes	traversing
40	11/07/96	VG	ver 2	ver 2	ver 3	none	yes	traversing
41	11/19/96	VG	ver 2	ver 2	ver 3	**ver 1**	yes	traversing
42	11/21/96	VG	ver 2	ver 2	ver 3	none	**none**	traversing
43	11/25/96	VG	ver 2	ver 2	**ver 3 mod**	none	none	traversing
55	3/13/97	VG	ver 3	ver 3	ver 4	none	none	traversing
56	3/18/97	VG	ver 3	ver 3	ver 4	none	none	traversing
57	3/20/97	VG	ver 3	ver 3	ver 4	none	none	traversing
58	3/26/97	VG	ver 3	ver 3	ver 4	none	none	traversing
64	5/06/97	VG	ver 3	ver 3	ver 14	none	none	traversing
65	5/07/97	VG	ver 3	ver 3	ver 14	none	none	traversing
66	5/23/97	VG	ver 3	ver 3	ver 11	none	none	traversing
67	5/28/97	VG	ver 3	ver 3	ver 11	none	none	traversing
134	3/10/98	FG	ver 3	ver 3	ver 15	none	none	traversing
135	3/11/98	FG	ver 3	ver 3	ver 15	none	none	traversing
136	3/13/98	FG	ver 3	ver 3	ver 15	none	none	traversing
137	3/22/98	FG	ver 3	ver 3	ver 15	none	none	traversing

Table VII - 1 Integrated Module Rig Reduced Scale Quench Convoluted Liner/Quench Plate Combustor Run Log and Configuration Summary

Testing of quench plate configuration #15 was focused on conditions taken from the HSR/CPC Program Coordination Memo GE97-002-C, summarized in Table VII - 2, with the primary intent of obtaining supersonic cruise emissions in support of the Combustor Downselect.

	T3 (F)	P3 (psia)	f/a
Nominal Supersonic Cruise	1200	150	0.0300
Nominal Subsonic Cruise	630	80	0.0200
100% Thrust LTO (Takeoff)	919	301	0.0329
65% Thrust LTO (Climb)	740	212	0.0248
34% Thrust LTO (Approach)	588	134	0.0187
15% Thrust LTO (Descent)	446	82	0.0141
5.8% Thrust LTO (Idle)	295	45	0.0113

Table VII - 2 Uniform Schedule of Test Points

Discussion of Reduced Scale Quench Convoluted Liner/Quench Plate Emissions Results

Summary

A summary of performance for all Reduced Scale Quench Convoluted Liner/Quench Plate combustor configurations is shown in Figure VII - 1 through Figure VII - 5. The first plot of FARR is for all fuel/air ratios tested while the second figure shows the behavior for fuel/air ratio = 0.030 supersonic cruise condition. From the figures, it is apparent that quench plate configuration #15 performed the best with the lowest NOx and CO emissions.

Effect of Gap Between Convoluted Rich Zone Liner and Quench Plate

The effect that the gap between the convoluted rich zone liner and the quench plate had on emissions performance can be assessed by comparing the results of the runs shown in Table VII - 3.

Run	Date	Injector	Liner	Insert	Quench Plate	Quench Extension	Liner-Quench Plate Gap	Emissions System
38	11/05/96	VG	ver 2	ver 2	ver 3	none	**yes**	traversing
39	11/06/96	VG	ver 2	ver 2	ver 3	none	**yes**	traversing
40	11/07/96	VG	ver 2	ver 2	ver 3	none	**yes**	traversing
42	11/21/96	VG	ver 2	ver 2	ver 3	none	**none**	traversing

Table VII - 3 Combustion Tests Evaluating the Influence of a Gap Between the Convoluted Rich Zone Liner and the Quench Plate

Figure VII - 6 and Figure VII - 7 show the impact of varying the gap between the convoluted rich zone liner and the quench plate. The NOx emissions appear un-affected by this geometric variation. However, The CO emissions were lower with the gap between the convoluted liner and the quench plate than without the gap. This behavior is not consistent with that observed in the wall-jet combustor configuration where the gap had a detrimental effect on unburned hydrocarbon emissions.

Effect of Quench Extension

The effect of an extended length of confined quench region immediately downstream of the quench air addition plane on emissions performance can be assessed by comparing the results of the runs shown in Table VII - 4.

Run	Date	Injector	Liner	Insert	Quench Plate	Quench Extension	Liner-Quench Plate Gap	Emissions System
38	11/05/96	VG	ver 2	ver 2	ver 3	**none**	yes	traversing
39	11/06/96	VG	ver 2	ver 2	ver 3	**none**	yes	traversing
40	11/07/96	VG	ver 2	ver 2	ver 3	**none**	yes	traversing
41	11/19/96	VG	ver 2	ver 2	ver 3	**ver 1**	yes	traversing

Table VII - 4 Combustion Tests Evaluating the Influence of an Extended Length of Confined Quench Region Downstream of the Quench Air Addition Plane

Figure VII - 8 and Figure VII - 9 show the impact of this quench extension. NOx emissions are un-affected while CO emissions are lower without the extended quench length for this lean zone residence time excursion. Again, this behavior is not consistent with that observed in the Wall-Jet Combustor where the extended quench was beneficial for lowering CO emissions. Durability was an issue for this quench extension and it was not pursued further in any of the other reduced scale quench configurations evaluated in this program.

Quench Plate #3

Results for Quench Plate Configuration #3 are shown in Figure VII - 10 through Figure VII - 21. In general, quench plate configuration #3 was determined to be similar to the wall-jet configurations in terms of its emissions performance. The lean zone residence time excursions showed NOx emissions increasing as a function of this residence time while CO decreased with residence time. This reduced scale quench configuration continued to show insensitivity to rich zone equivalence ratio. However, the wide spread in emissions shown in the inlet temperature excursion figures, as a function of various emissions probe orientations, was a result of the relative non-uniformity of this configuration. A significant contributor to this non-uniformity was the large region associated with the spacing of the convolutions in the Gen I liner. An attempt to modify quench plate configuration #3 by re-operating the quench plate teeth to improve its uniformity was not successful at significantly improving the emissions performance as shown in Figure VII - 22 and Figure VII - 23.

Quench Plate #4

Results for Quench Plate Configuration #4 are shown in Figure VII - 24 through Figure VII - 36. Again, non-uniformity at the quench region appeared to dominate the emissions performance behavior of this configuration as shown in the inlet temperature excursion results. The reduced scale quench configurations had low CO emissions and could achieve 99.9% efficiency (approximately 4 EI of CO) at about 1 millisecond of residence time (approximately 4") downstream of the quench air addition. This CO oxidation rate appears to be significantly faster than that observed in the wall-jet combustor configurations, presumably due to the more intimate mixing of quench air with the rich zone gas effluent in these reduced scale quench configurations.

Quench Plate #11

Results for Quench Plate Configuration #11 are shown in Figure VII - 37 through Figure VII - 40 with emissions contours shown in Figure VII - 41 through Figure VII - 50. Non-uniformities, especially as demonstrated by the full contour maps of emissions, still are apparent in this version of an optimized quench plate. However, the non-uniformities were reduced in magnitude relative to the previous versions of the reduced scale quench plates and a comensurate decrease in NOx emissions was observed.

Quench Plate #14

Results for Quench Plate Configuration #14 are shown in Figure VII - 51 through Figure VII - 54 with emissions contours shown Figure VII - 55 through Figure VII - 59. While improvements were made in tailoring the quench plate to improve the uniformity, some non-uniformities still existed as shown in the graphs, which show the varying emissions behavior as a function of emissions probe orientation, as well as in the contour plots, especially the FARR plot. It should be noted that these contour plots are acquired 1" downstream of the quench plane. It was found that the uniformity associated with the vicinity immediately downstream of the quench region was essential for providing low emissions.

Quench Plate #15

Continued optimization of the quench air addition resulted in the generation of quench plate configuration #15, the best emissions performer for the Integrated Module Rig Tests. The emissions results for this configuration are comprehensively documented in Figure VII - 60 through Figure VII - 90. For the LTO conditions where a fullscale HSCT combustor is anticipated to operate in a uniform, non-fuel-shifted mode, a notation on the graphs show the nominal fuel/air ratio of that condition, assuming 5% of combustor air is reserved for providing cooling of the lean zone liners. This includes the takeoff, climb, subsonic cruise and idle conditions. The approach and descent conditions are anticipated to operate in a fuel shifted mode and those graphs are marked with additional lines signifying the fuel/air ratios that each of those modules would operate at in a fuel-shifted mode. In addition, facility limitations precluded operation at full pressure for the takeoff condition. Data was acquired as a function of inlet pressure at

this condition to support extrapolation of the combustor behavior to the higher inlet pressures. However, scatter in the data associated with day-to-day variations in emissions readings as well as non-uniformities associated with various emissions probe orientations makes determination of a pressure coefficient difficult. Emissions contour plots are shown in Figure VII - 91 through Figure VII - 99. The improved uniformity, and subsequently lower emissions are exemplified in the emissions contour plots.

Section VIII - Conclusions

The low emissions potential of a Rich-Quench-Lean (RQL) combustor for use in the High Speed Civil Transport (HSCT) application was demonstrated.

Specifically:

1. A Rich-Quench-Lean combustor, utilizing wall-jet technology, demonstrated the capability of achieving an emissions index of nitrogen oxides (NO_X EI) of 13.6 gm/Kg fuel at the supersonic flight condition (relative to the program goal of 5 gm/Kg fuel). An elevated pressure drop of approximately 8.5% (relative to a design target combustor pressure drop of 5%) was required to achieve this performance.

2. A Rich-Quench-Lean combustor, utilizing reduced scale quench technology implemented in a convoluted liner/quench plate configuration, demonstrated the capability of achieving an emissions index of nitrogen oxides (NO_X EI) of 9.2 gm/Kg fuel at the supersonic flight condition (relative to the program goal of 5 gm/Kg fuel).

3. The reduced scale quench configurations demonstrated exceptional efficiencies at supersonic cruise conditions.

4. The quench throat diameter and quench extension length were found to be important geometric parameters for effecting the emissions performance of the wall-jet combustor configuration.

5. Uniformity was determined to play an important role in determining the emissions performance of the reduced scale quench convoluted liner/quench plate combustor configuration.

References

1. The Atmospheric Effects of Stratospheric Aircraft: A Fourth Program Report, NASA Reference Publication 1359, January 1995

2. Rosfjord, T. J. and Padget, F. C., Experimental Assessment of the Rich/Quench/Lean Combustor for High Speed Civil Transport Aircraft Engines, Final Report on Task 3 of NASA Contract NAS3-25952, December 1995.

3. Lohmann, R. P., et. al., Variable Geometry Concepts for Rich-Quench-Lean Combustors, Final Report on Task 22 of NASA Contract NAS3-26618.

4. Siskind, K. S. et. al., Multi-Module Fuel Shifting Sector Test Complete - MT410255, Informal Test Report, NASA Contract NAS3-27235, March 1998

5. Chiappetta, L., et. al., Design Considerations for Aerodynamically Quenching Gas Sampling Probes, ASME 82-HT-39.

6. Spindt, R. S., Air-Fuel Ratios from Exhaust Gas Analysis, SAE Paper 650507, Jan, 1965.

Section II Figures

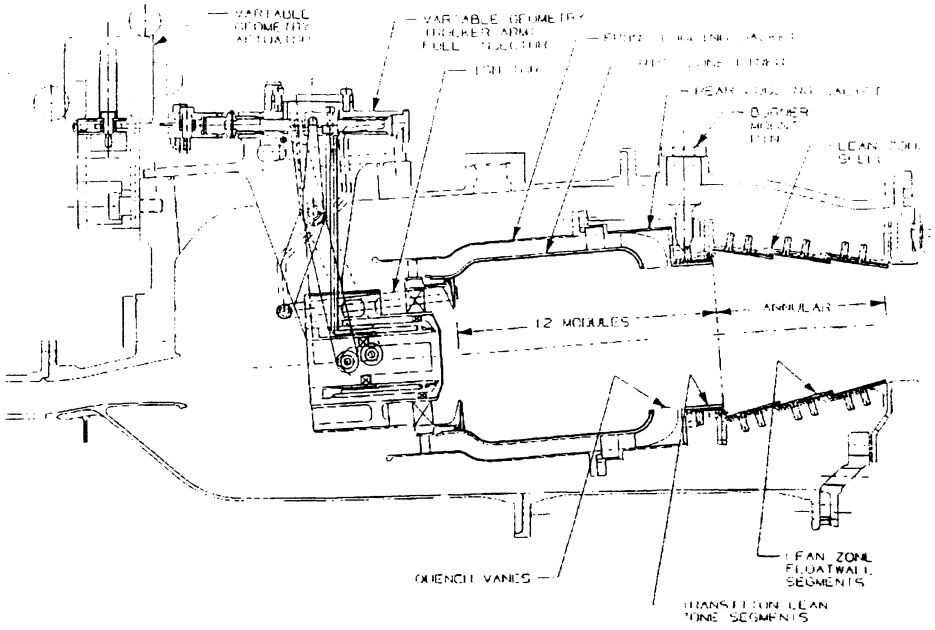

Figure II - 1 Multi-Modular Rich-Quench-Lean Subscale Combustor

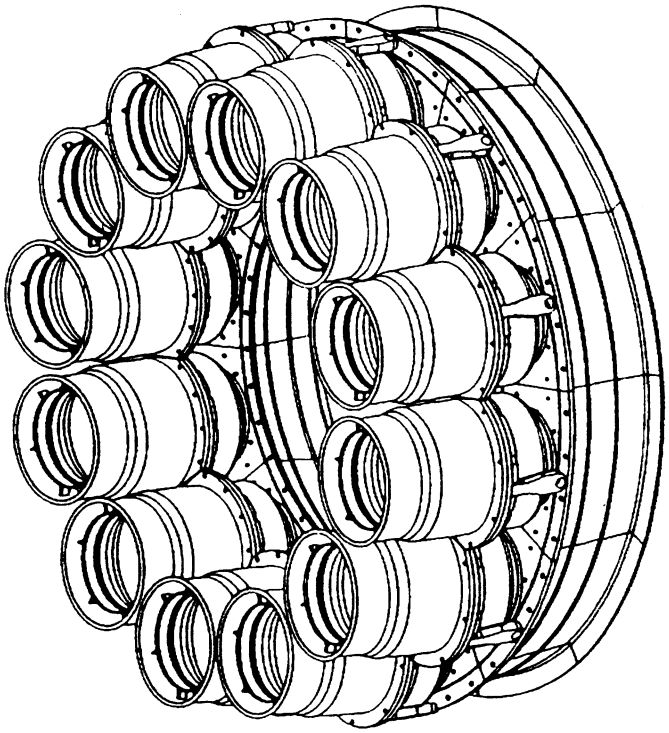

Figure II - 2Isometric view of Multi-Modular Rich-Quench-Lean Subscale Combustor

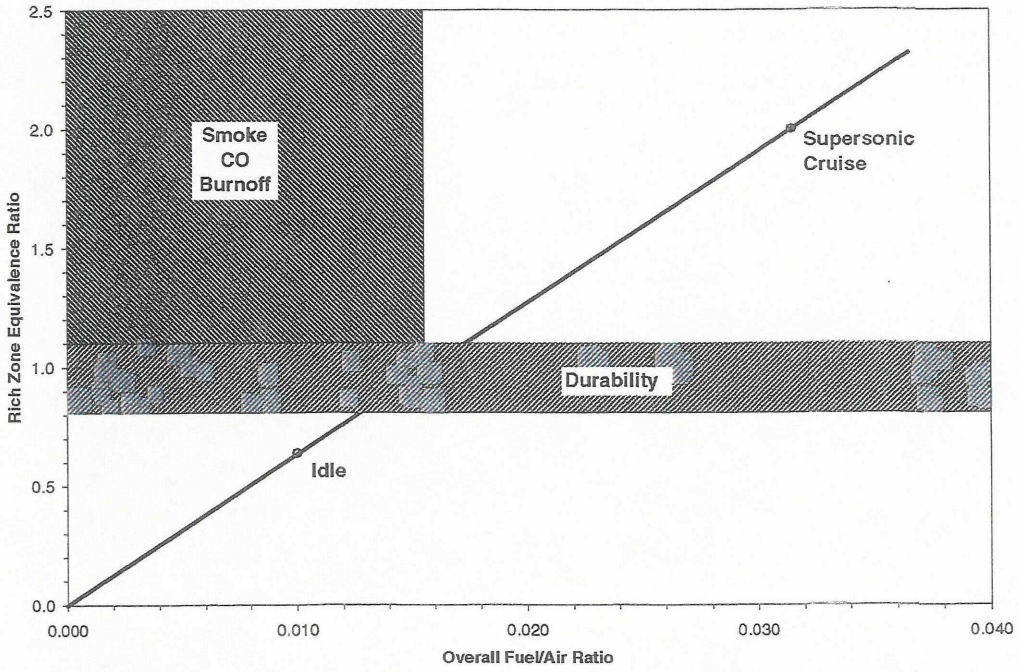

Figure II - 3 Rich Zone Stoichiometry of a Fixed Geometry RQL Combustor (22% rich zone, 73% quench zone, 5% lean zone cooling)

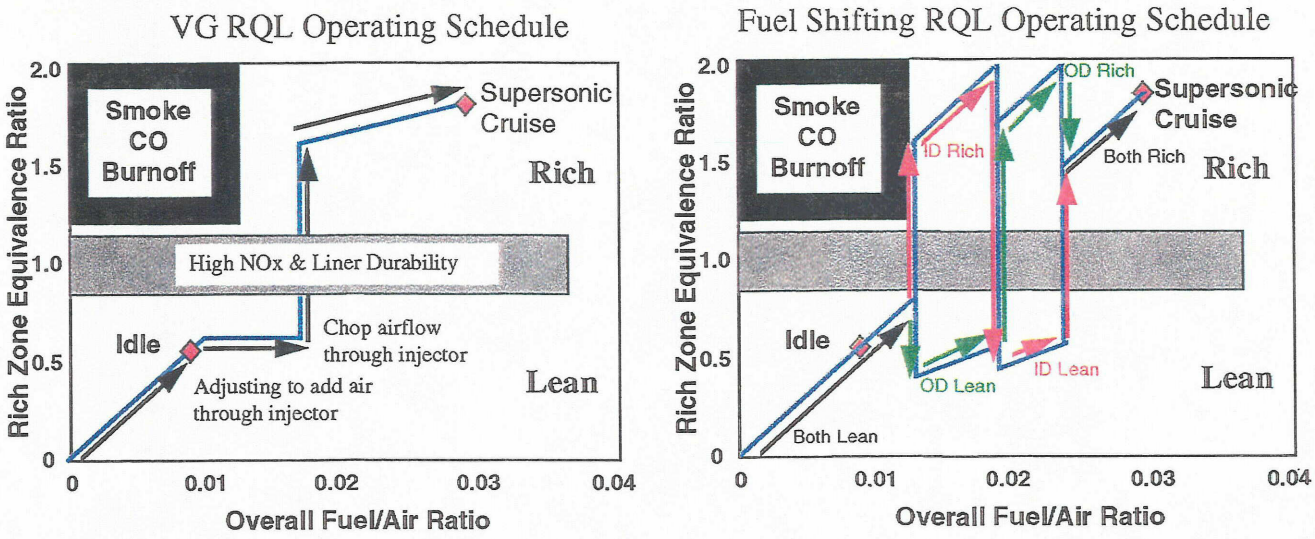

Figure II - 4 Rich Zone Stoichiometry of a Variable Geometry RQL Combustor (left) and a Fuel-Shifted RQL Combustor (right)

Section III Figures

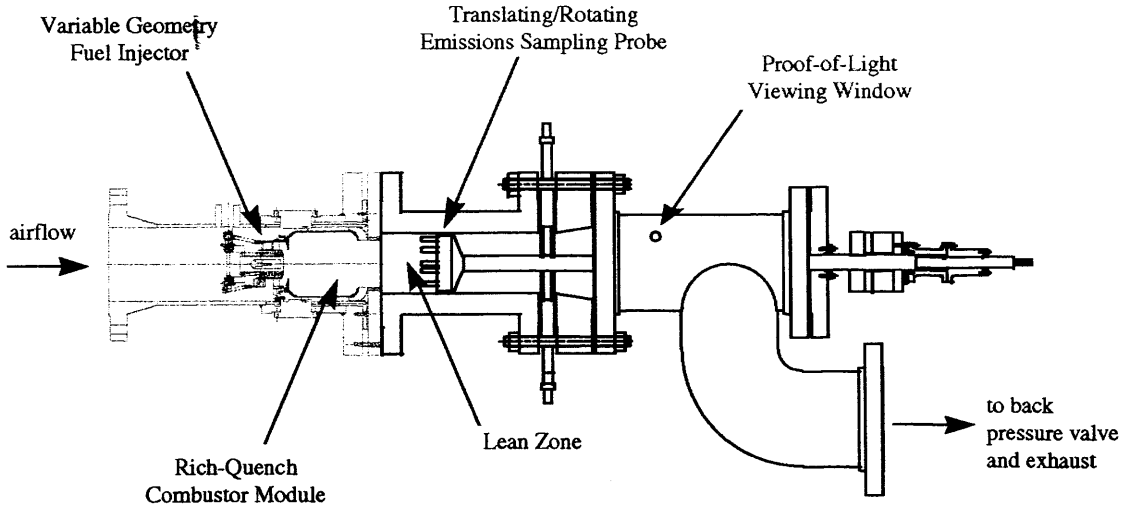

Figure III - 1 Integrated Module Rig Layout with Wall-Jet Combustor Configuration and Translating/Rotating Emission Probe System

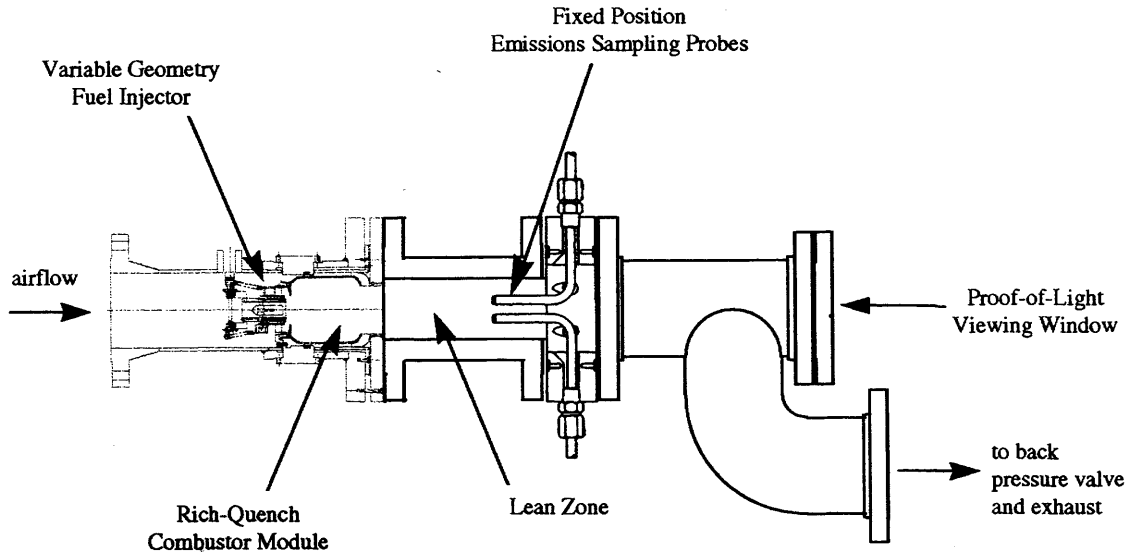

Figure III - 2 Integrated Module Rig Layout with Wall-Jet Combustor Configuration and Fixed Position Emission Probe System

Section IV Figures

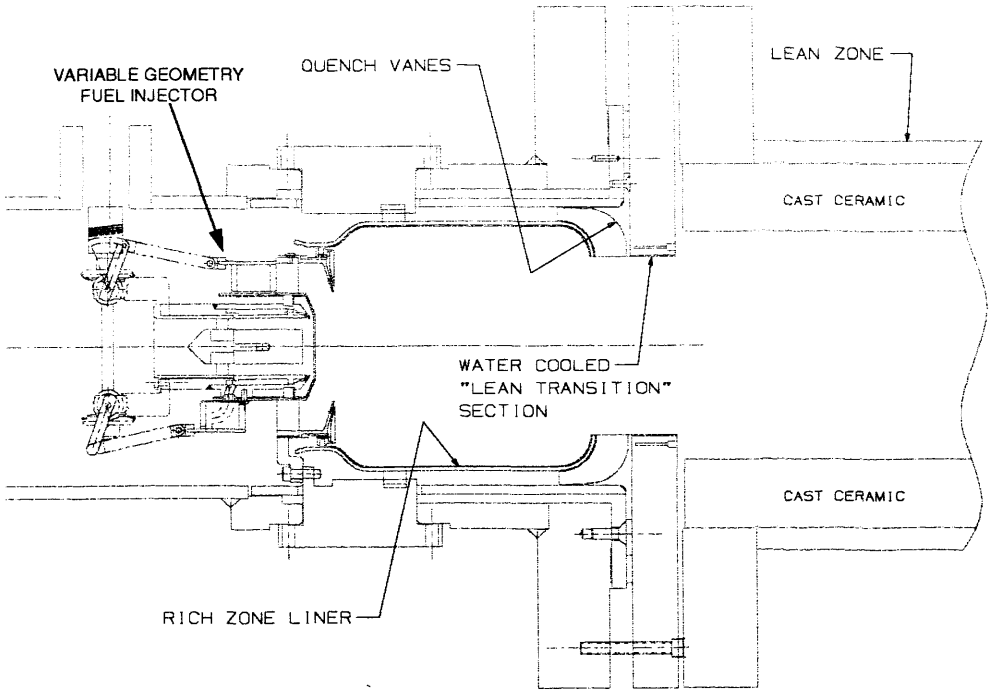

Figure IV - 1 Integrated Module Rig Layout with Wall-Jet Combustor Configuration

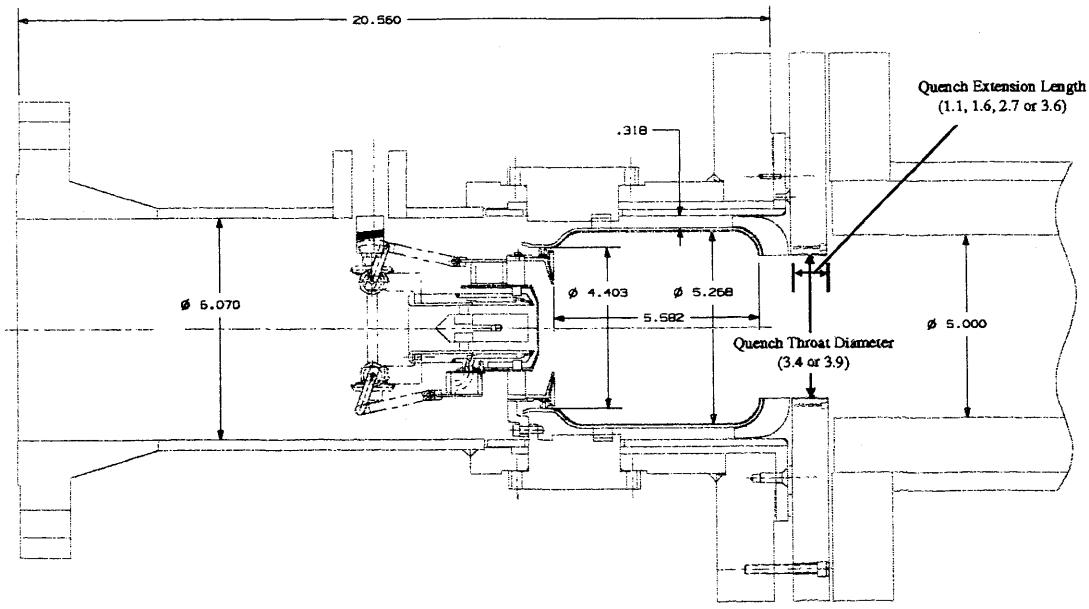

Figure IV - 2 Integrated Module Rig Wall-Jet Combustor Design Dimensions

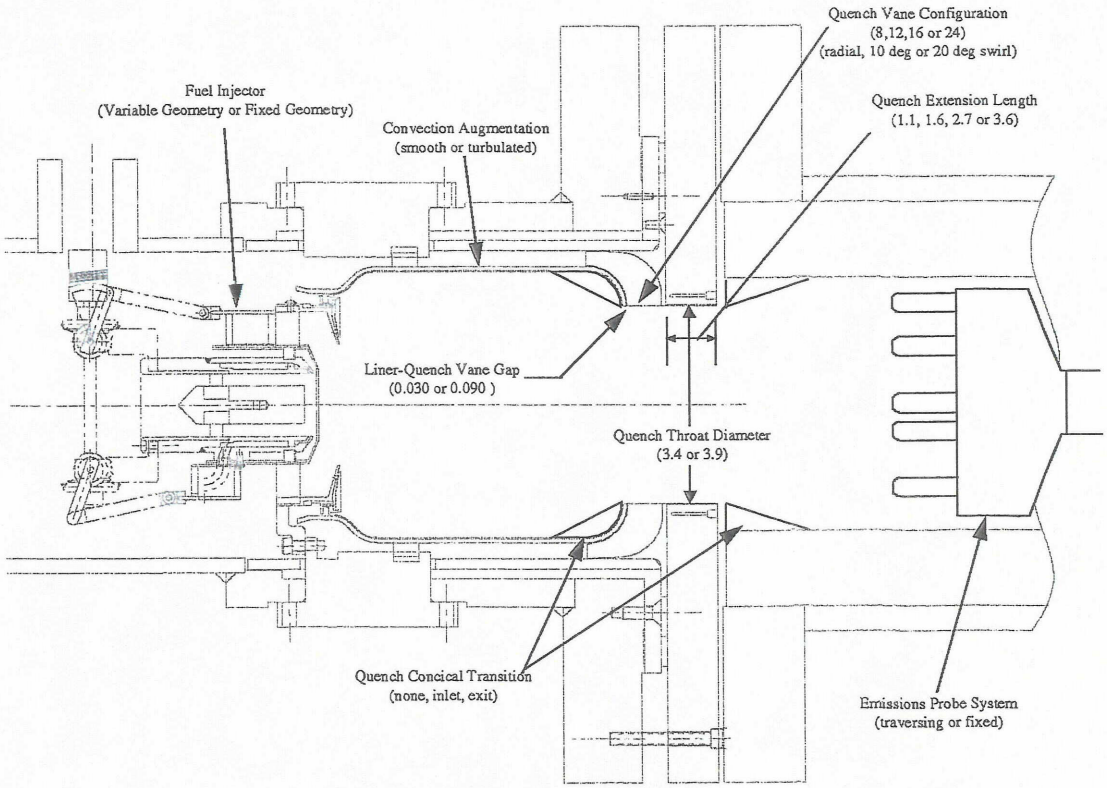

Figure IV - 3 Key Configuration Variables Evaluated During Integrated Module Rig Testing of the Wall-Jet Combustor Configuration

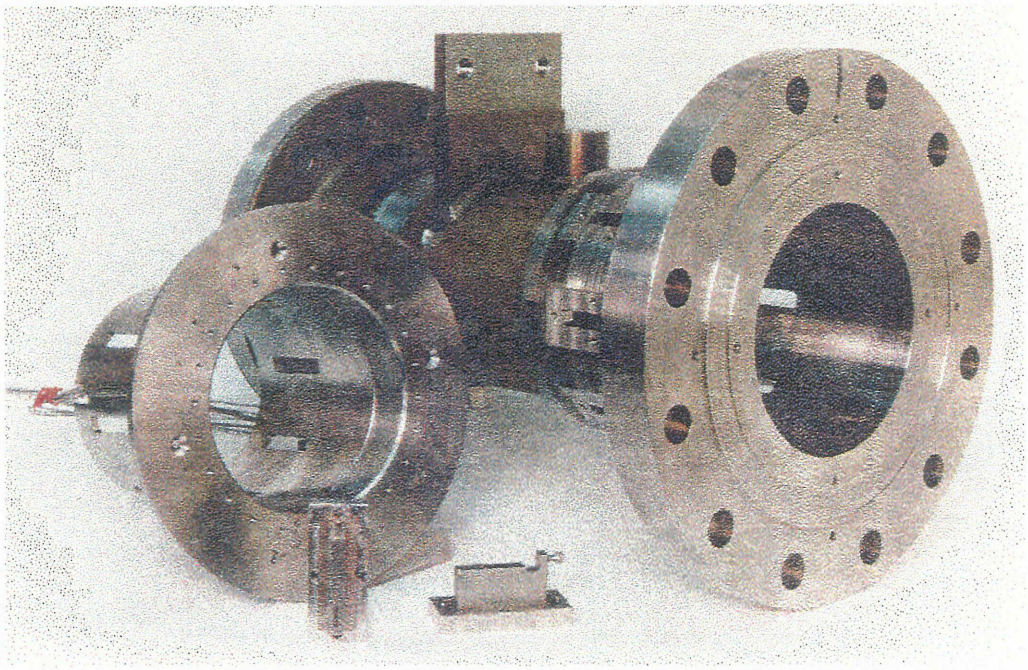

Figure IV - 4 RQL Integrated Module Rig Test Spool Section, Quench Mount Cylinder/Flange and Rich Zone Liner Mount Blocks

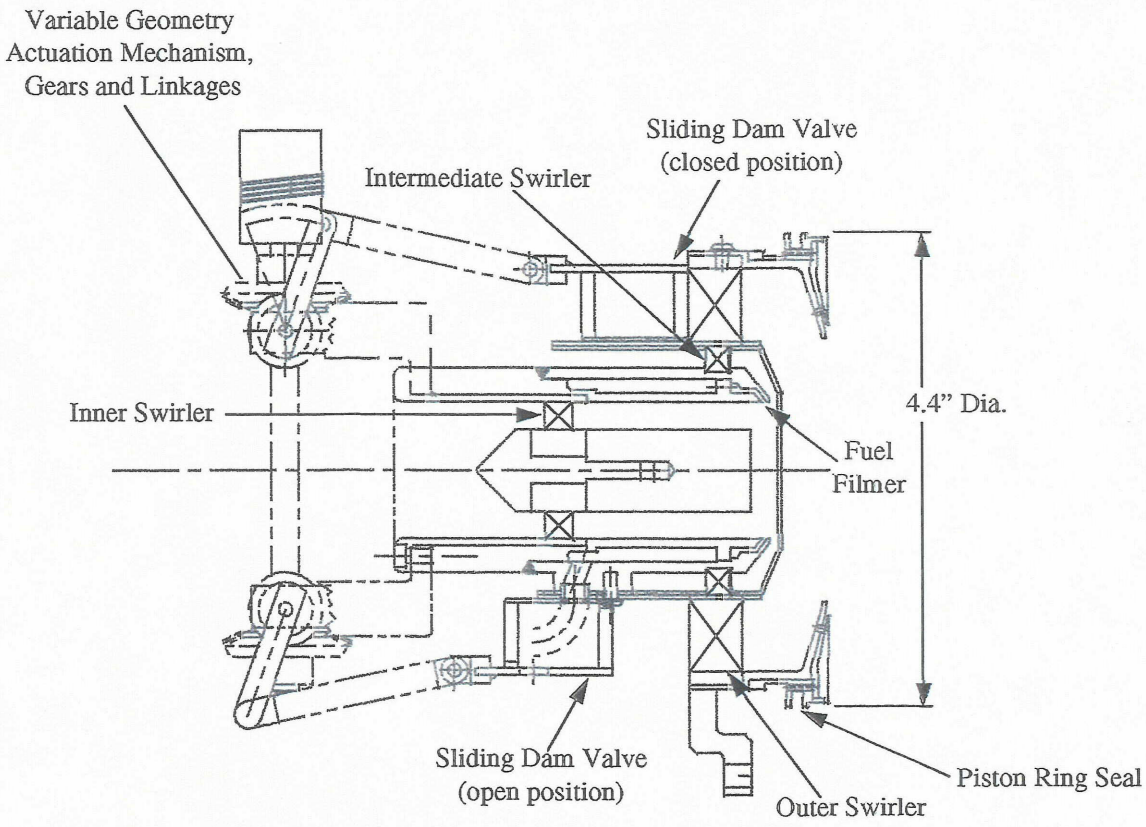

Figure IV - 5 Variable Geometry Fuel Injector Cross Section

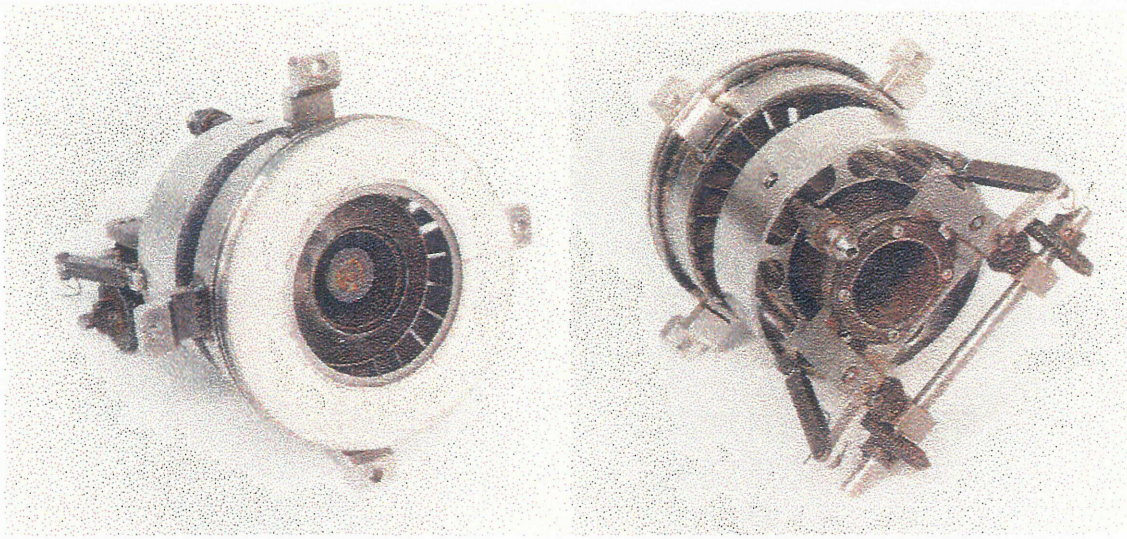

Figure IV - 6 Variable Geometry Fuel Injector for the Integrated Module Rig

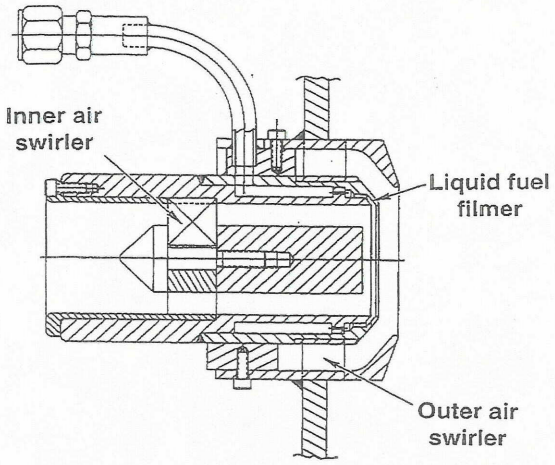

Figure IV - 7 Fixed Geometry Fuel Injector for the Integrated Module Rig

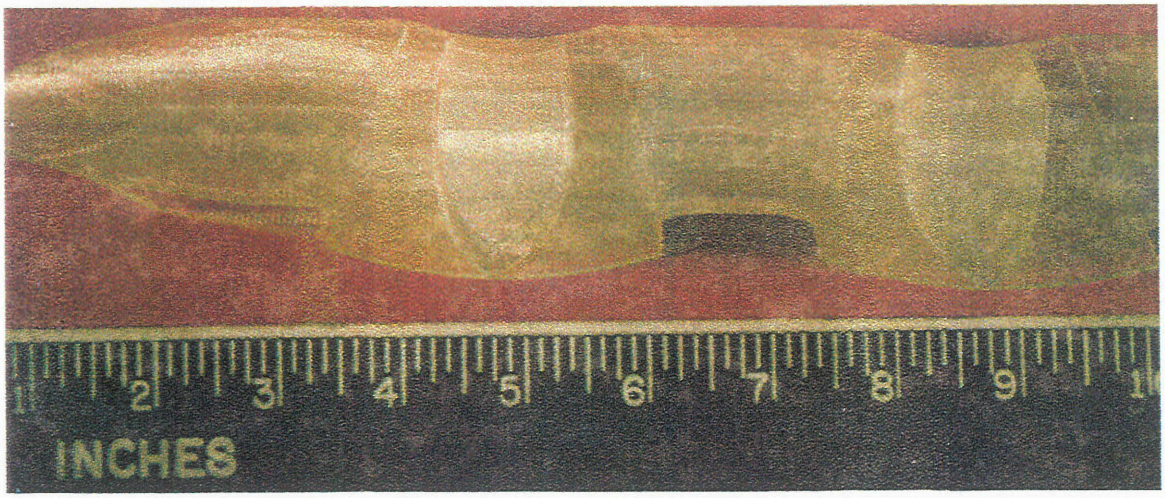

Figure IV - 8 Stereolithography Pattern used for Casting Quench Vanes for the Integrated Module Rig

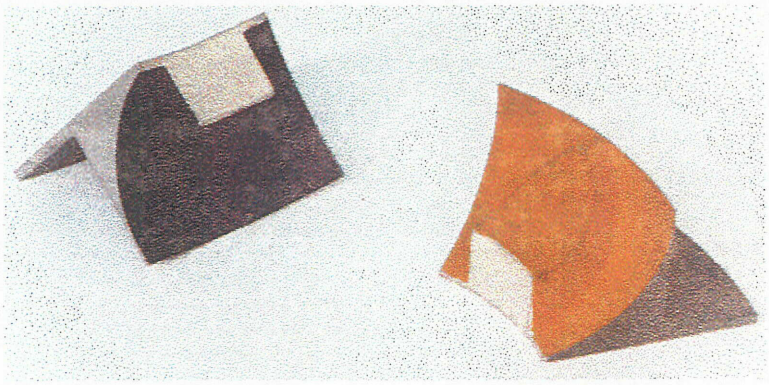

Figure IV - 9 Quench Vanes (Thermal Paint Applied to surface for Heat Transfer Evaluation)

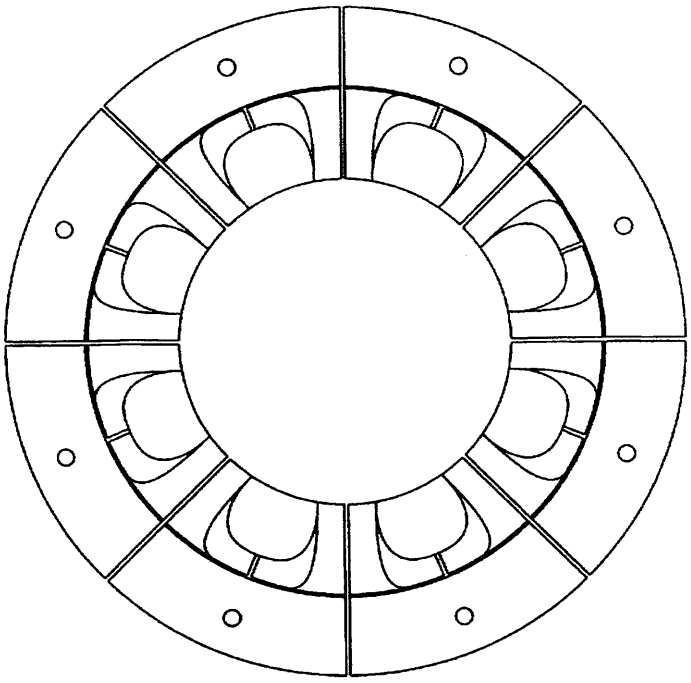

Figure IV - 10 Forward-Looking Aft view of Quench Vane Design; 8 Vane Configuration

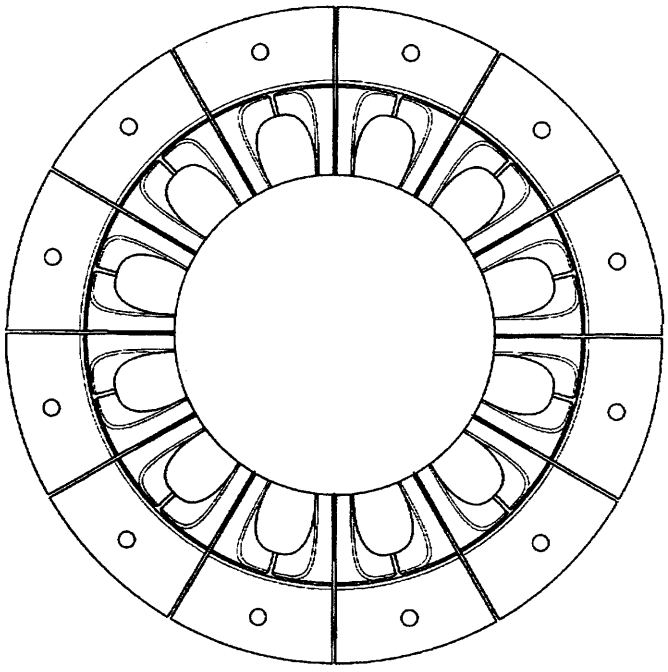

Figure IV - 11 Forward-Looking Aft view of Quench Vane Design; 12 Vane Configuration

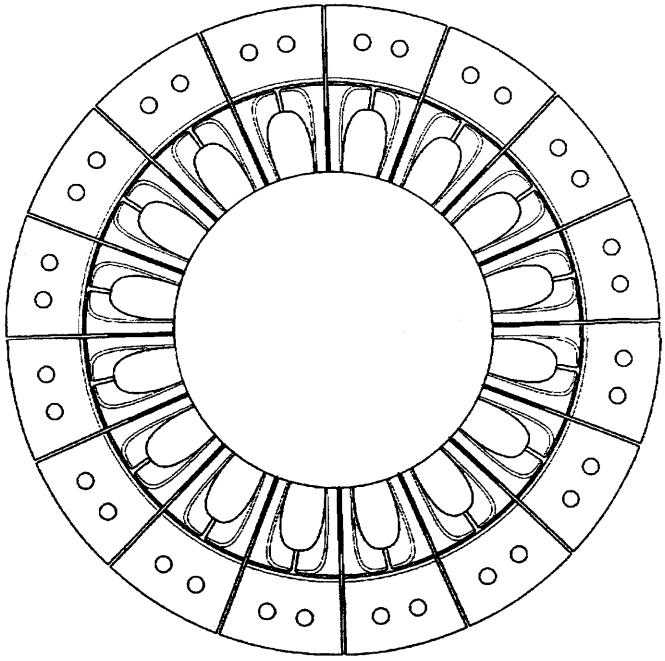

Figure IV - 12 Forward-Looking Aft view of Quench Vane Design; 16 Vane Configuration

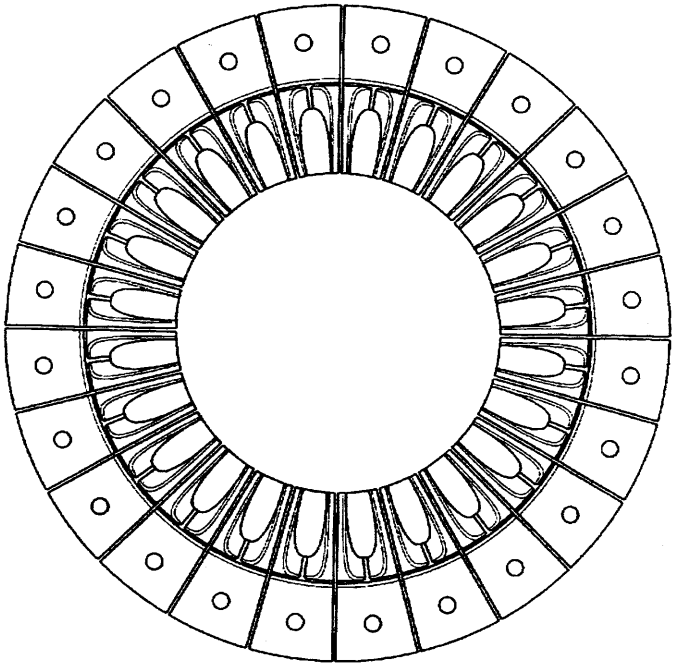

Figure IV - 13 Forward-Looking Aft view of Quench Vane Design; 24 Vane Configuration

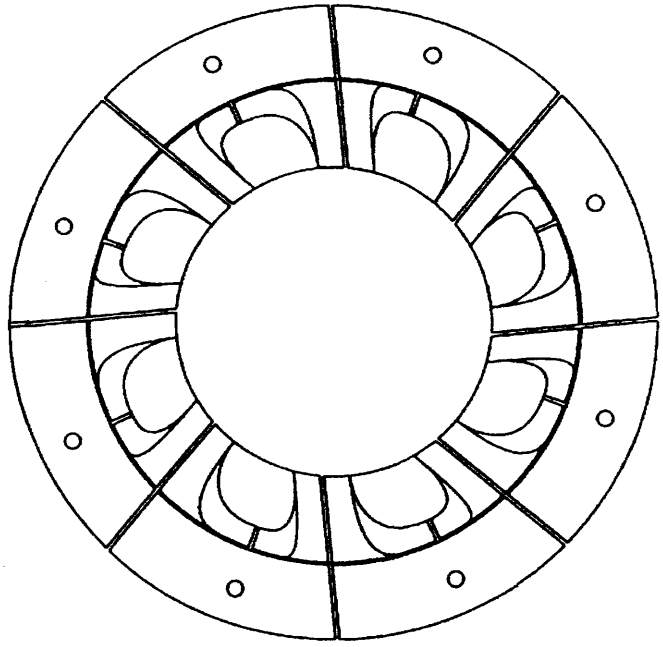

Figure IV - 14 Forward-Looking Aft view of Quench Vane Design; 8 Vane Configuration 10 degree swirl

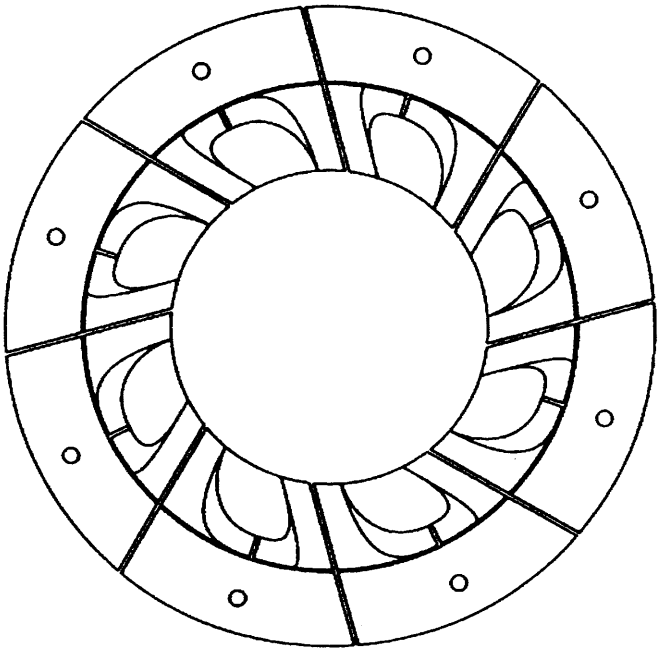

Figure IV - 15 Forward-Looking Aft view of Quench Vane Design; 8 Vane Configuration 20 degree swirl

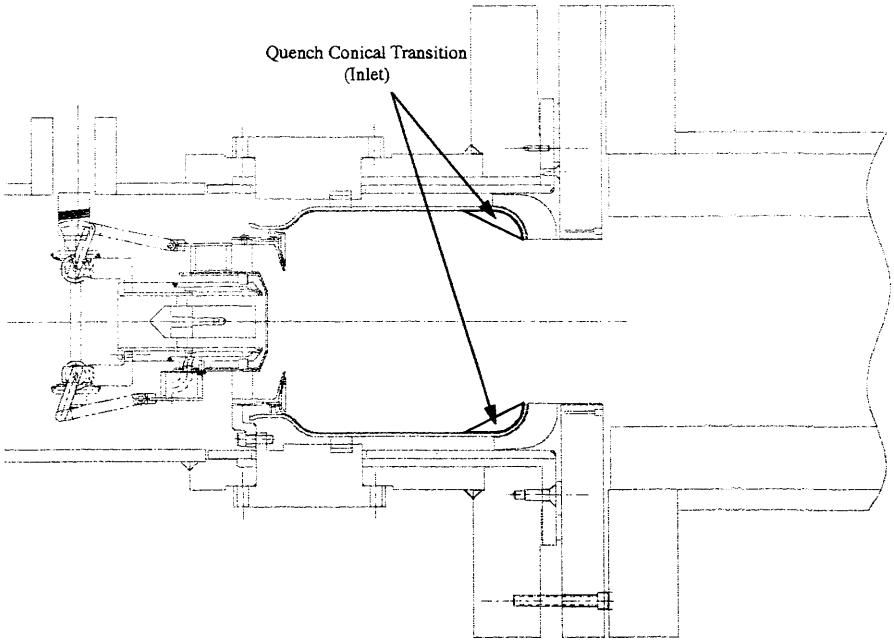

Figure IV - 16 Quench Conical Transition at the inlet to the Quench Region formed by Cast Ceramic Inserts

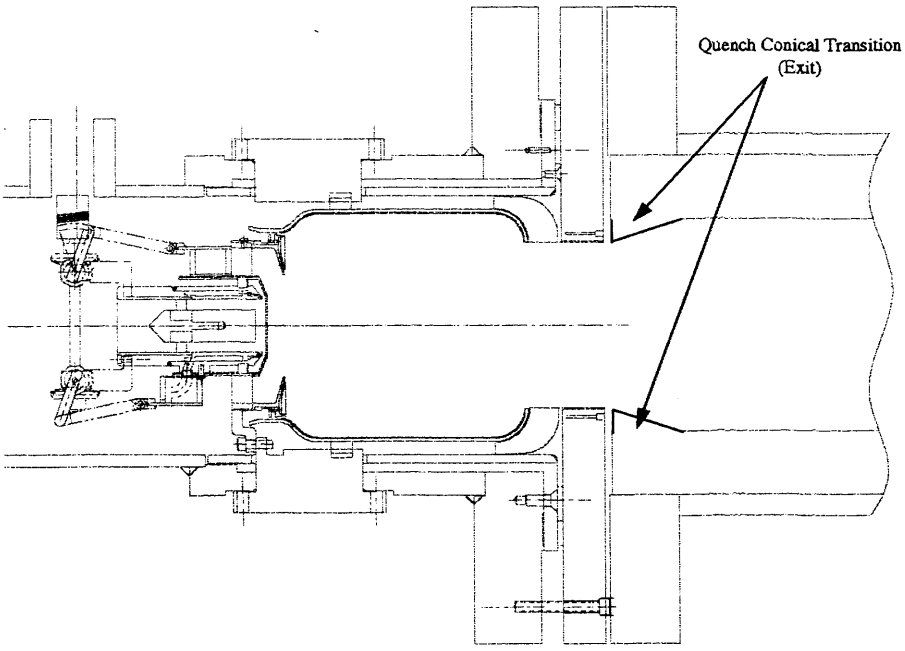

Figure IV - 17 Quench Conical Transition at the exit of the Quench Region formed by Cast Ceramic lean Zone Liner

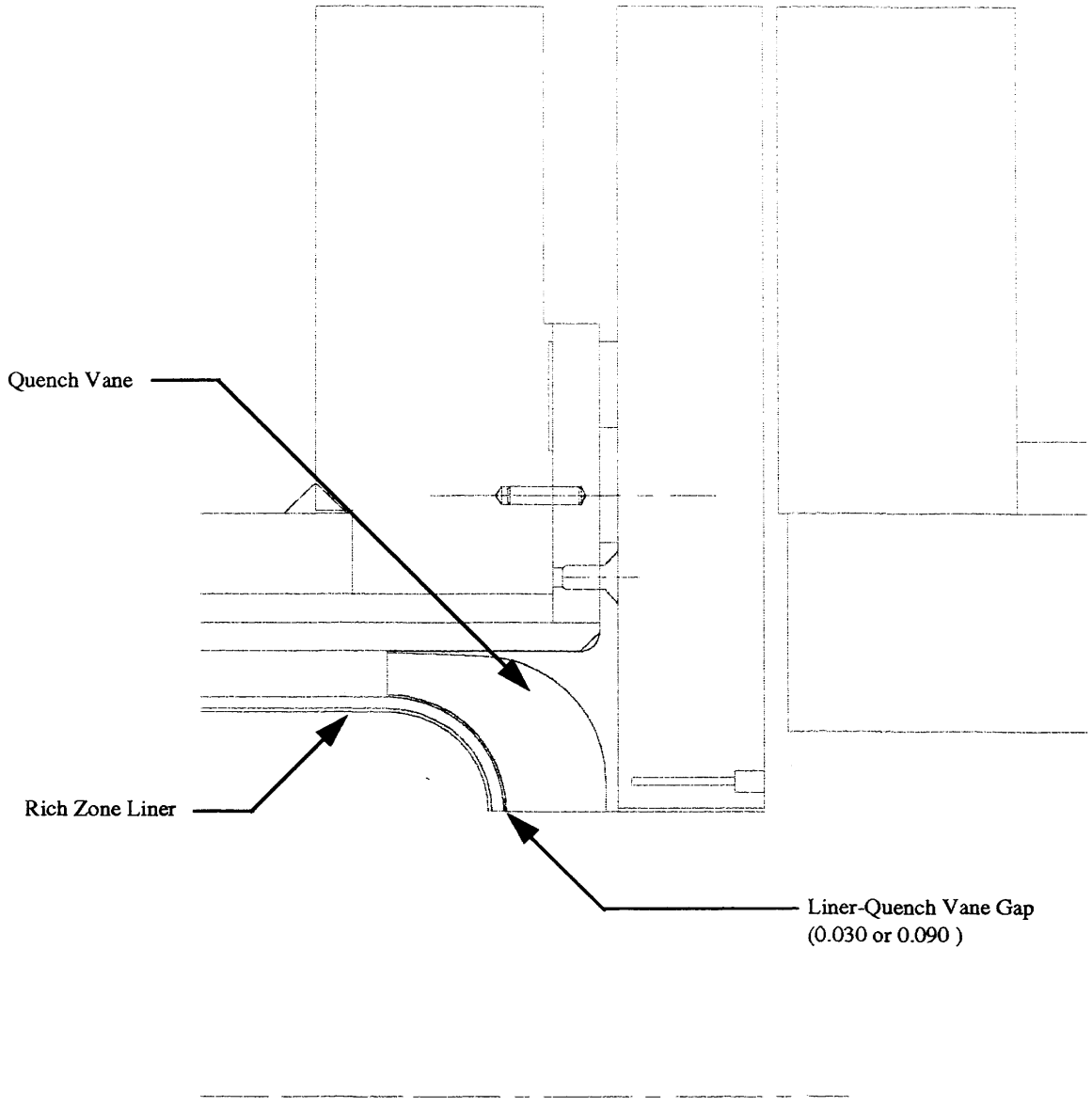

Figure IV - 18 Gap Between Rich Zone Liner and Quench Vane

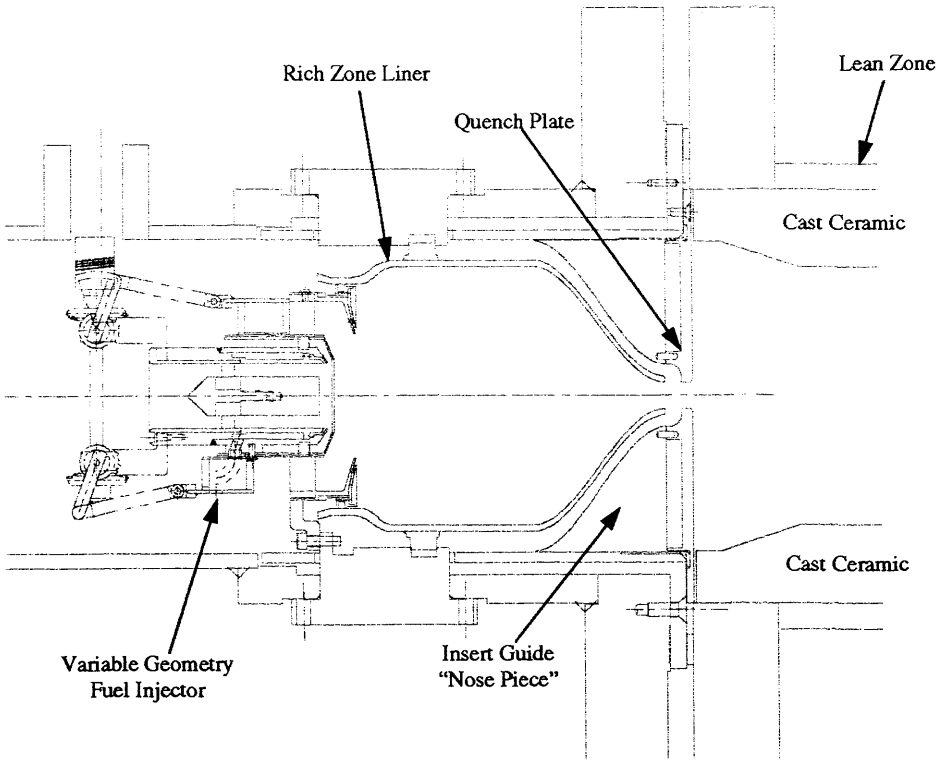

Figure IV - 19 Integrated Module Rig Layout with Reduced Scale Quench Convoluted Liner/Quench Plate Combustor Configuration

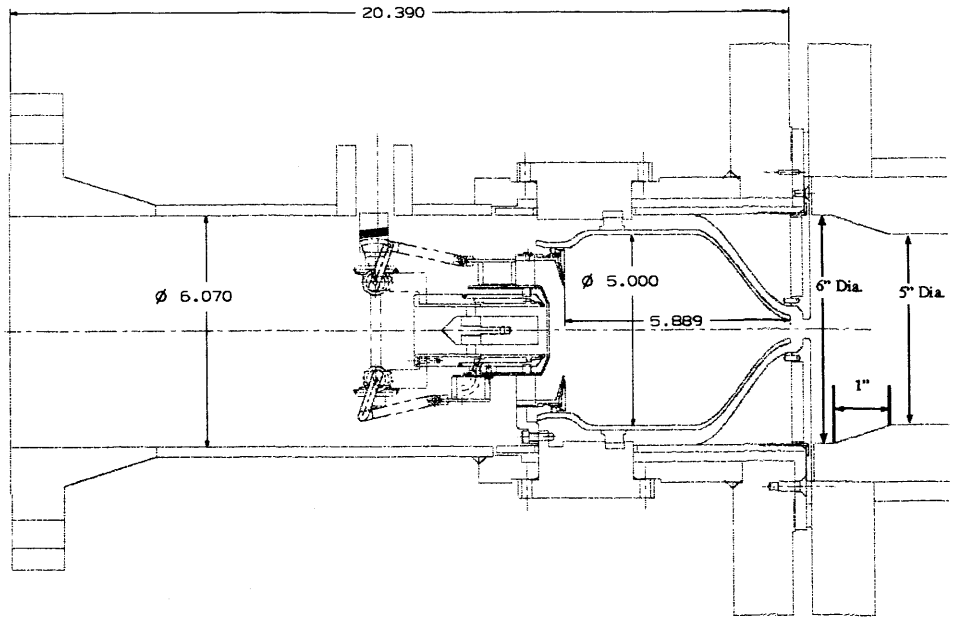

Figure IV - 20 Integrated Module Rig Reduced Scale Quench Convoluted Liner/Quench Plate Combustor Design Dimensions

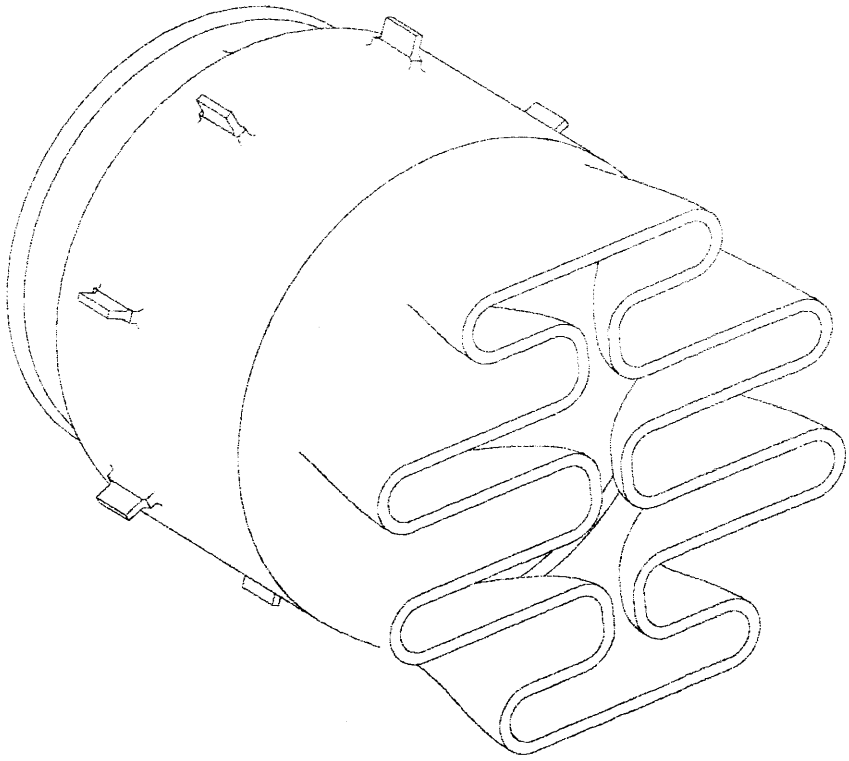

Figure IV - 21 Rich Zone Convoluted Liner

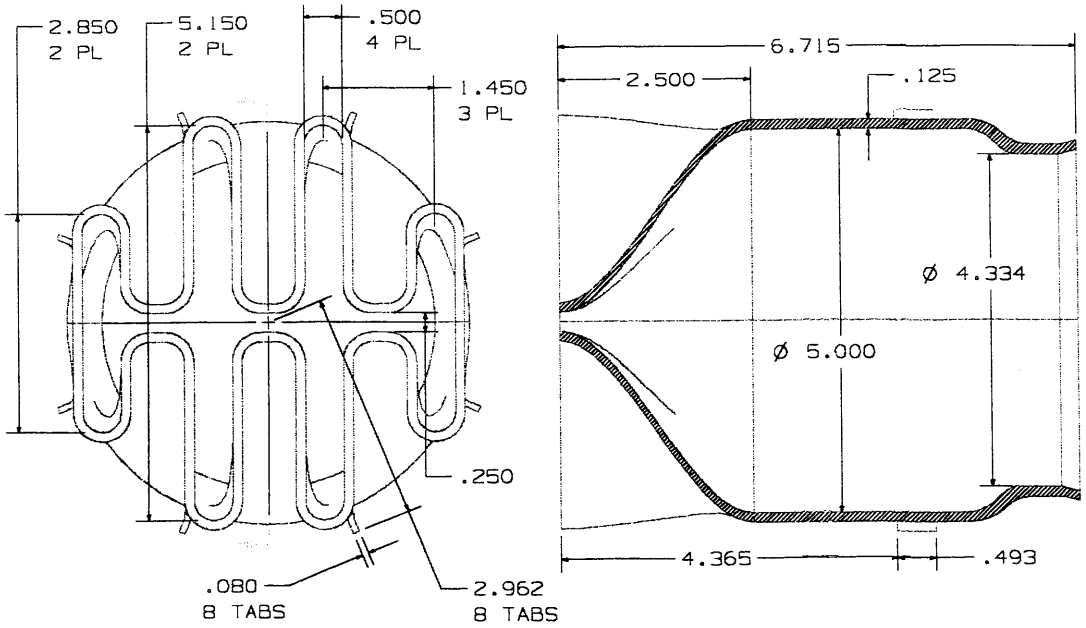

Figure IV - 22 Rich Zone Convoluted Liner Design; Gen II shown

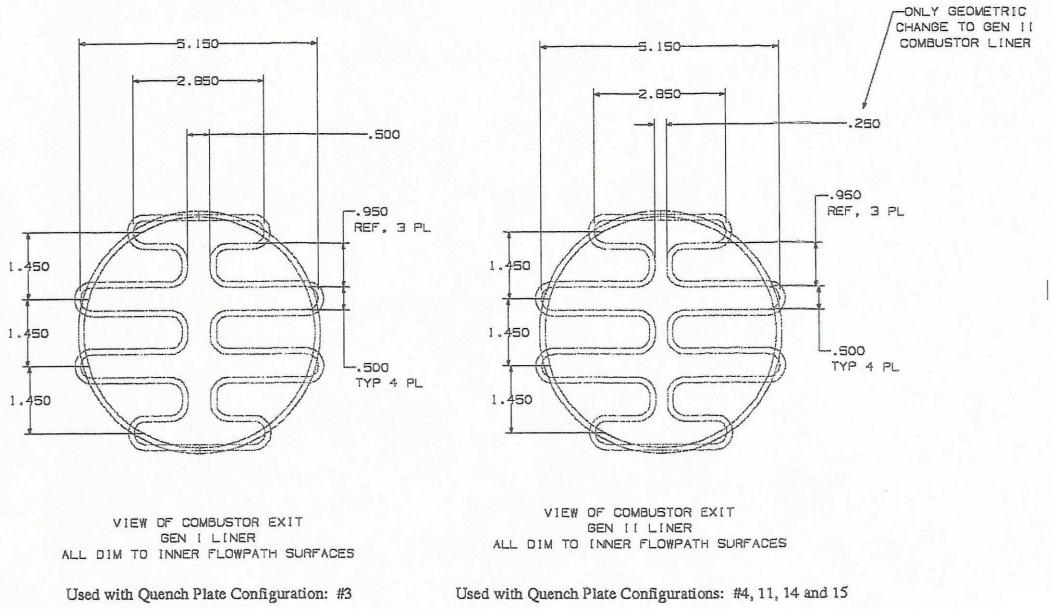

Figure IV - 23 Rich Zone Convoluted Liner Design; Gen I and Gen II

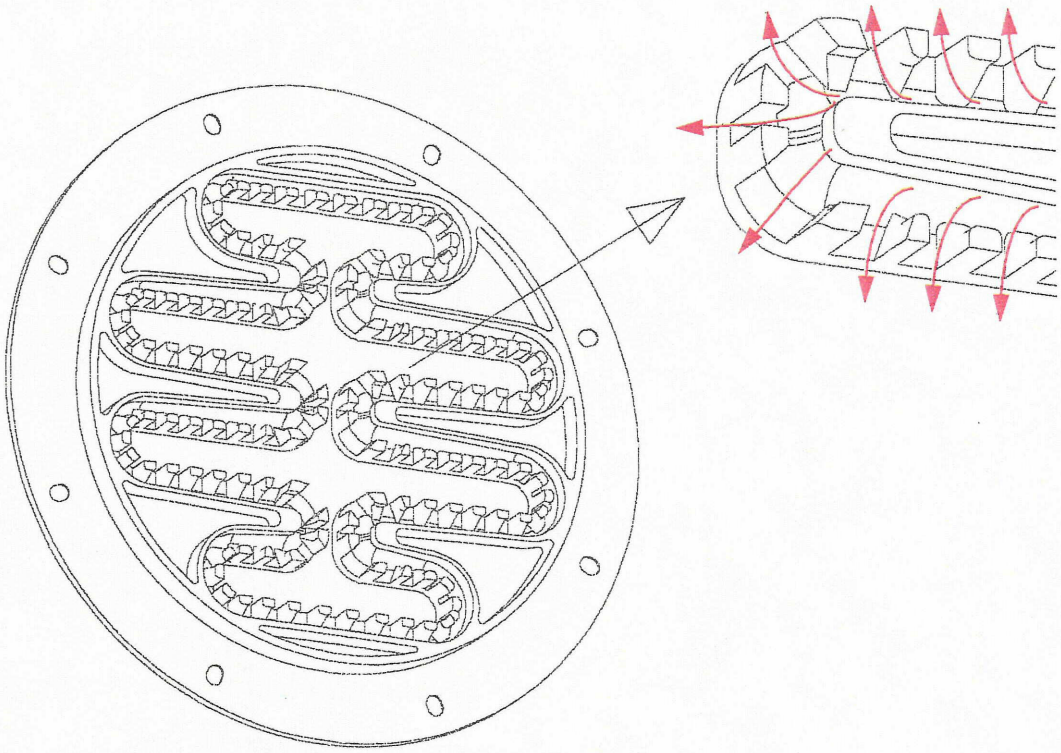

Figure IV - 24 Isometric View of Quench Plate with Flowpath

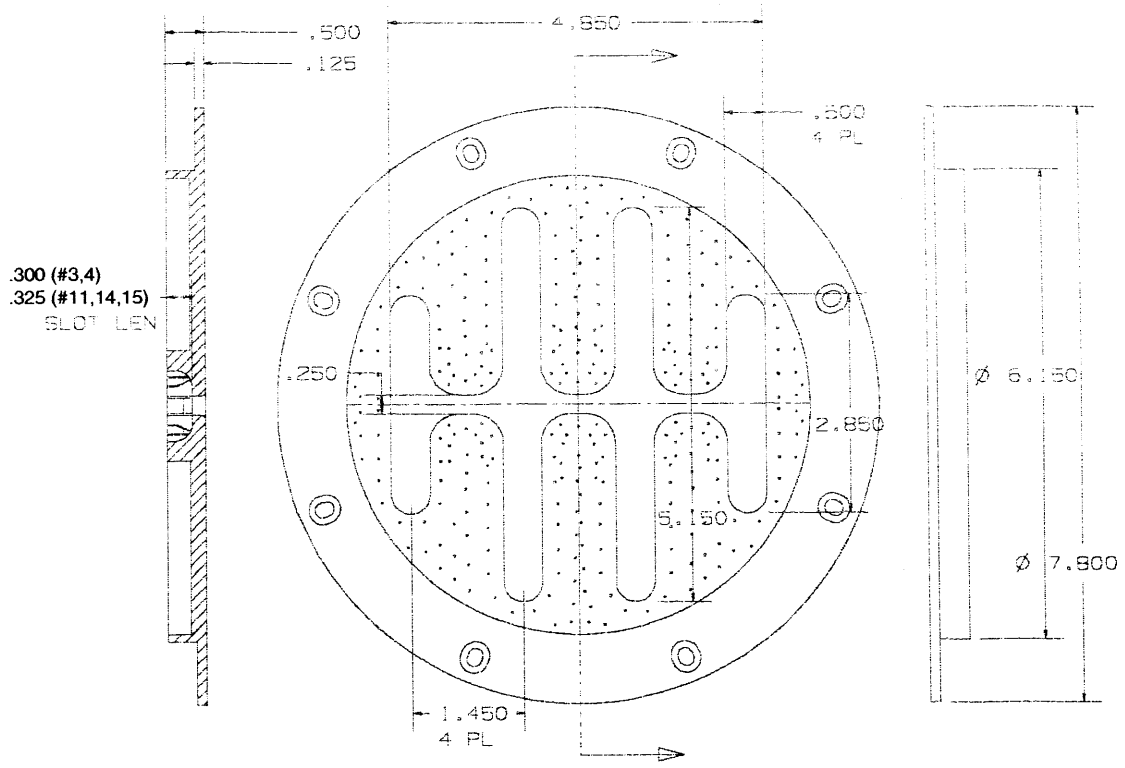

Figure IV - 25 Reduced Scale Quench Plate Design

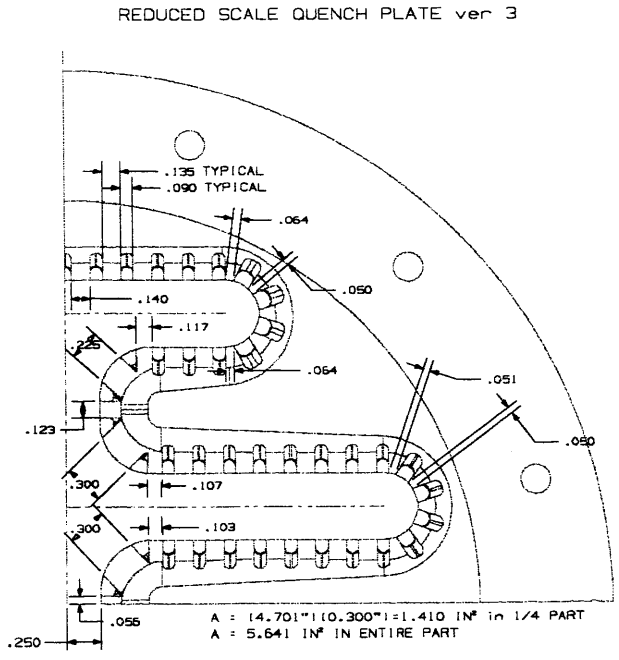

Figure IV - 26 Reduced Scale Quench Plate Configuration #3 Design

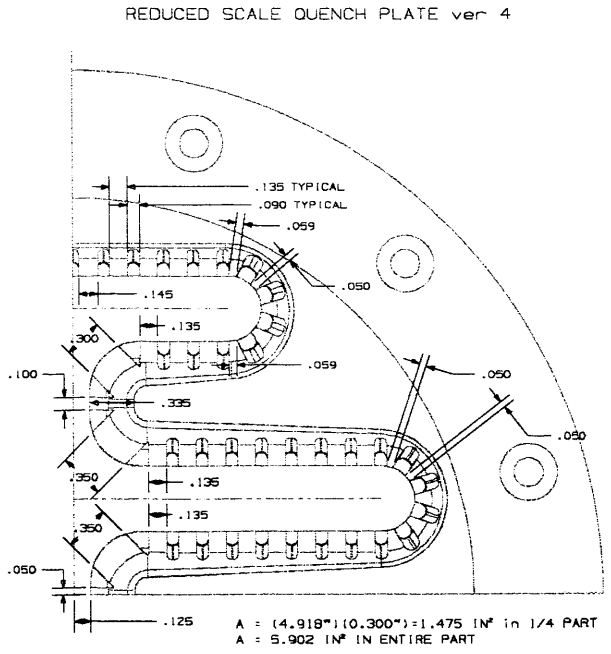

Figure IV - 27 Reduced Scale Quench Plate Configuration #4 Design

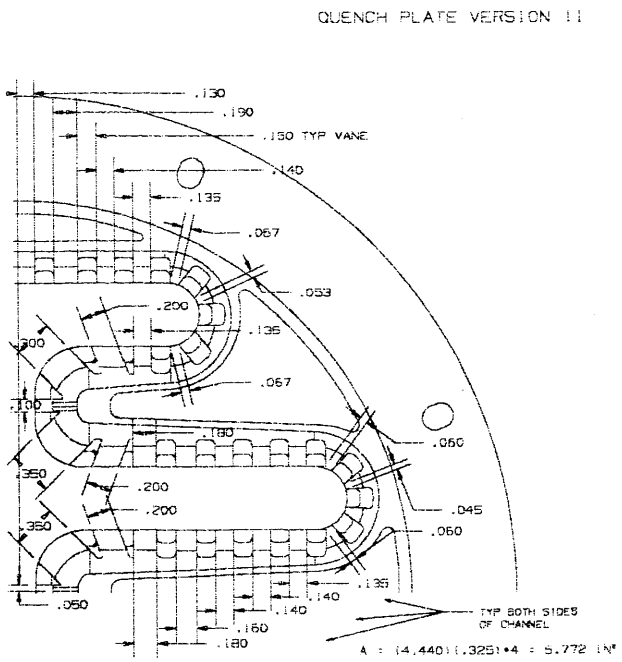

Figure IV - 28 Reduced Scale Quench Plate Configuration #11 Design

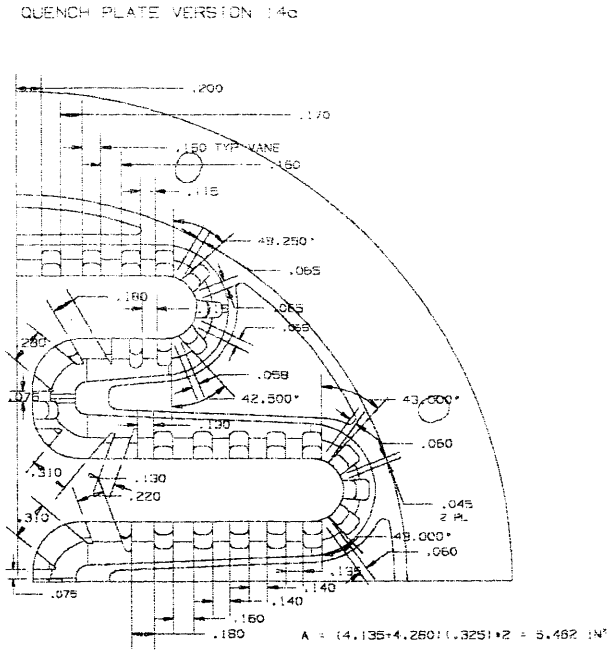

Figure IV - 29 Reduced Scale Quench Plate Configuration #14 Design

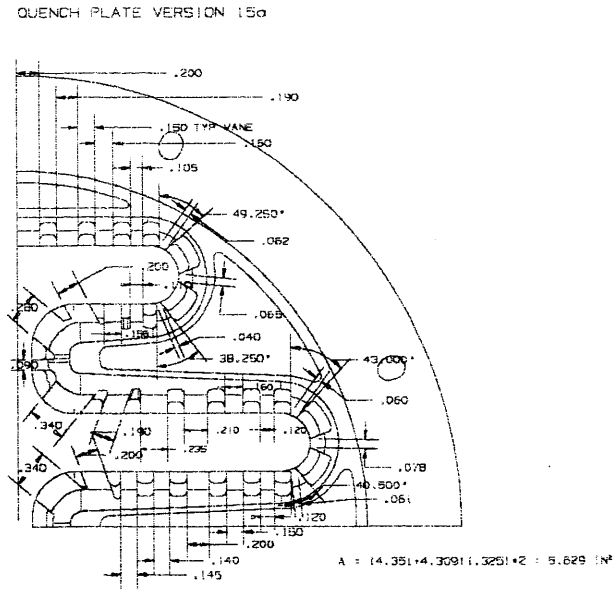

Figure IV - 30 Reduced Scale Quench Plate Configuration #15 Design

Section V Figures

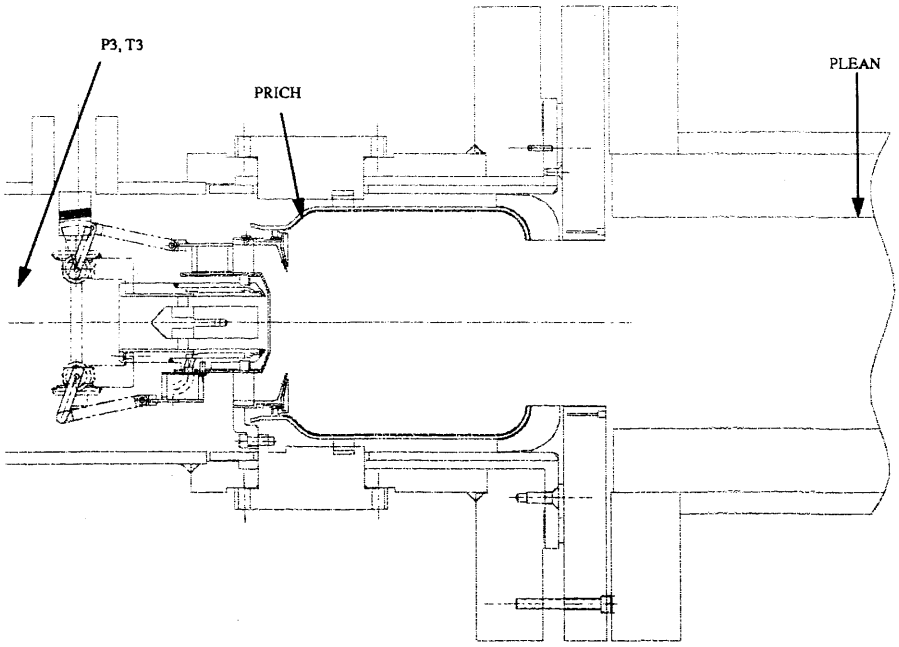

Figure V - 1 Operational Static Pressure and Temperature Instrumentation on Integrated Module Rig Wall-Jet Combustor Configuration

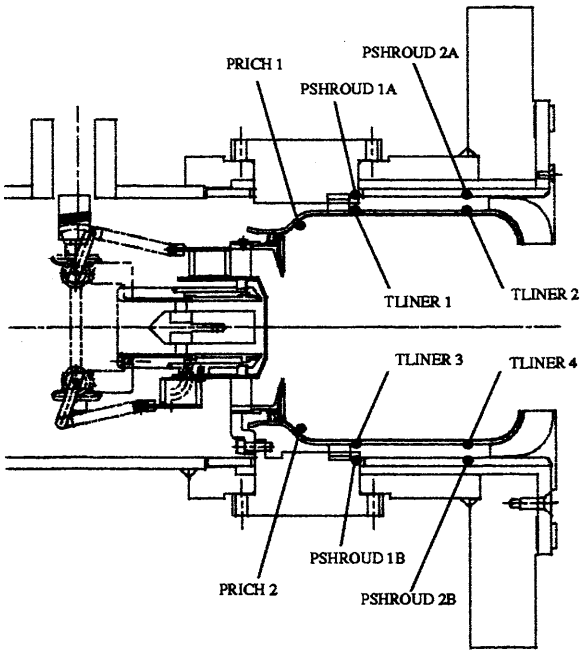

Figure V - 2 Additional Instrumentation on Wall-Jet Combustor Configuration

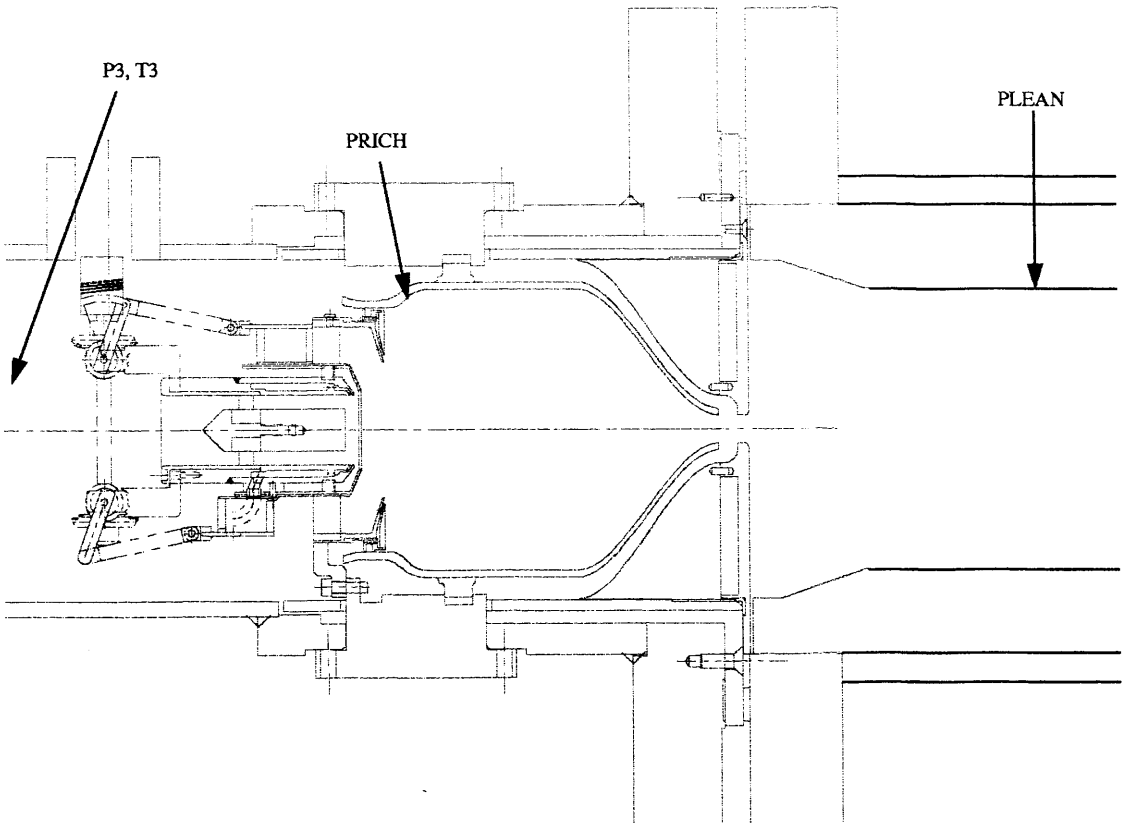

Figure V - 3 Operational Static Pressure and Temperature Instrumentation on Integrated Module Rig Reduced Scale Quench Convoluted Liner/Quench Plate Combustor Configuration

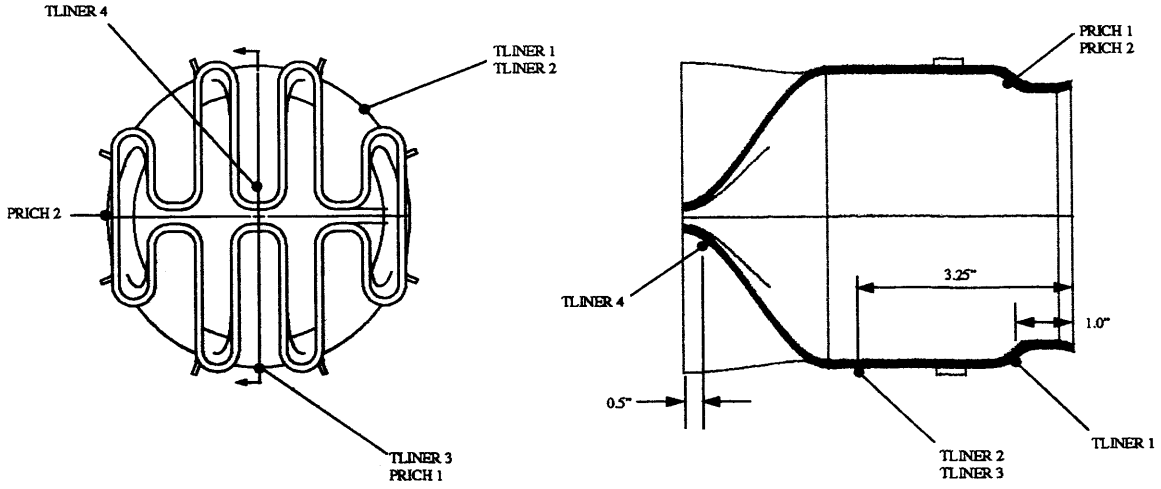

Figure V - 4 Additional Instrumentation on Reduced Scale Quench Convoluted Liner Combustor Configuration

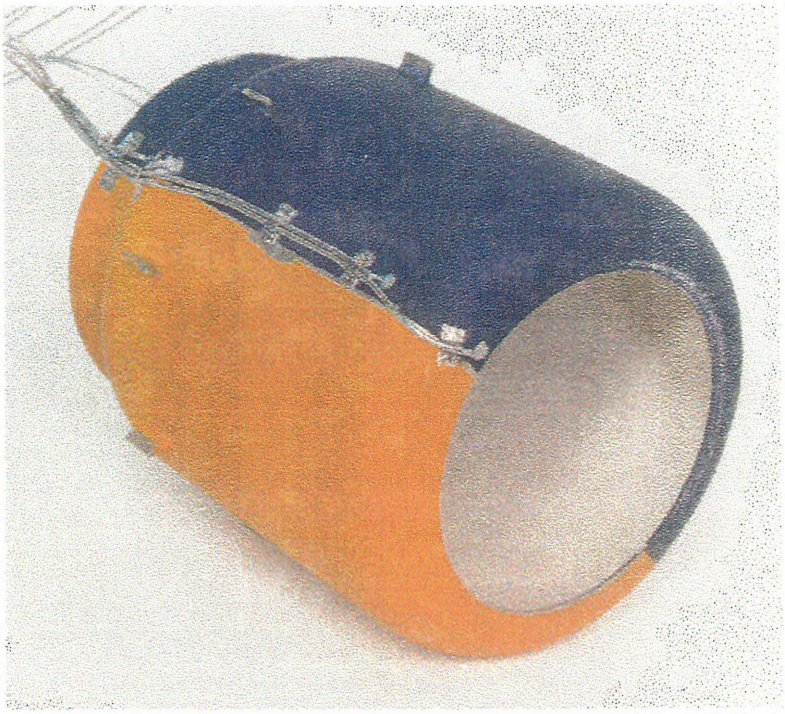

Figure V - 5 Rich Zone Liner with Thermocouples; Thermal Paint Applied for Heat Transfer Evaluation; Aft-Looking-Forward Isometric View

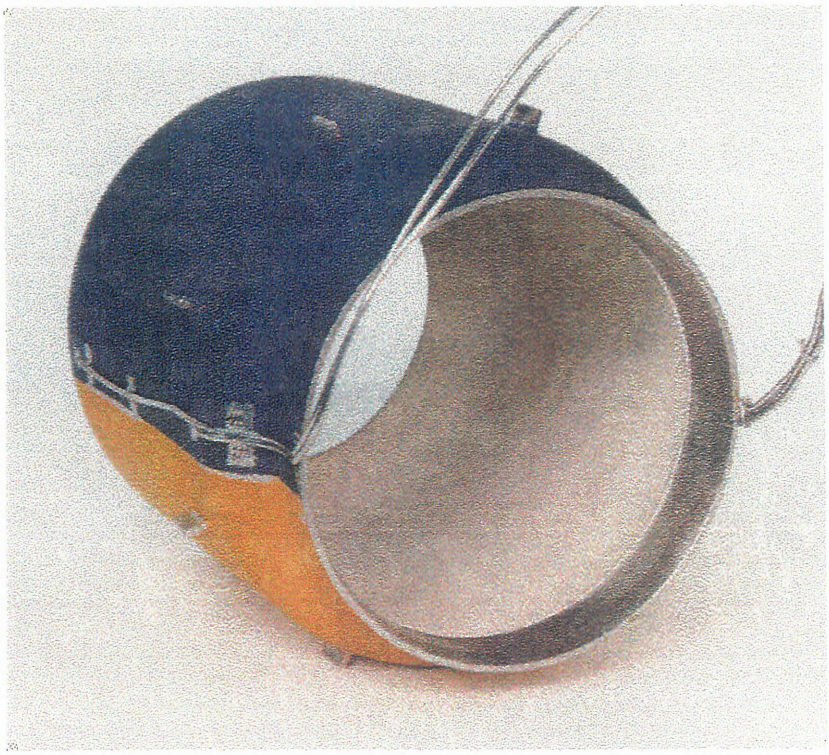

Figure V - 6 Rich Zone Liner with Thermocouples; Thermal Paint Applied for Heat Transfer Evaluation; Forward-Looking-Aft Isometric View

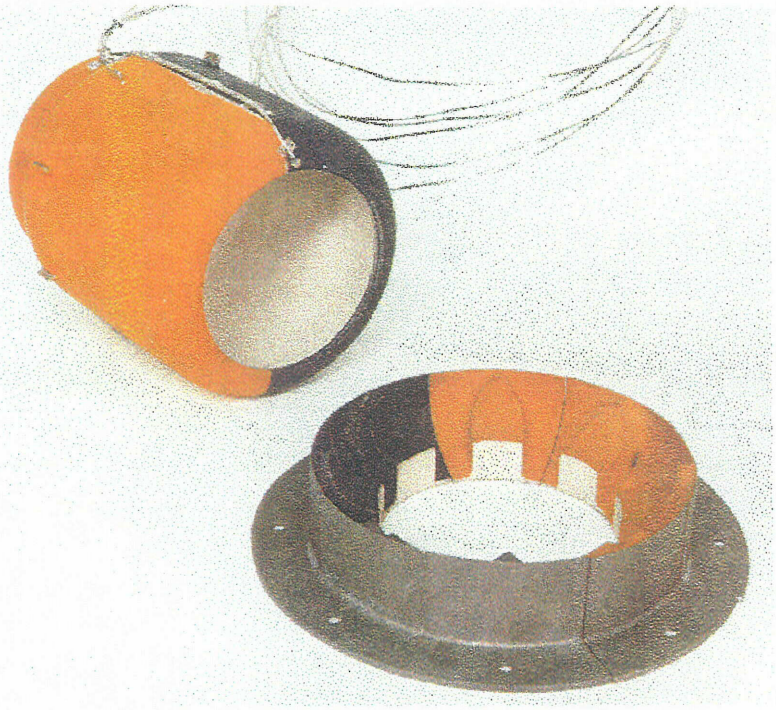

Figure V - 7 Rich Zone Liner with Thermocouples and Quench Vanes; Thermal Paint Applied for Heat Transfer Evaluation

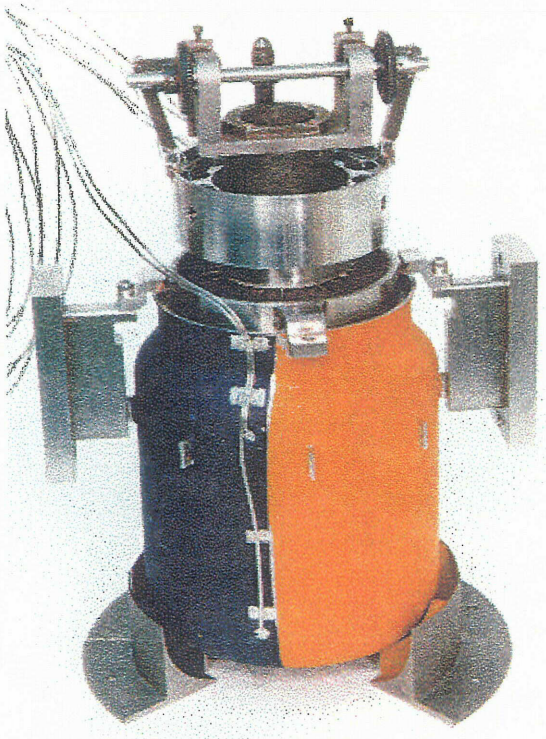

Figure V - 8 Rich Zone Liner with Thermocouples, Quench Vanes and Variable Geometry Injector; Thermal Paint Applied for Heat Transfer Evaluation

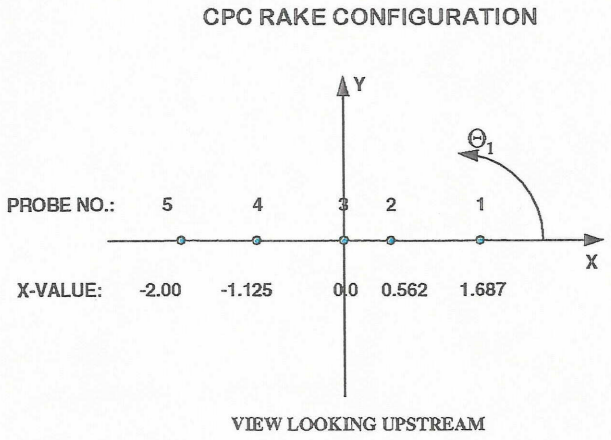

$$y = r \cdot \sin \Theta_2 \; ; \; x = r \cdot \cos \Theta_2$$

$$\text{if } \Theta_1 > 0, \Theta_2 = \Theta_1, \text{ else } \Theta_2 = 360 + \Theta_1$$

Figure V - 9 Translating/Rotating Emissions Sampling Probe Rotational Position Definition

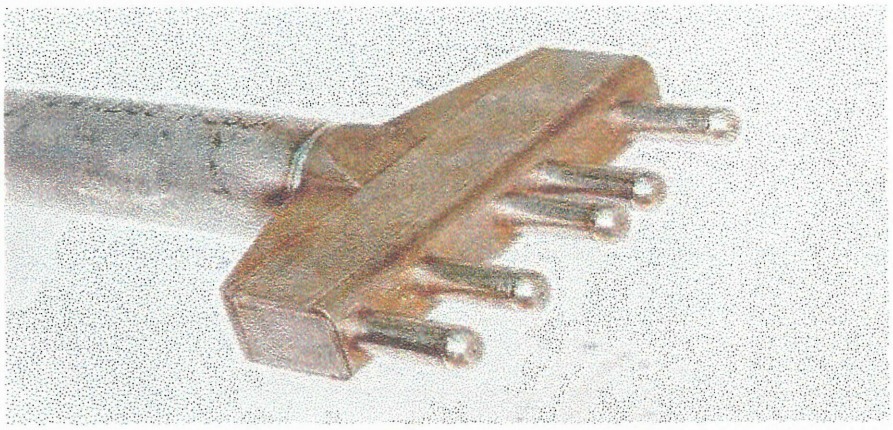

Figure V - 10 Translating/Rotating Emissions Sampling Probe System used in Integrated Module Rig Tests

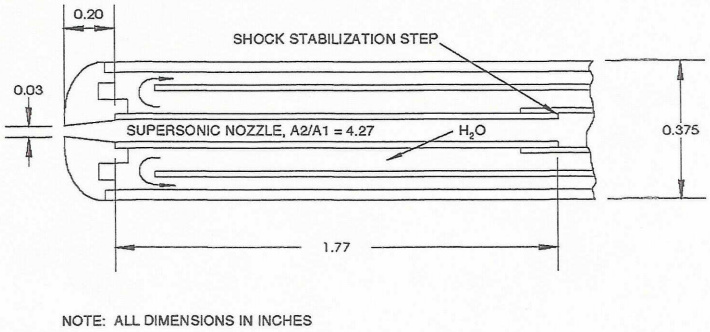

Figure V - 11 Aerodynamic Quenching Emissions Probe Tip Design of Translating/Rotating Emissions Sampling Probe System

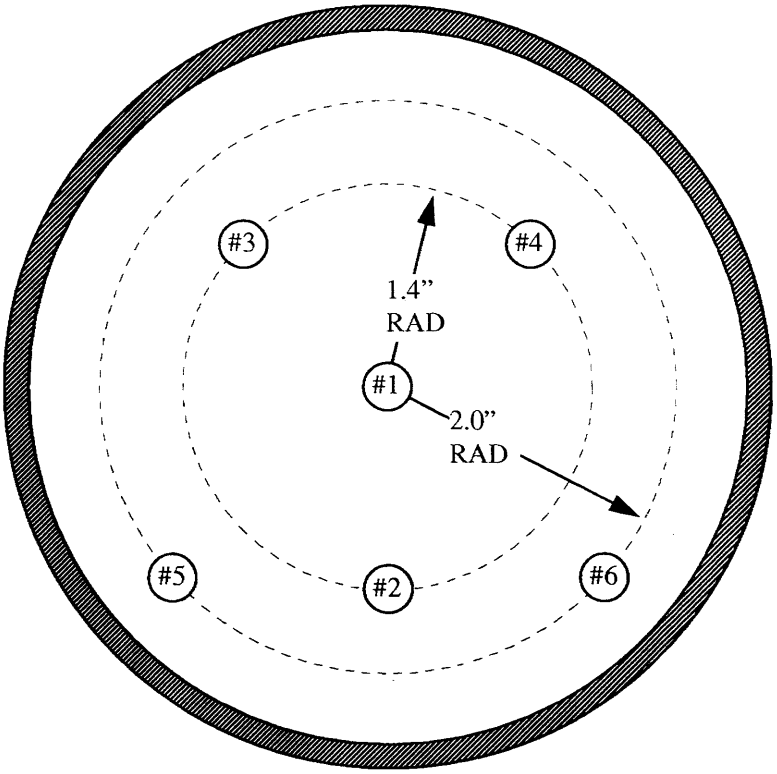

Figure V - 12 Fixed Location Emissions Sampling Probe Position Definition

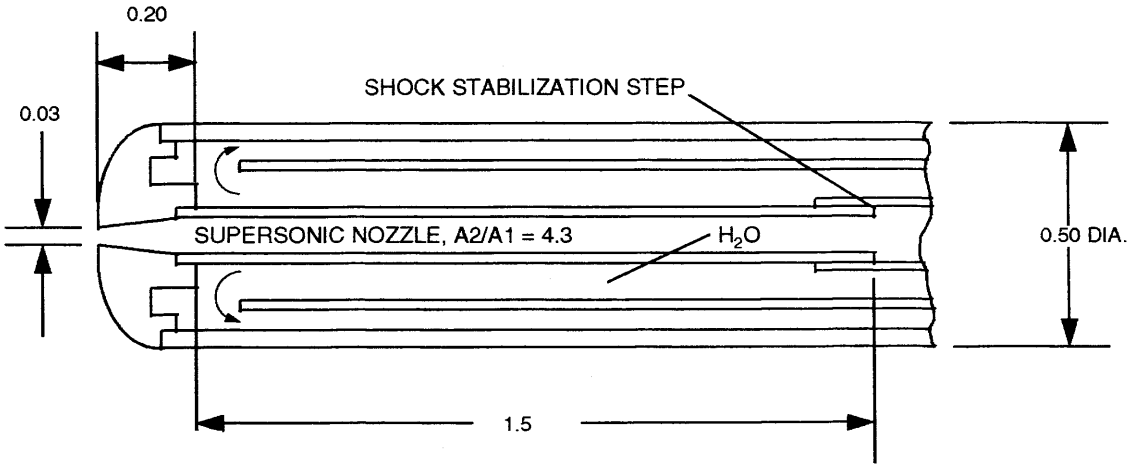

NOTE: ALL DIMENSIONS IN INCHES

Figure V - 13 Aerodynamic Quenching Emissions Probe Tip Design of Fixed Location Emissions Sampling Probe System

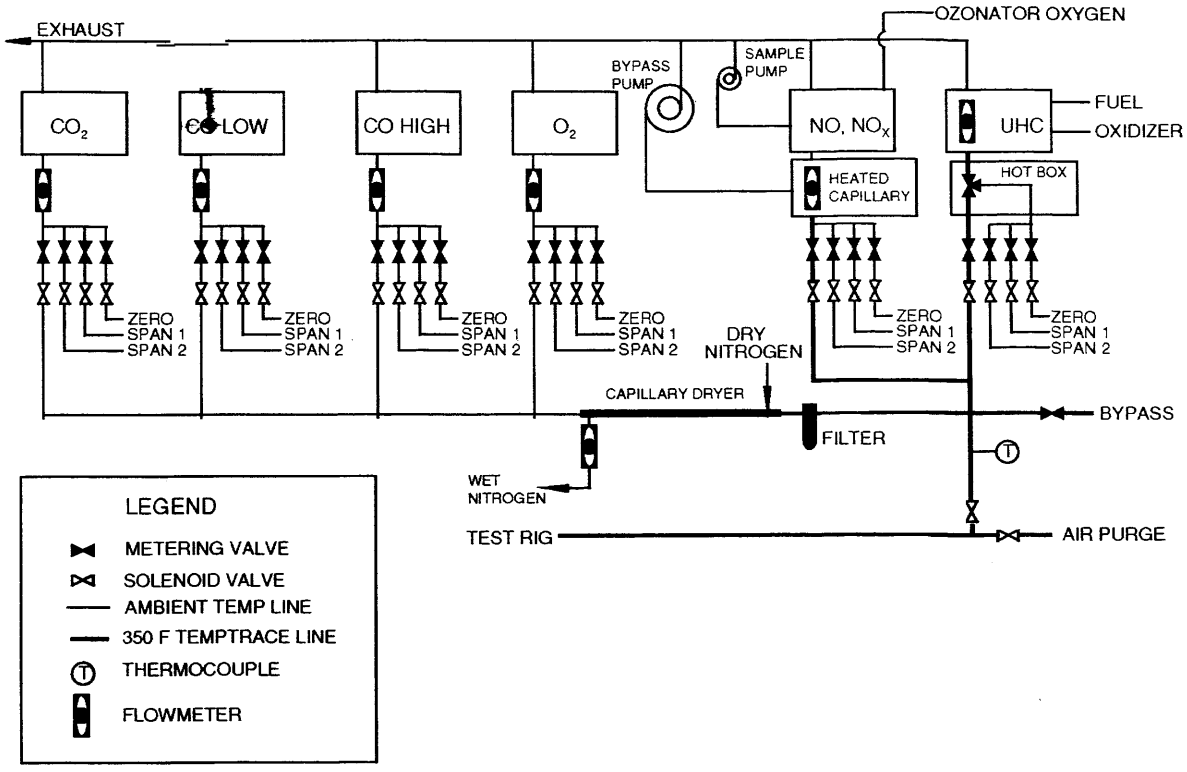

Figure V - 14 Emissions Analysis System Schematic

Section VI Figures

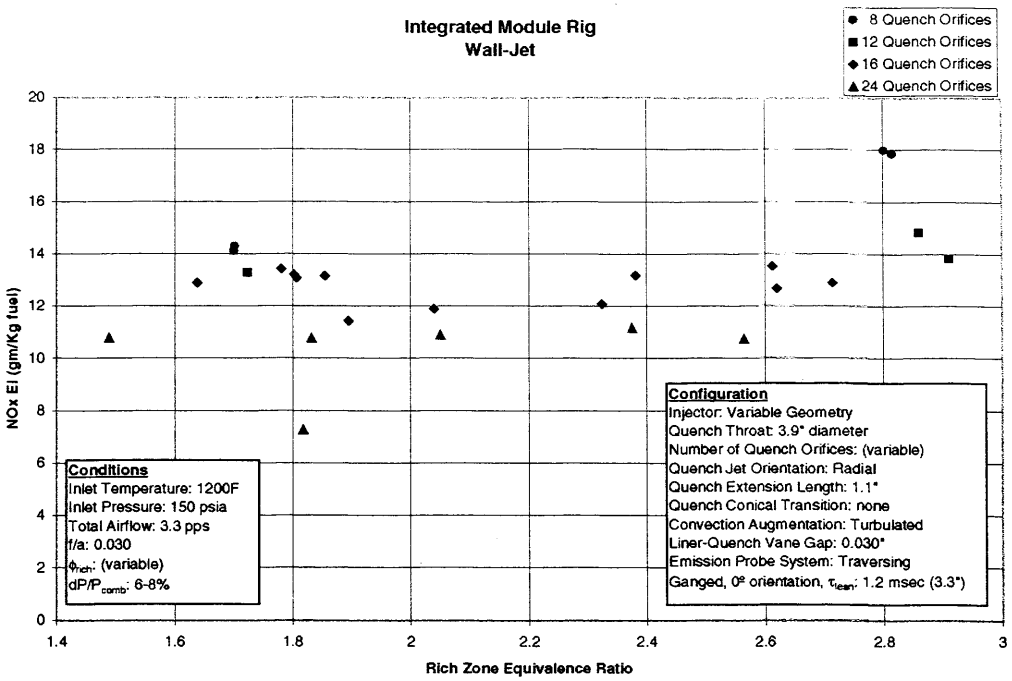

Figure VI - 1 Effect of Number of Quench Vanes on NOx Emissions as a Function of Rich Zone Equivalence Ratio

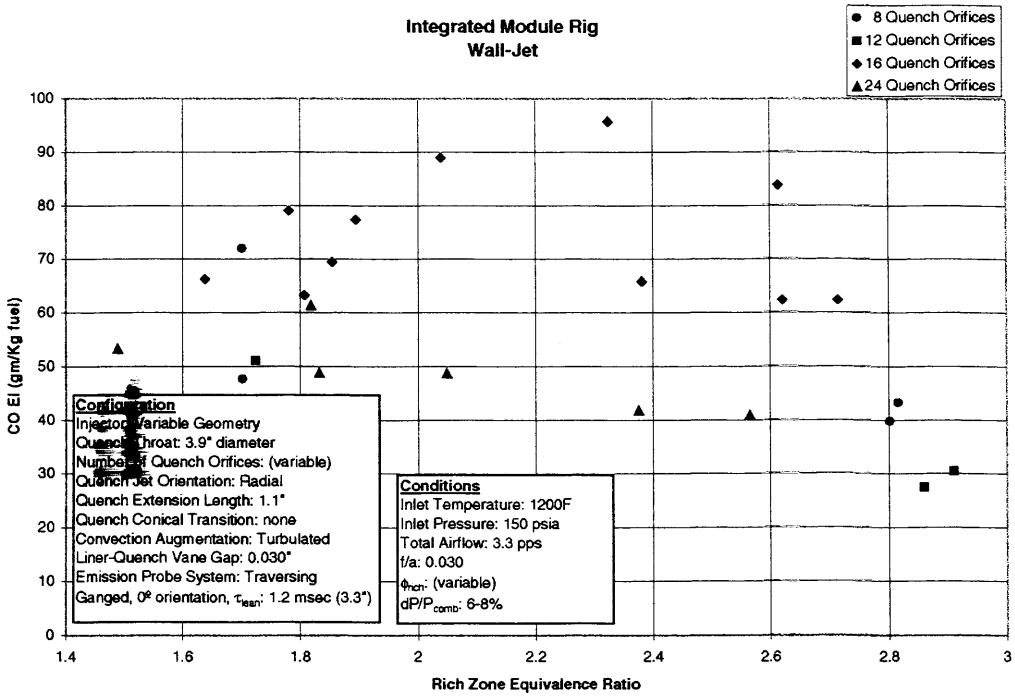

Figure VI - 2 Effect of Number of Quench Vanes on CO Emissions as a Function of Rich Zone Equivalence Ratio

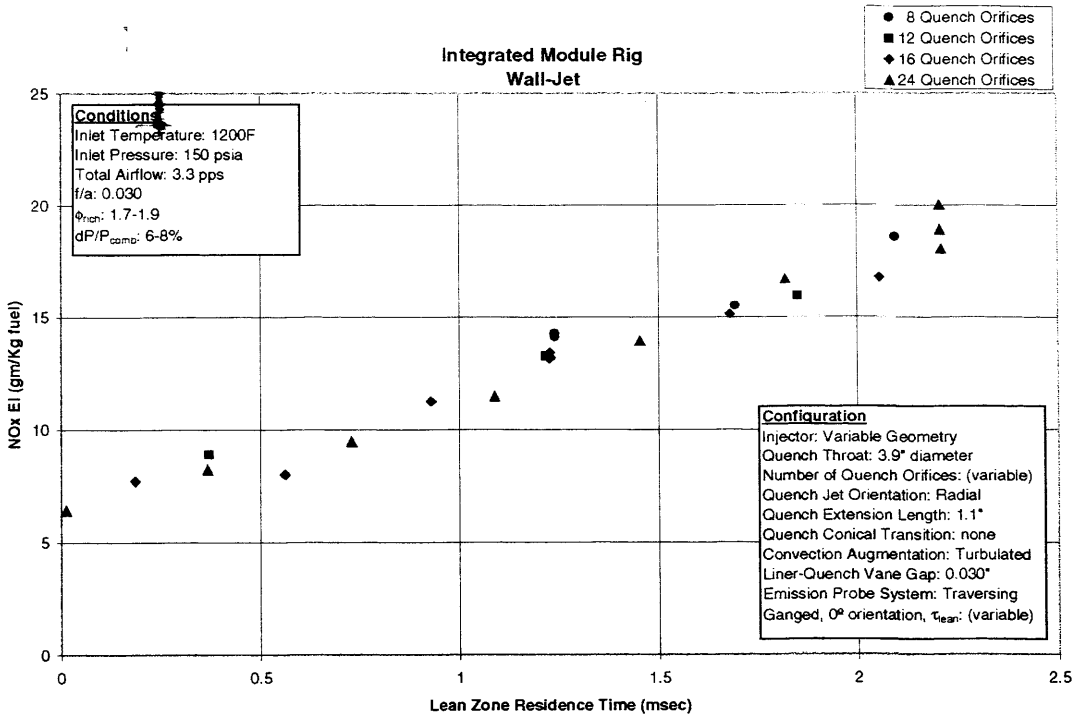

Figure VI - 3 Effect of Number of Quench Vanes on NOx Emissions as a Function of Lean Zone Residence Time

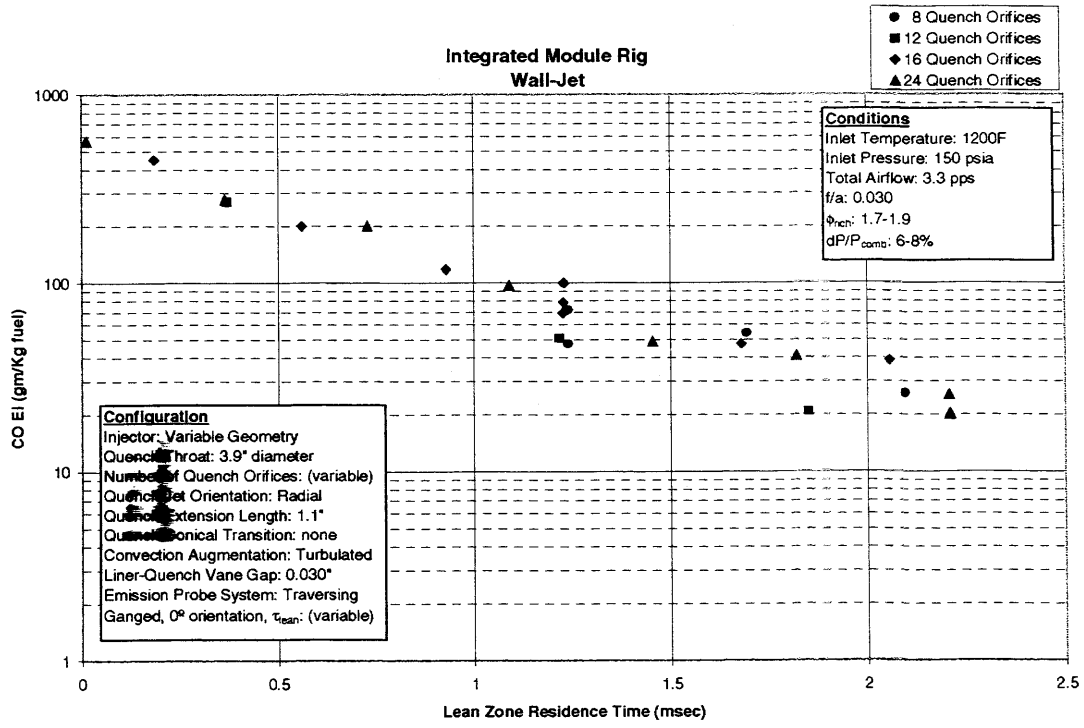

Figure VI - 4 Effect of Number of Quench Vanes on CO Emissions as a Function of Lean Zone Residence Time

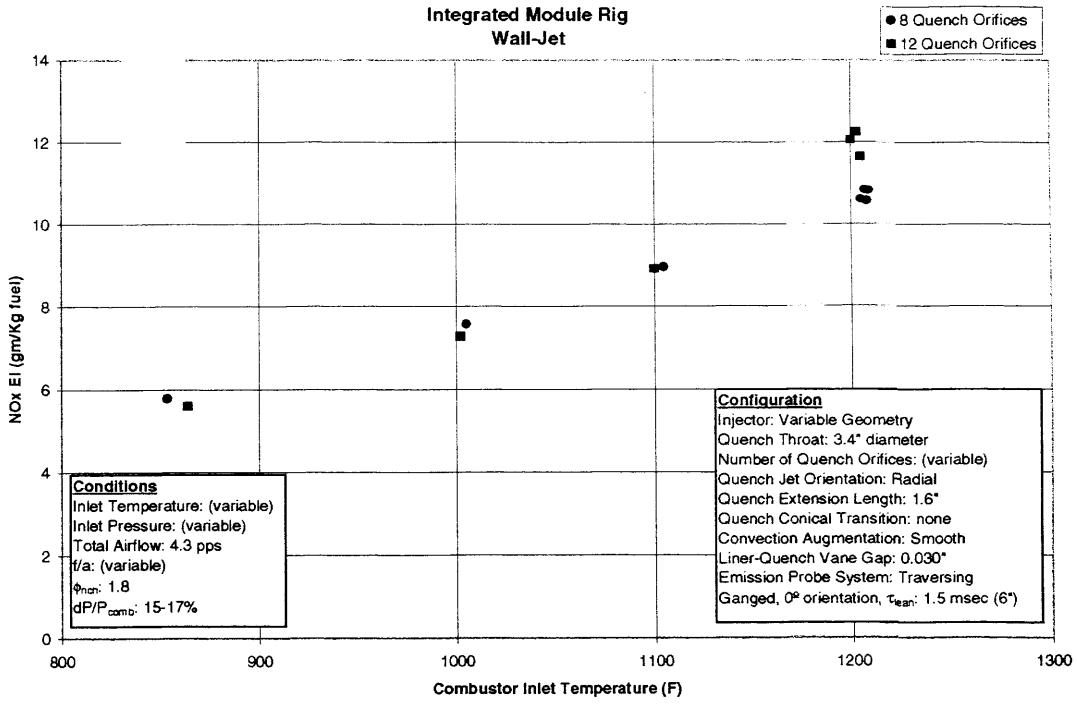

Figure VI - 5 Effect of 8 vs 12 Quench Vanes on NOx Emissions as a Function of Inlet Temperature

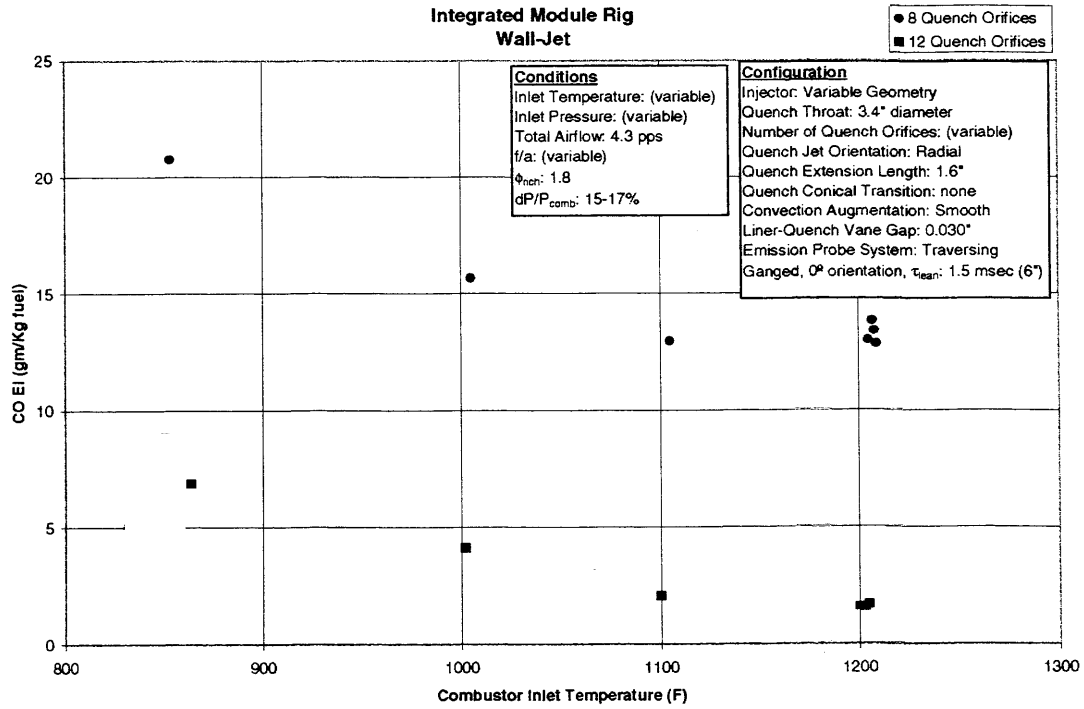

Figure VI - 6 Effect of 8 vs 12 Quench Vanes on CO Emissions as a Function of Inlet Temperature

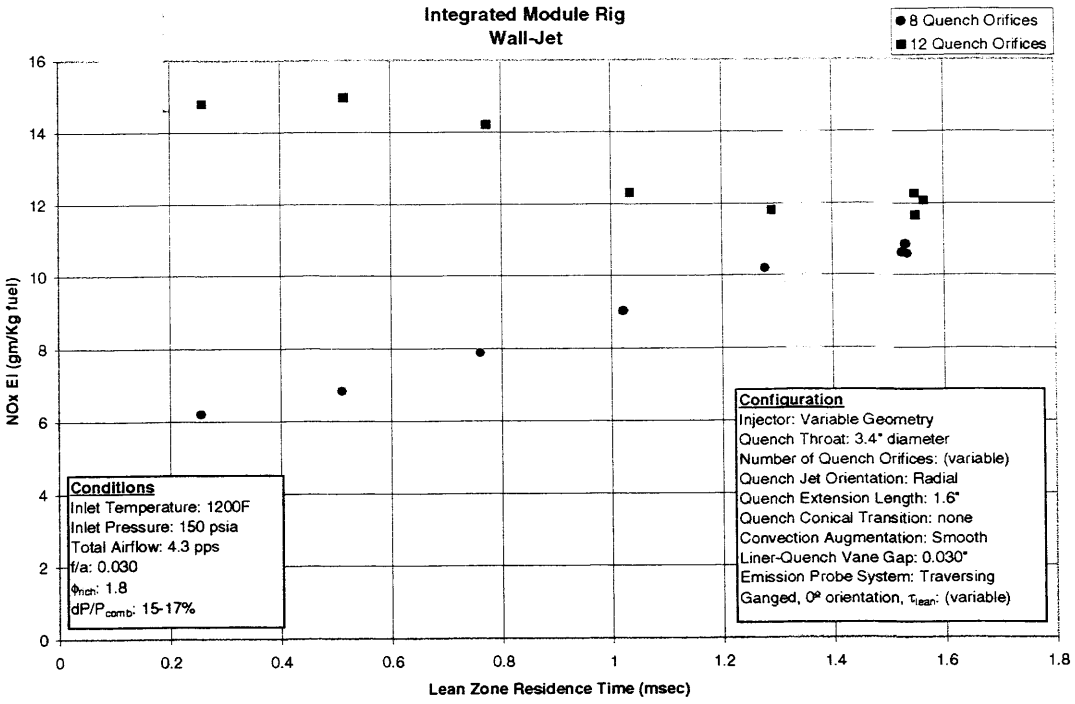

Figure VI - 7 Effect of 8 vs 12 Quench Vanes on NOx Emissions as a Function of Lean Zone Residence Time

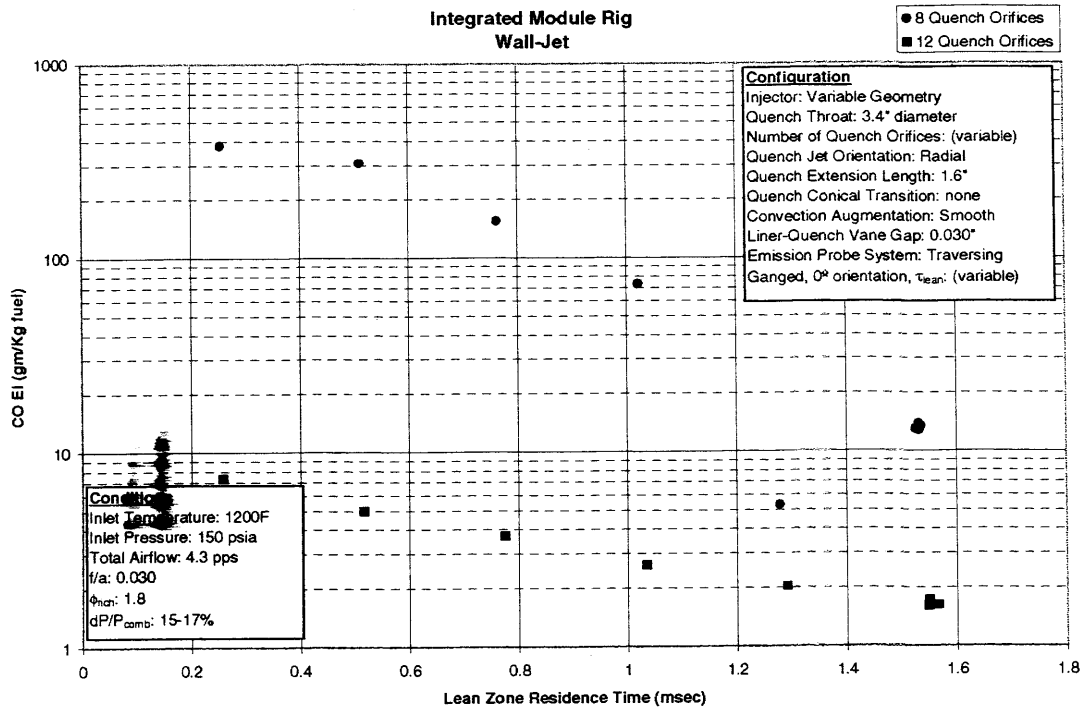

Figure VI - 8 Effect of 8 vs 12 Quench Vanes on CO Emissions as a Function of Lean Zone Residence Time

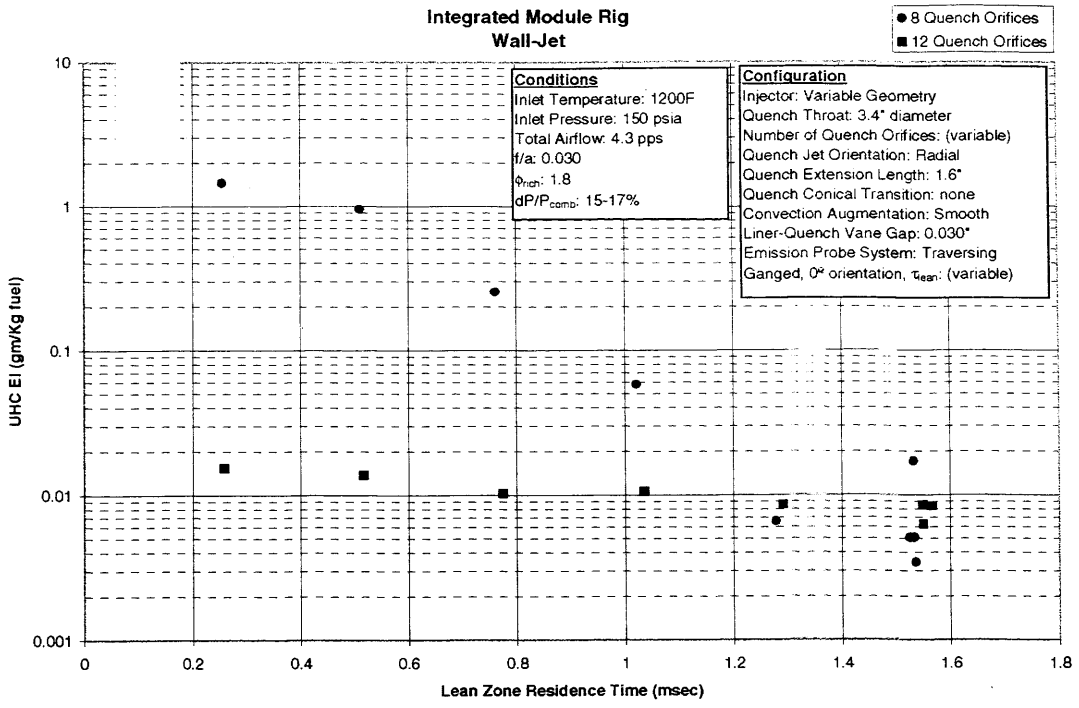

Figure VI - 9 Effect of 8 vs 12 Quench Vanes on UHC Emissions as a Function of Lean Zone Residence Time

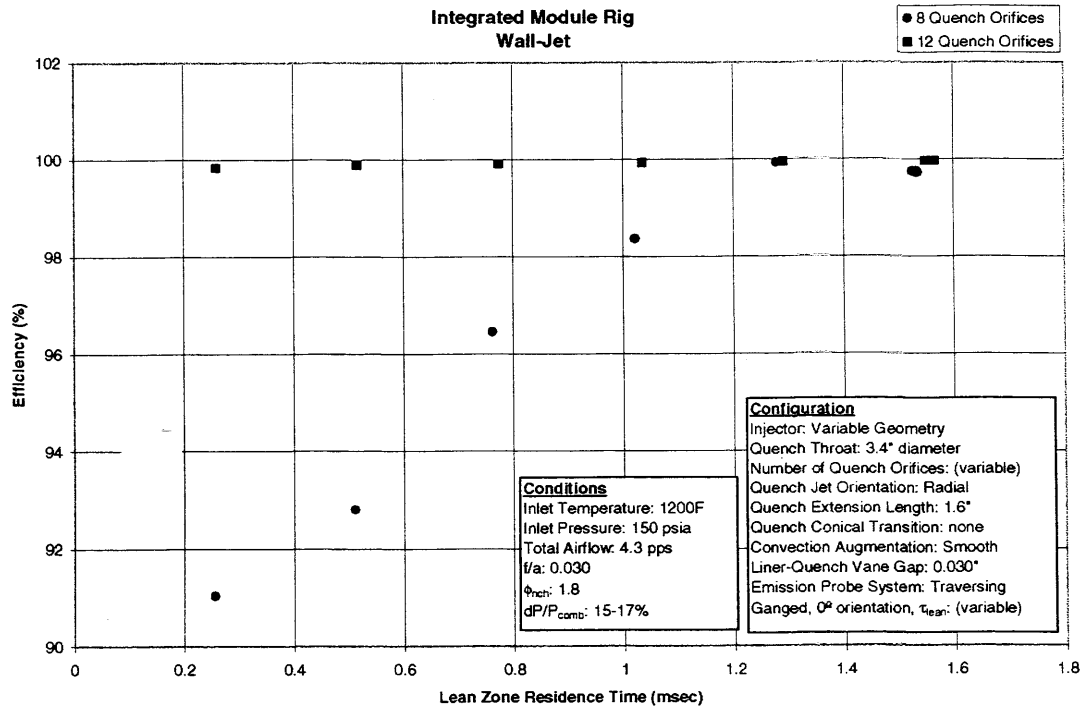

Figure VI - 10 Effect of 8 vs 12 Quench Vanes on Efficiency as a Function of Lean Zone Residence Time

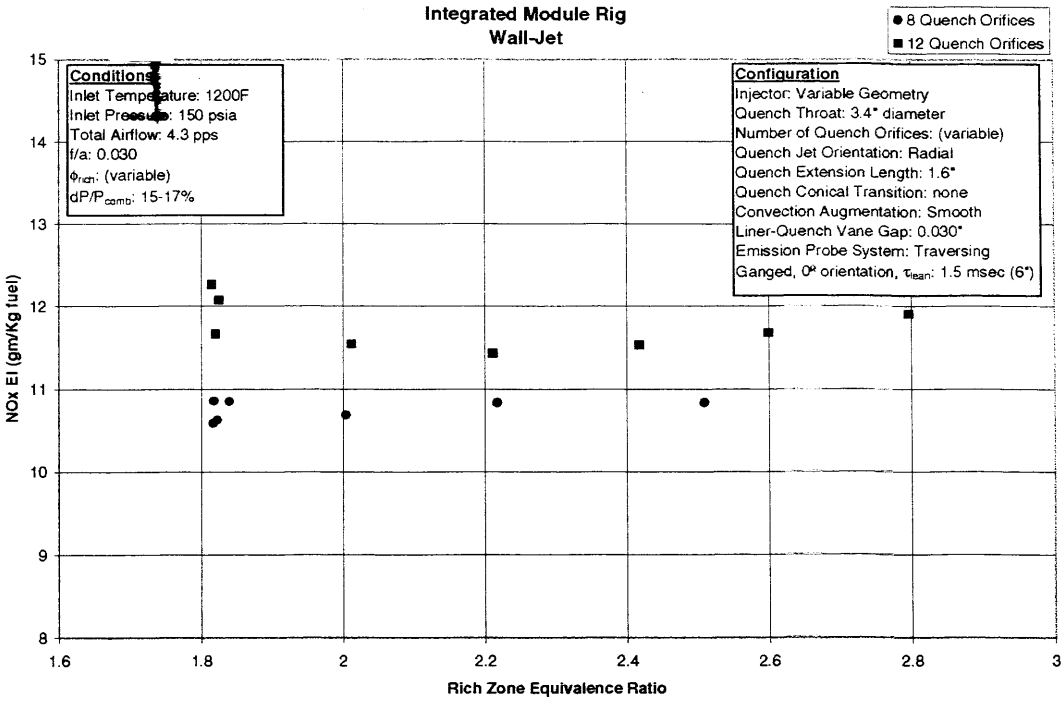

Figure VI - 11 Effect of 8 vs 12 Quench Vanes on NOx Emissions as a Function of Rich Zone Equivalence Ratio

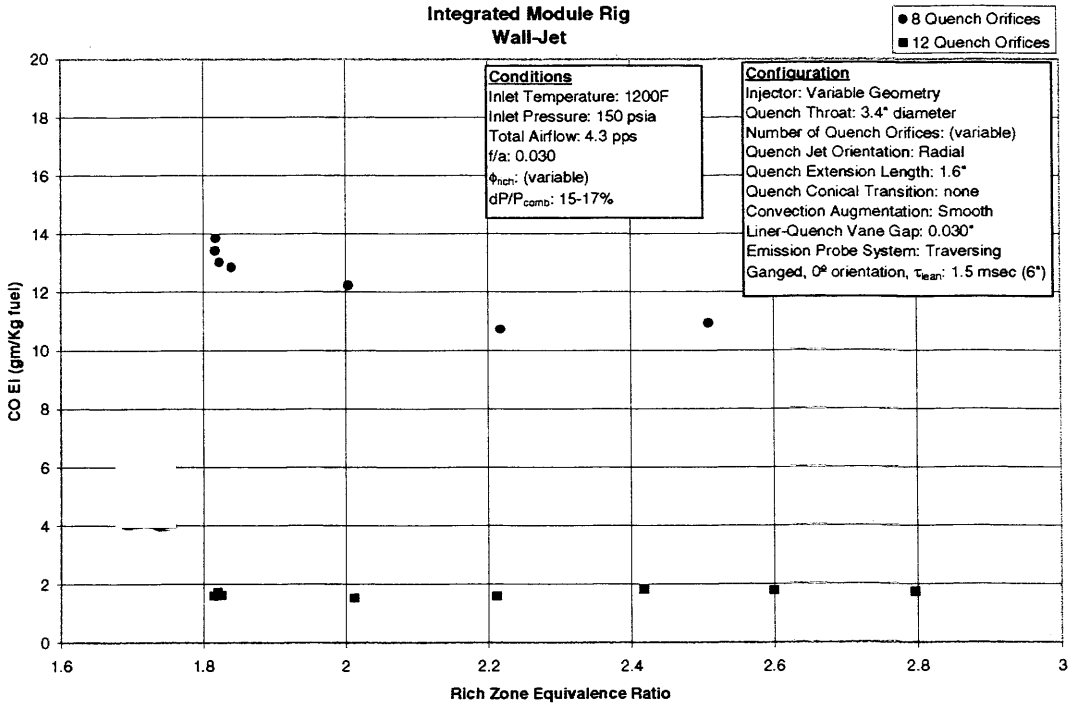

Figure VI - 12 Effect of 8 vs 12 Quench Vanes on CO Emissions as a Function of Rich Zone Equivalence Ratio

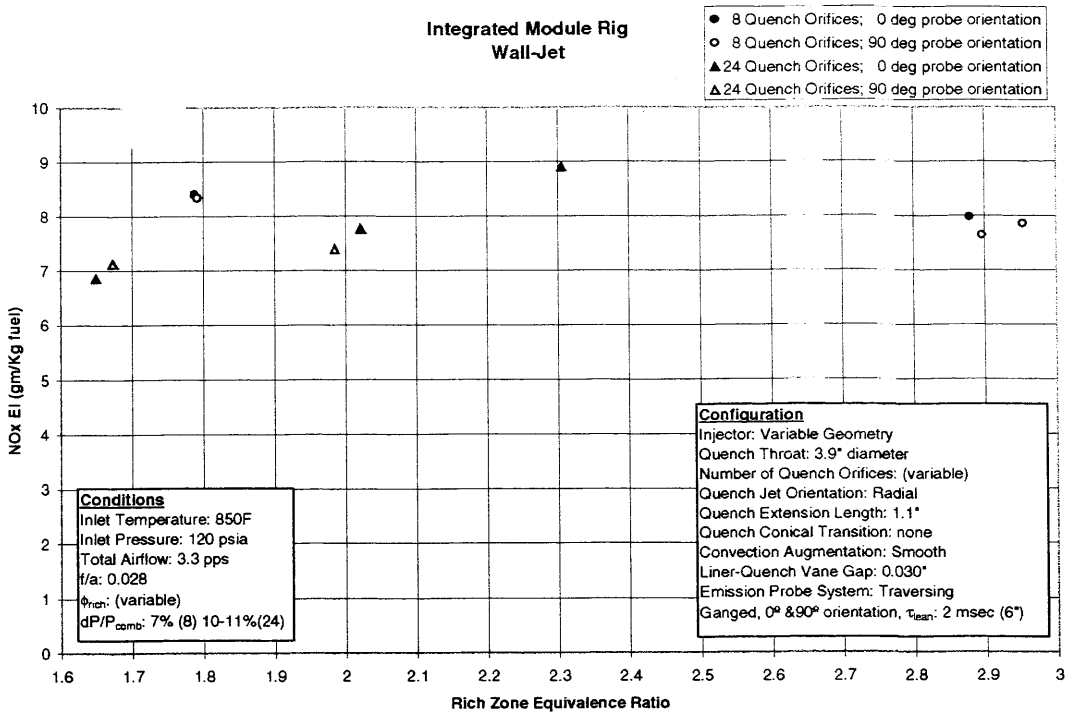

Figure VI - 13 Effect of 8 vs 24 Quench Vanes on NOx Emissions as a Function of Rich Zone Equivalence Ratio

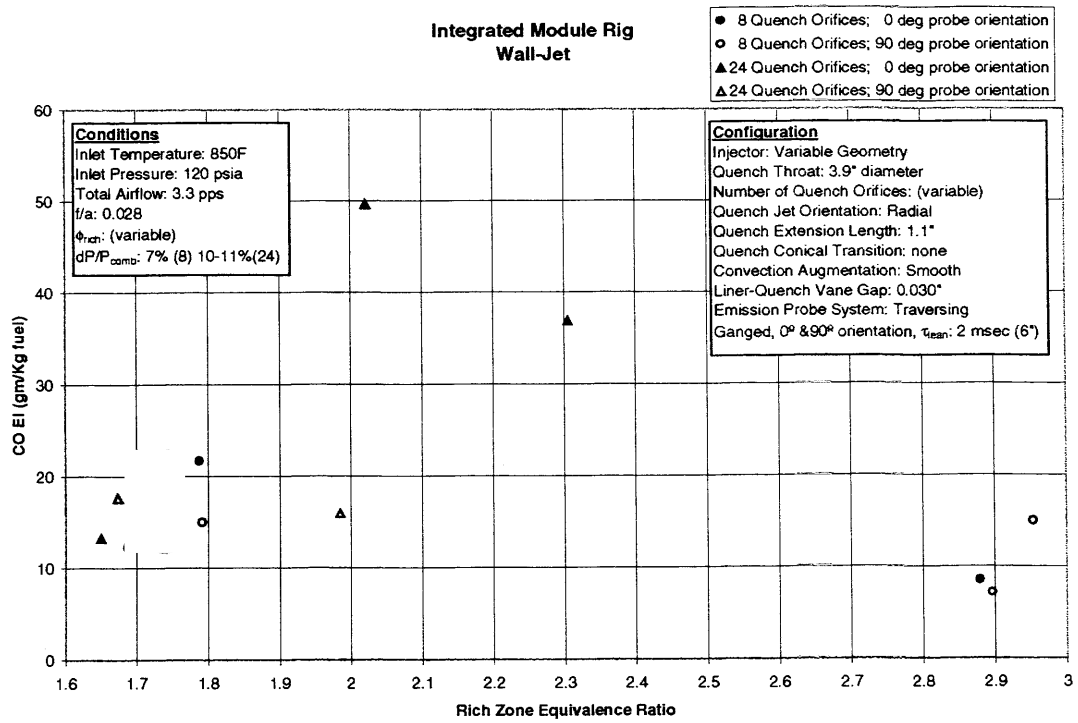

Figure VI - 14 Effect of 8 vs 24 Quench Vanes on CO Emissions as a Function of Rich Zone Equivalence Ratio

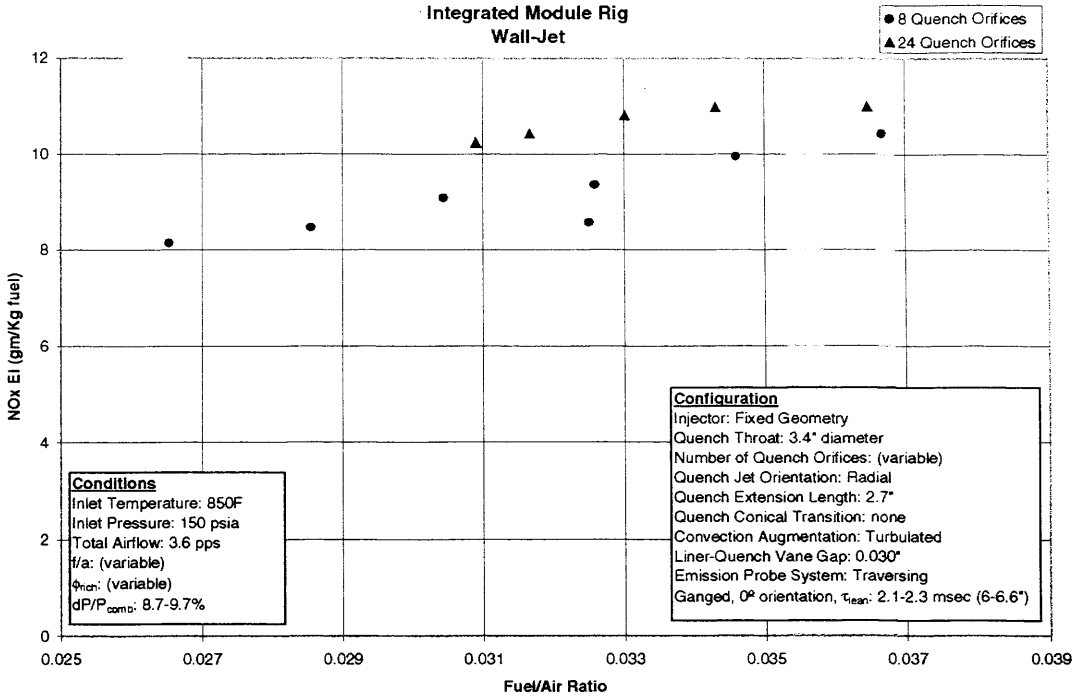

Figure VI - 15 Effect of 8 vs 24 Quench Vanes on NOx Emissions as a Function of Fuel/Air Ratio

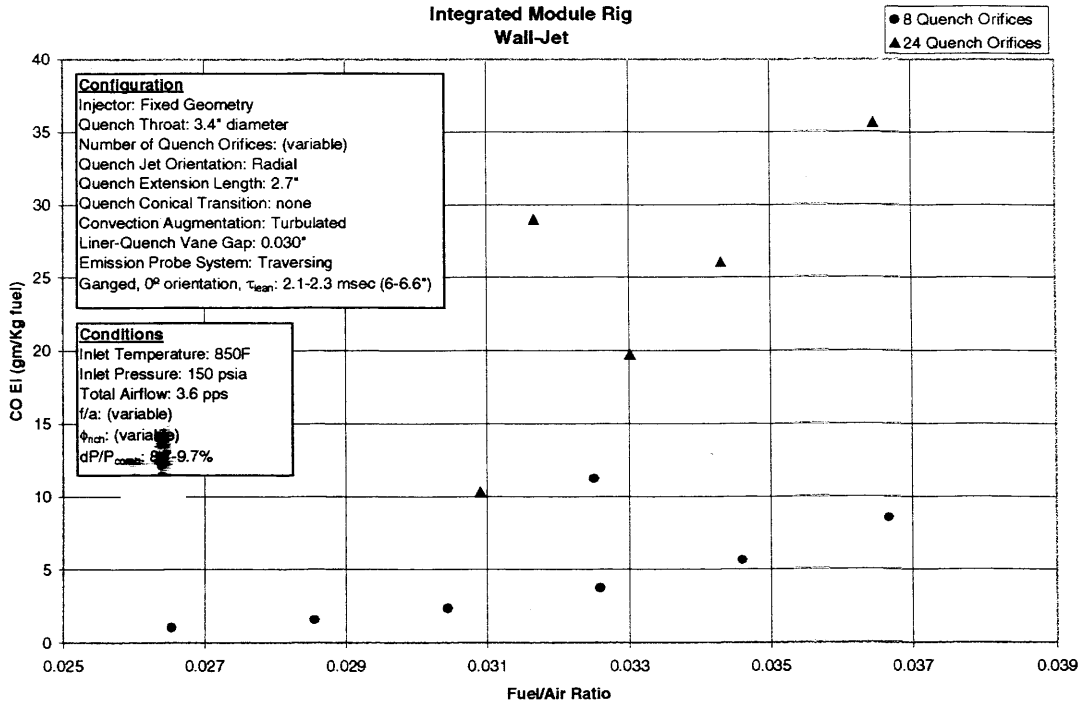

Figure VI - 16 Effect of 8 vs 24 Quench Vanes on CO Emissions as a Function of Fuel/Air Ratio

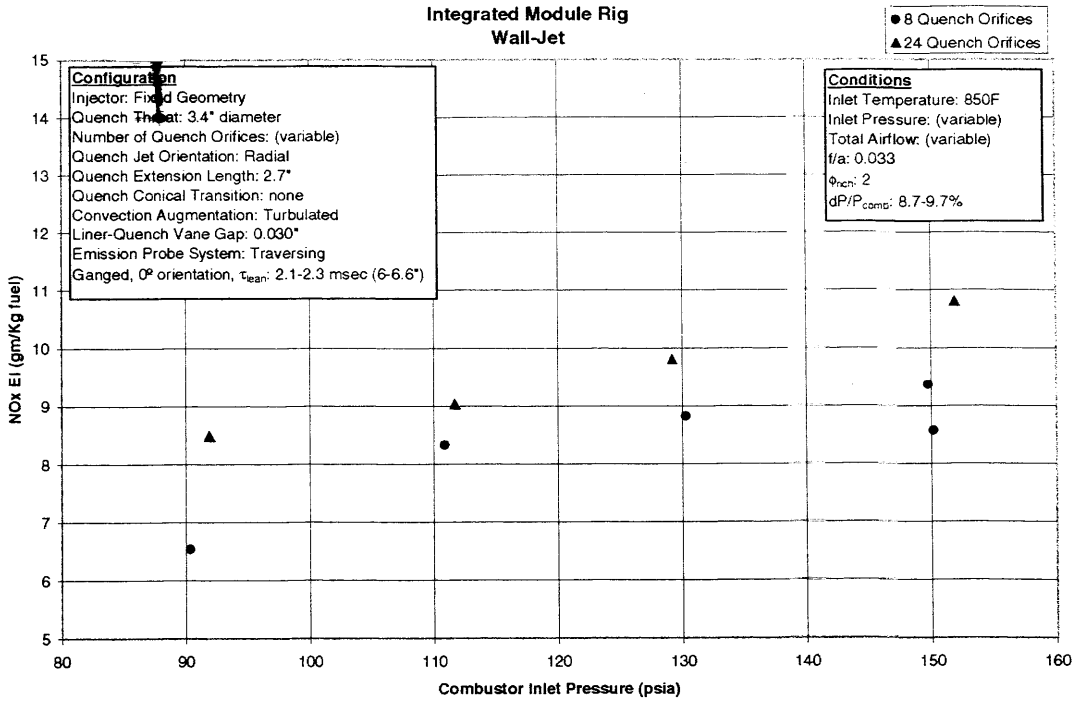

Figure VI - 17 Effect of 8 vs 24 Quench Vanes on NOx Emissions as a Function of Inlet Pressure

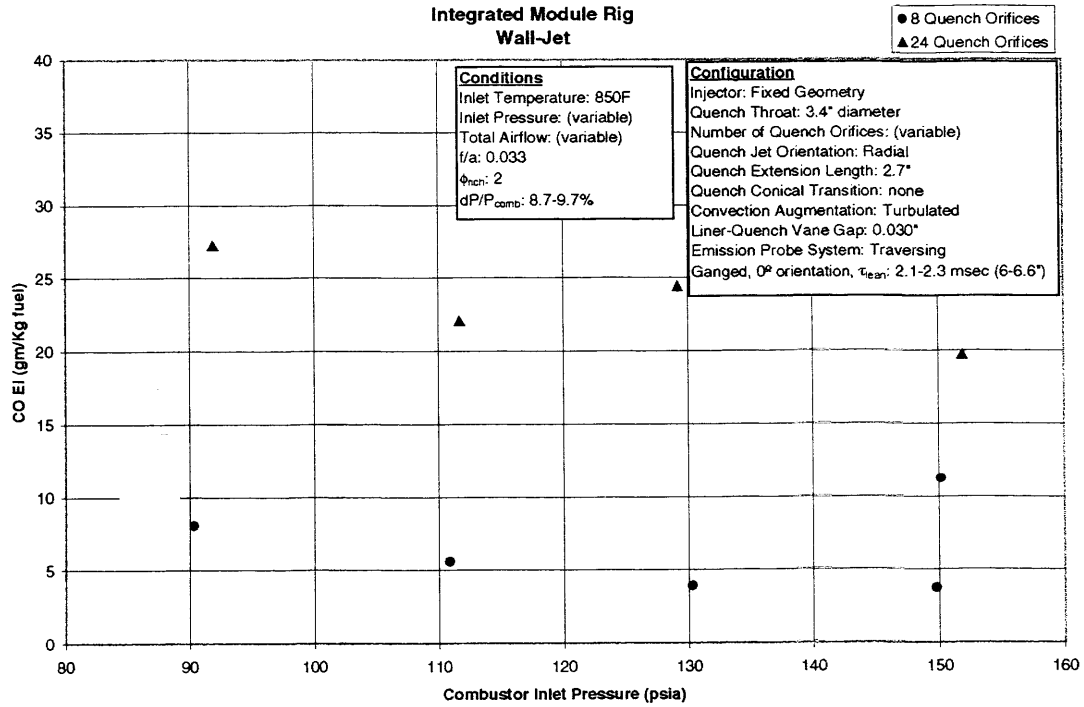

Figure VI - 18 Effect of 8 vs 24 Quench Vanes on CO Emissions as a Function of Inlet Pressure

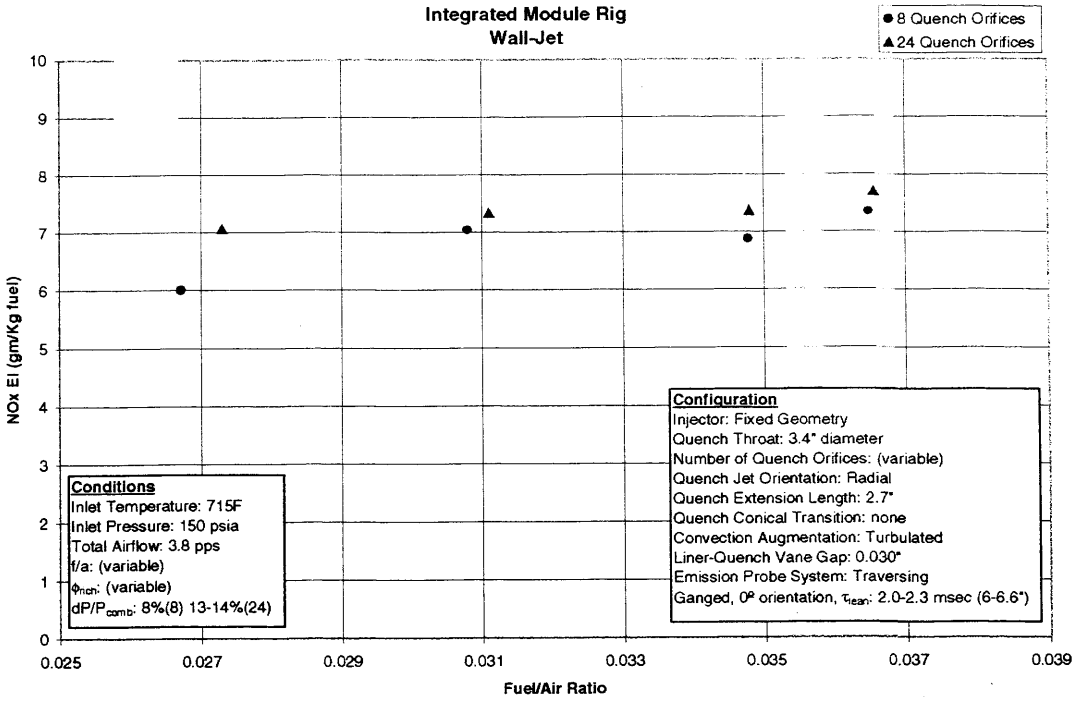

Figure VI - 19 Effect of 8 vs 24 Quench Vanes on NOx Emissions as a Function of Fuel/Air Ratio

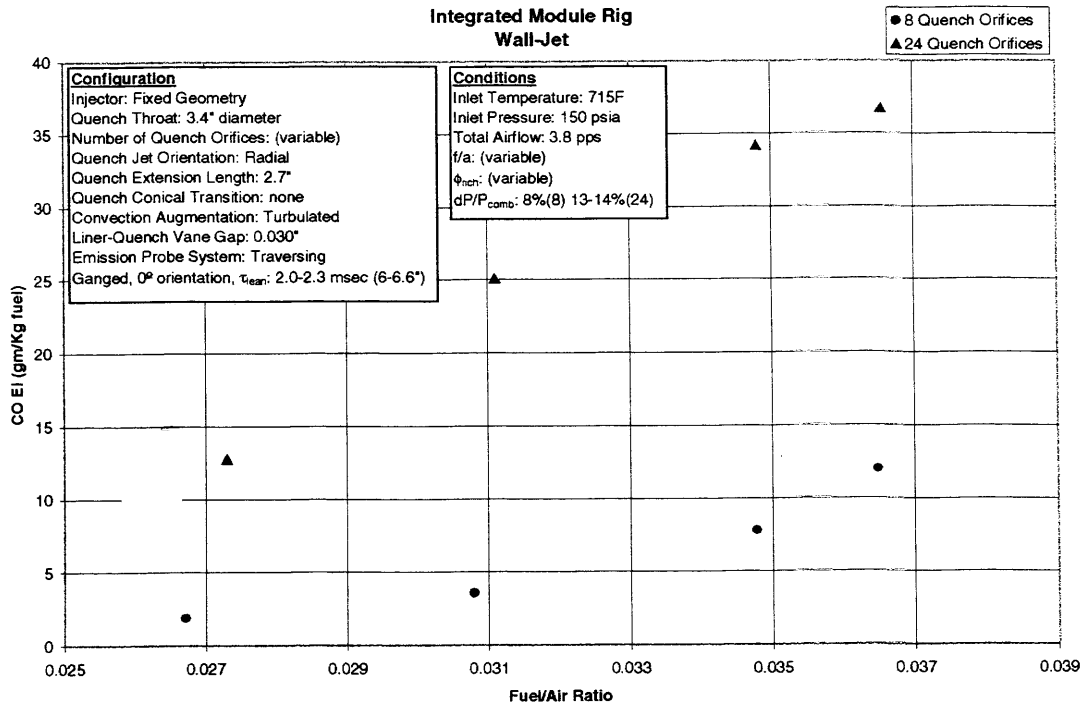

Figure VI - 20 Effect of 8 vs 24 Quench Vanes on CO Emissions as a Function of Fuel/Air Ratio

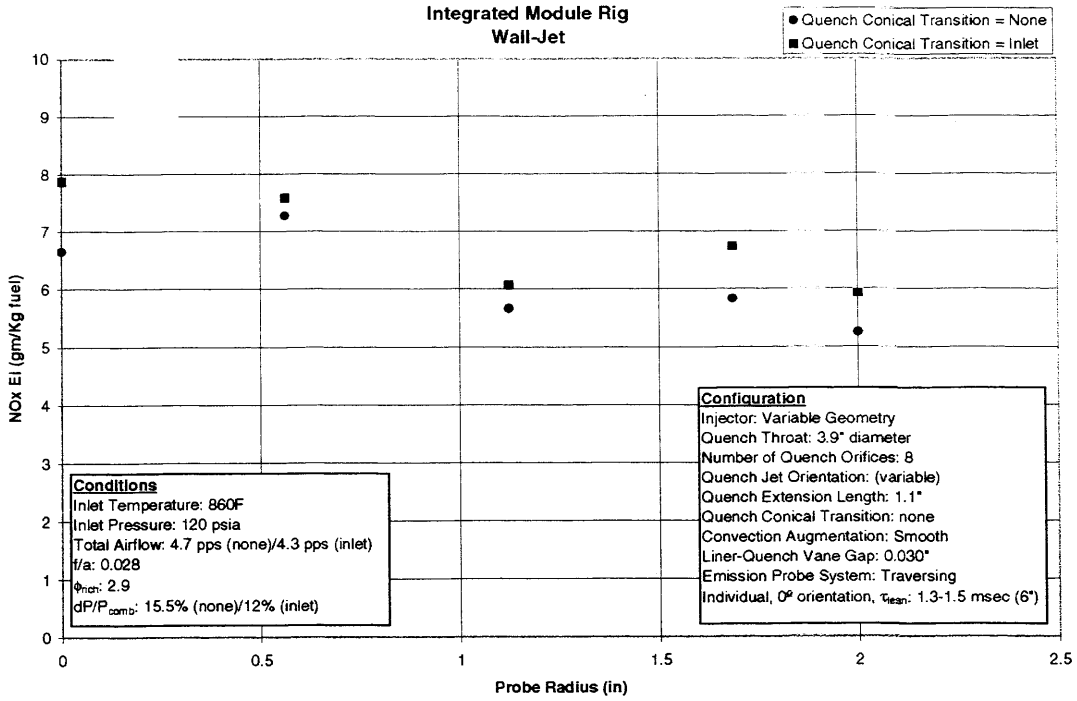

Figure VI - 21 Effect of Inlet Geometry to Quench Region on NOx Emissions as a Function of Probe Radius

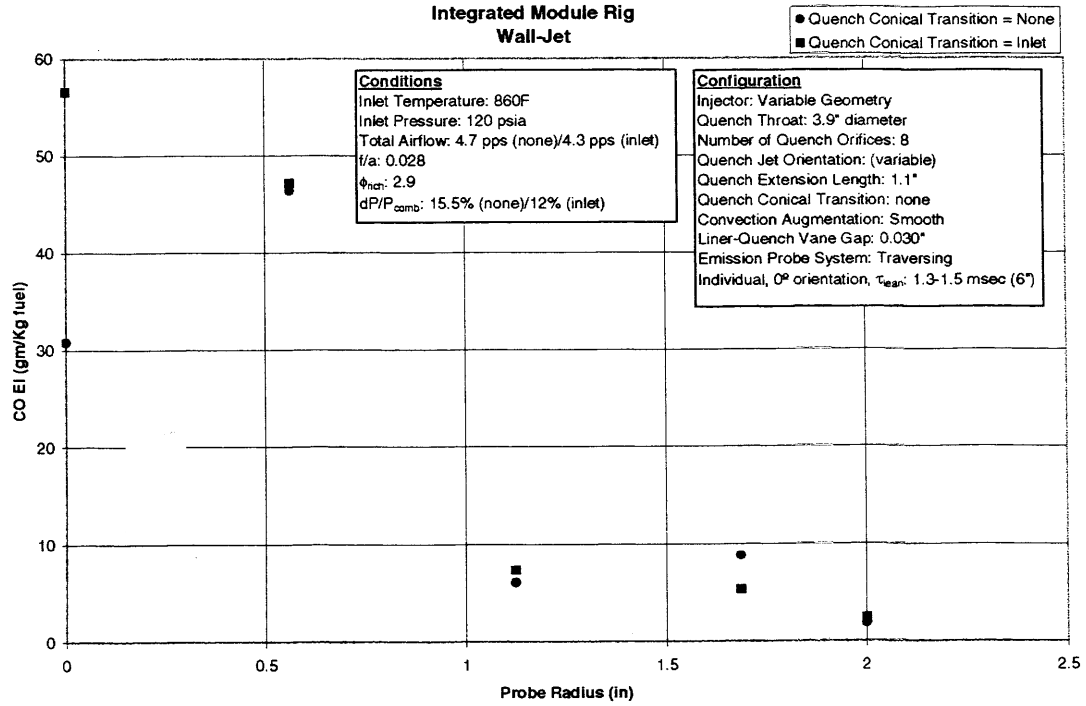

Figure VI - 22 Effect of Inlet Geometry to Quench Region on CO Emissions as a Function of Probe Radius

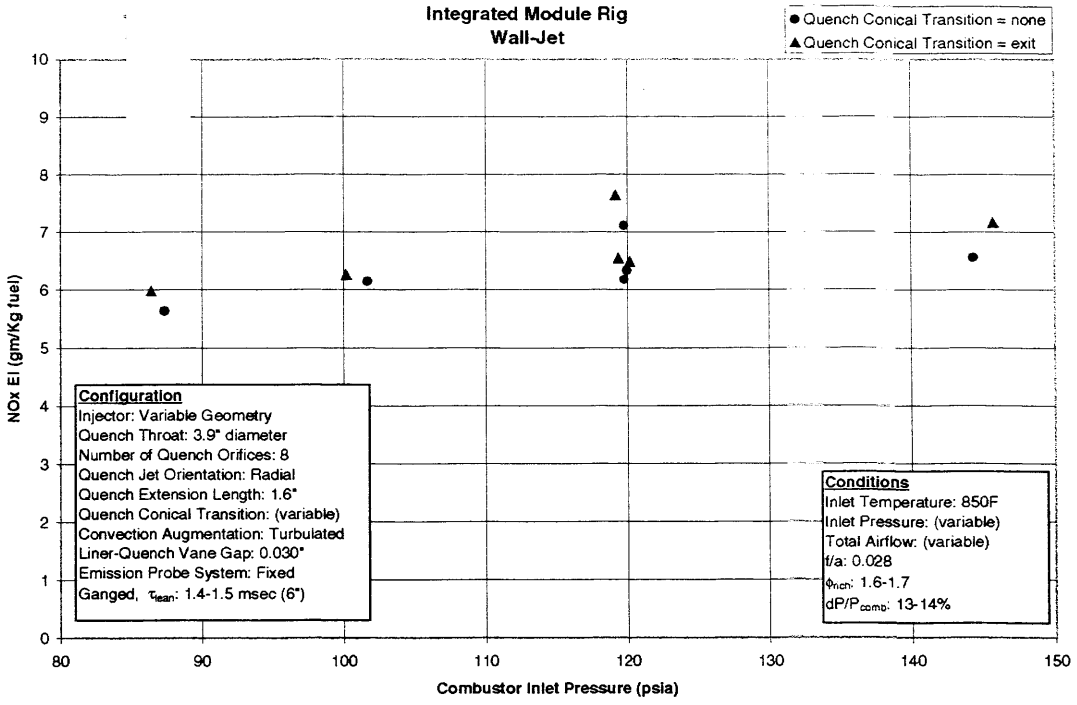

Figure VI - 23 Effect of Exit Geometry from Quench Region on NOx Emissions as a Function of Inlet Pressure

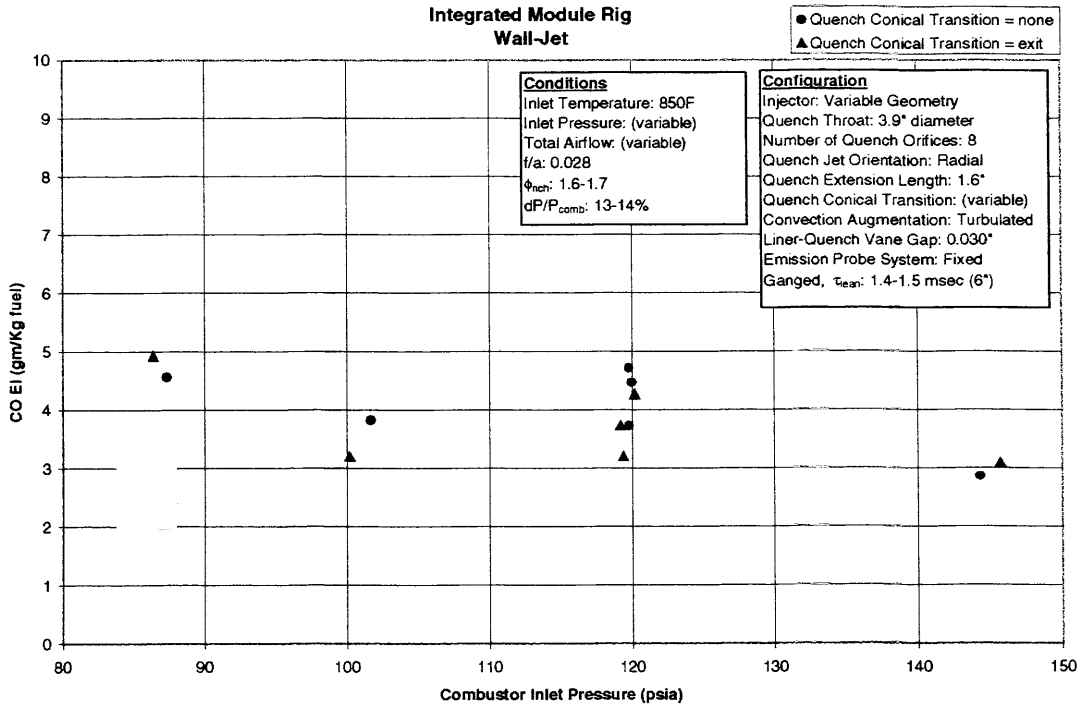

Figure VI - 24 Effect of Exit Geometry from Quench Region on CO Emissions as a Function of Inlet Pressure

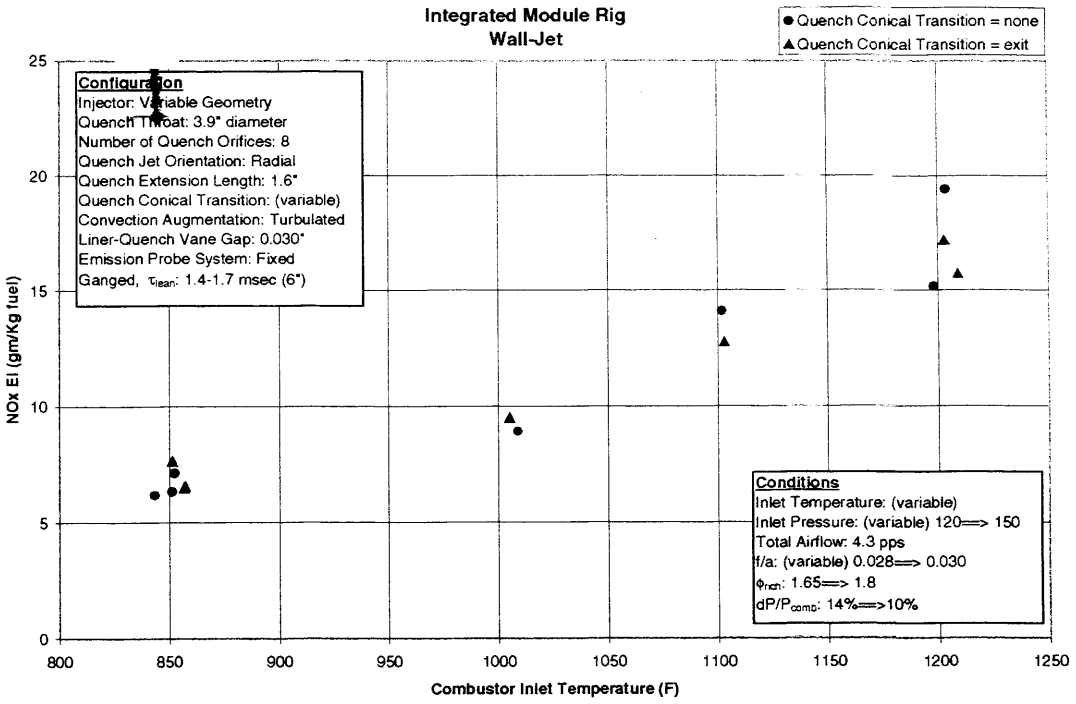

Figure VI - 25 Effect of Exit Geometry from Quench Region on NOx Emissions as a Function of Inlet Temperature

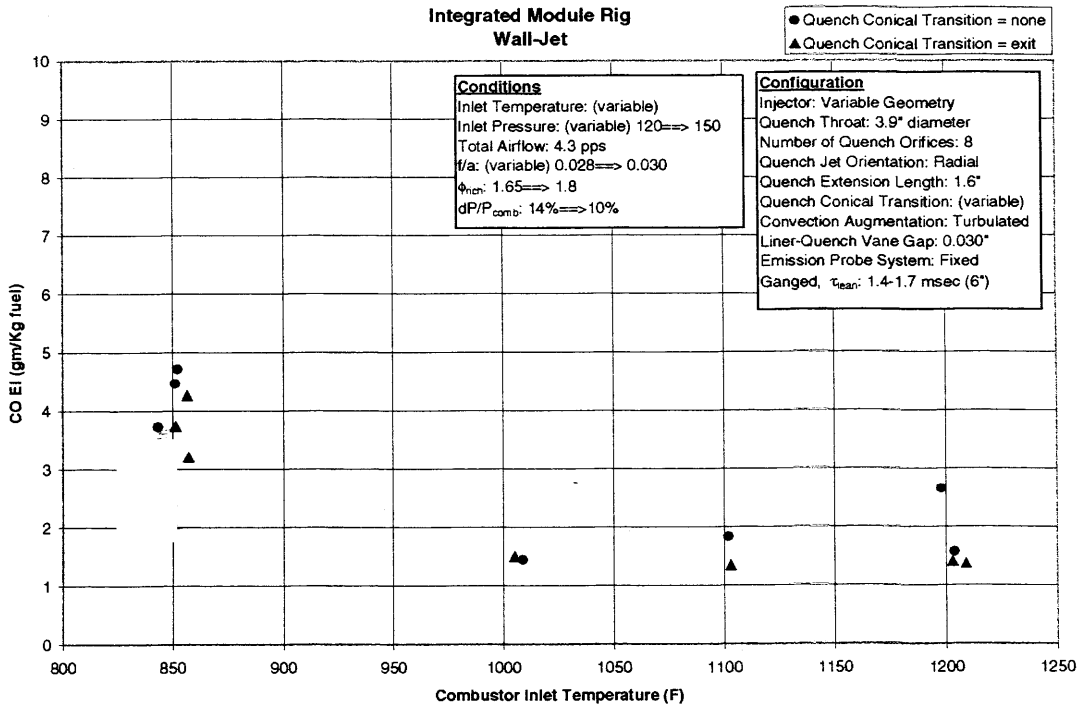

Figure VI - 26 Effect of Exit Geometry from Quench Region on CO Emissions as a Function of Inlet Temperature

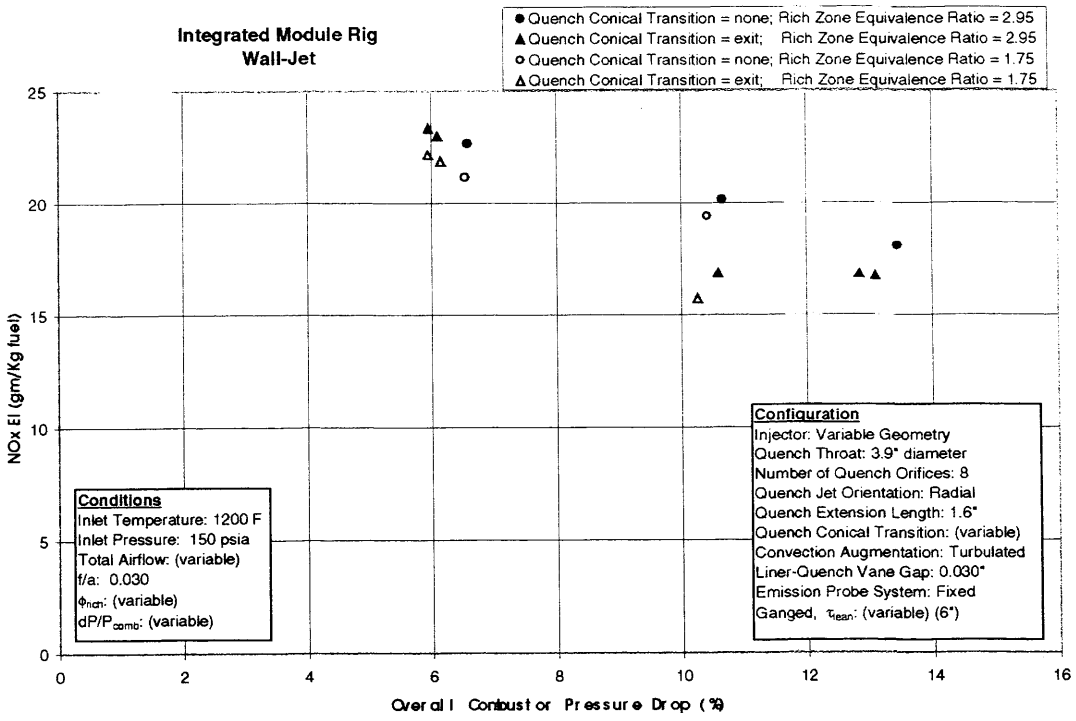

Figure VI - 27 Effect of Exit Geometry from Quench Region on NOx Emissions as a Function of Combustor Pressure Drop and Rich Zone Equivalence Ratio

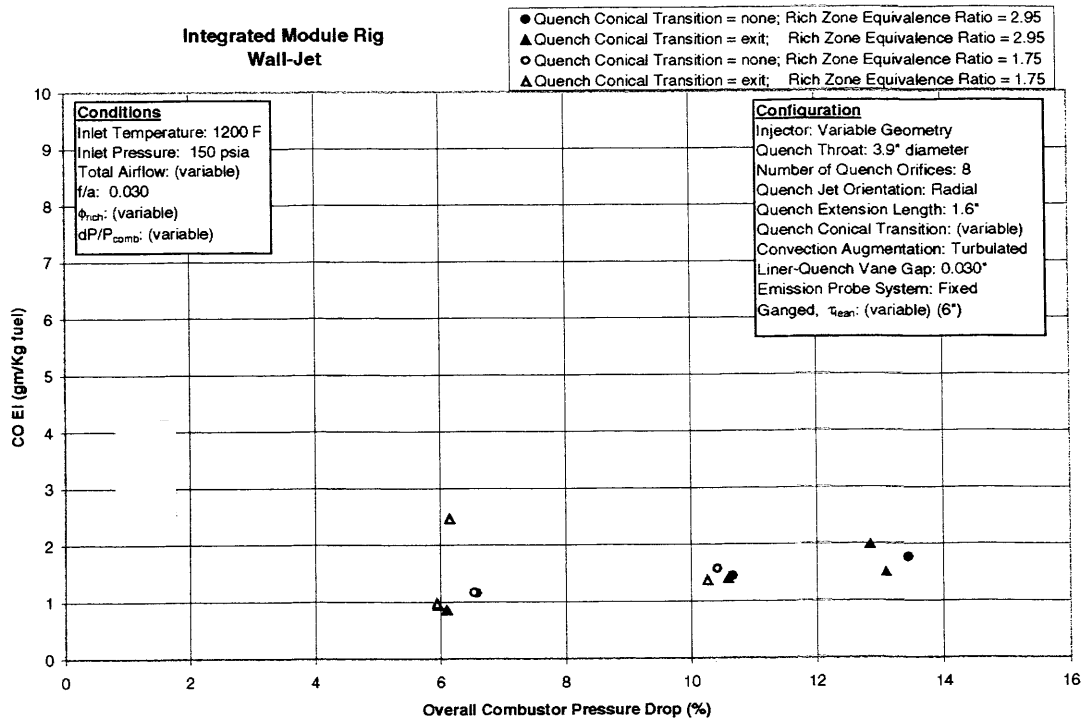

Figure VI - 28 Effect of Exit Geometry from Quench Region on CO Emissions as a Function of Combustor Pressure Drop and Rich Zone Equivalence Ratio

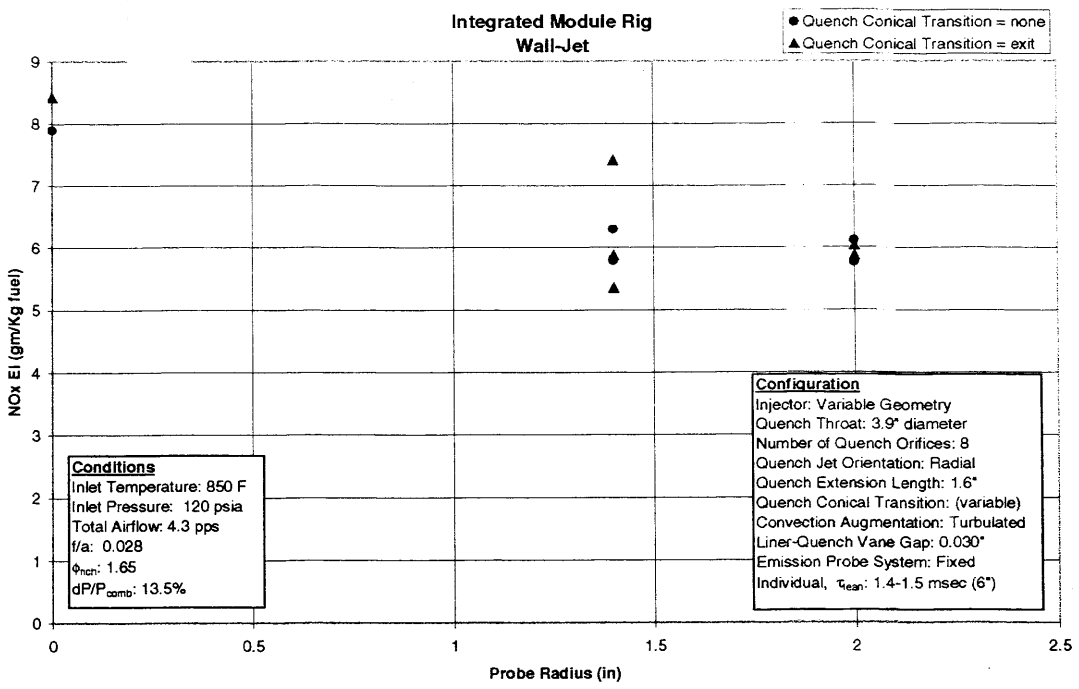

Figure VI - 29 Effect of Exit Geometry from Quench Region on NOx Emissions as a Function of Radial Location

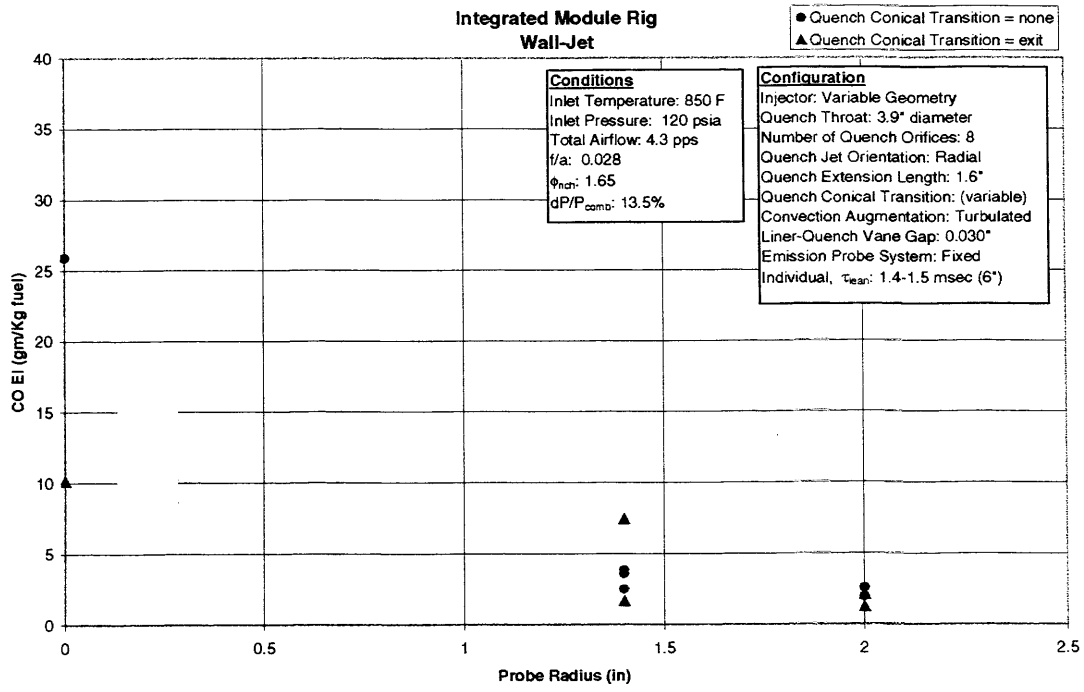

Figure VI - 30 Effect of Exit Geometry from Quench Region on CO Emissions as a Function of Radial Location

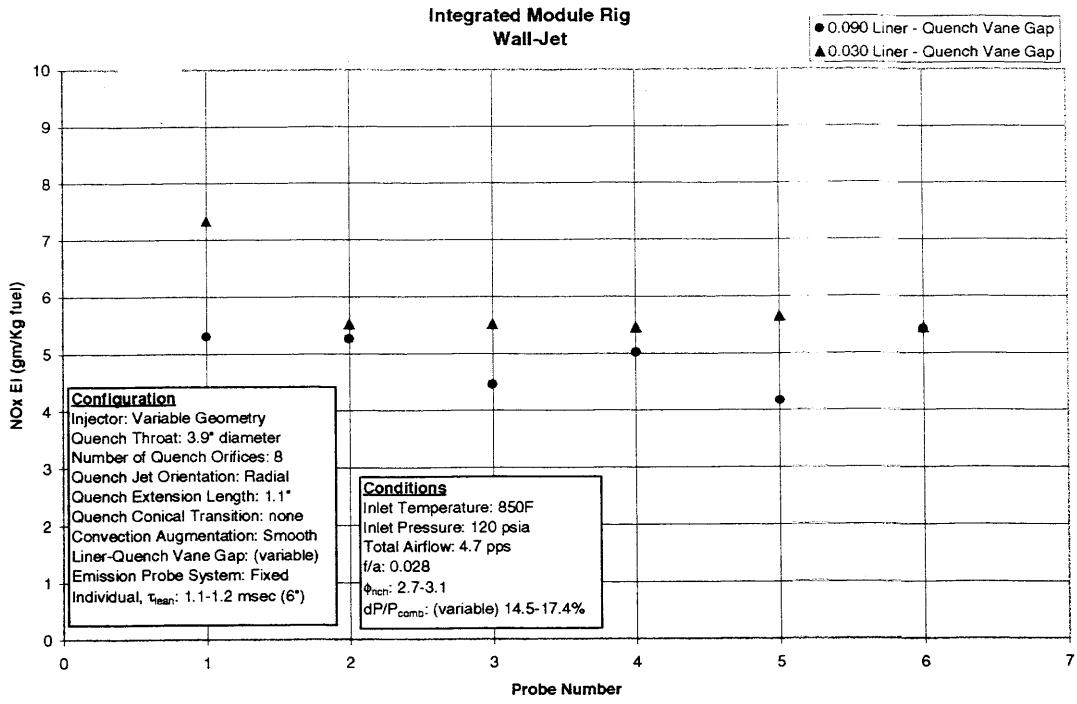

Figure VI - 31 Effect of Gap Between Rich Zone Liner and Quench Vanes on NOx Emissions as a Function of Probe Location

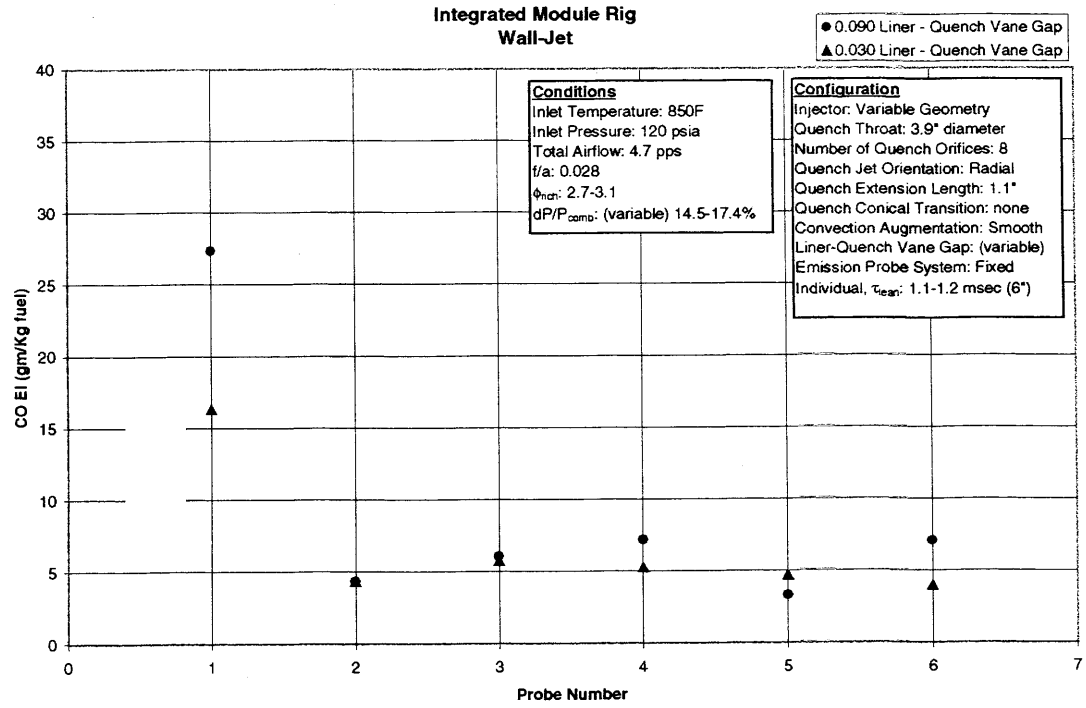

Figure VI - 32 Effect of Gap Between Rich Zone Liner and Quench Vanes on CO Emissions as a Function of Probe Location

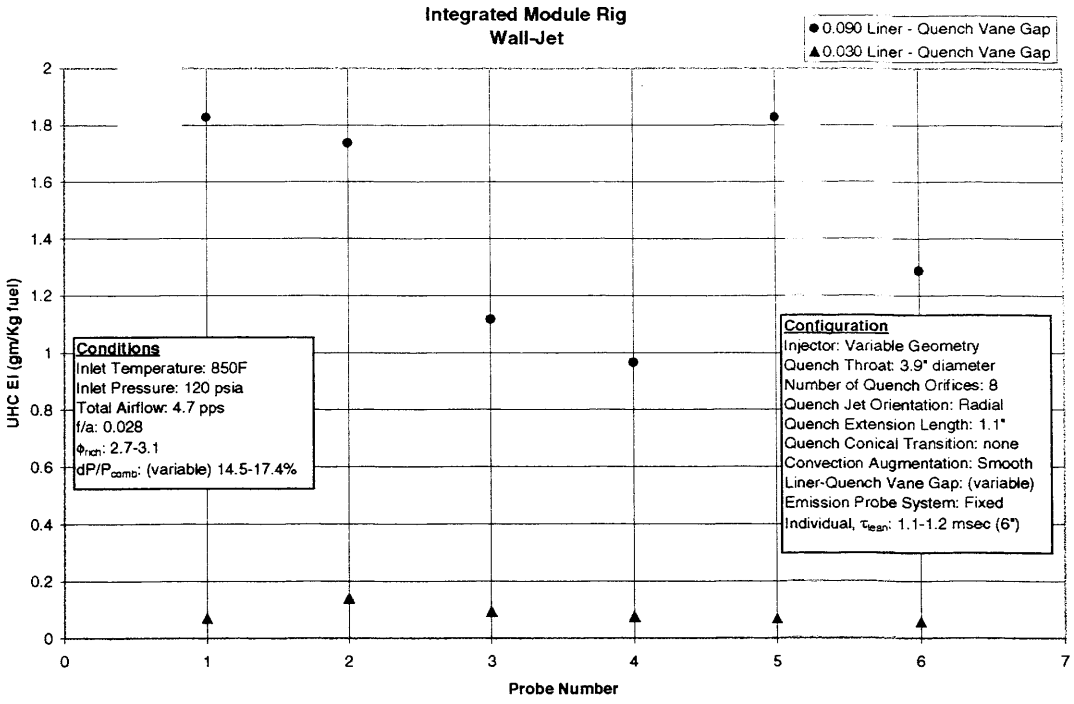

Figure VI - 33 Effect of Gap Between Rich Zone Liner and Quench Vanes on UHC Emissions as a Function of Probe Location

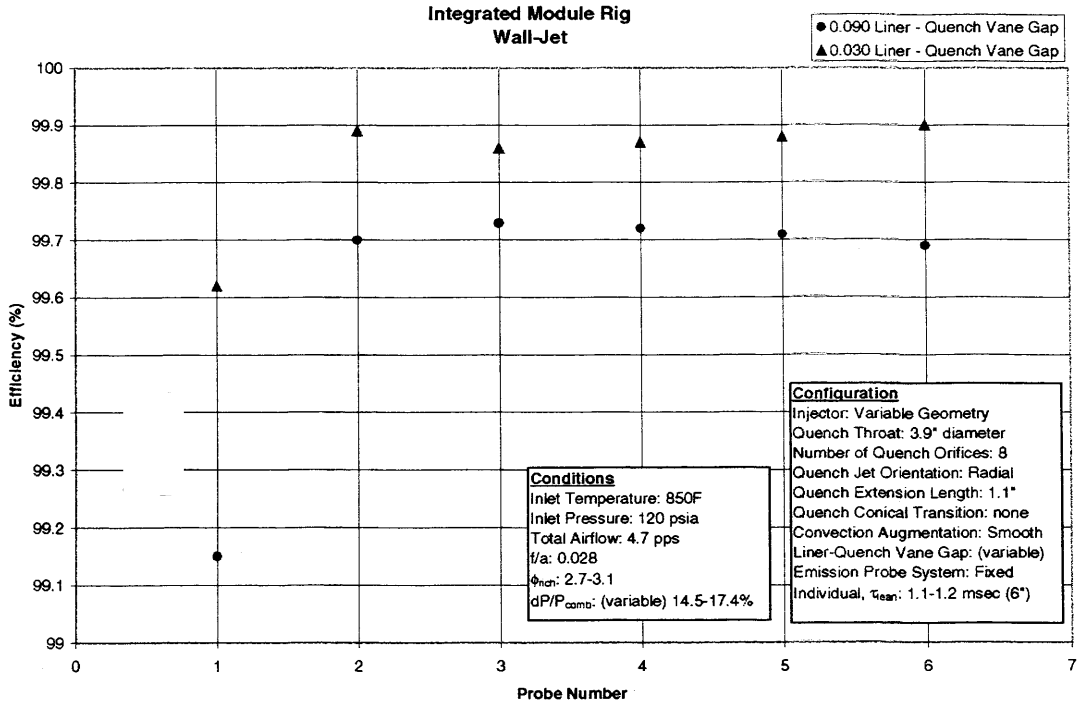

Figure VI - 34 Effect of Gap Between Rich Zone Liner and Quench Vanes on Efficiency as a Function of Probe Location

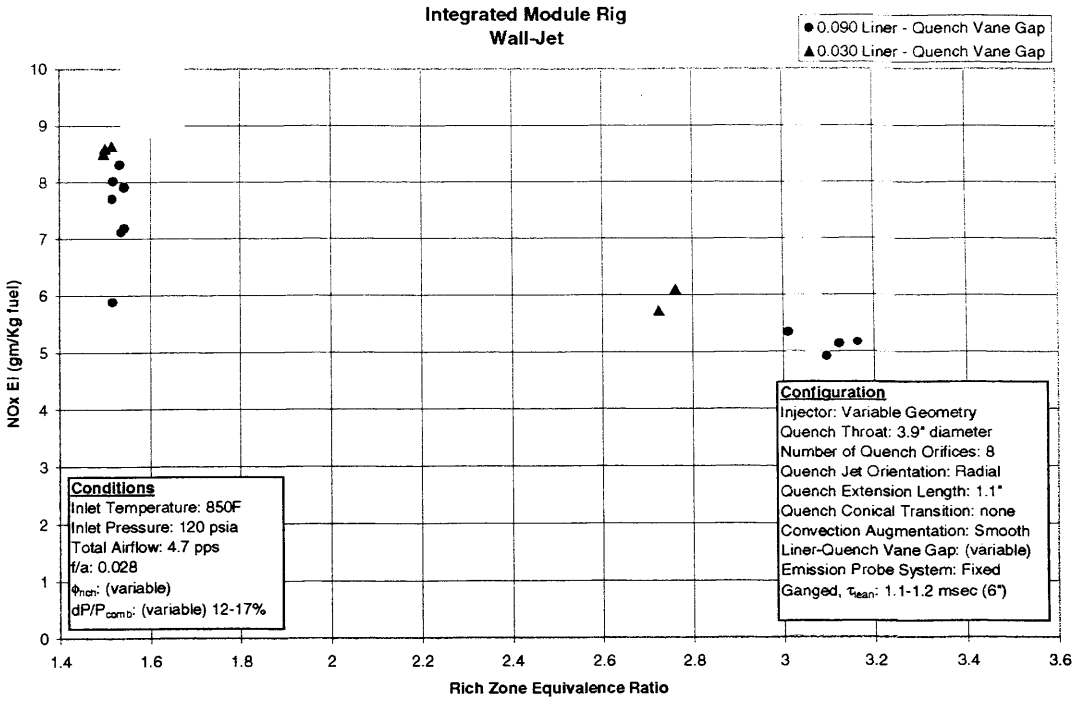

Figure VI - 35 Effect of Gap Between Rich Zone Liner and Quench Vanes on NOx Emissions as a Function of Rich Zone Equivalence Ratio

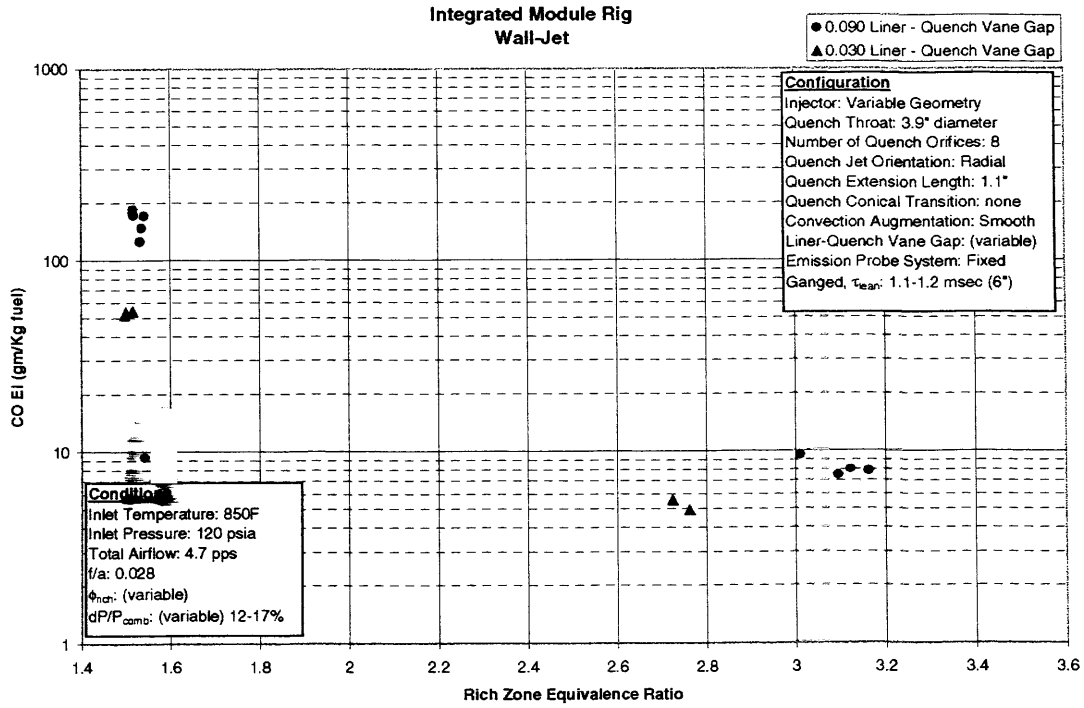

Figure VI - 36 Effect of Gap Between Rich Zone Liner and Quench Vanes on CO Emissions as a Function of Rich Zone Equivalence Ratio

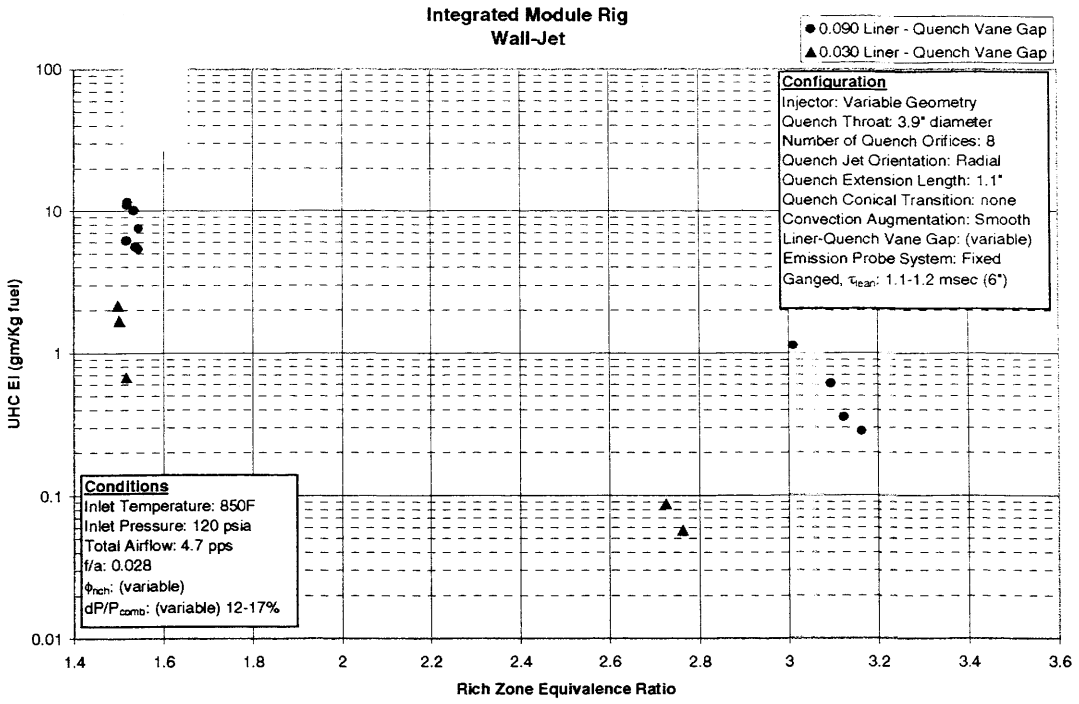

Figure VI - 37 Effect of Gap Between Rich Zone Liner and Quench Vanes on UHC Emissions as a Function of Rich Zone Equivalence Ratio

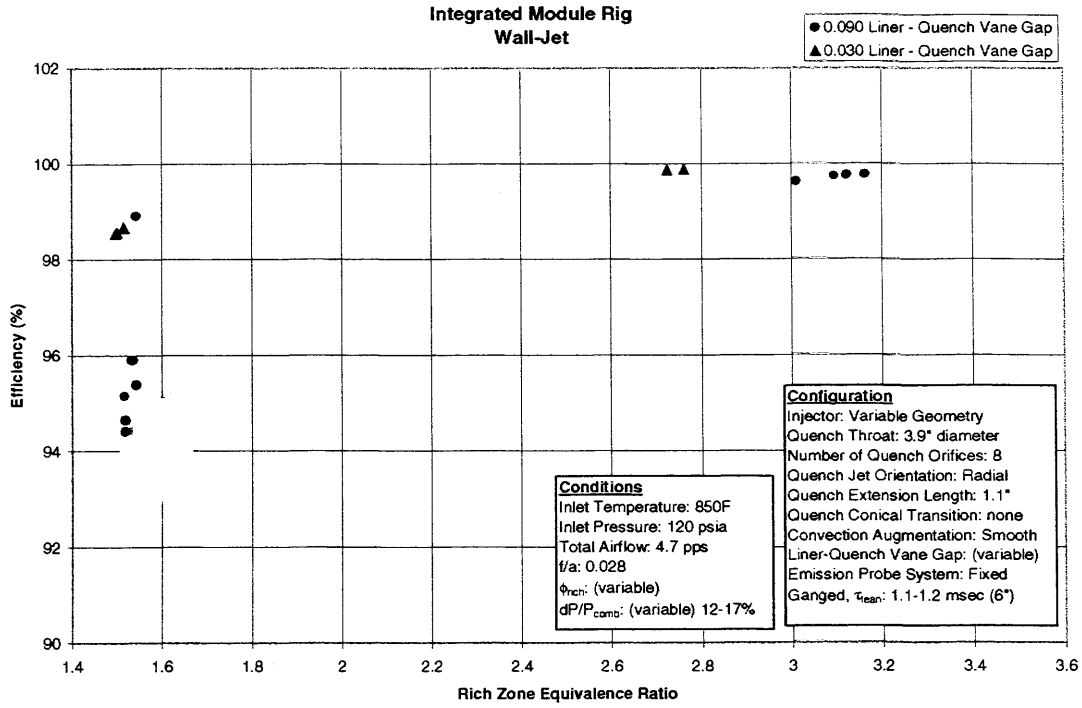

Figure VI - 38 Effect of Gap Between Rich Zone Liner and Quench Vanes on Efficiency as a Function of Rich Zone Equivalence Ratio

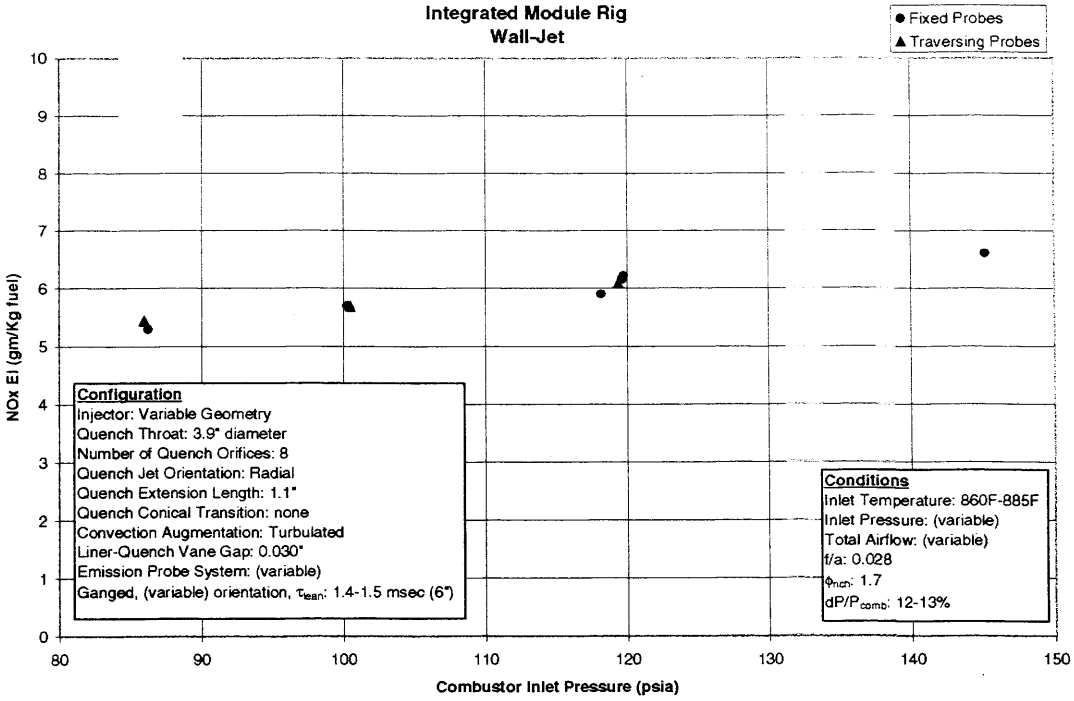

Figure VI - 39 Effect of Emissions Probe System on NOx Emissions as a Function of Inlet Pressure

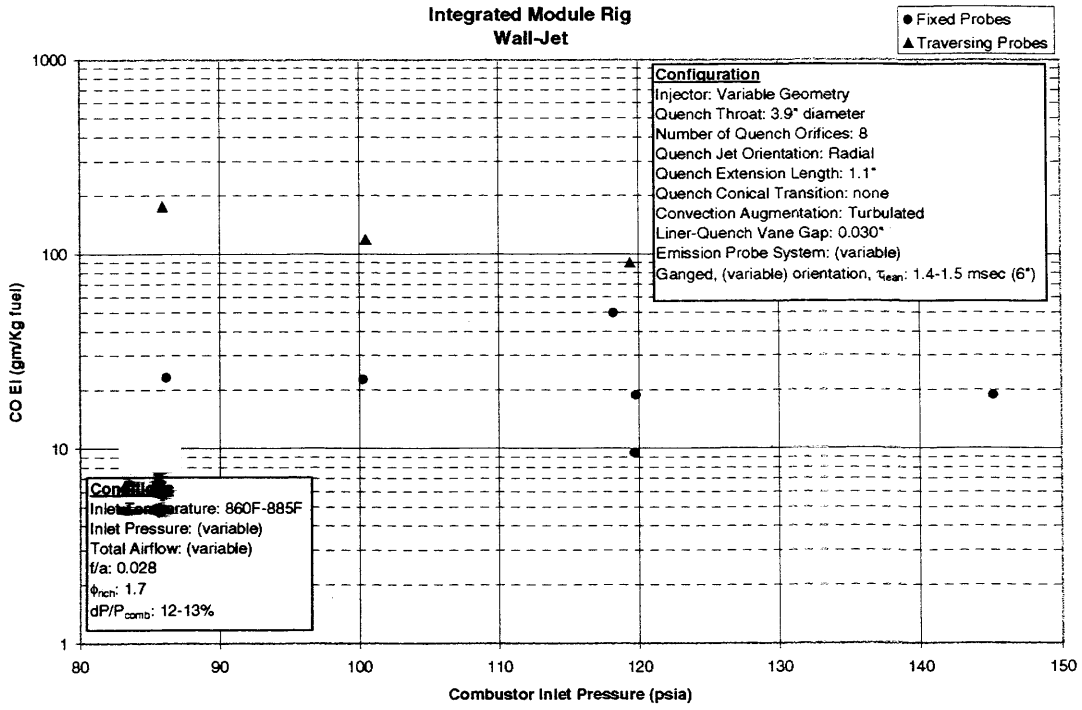

Figure VI - 40 Effect of Emissions Probe System on CO Emissions as a Function of Inlet Pressure

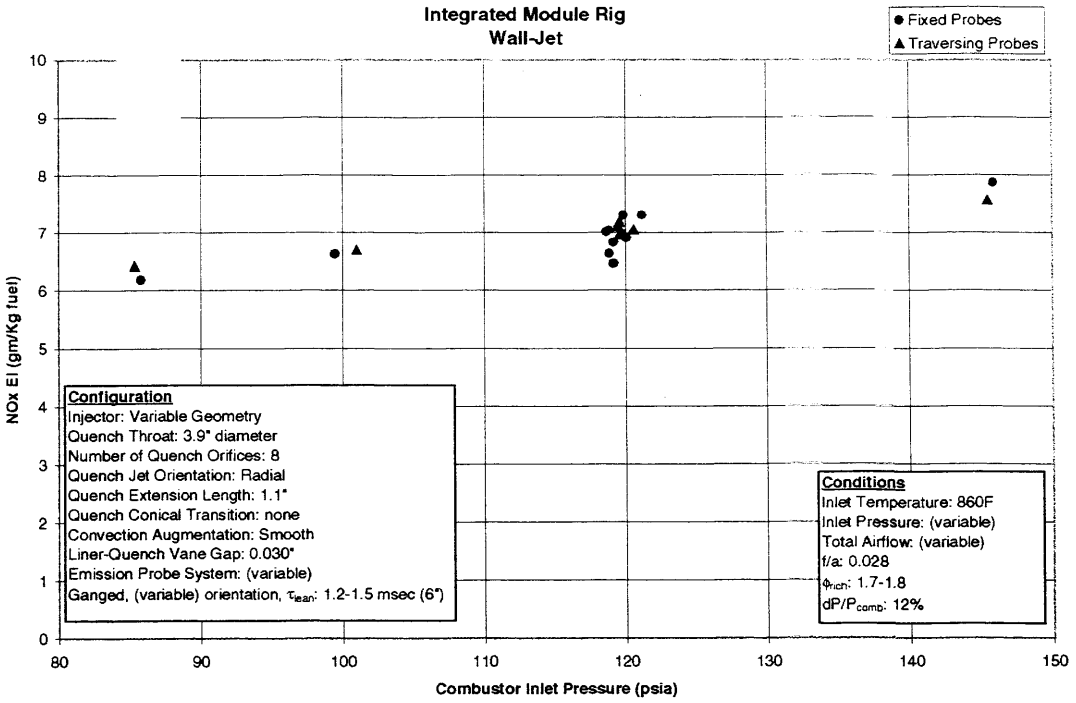

Figure VI - 41 Effect of Emissions Probe System on NOx Emissions as a Function of Inlet Pressure

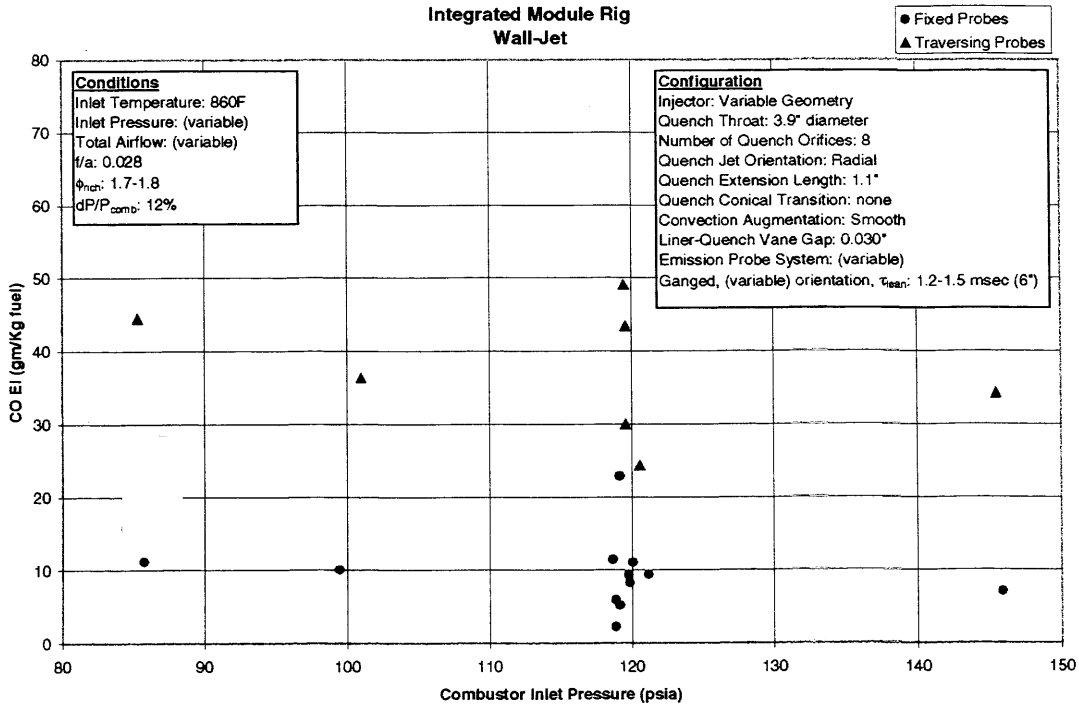

Figure VI - 42 Effect of Emissions Probe System on CO Emissions as a Function of Inlet Pressure

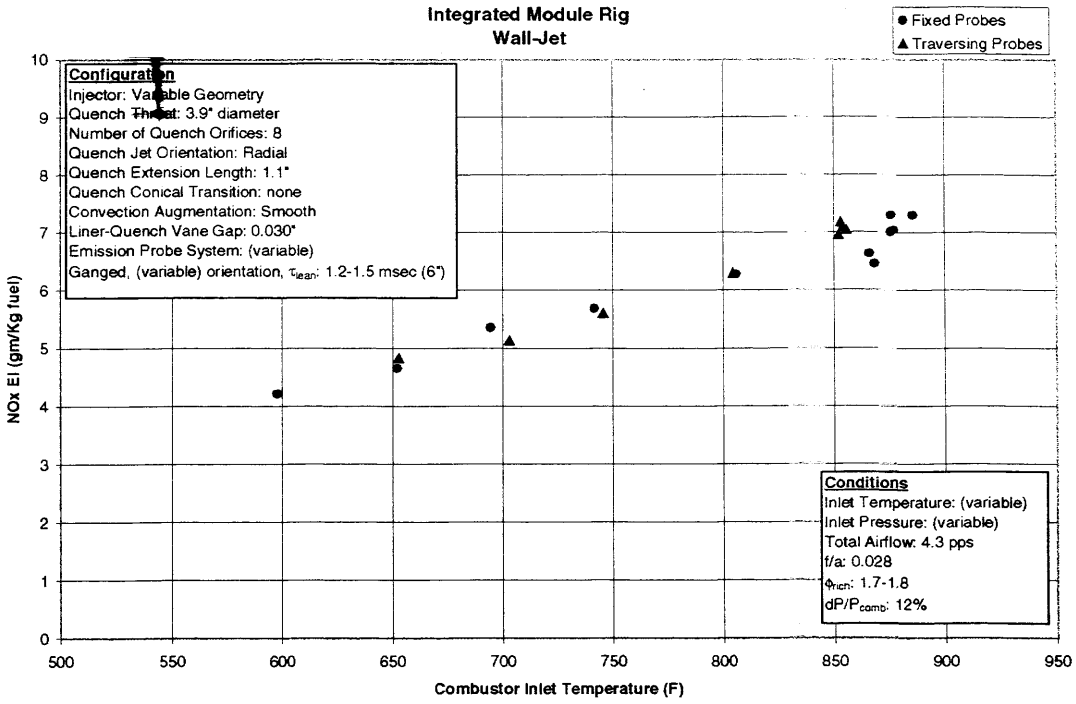

Figure VI - 43 Effect of Emissions Probe System on NOx Emissions as a Function of Inlet Temperature

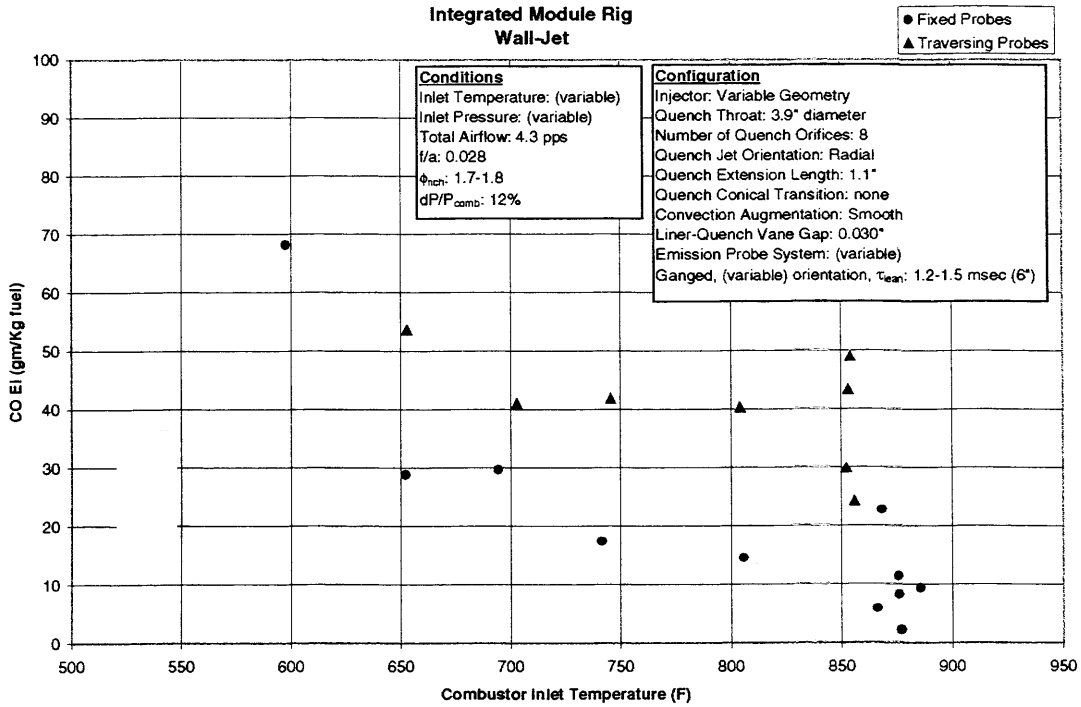

Figure VI - 44 Effect of Emissions Probe System on CO Emissions as a Function of Inlet Temperature

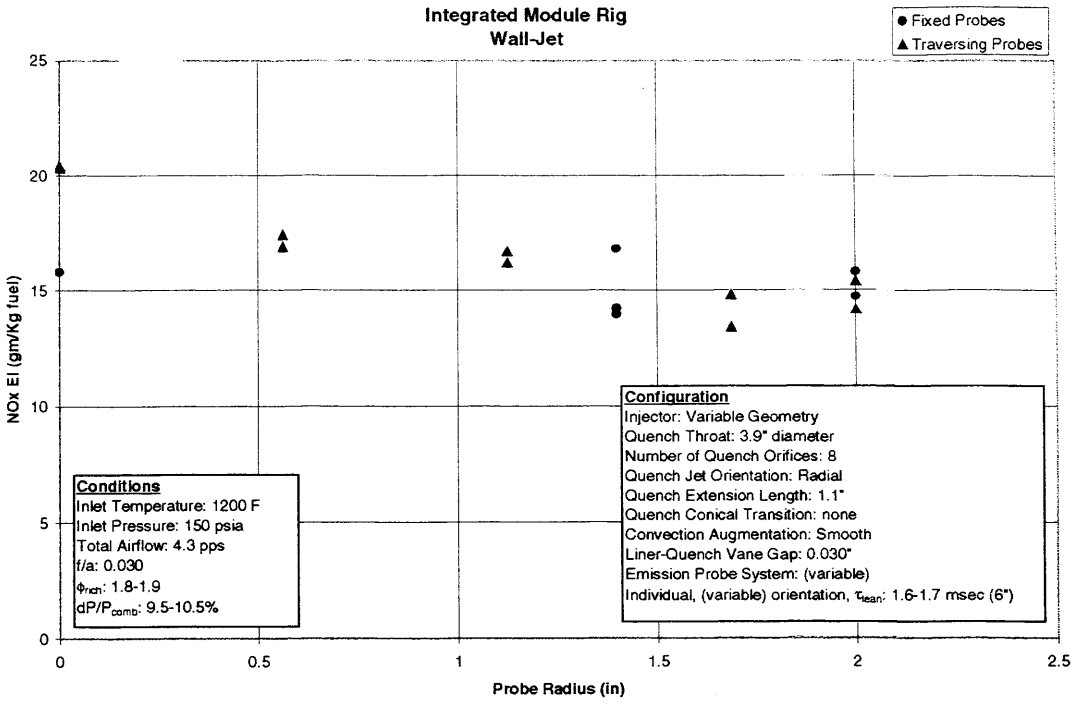

Figure VI - 45 Effect of Emissions Probe System on NOx Emissions as a Function of Radial Location

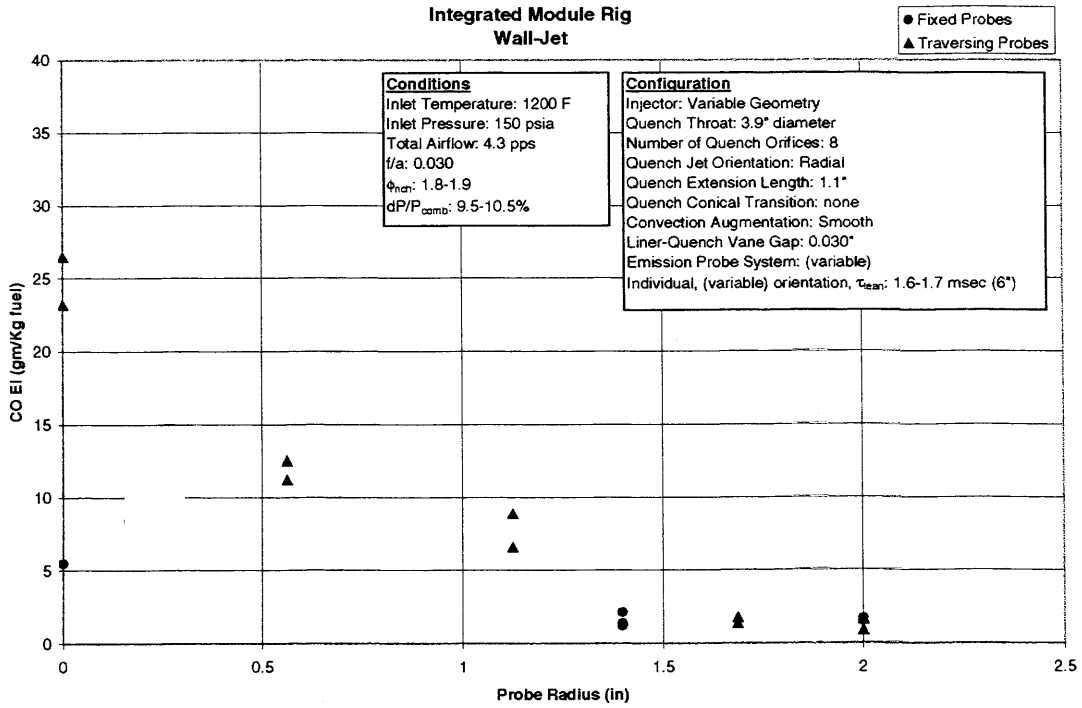

Figure VI - 46 Effect of Emissions Probe System on CO Emissions as a Function of Radial Location

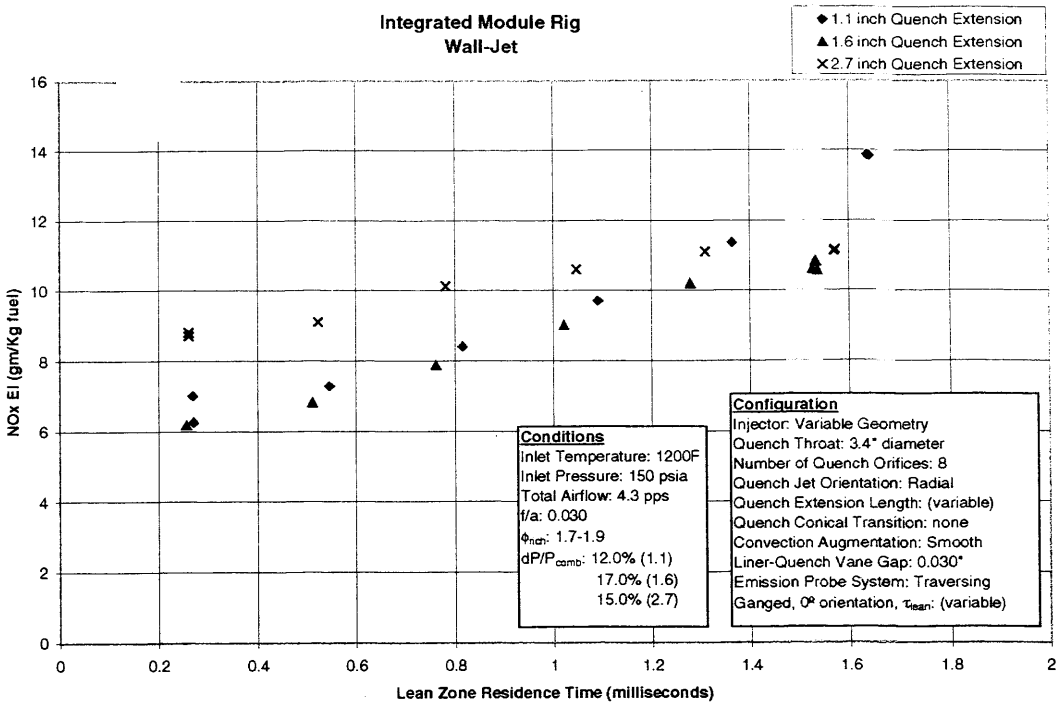

Figure VI - 47 Effect of Quench Extension Length on NOx Emissions as a Function of Lean Zone Residence Time

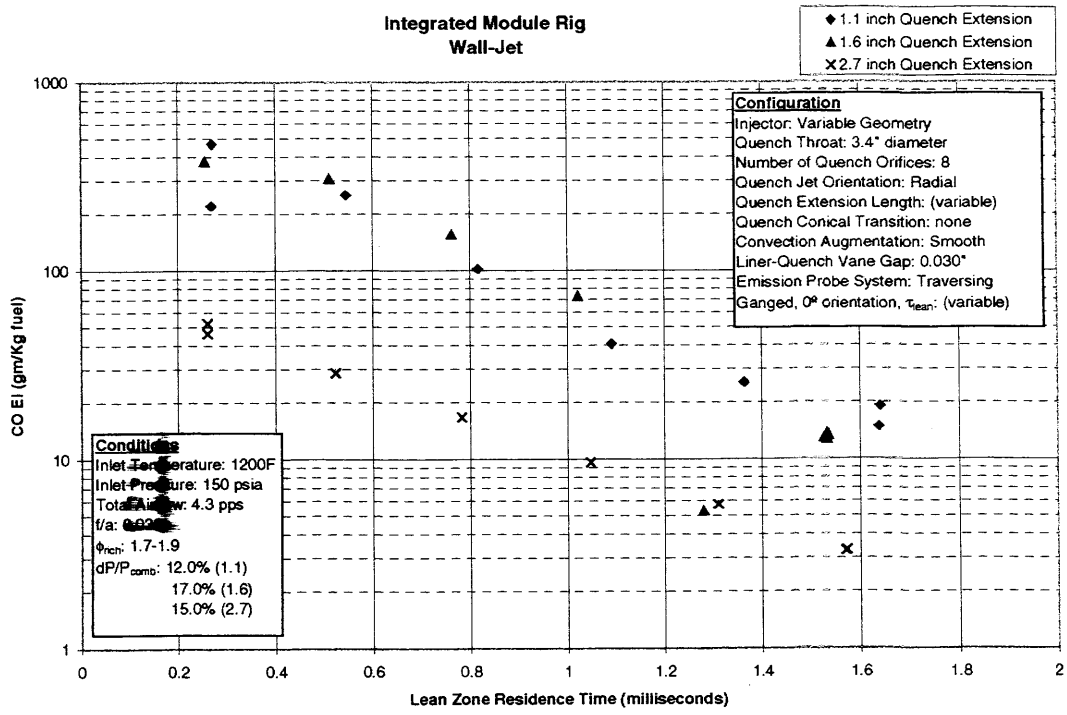

Figure VI - 48 Effect of Quench Extension Length on CO Emissions as a Function of Lean Zone Residence Time

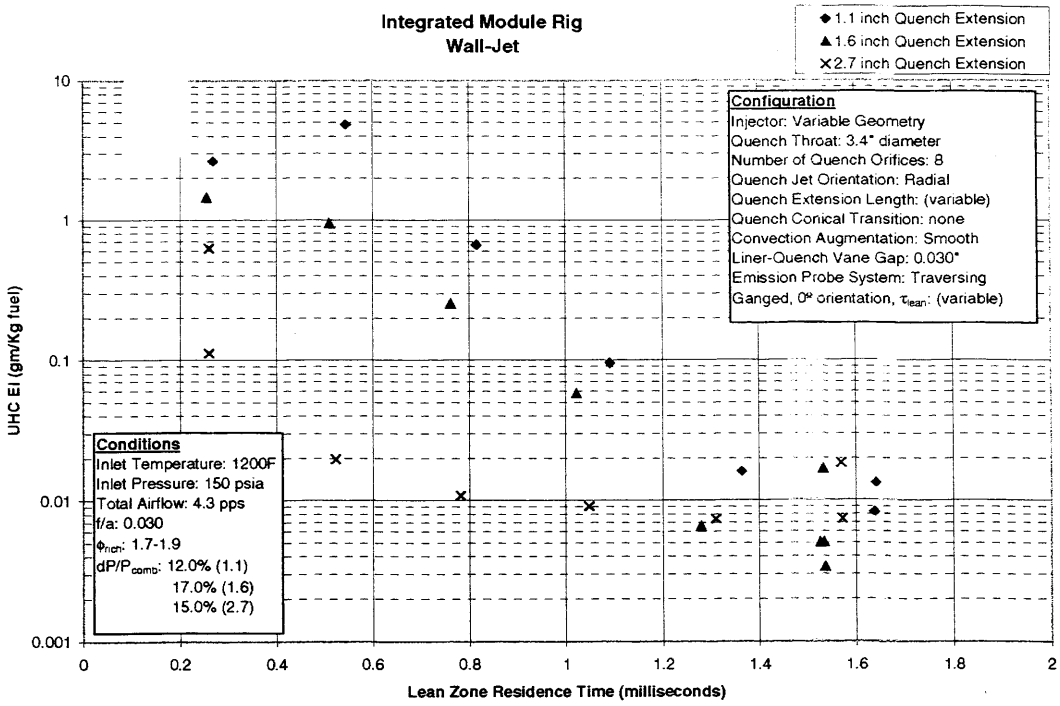

Figure VI - 49 Effect of Quench Extension Length on UHC Emissions as a Function of Lean Zone Residence Time

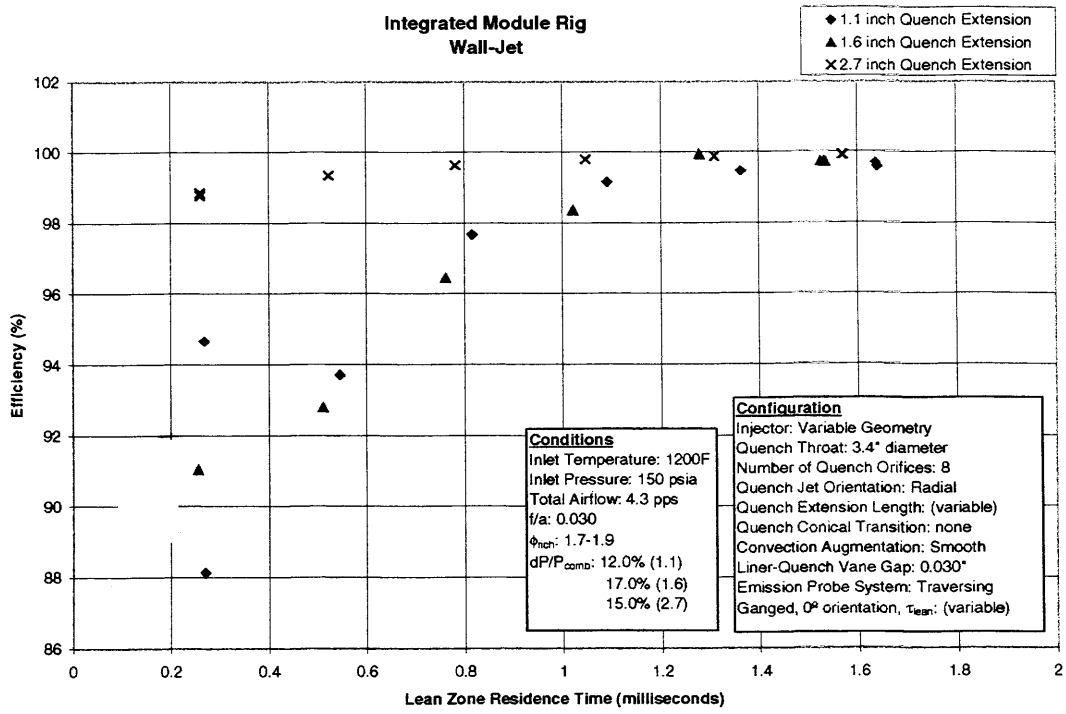

Figure VI - 50 Effect of Quench Extension Length on Efficiency as a Function of Lean Zone Residence Time

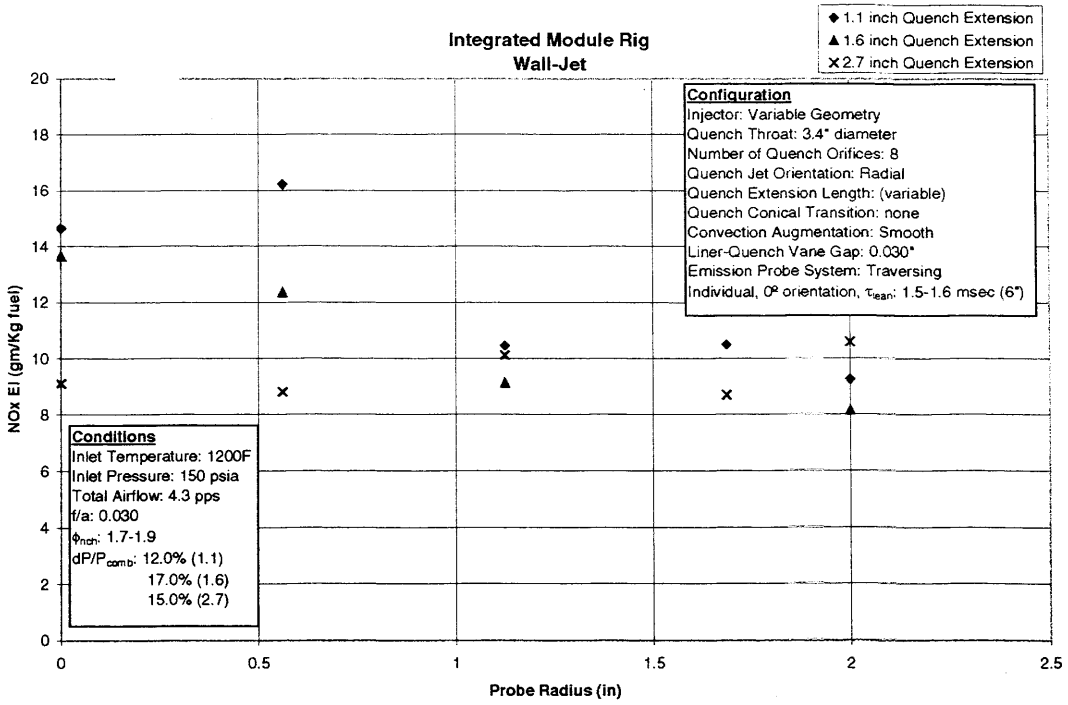

Figure VI - 51 Effect of Quench Extension Length on NOx Emissions as a Function of Radial Location

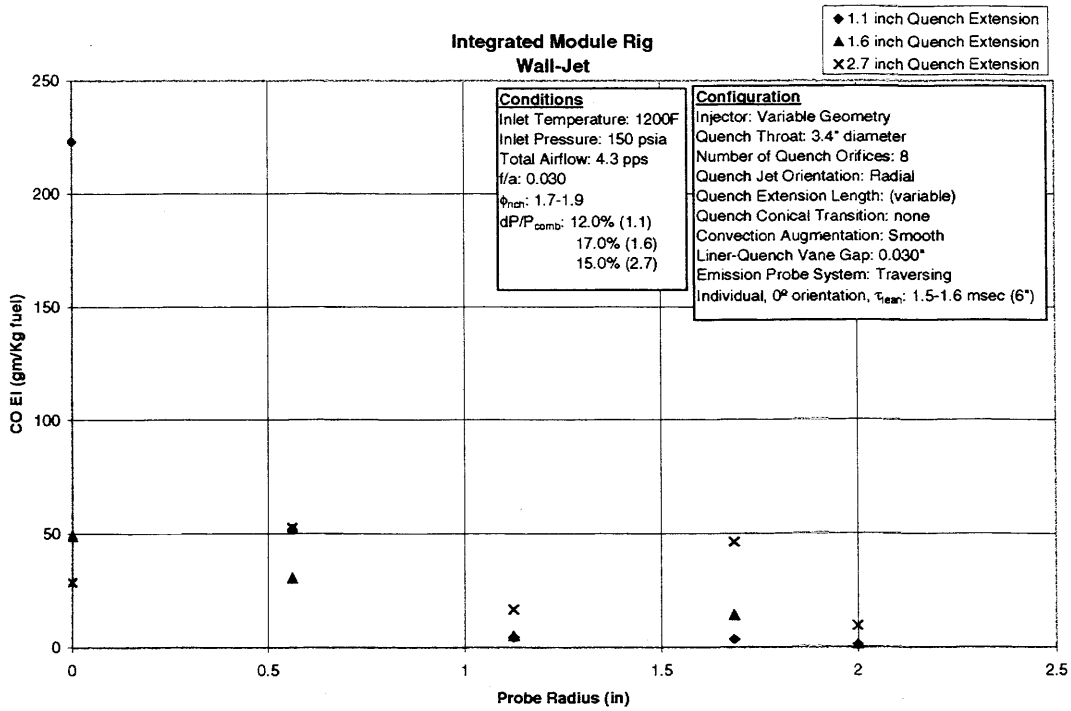

Figure VI - 52 Effect of Quench Extension Length on CO Emissions as a Function of Radial Location

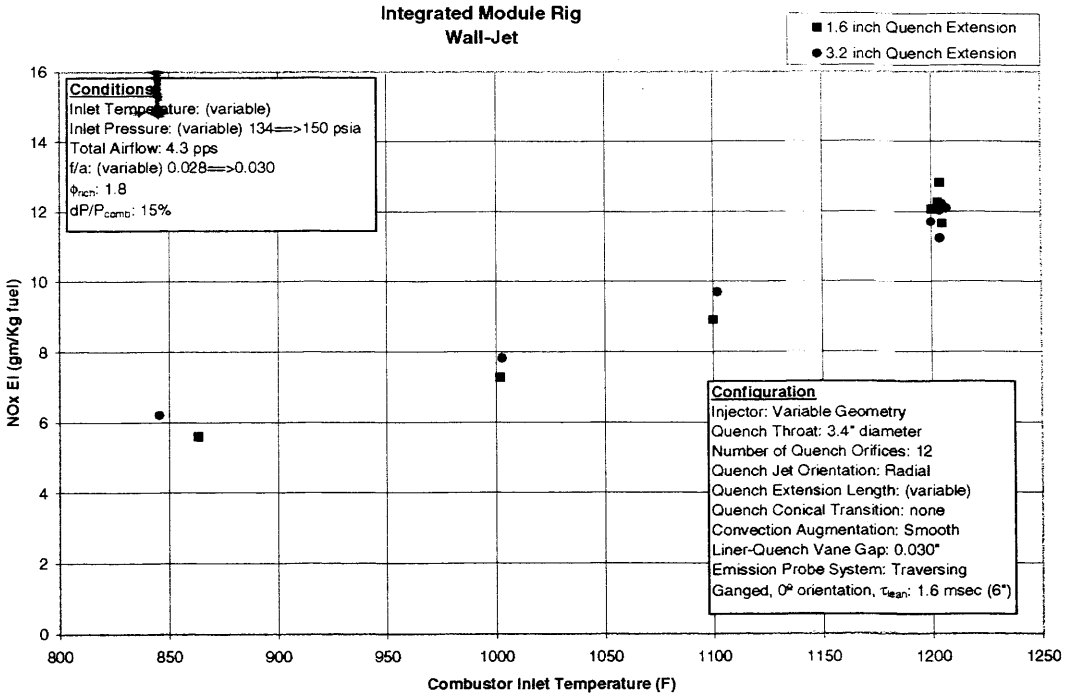

Figure VI - 53 Effect of Quench Extension Length on NOx Emissions as a Function of Inlet Temperature

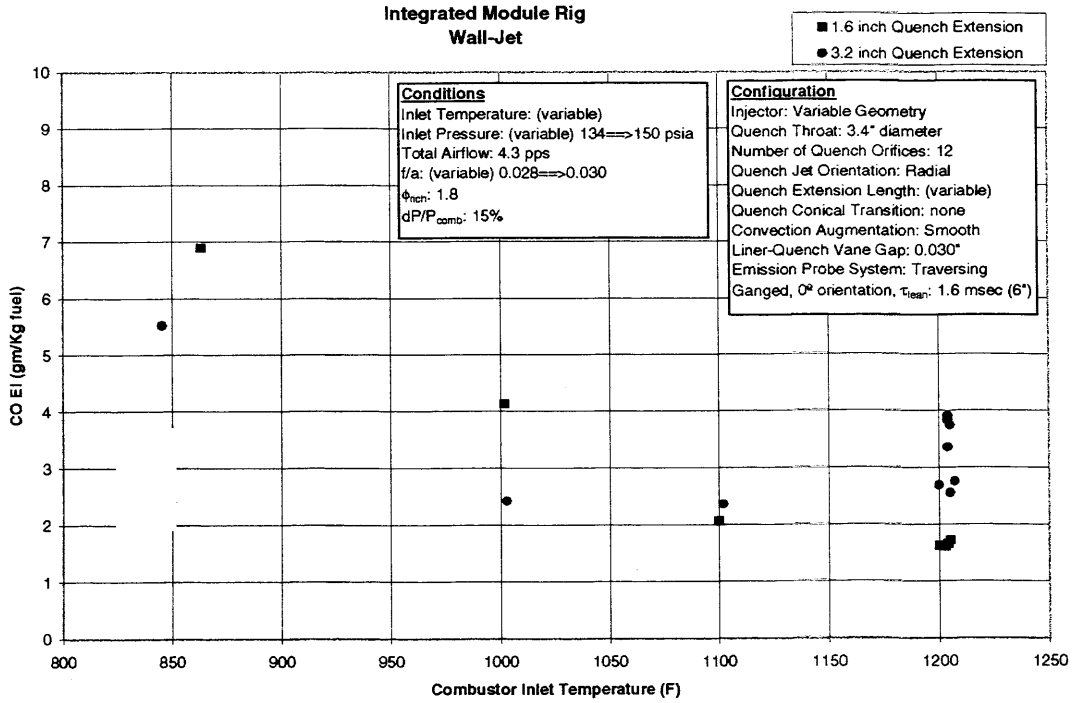

Figure VI - 54 Effect of Quench Extension Length on CO Emissions as a Function of Inlet Temperature

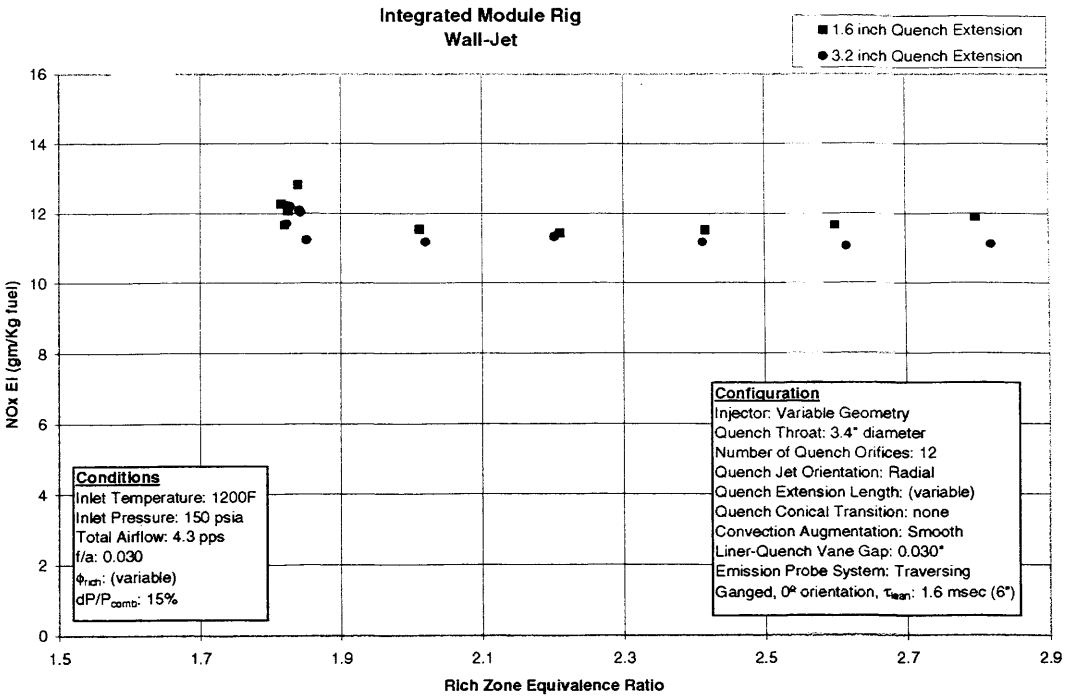

Figure VI - 55 Effect of Quench Extension Length on NOx Emissions as a Function of Rich Zone Equivalence Ratio

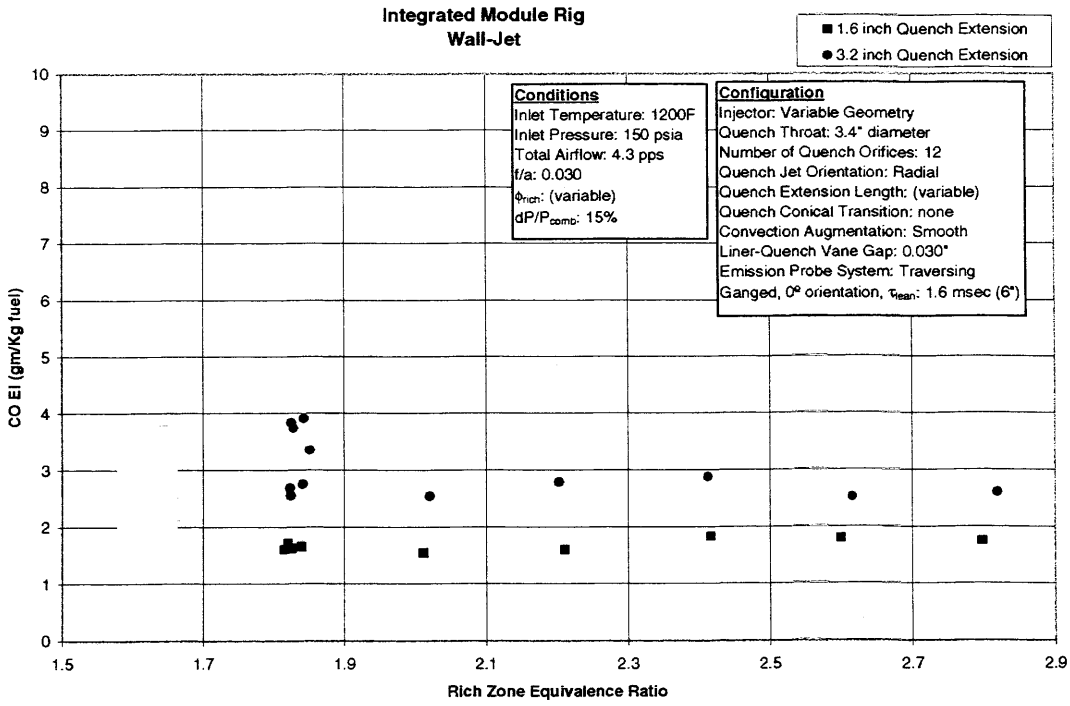

Figure VI - 56 Effect of Quench Extension Length on CO Emissions as a Function of Rich Zone Equivalence Ratio

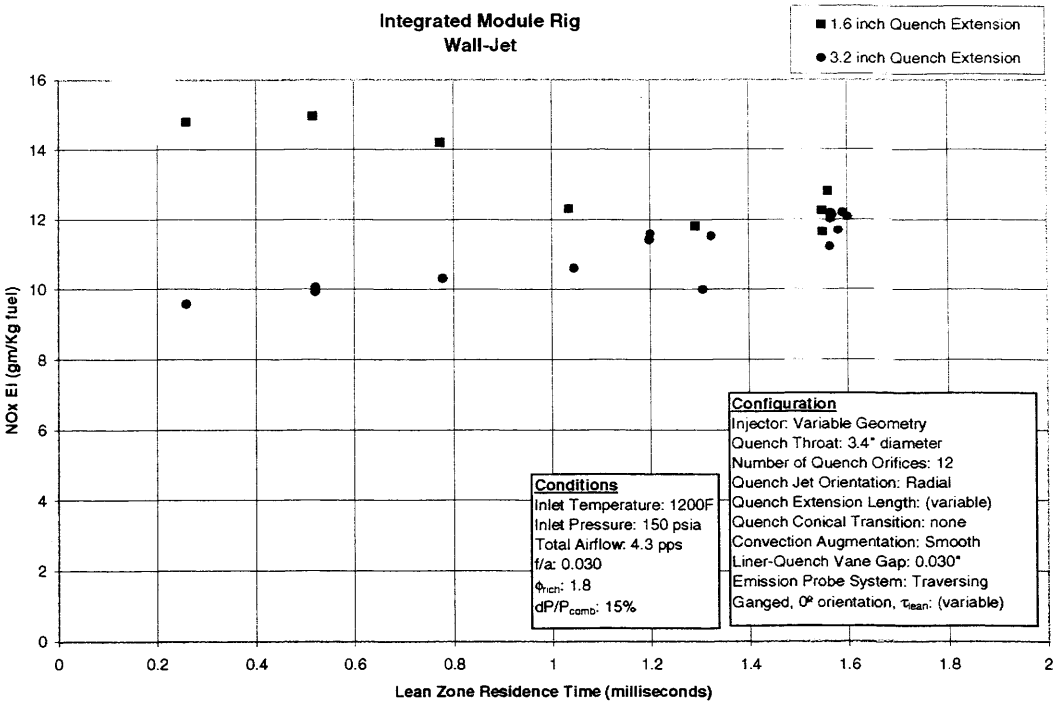

Figure VI - 57 Effect of Quench Extension Length on NOx Emissions as a Function of Lean Zone Residence Time

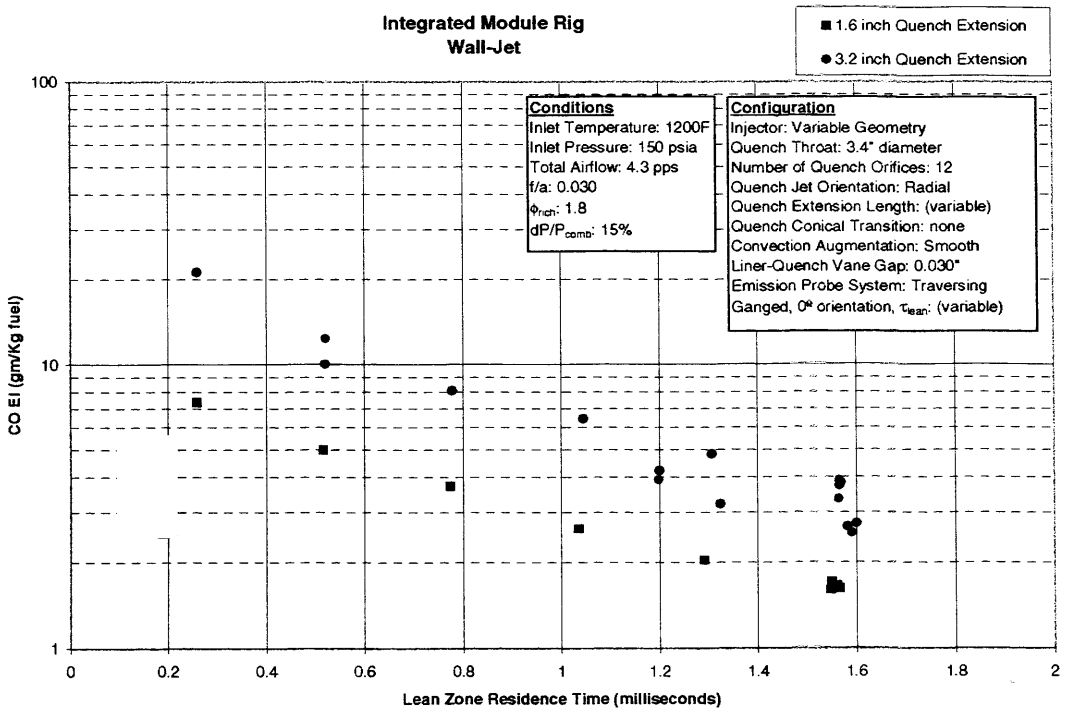

Figure VI - 58 Effect of Quench Extension Length on CO Emissions as a Function of Lean Zone Residence Time

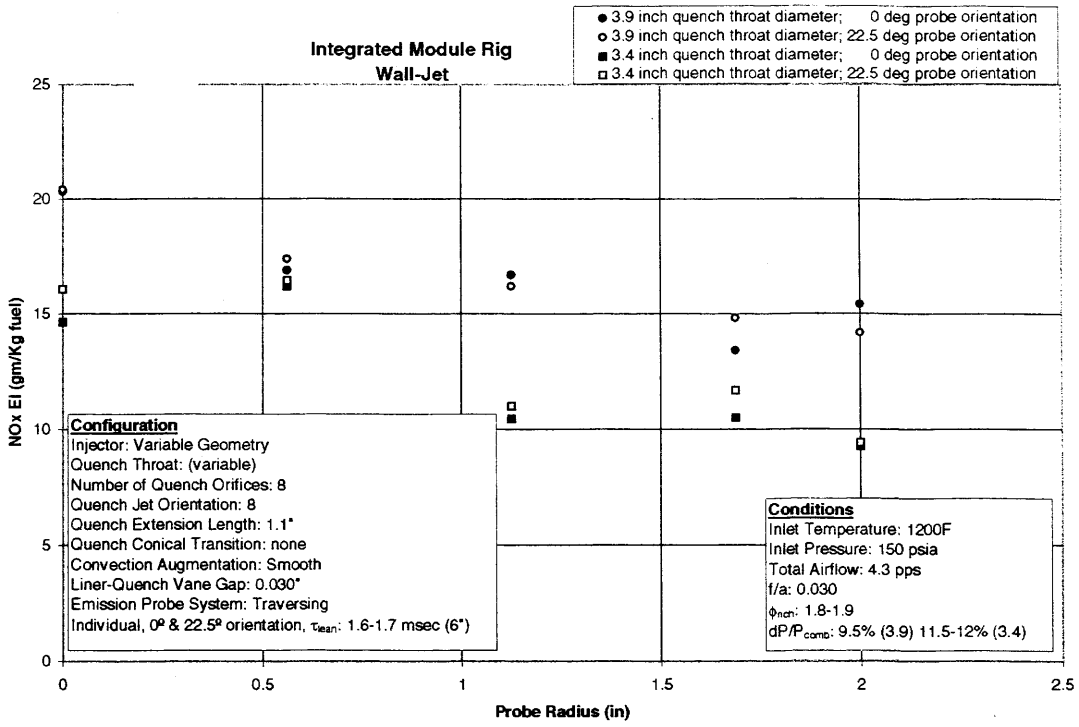

Figure VI - 59 Effect of Quench Throat Diameter on NOx Emissions as a Function of Radial Location

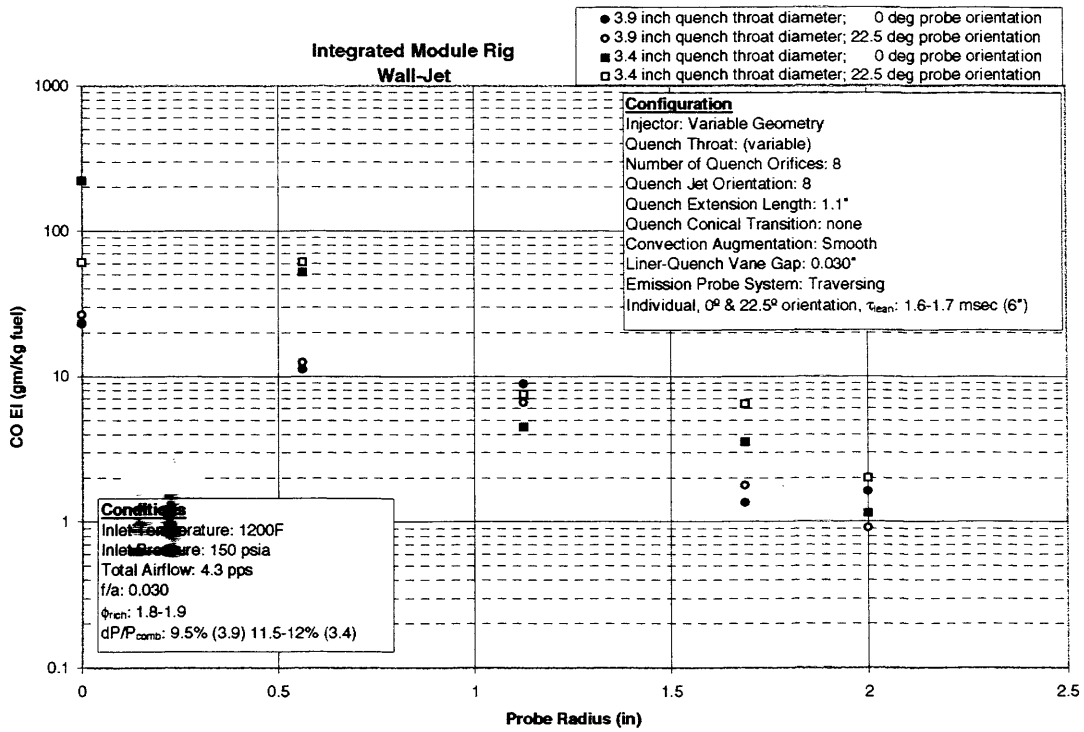

Figure VI - 60 Effect of Quench Throat Diameter on CO Emissions as a Function of Radial Location

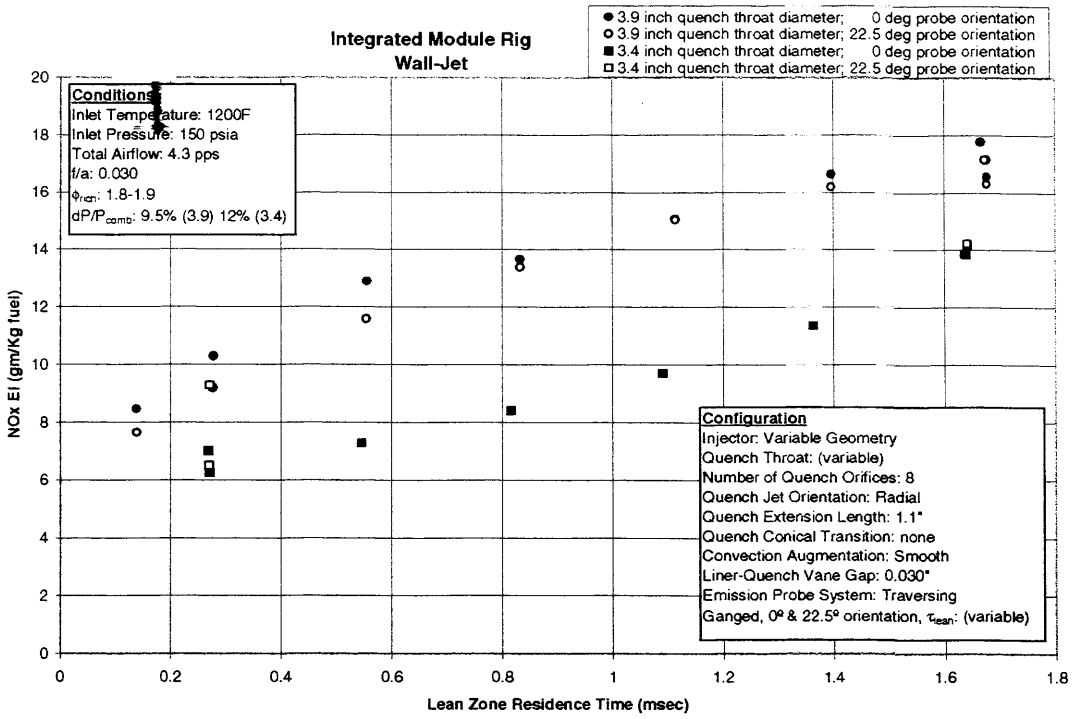

Figure VI - 61 Effect of Quench Throat Diameter on NOx Emissions as a Function of Lean Zone Residence Time

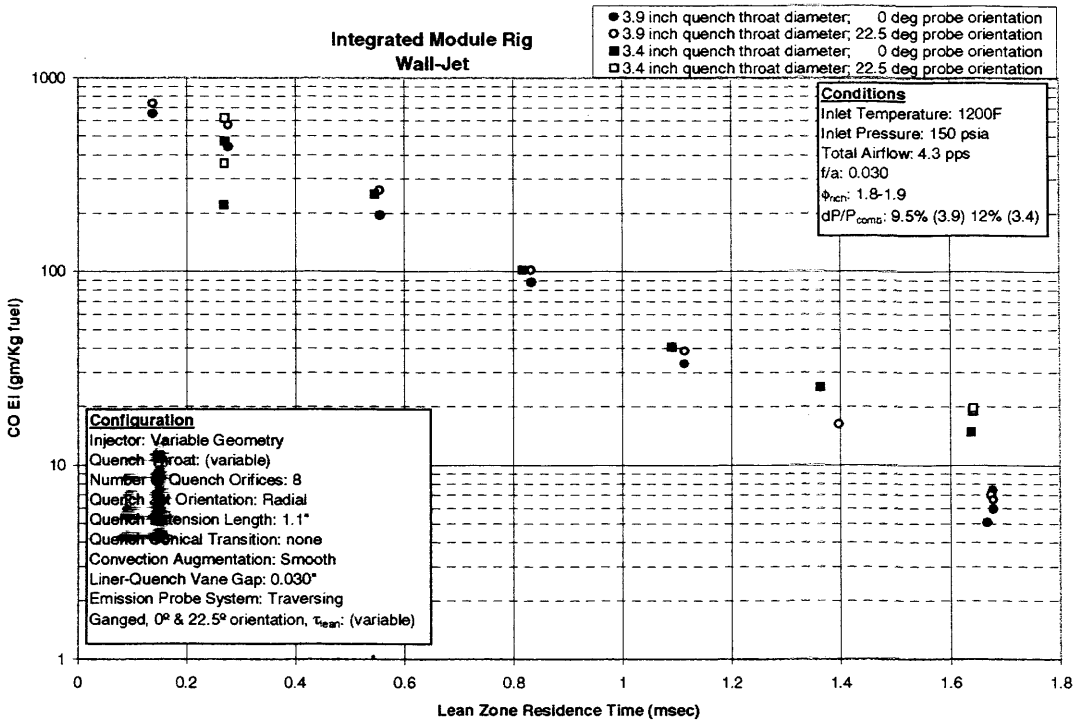

Figure VI - 62 Effect of Quench Throat Diameter on CO Emissions as a Function of Lean Zone Residence Time

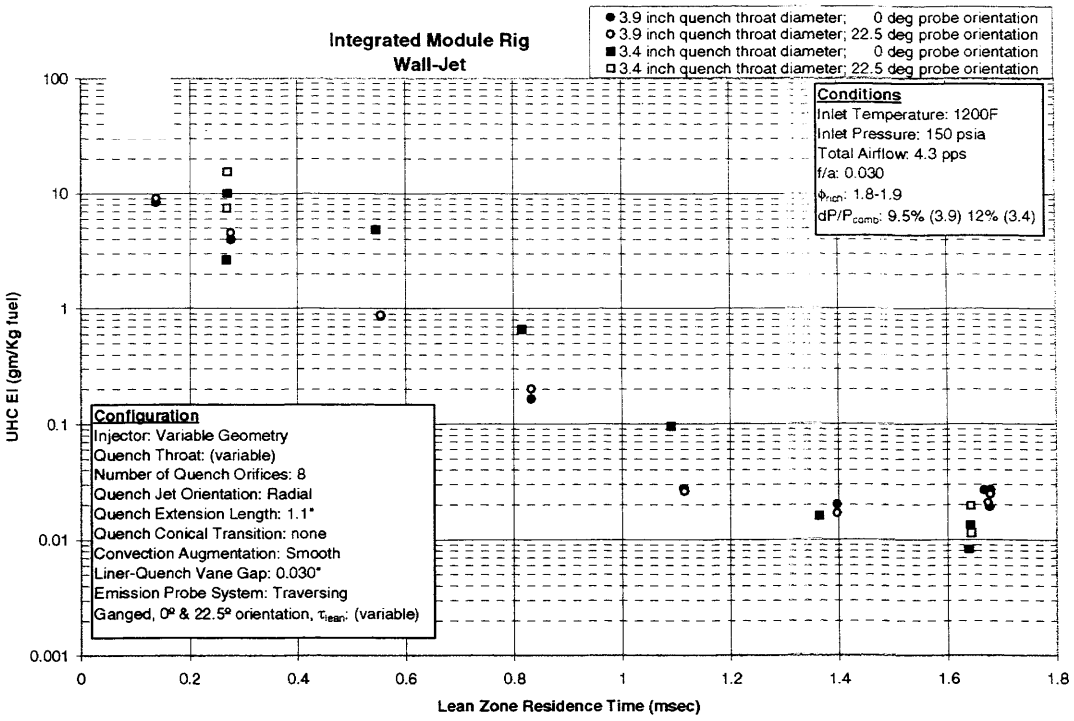

Figure VI - 63 Effect of Quench Throat Diameter on UHC Emissions as a Function of Lean Zone Residence Time

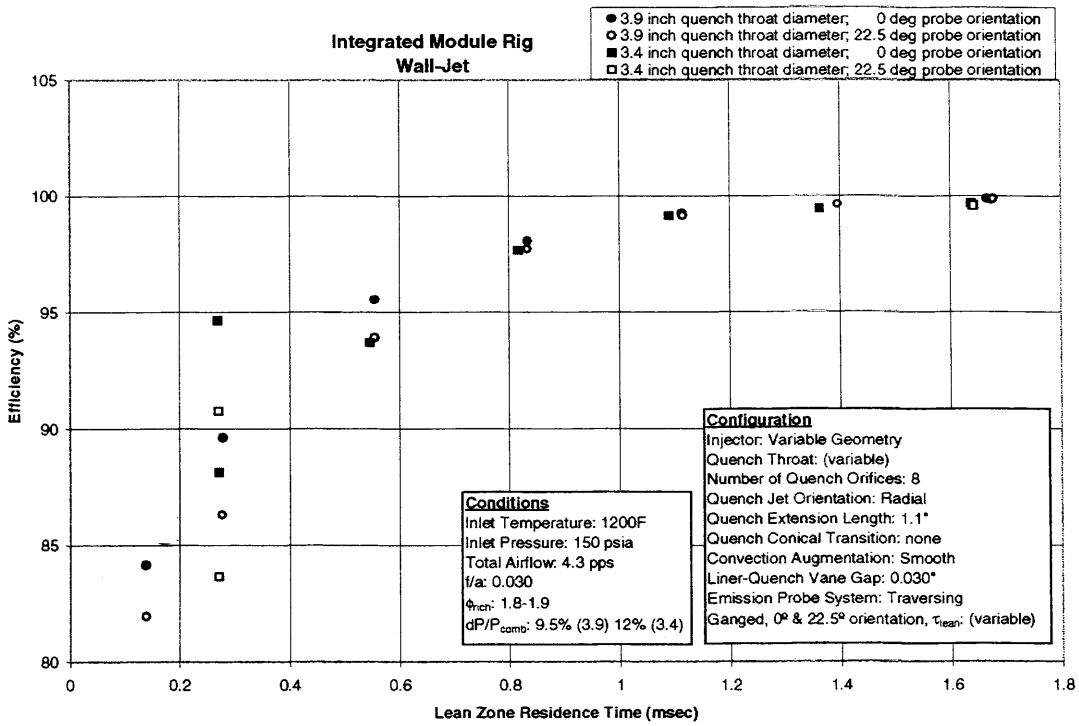

Figure VI - 64 Effect of Quench Throat Diameter on Efficiency as a Function of Lean Zone Residence Time

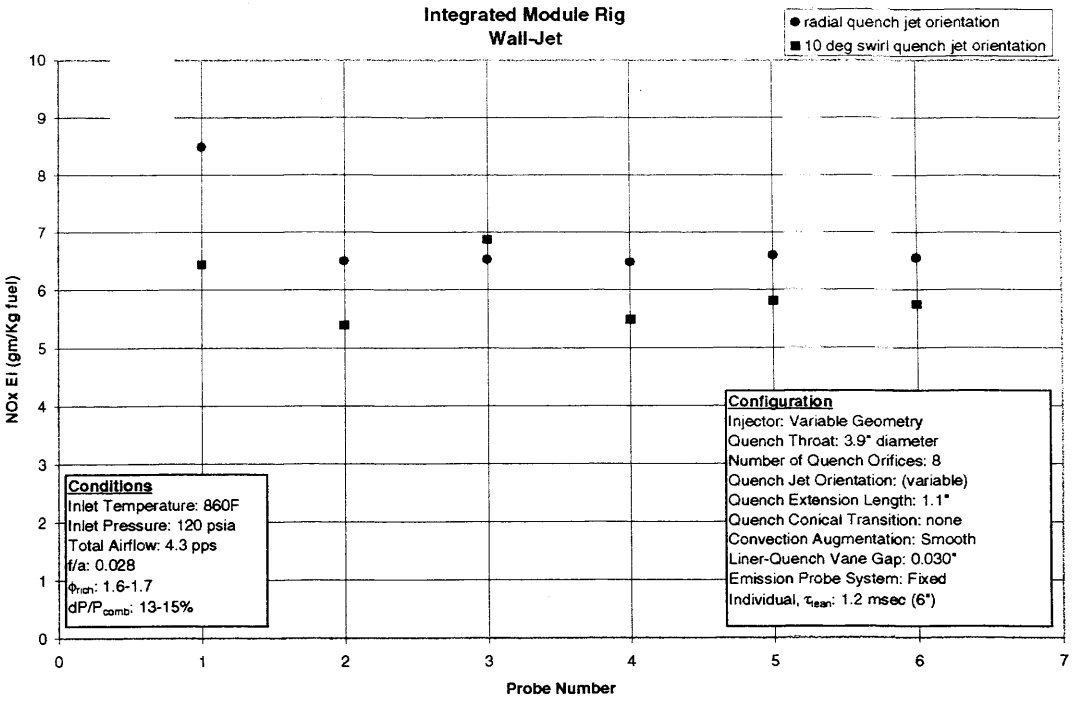

Figure VI - 65 Effect of Quench Jet Orientation on NOx Emissions as a Function of Probe Location

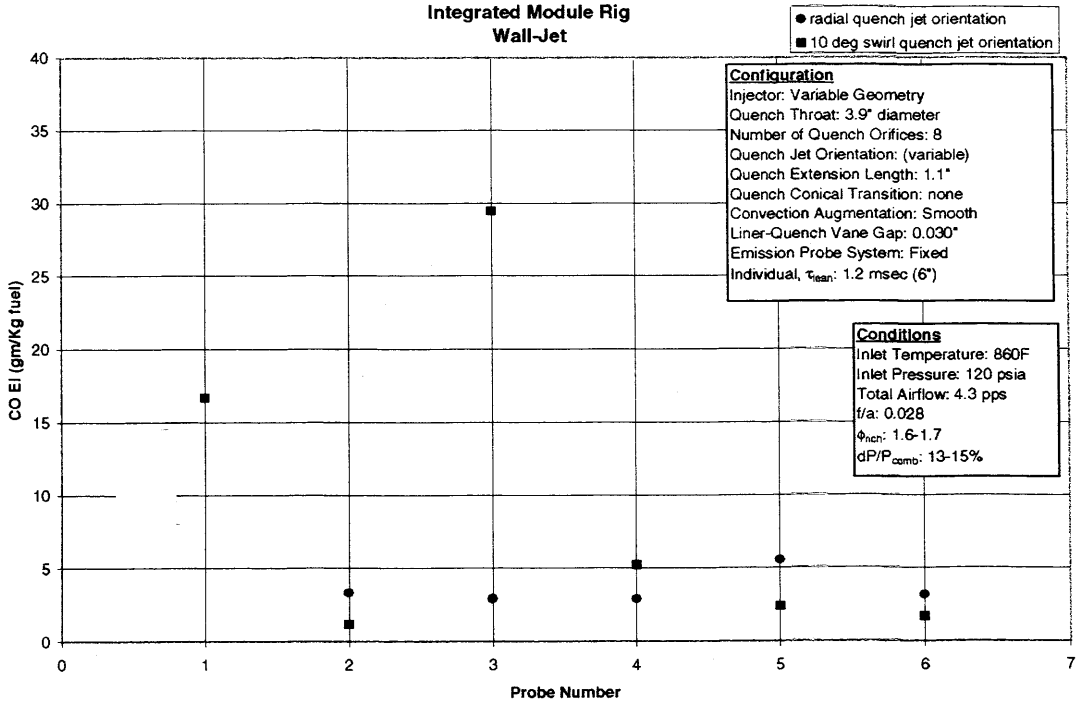

Figure VI - 66 Effect of Quench Jet Orientation on CO Emissions as a Function of Probe Location

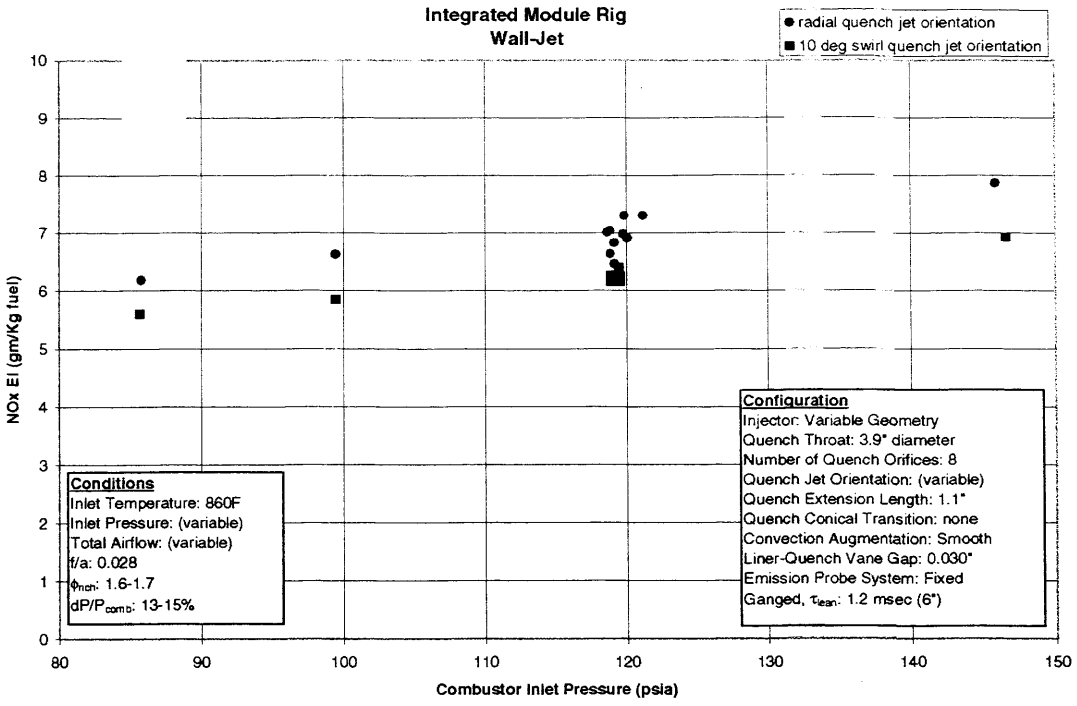

Figure VI - 67 Effect of Quench Jet Orientation on NOx Emissions as a Function of Inlet Pressure

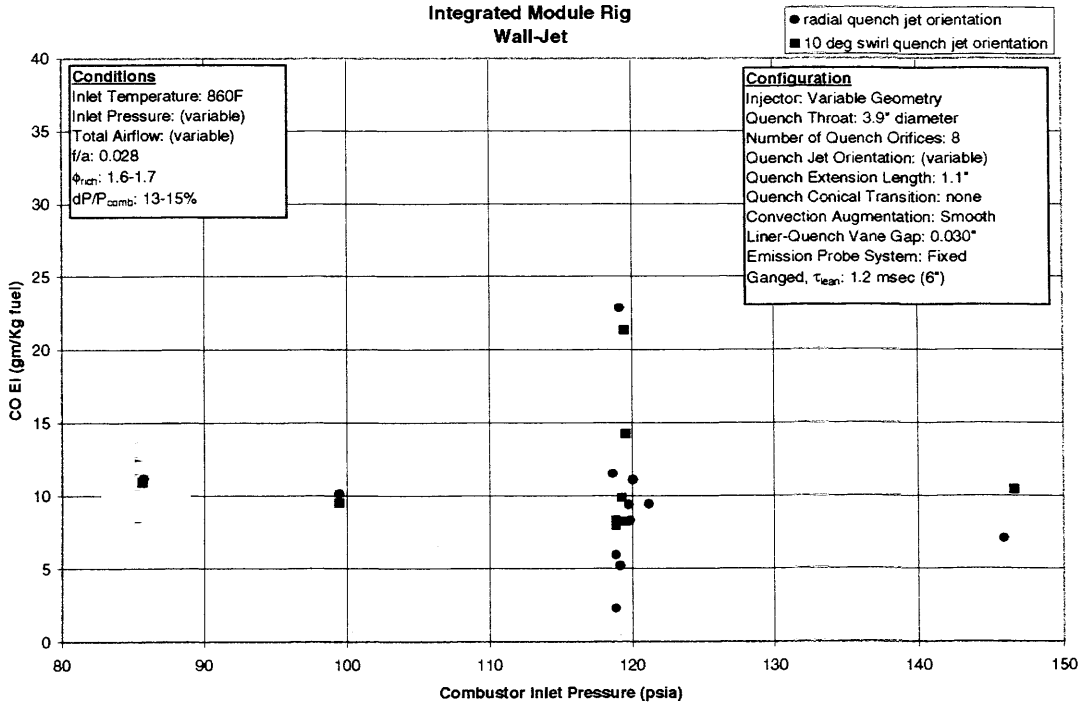

Figure VI - 68 Effect of Quench Jet Orientation on CO Emissions as a Function of Inlet Pressure

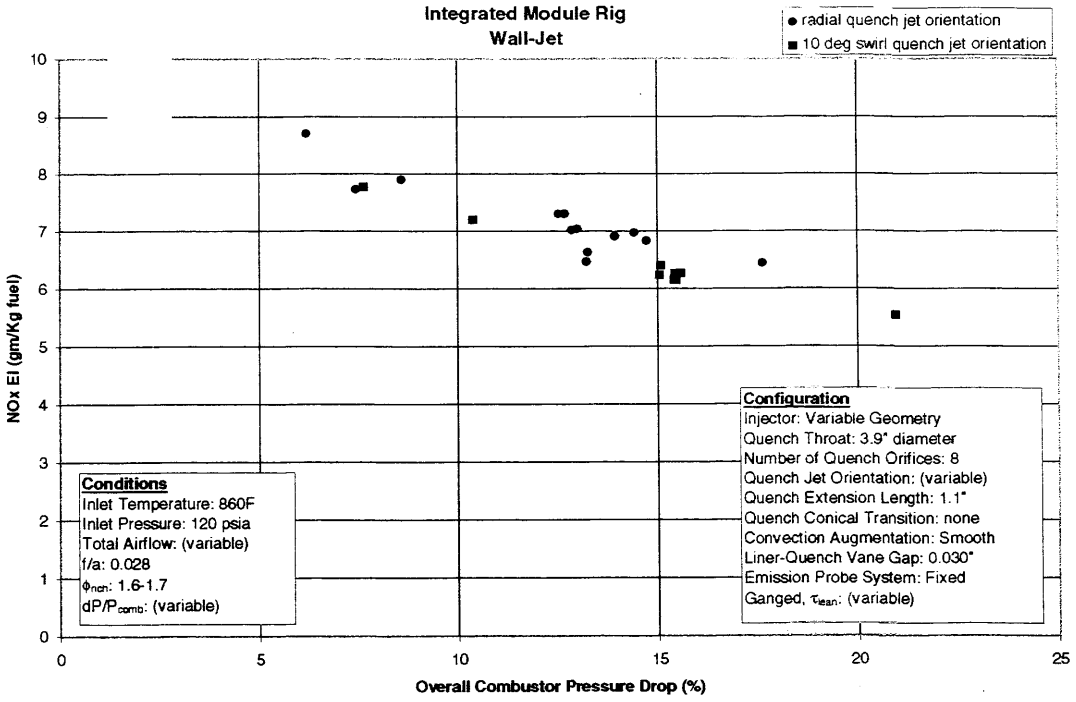

Figure VI - 69 Effect of Quench Jet Orientation on NOx Emissions as a Function of Combustor Pressure Drop

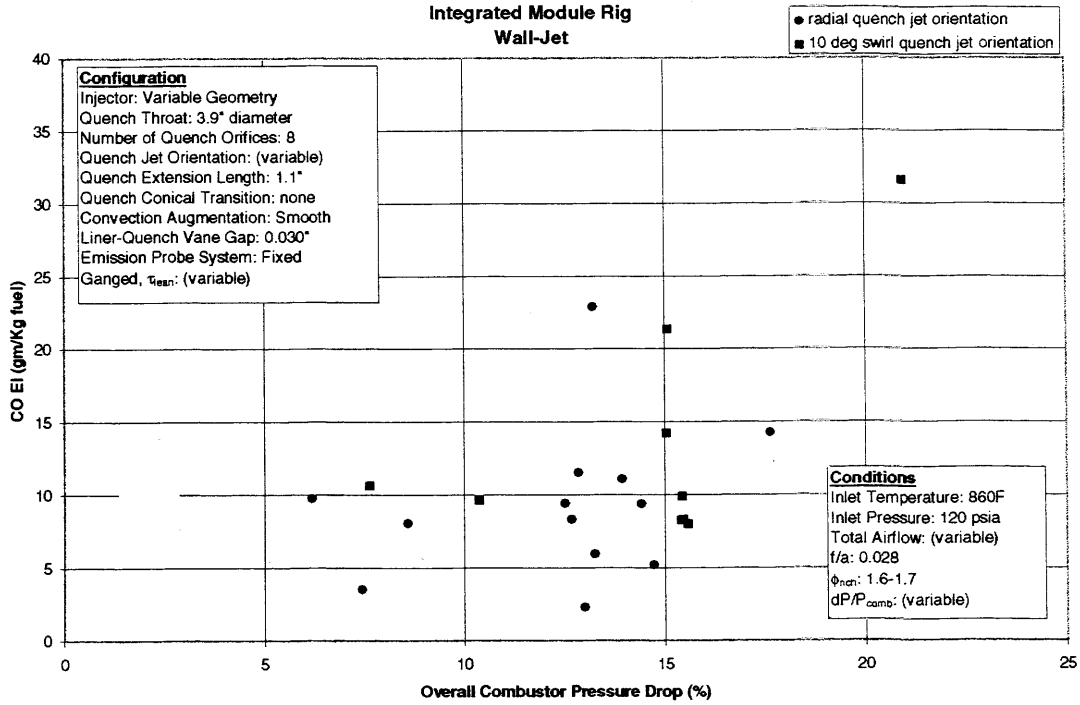

Figure VI - 70 Effect of Quench Jet Orientation on CO Emissions as a Function of Combustor Pressure Drop

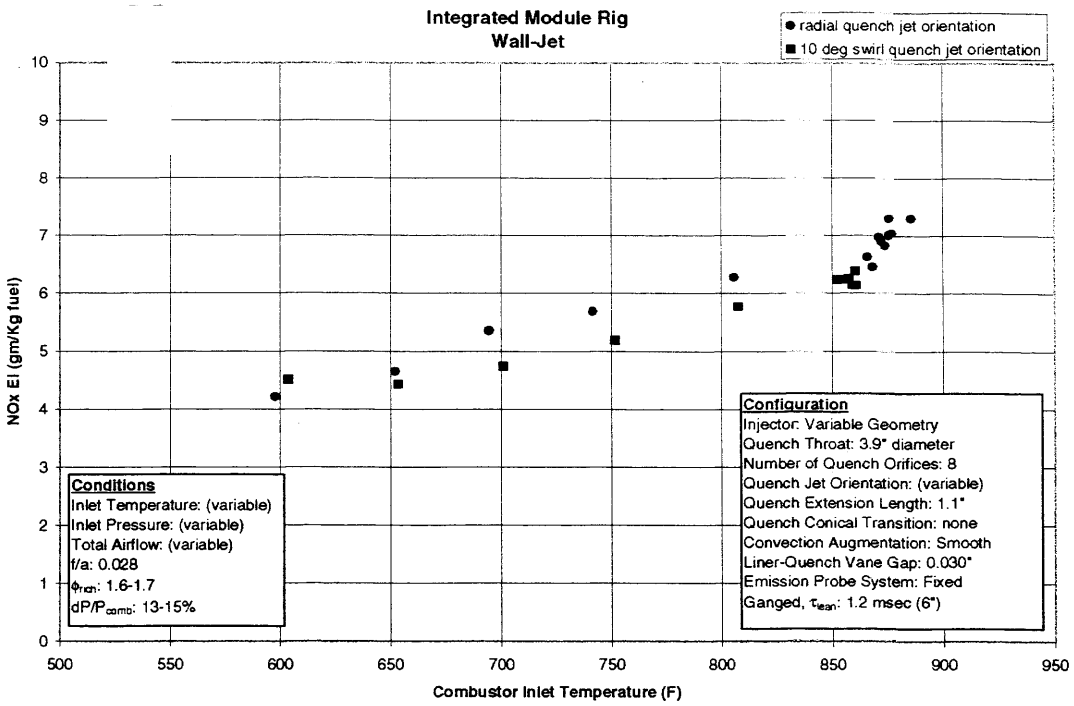

Figure VI - 71 Effect of Quench Jet Orientation on NOx Emissions as a Function of Inlet Temperature

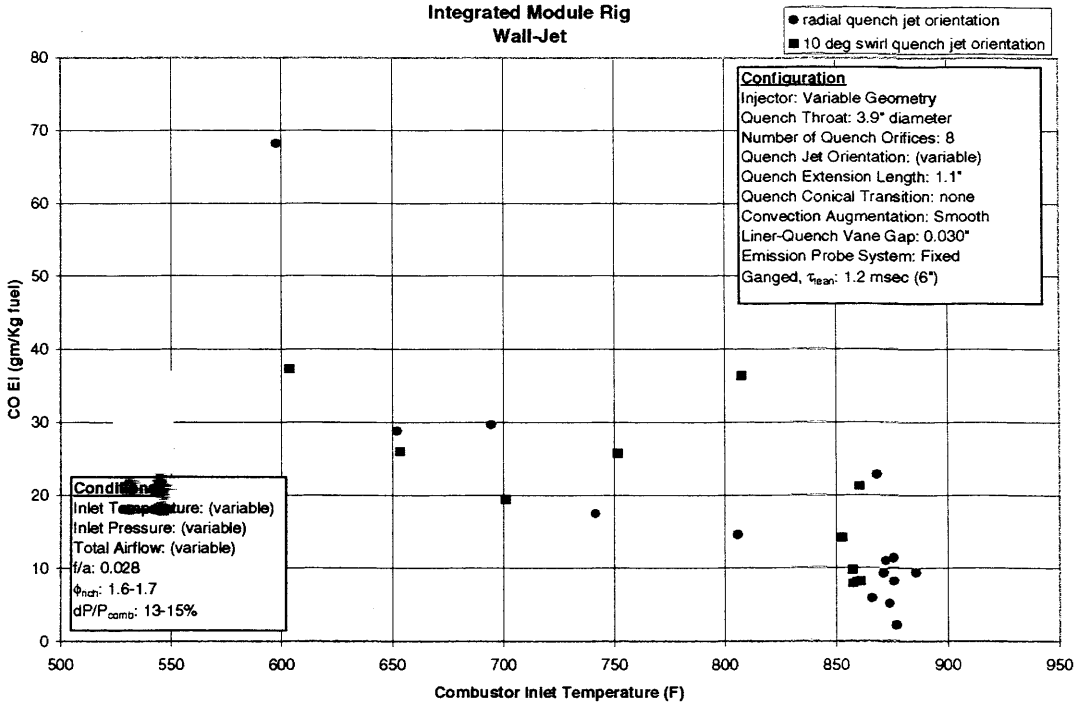

Figure VI - 72 Effect of Quench Jet Orientation on CO Emissions as a Function of Inlet Temperature

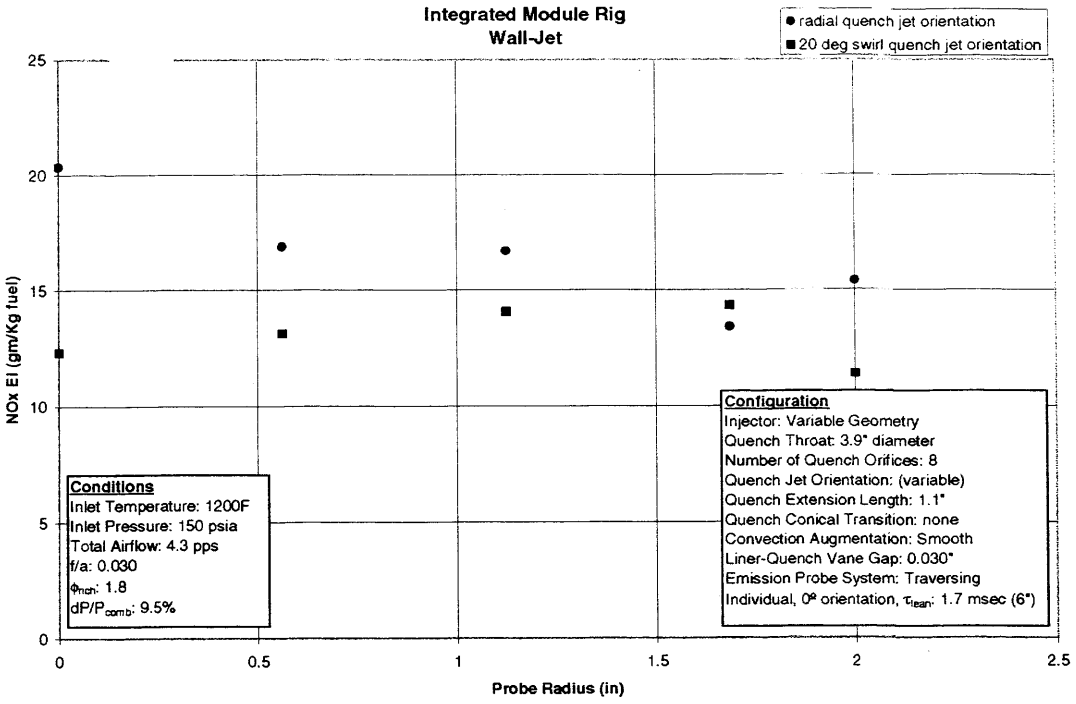

Figure VI - 73 Effect of Quench Jet Orientation on NOx Emissions as a Function of Radial Location

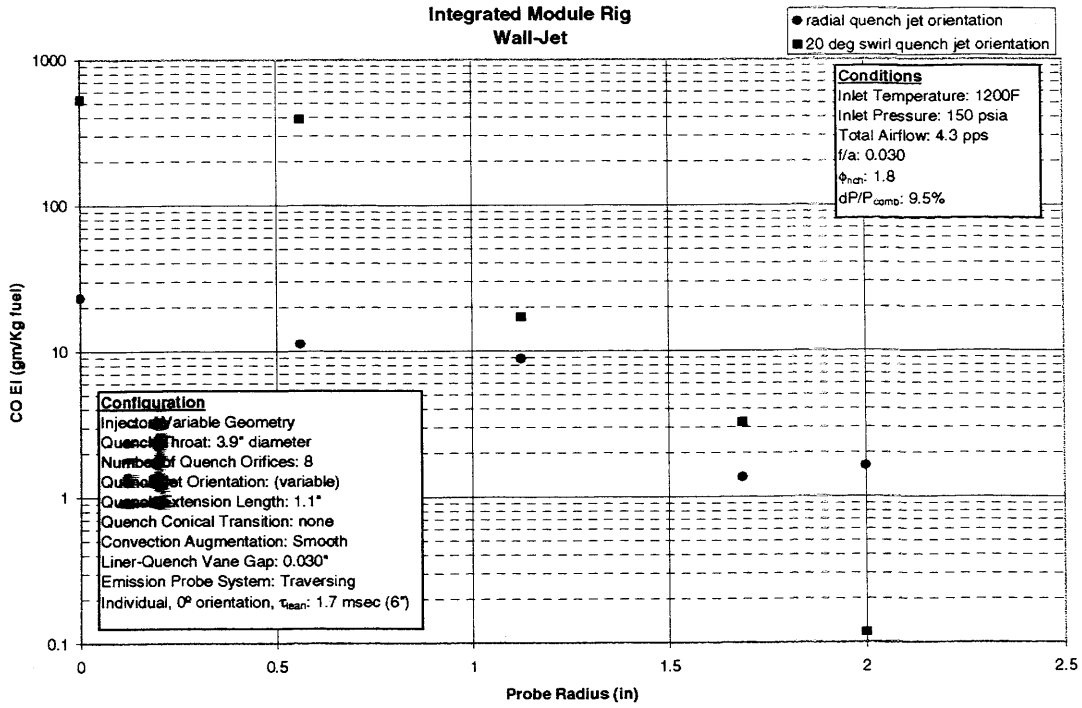

Figure VI - 74 Effect of Quench Jet Orientation on CO Emissions as a Function of Radial Location

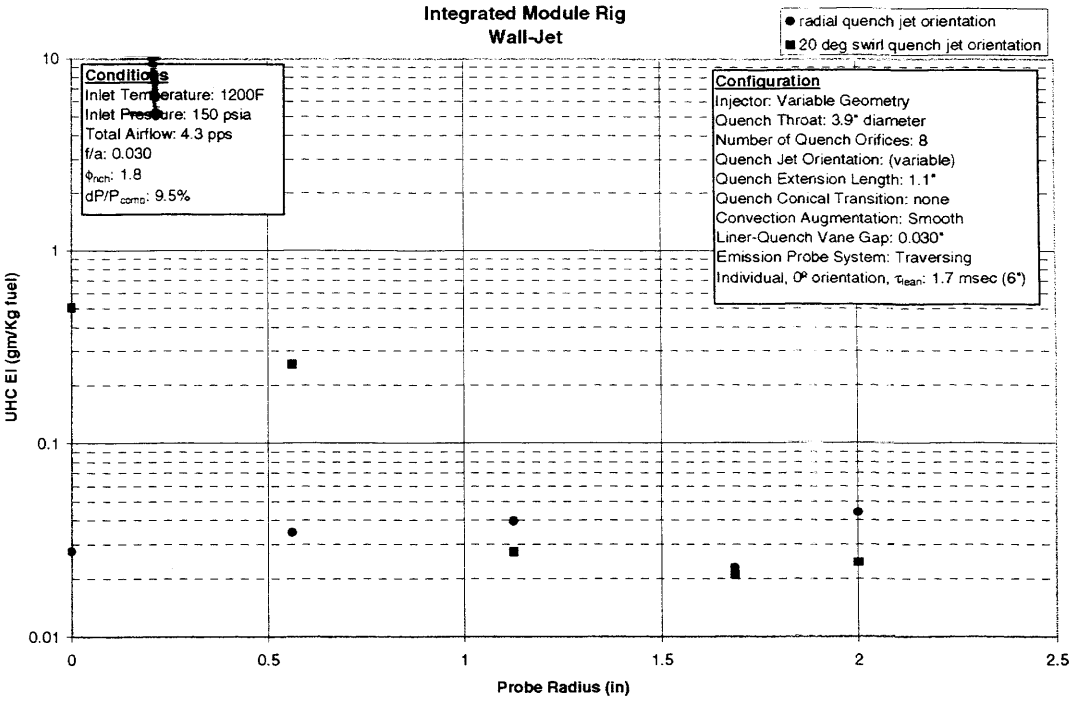

Figure VI - 75 Effect of Quench Jet Orientation on UHC Emissions as a Function of Radial Location

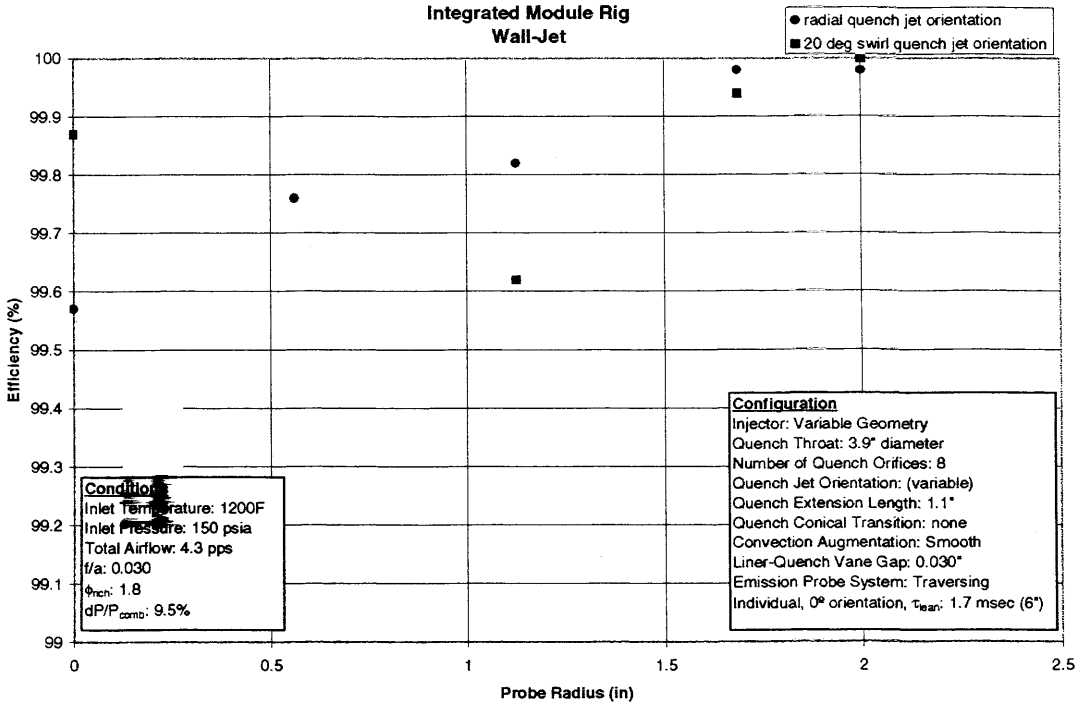

Figure VI - 76 Effect of Quench Jet Orientation on Efficiency as a Function of Radial Location

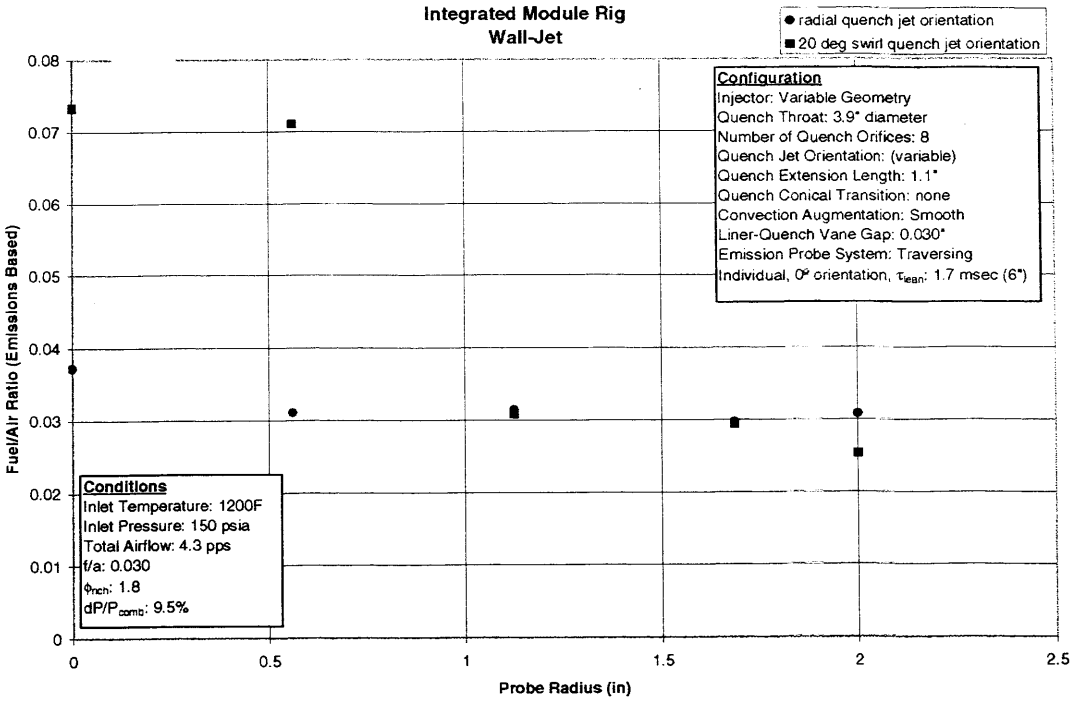

Figure VI - 77 Effect of Quench Jet Orientation on Emissions Fuel/Air Ratio as a Function of Radial Location

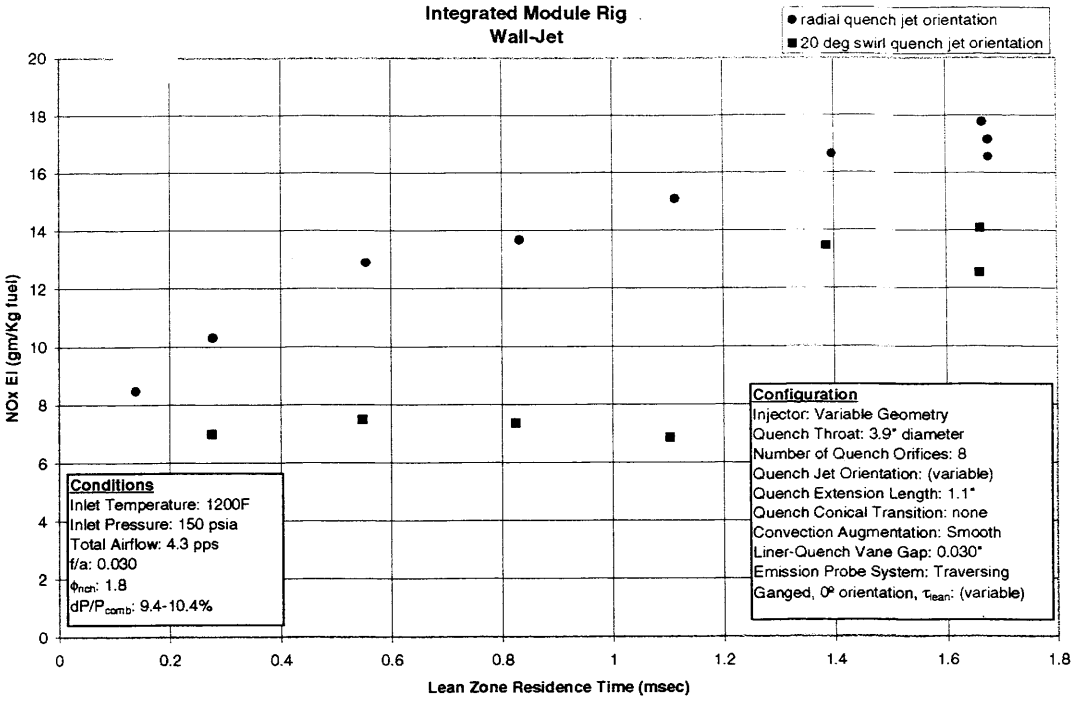

Figure VI - 78 Effect of Quench Jet Orientation on NOx Emissions as a Function of Lean Zone Residence Time

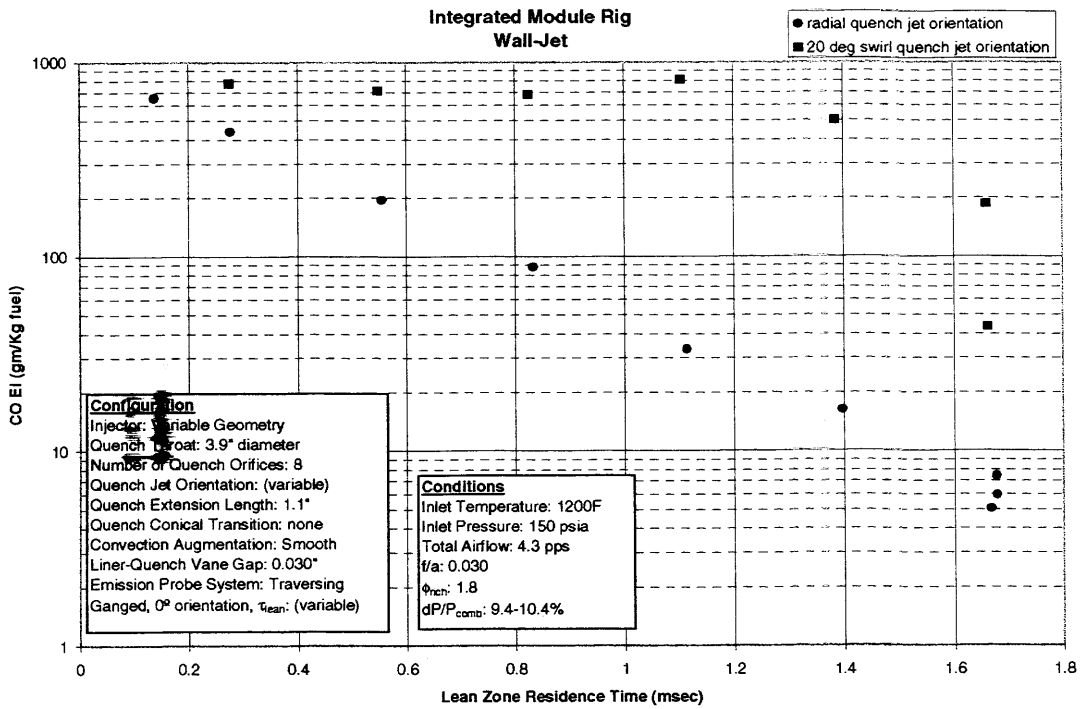

Figure VI - 79 Effect of Quench Jet Orientation on CO Emissions as a Function of Lean Zone Residence Time

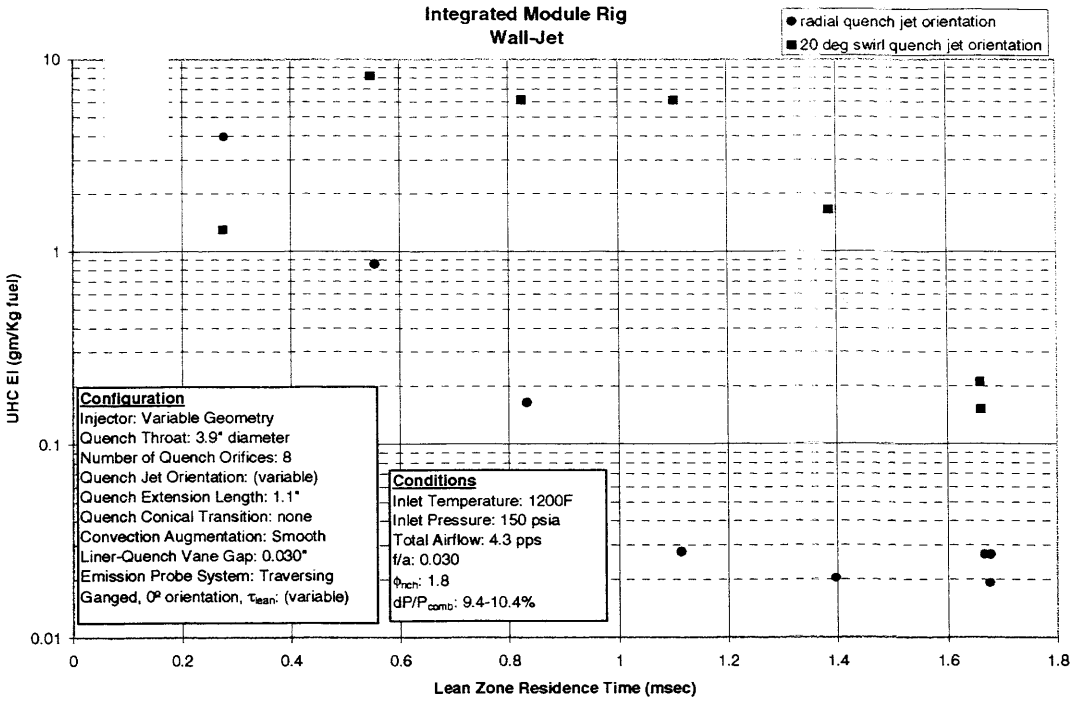

Figure VI - 80 Effect of Quench Jet Orientation on UHC Emissions as a Function of Lean Zone Residence Time

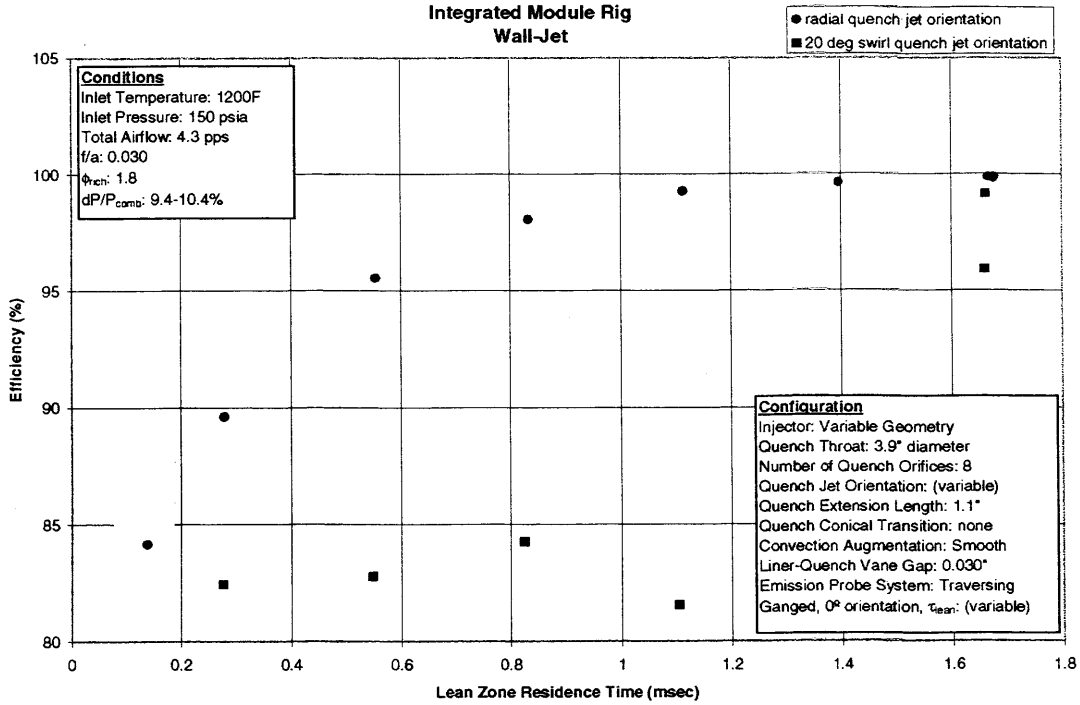

Figure VI - 81 Effect of Quench Jet Orientation on Efficiency as a Function of Lean Zone Residence Time

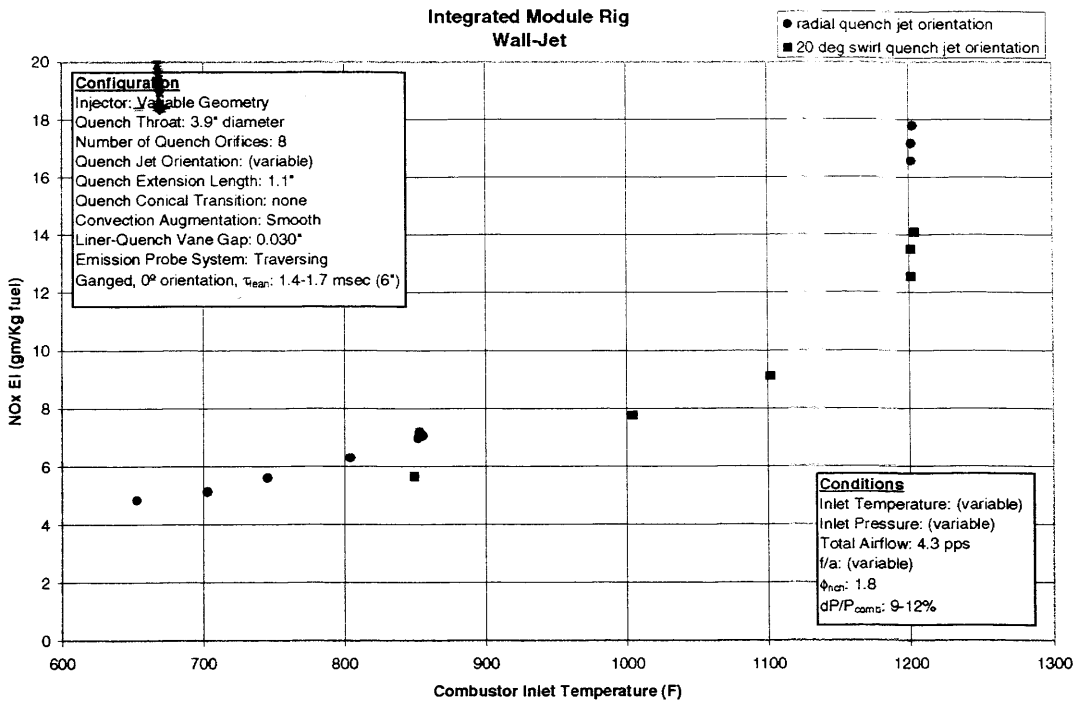

Figure VI - 82 Effect of Quench Jet Orientation on NOx Emissions as a Function of Inlet Temperature

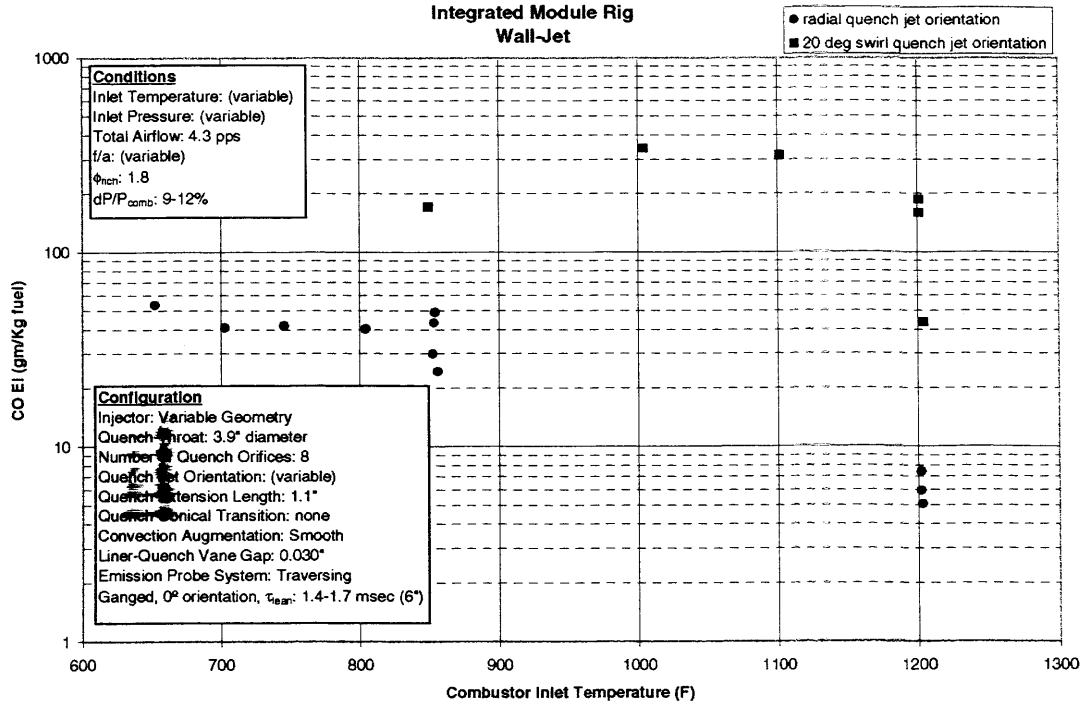

Figure VI - 83 Effect of Quench Jet Orientation on CO Emissions as a Function of Inlet Temperature

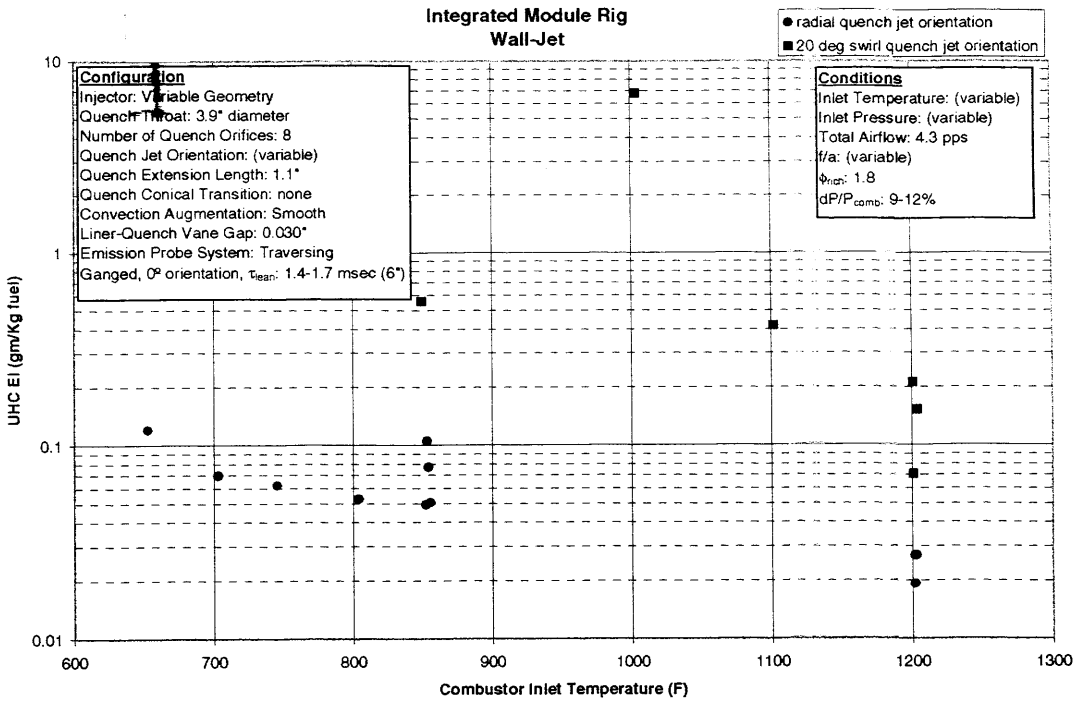

Figure VI - 84 Effect of Quench Jet Orientation on UHC Emissions as a Function of Inlet Temperature

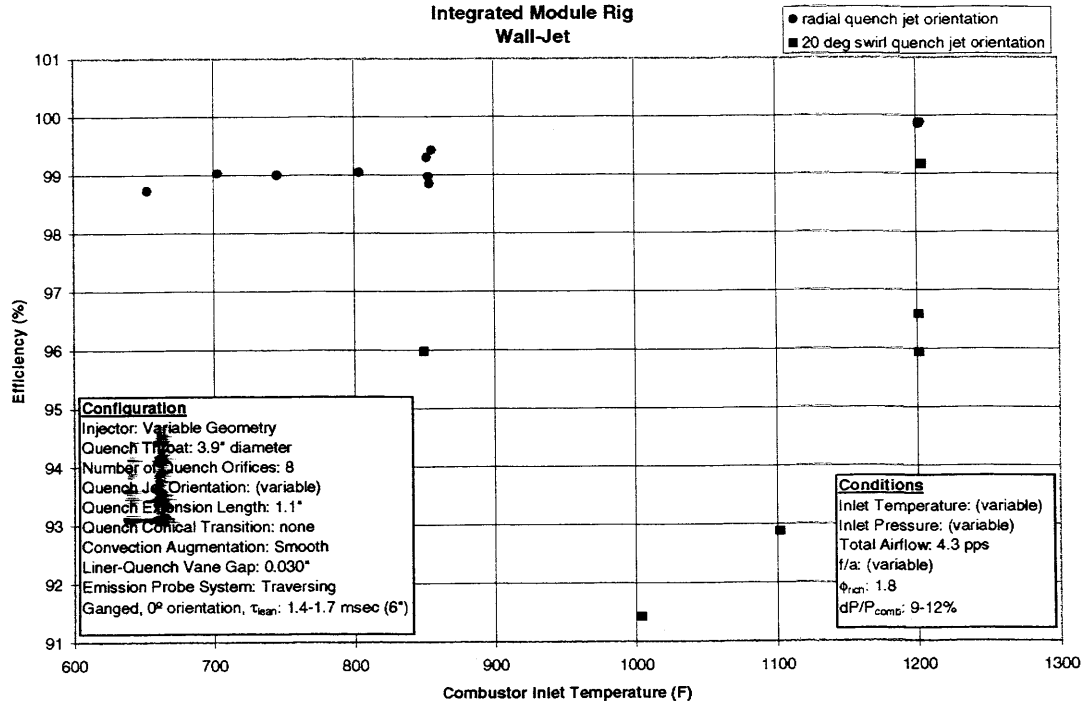

Figure VI - 85 Effect of Quench Jet Orientation on Efficiency as a Function of Inlet Temperature

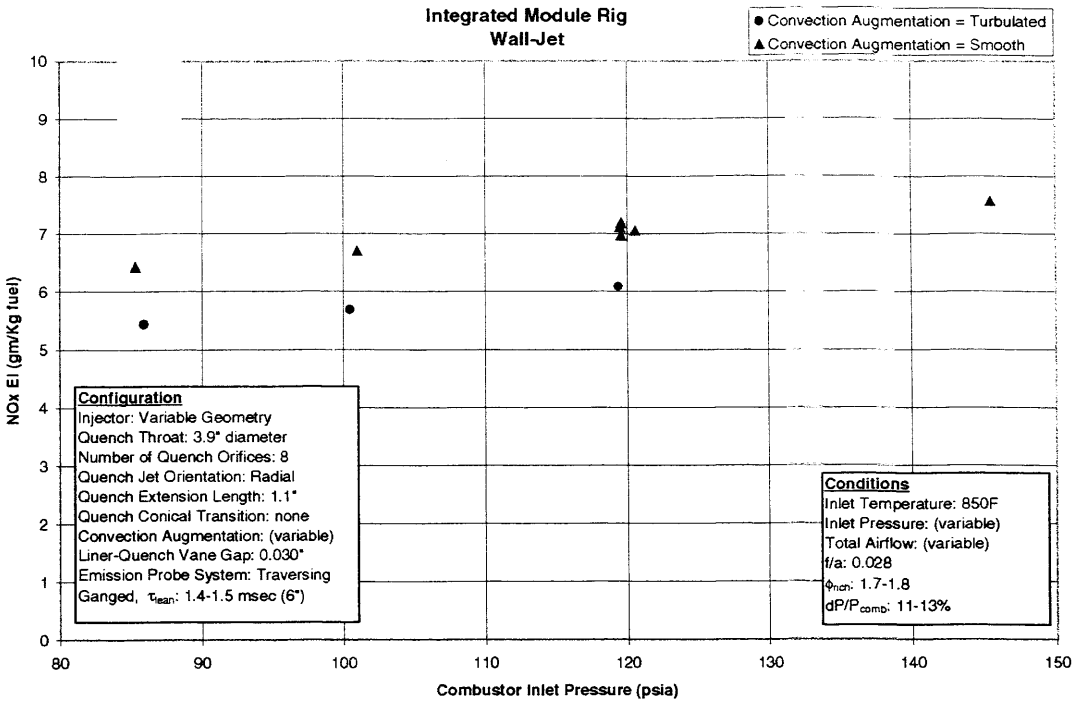

Figure VI - 86 Effect of Rich Zone Liner Backside Cooling Convection Augmentation on NOx Emissions as a Function of Inlet Pressure

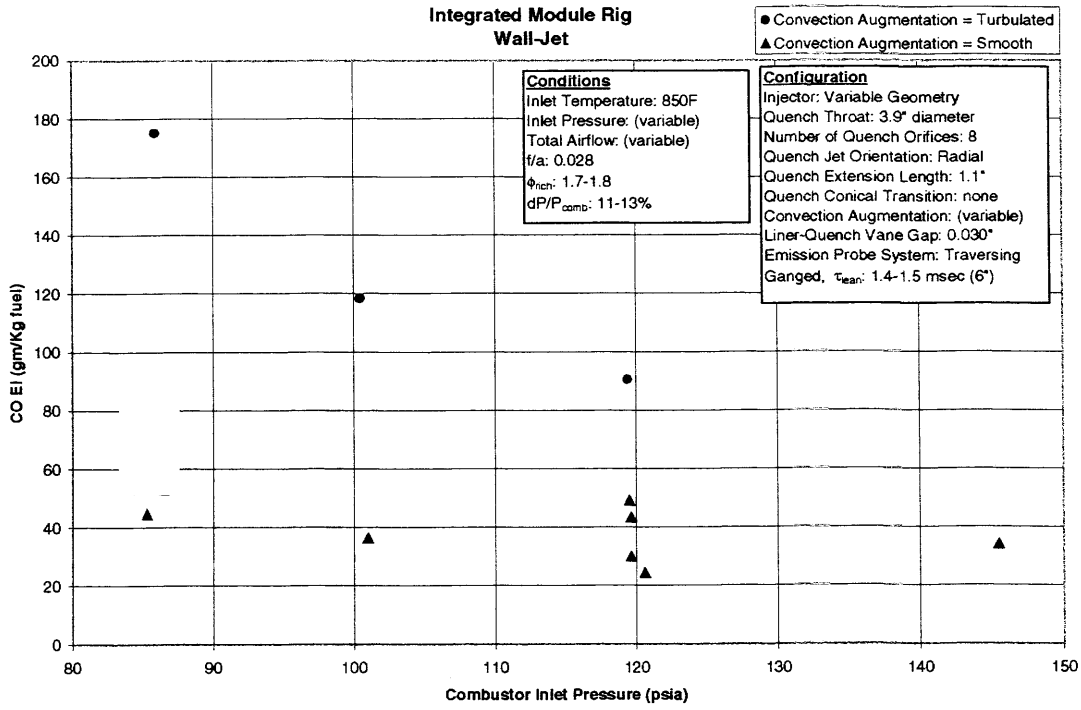

Figure VI - 87 Effect of Rich Zone Liner Backside Cooling Convection Augmentation on CO Emissions as a Function of Inlet Pressure

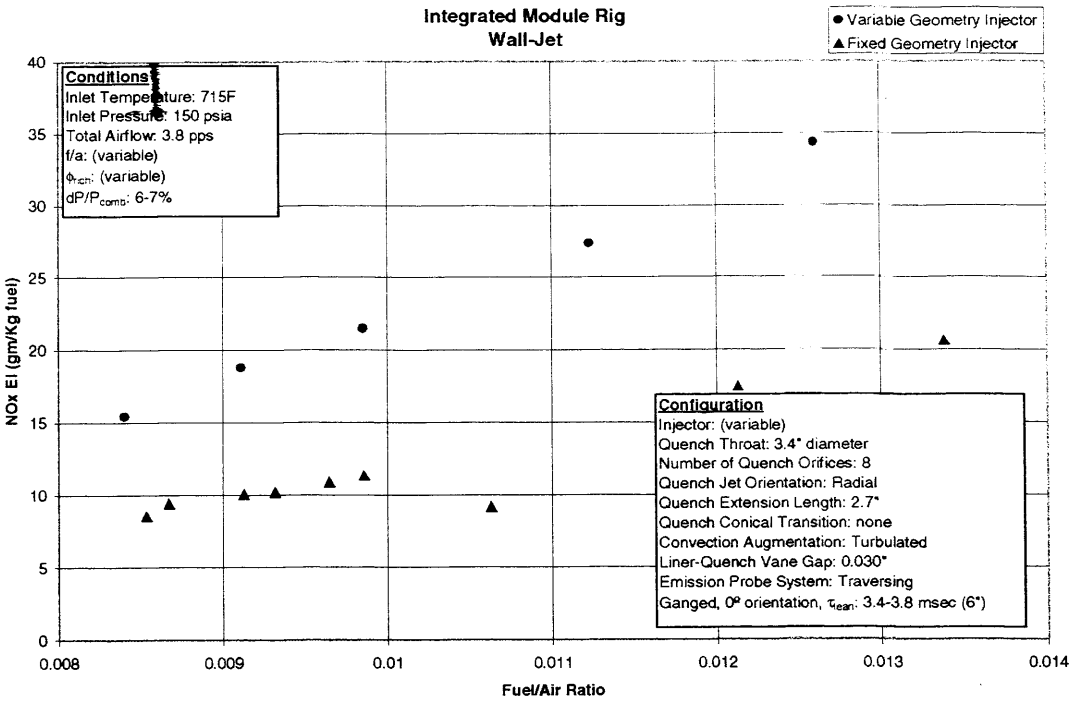

Figure VI - 88 Effect of Fuel Injector on NOx Emissions as a Function of Fuel/Air Ratio

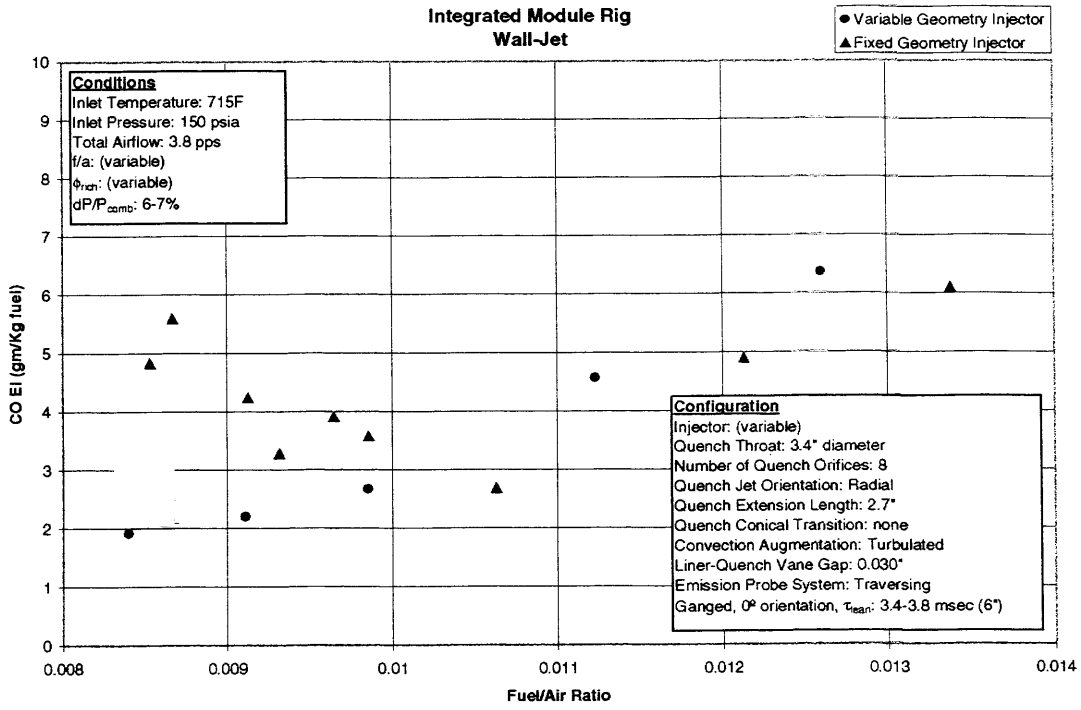

Figure VI - 89 Effect of Fuel Injector on CO Emissions as a Function of Fuel/Air Ratio

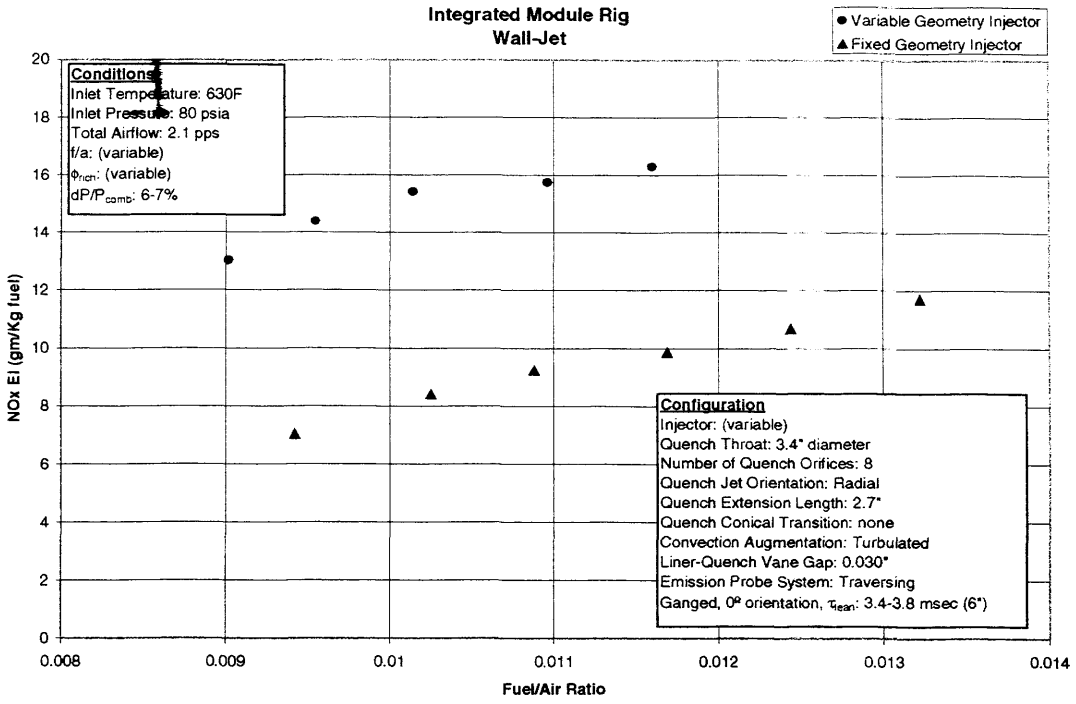

Figure VI - 90 Effect of Fuel Injector on NOx Emissions as a Function of Fuel/Air Ratio

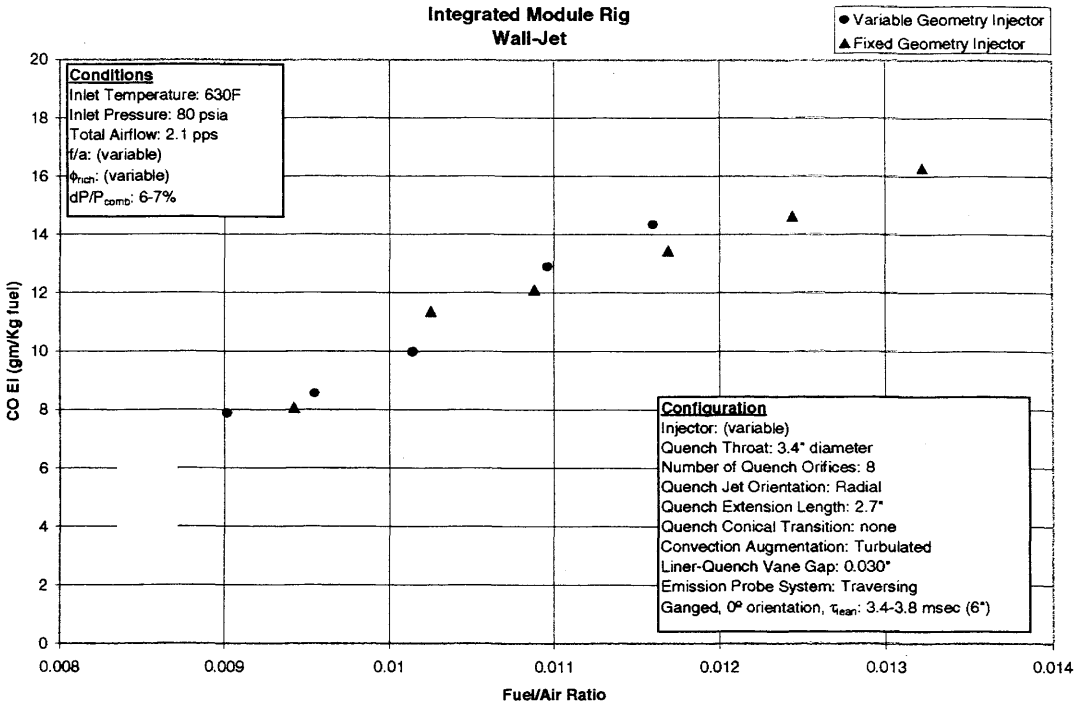

Figure VI - 91 Effect of Fuel Injector on CO Emissions as a Function of Fuel/Air Ratio

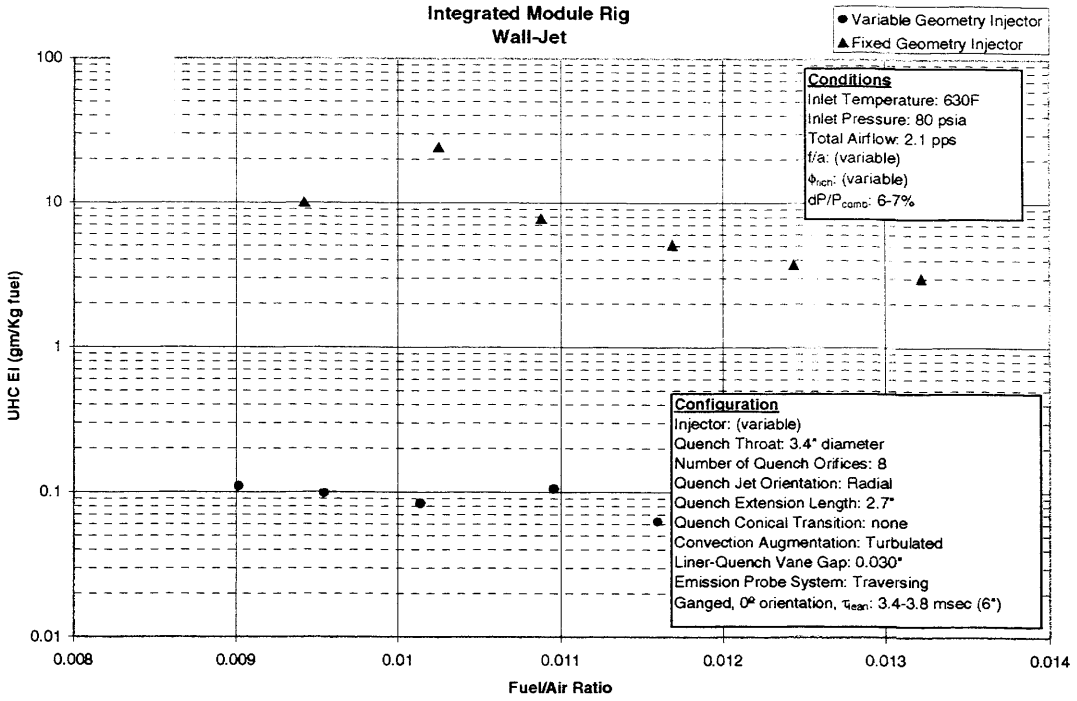

Figure VI - 92 Effect of Fuel Injector on UHC Emissions as a Function of Fuel/Air Ratio

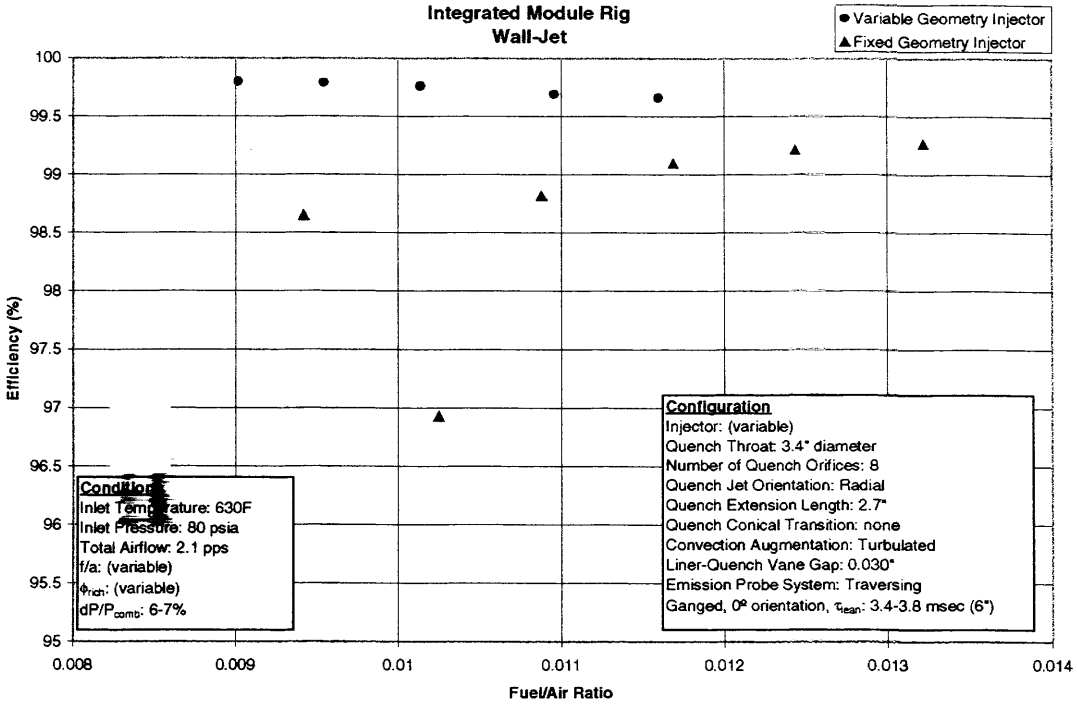

Figure VI - 93 Effect of Fuel Injector on Efficiency as a Function of Fuel/Air Ratio

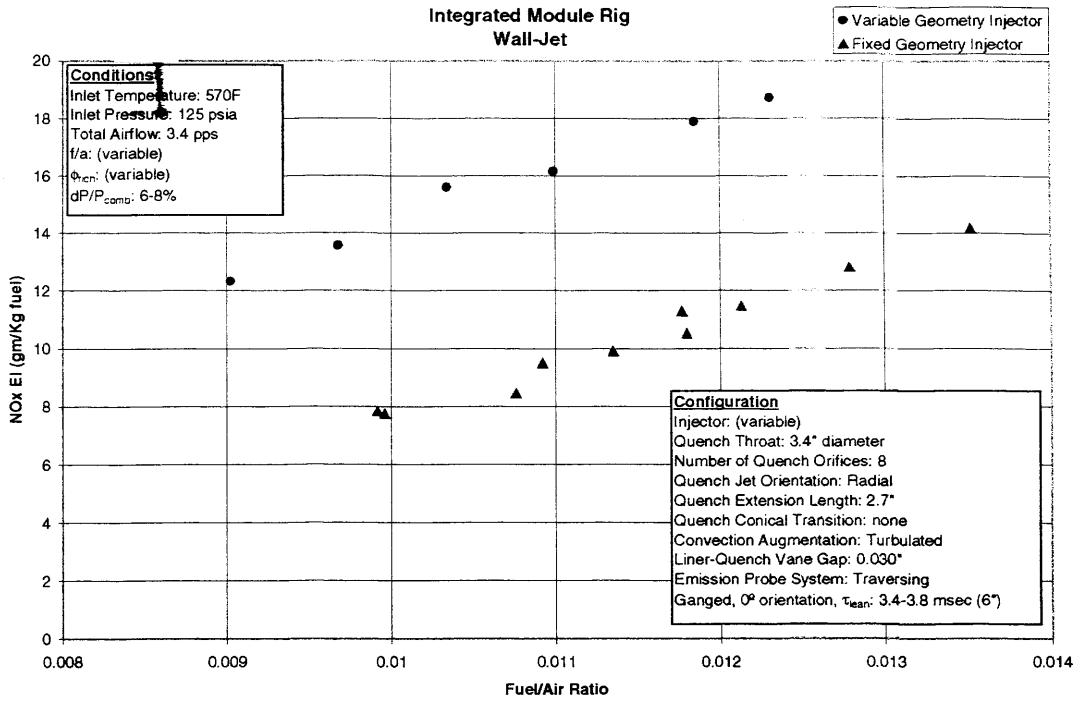

Figure VI - 94 Effect of Fuel Injector on NOx Emissions as a Function of Fuel/Air Ratio

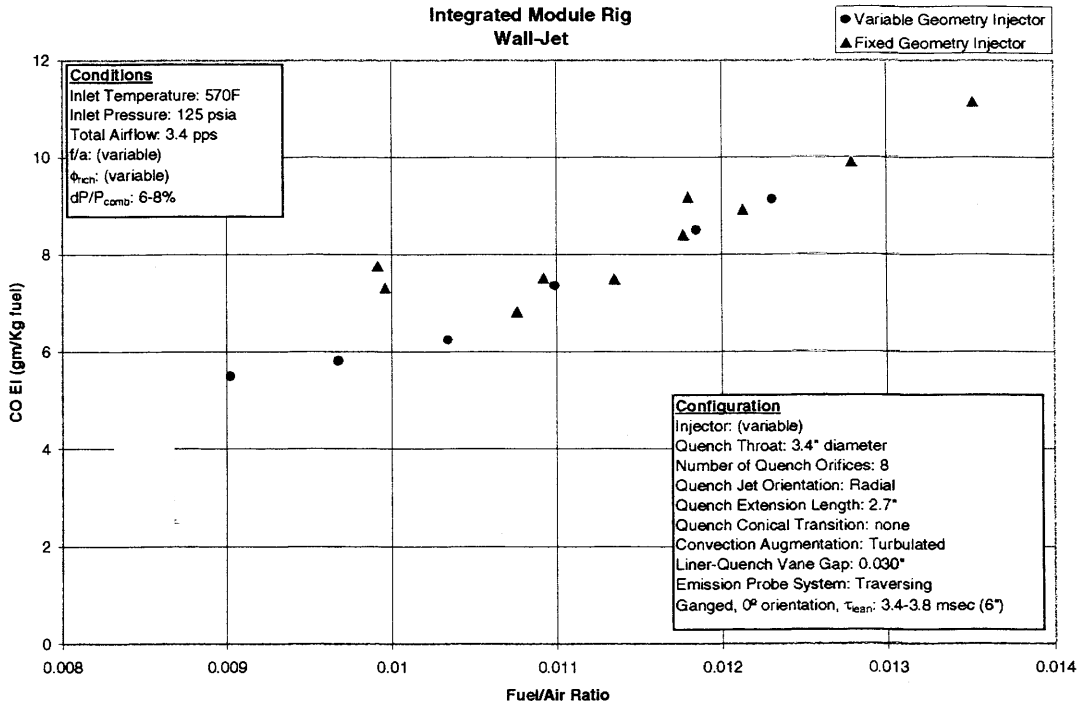

Figure VI - 95 Effect of Fuel Injector on CO Emissions as a Function of Fuel/Air Ratio

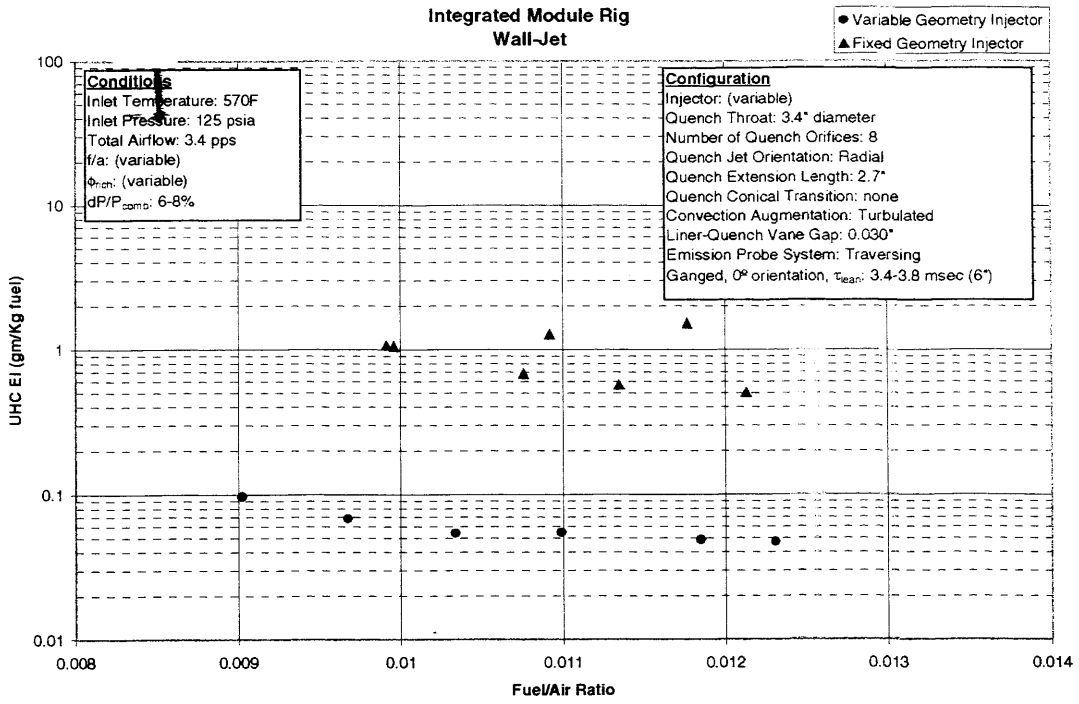

Figure VI - 96 Effect of Fuel Injector on UHC Emissions as a Function of Fuel/Air Ratio

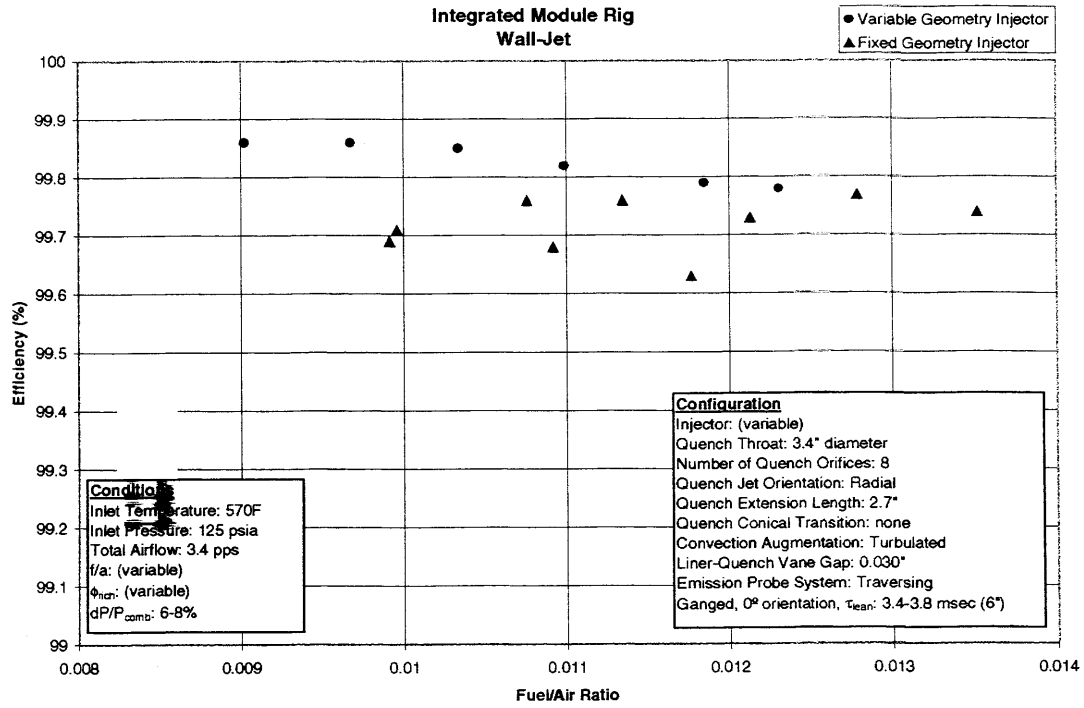

Figure VI - 97 Effect of Fuel Injector on Efficiency as a Function of Fuel/Air Ratio

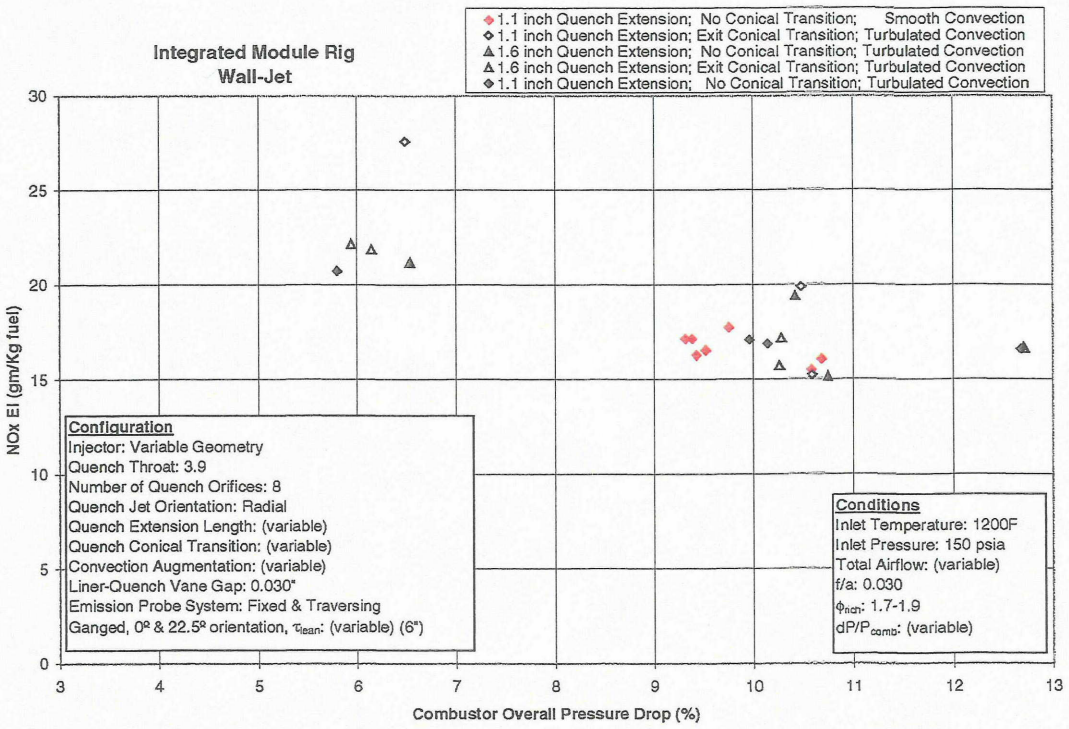

Figure VI - 98 NOx Emissions as a Function of Combustor Pressure Drop

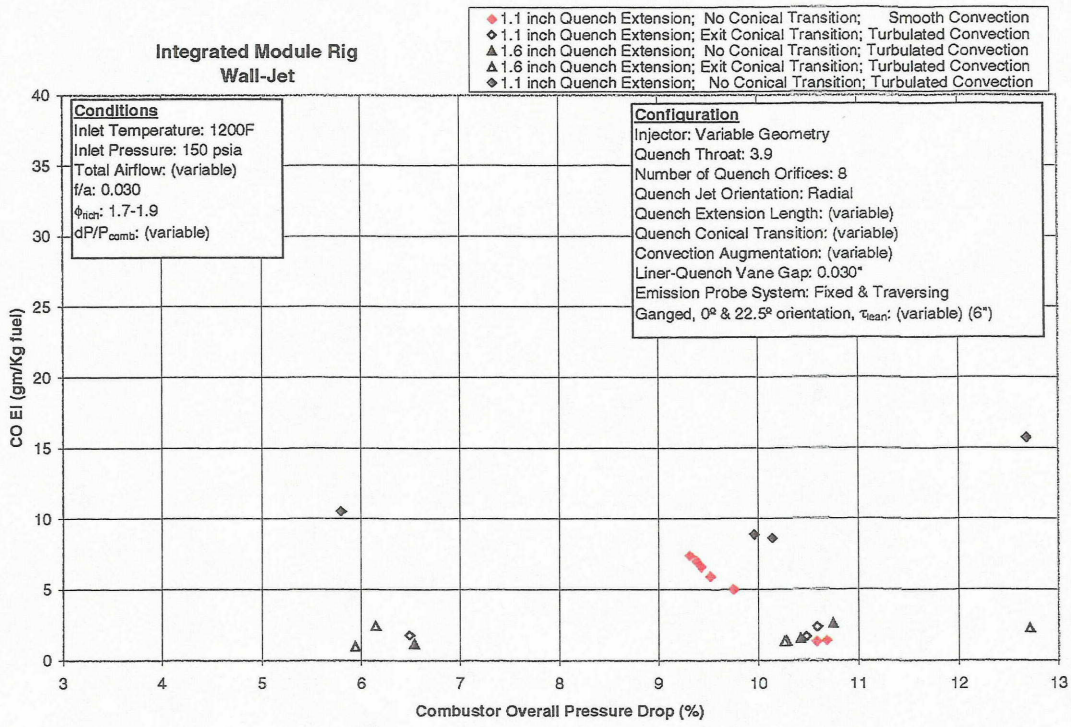

Figure VI - 99 CO Emissions as a Function of Combustor Pressure Drop

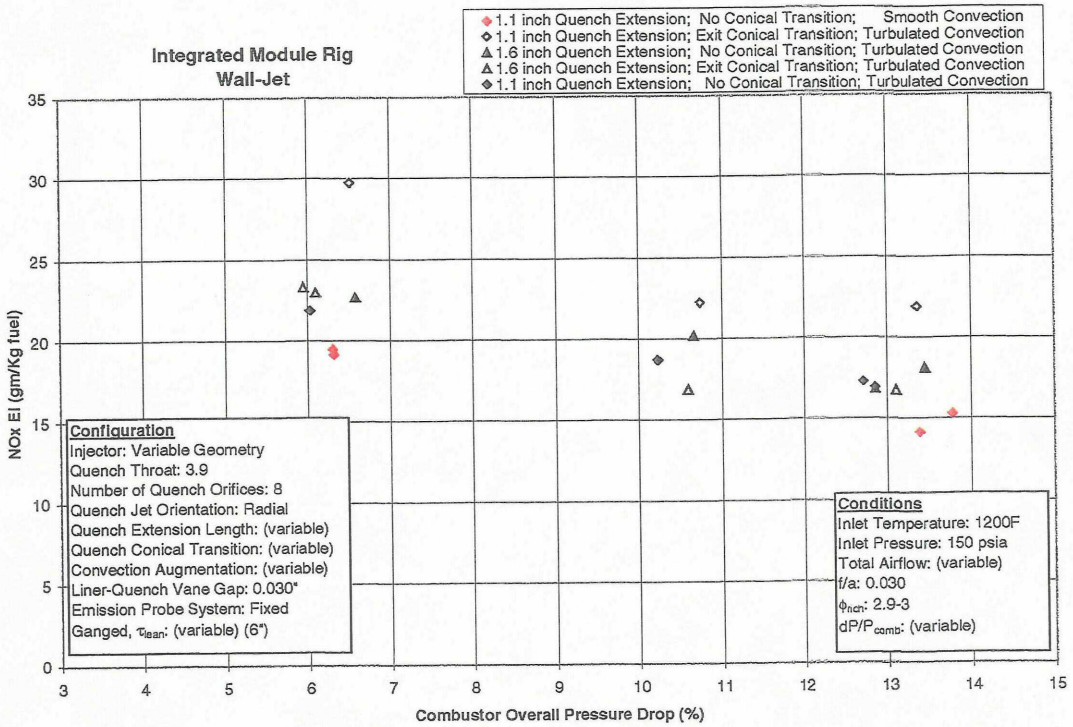

Figure VI - 100 NOx Emissions as a Function of Combustor Pressure Drop

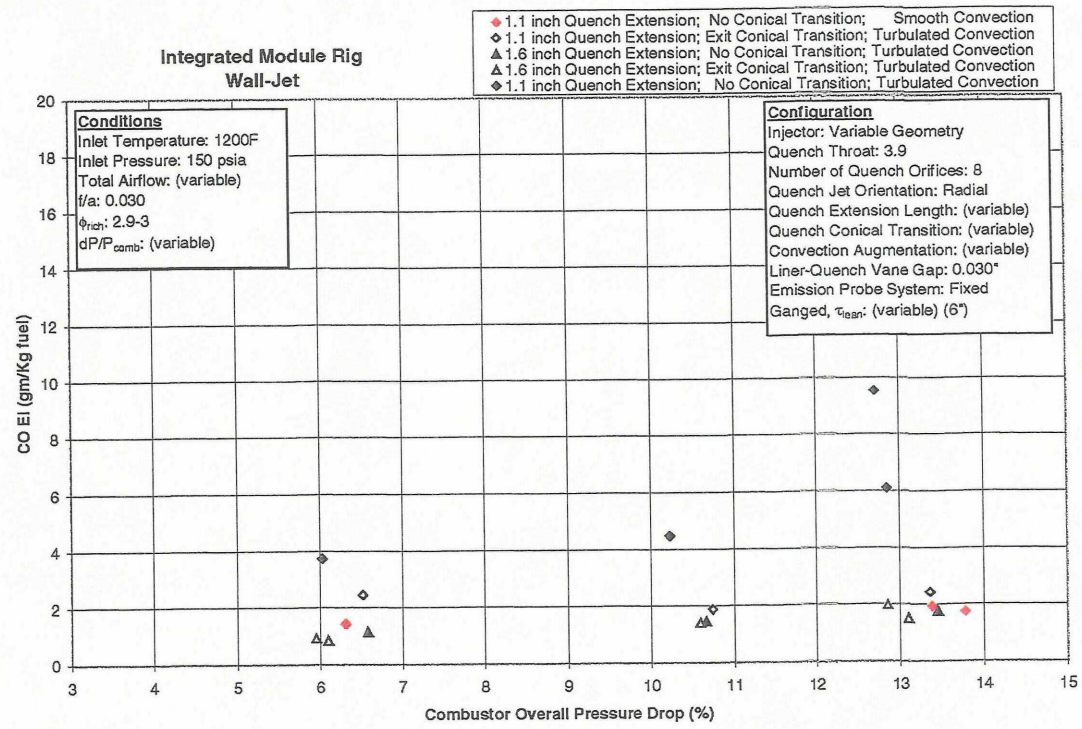

Figure VI - 101 CO Emissions as a Function of Combustor Pressure Drop

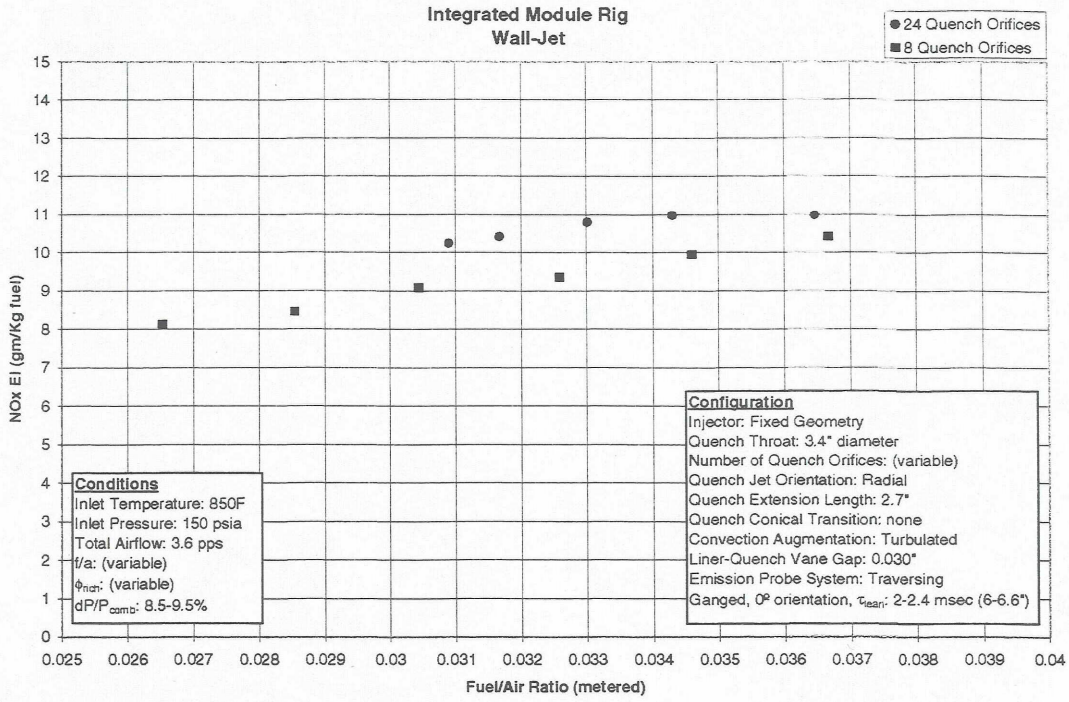

Figure VI - 102 NOx Emissions as a Function of Metered Fuel/Air Ratio

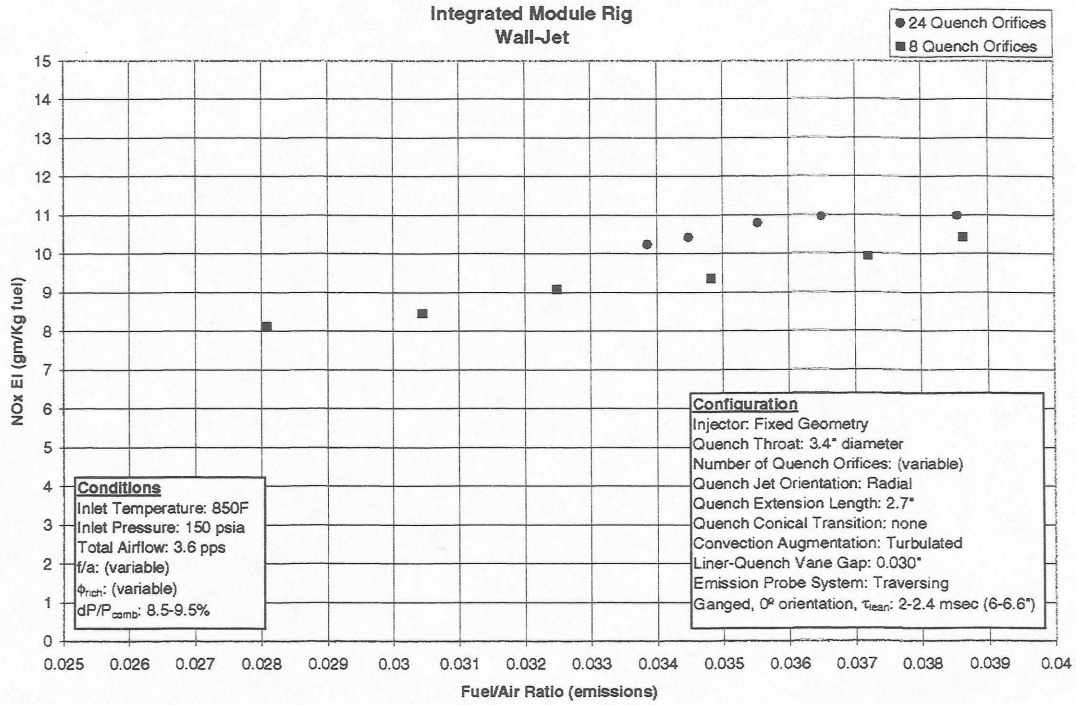

Figure VI - 103 NOx Emissions as a Function of Emissions Fuel/Air Ratio

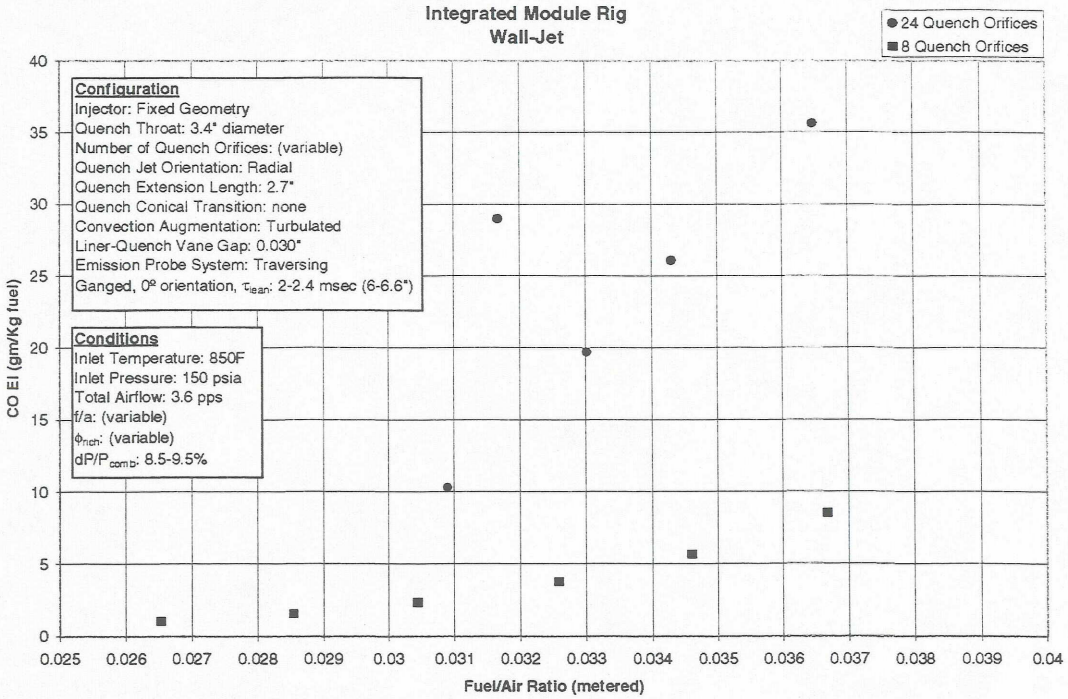

Figure VI - 104 CO Emissions as a Function of Metered Fuel/Air Ratio

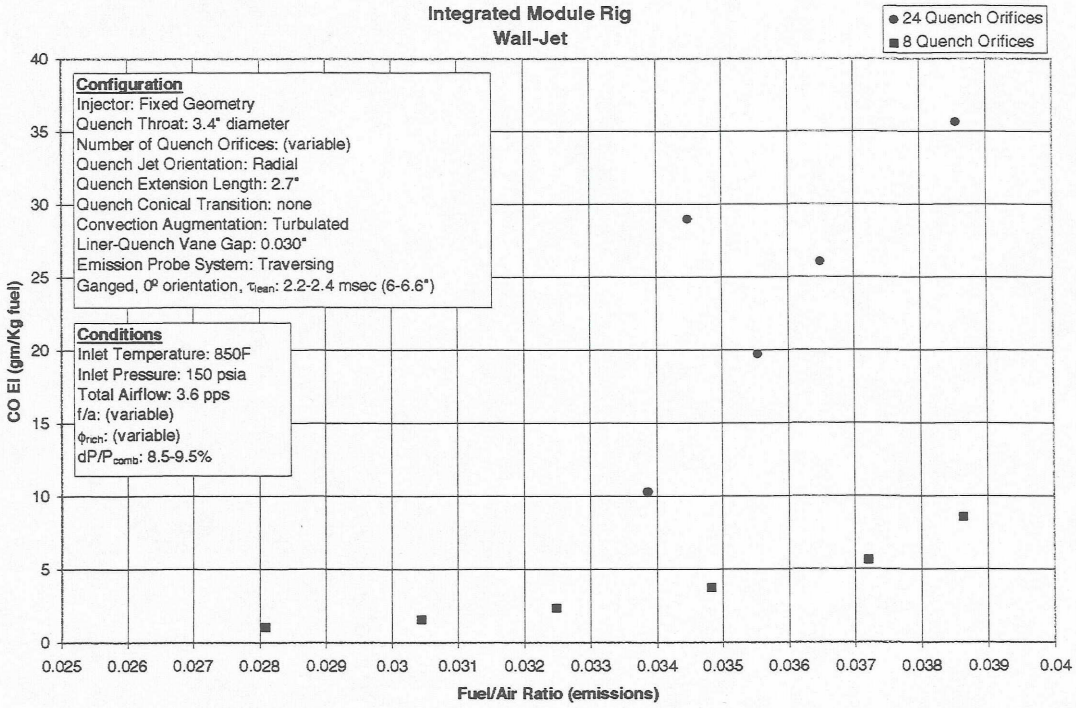

Figure VI - 105 CO Emissions as a Function of Emissions Fuel/Air Ratio

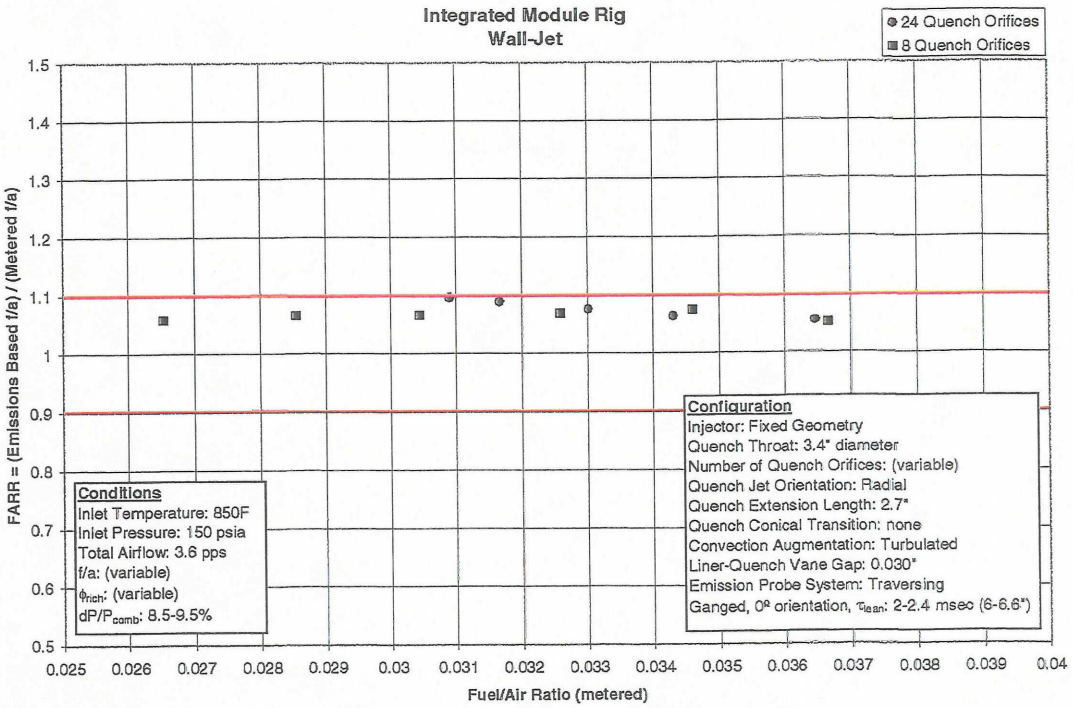

Figure VI - 106 FARR (Emissions Fuel/Air Ratio relative to Metered Fuel Air Ratio) as a Function of Metered Fuel/Air Ratio

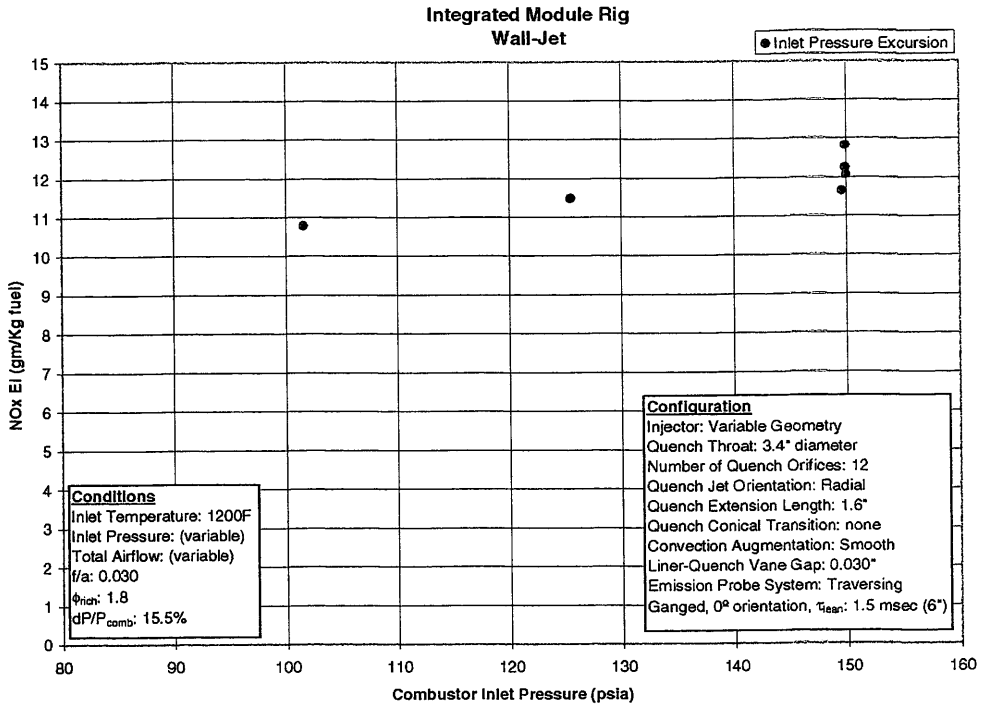

Figure VI - 107 NOx Emissions as a Function of Inlet Pressure

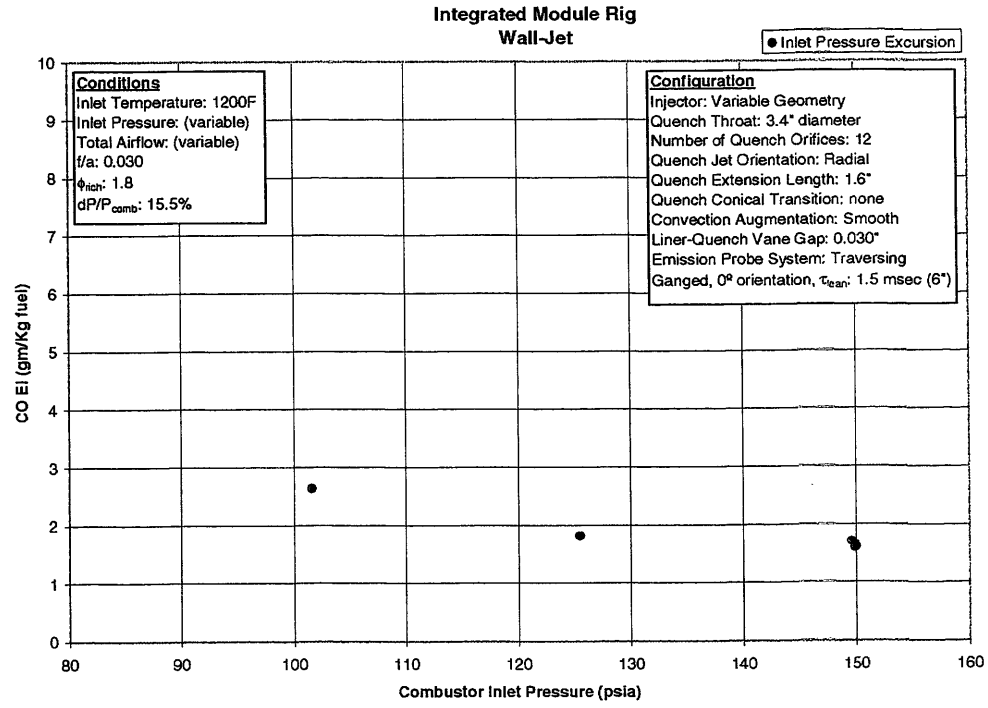

Figure VI - 108 CO Emissions as a Function of Inlet Pressure

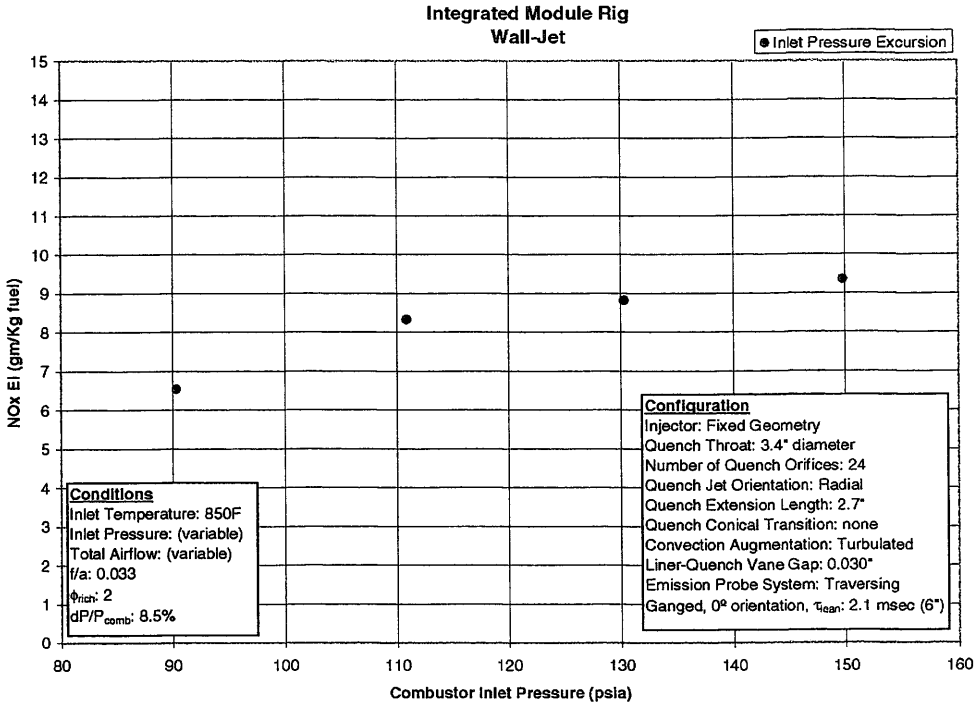

Figure VI - 109 NOx Emissions as a Function of Inlet Pressure

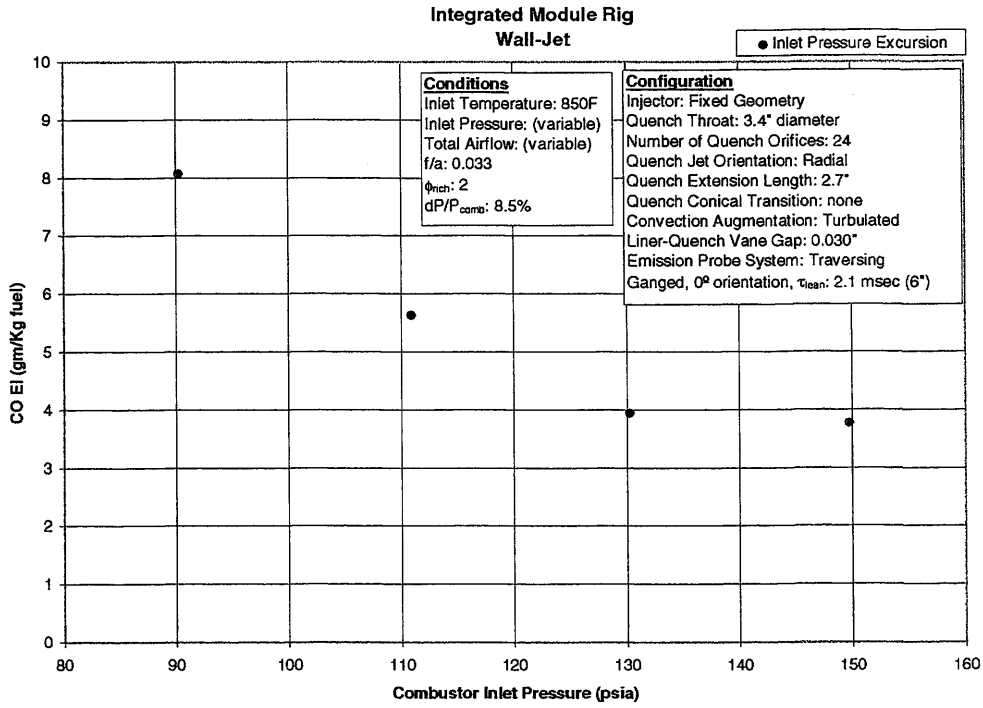

Figure VI - 110 CO Emissions as a Function of Inlet Pressure

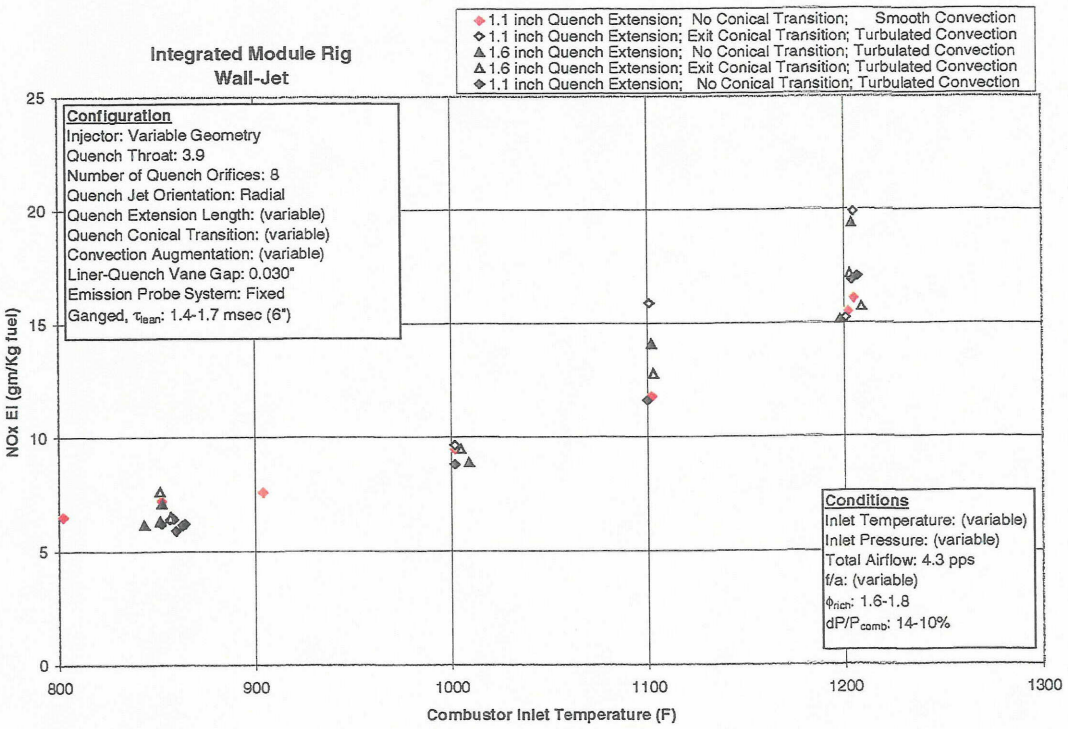

Figure VI - 111 NOx Emissions as a Function of Inlet Temperature

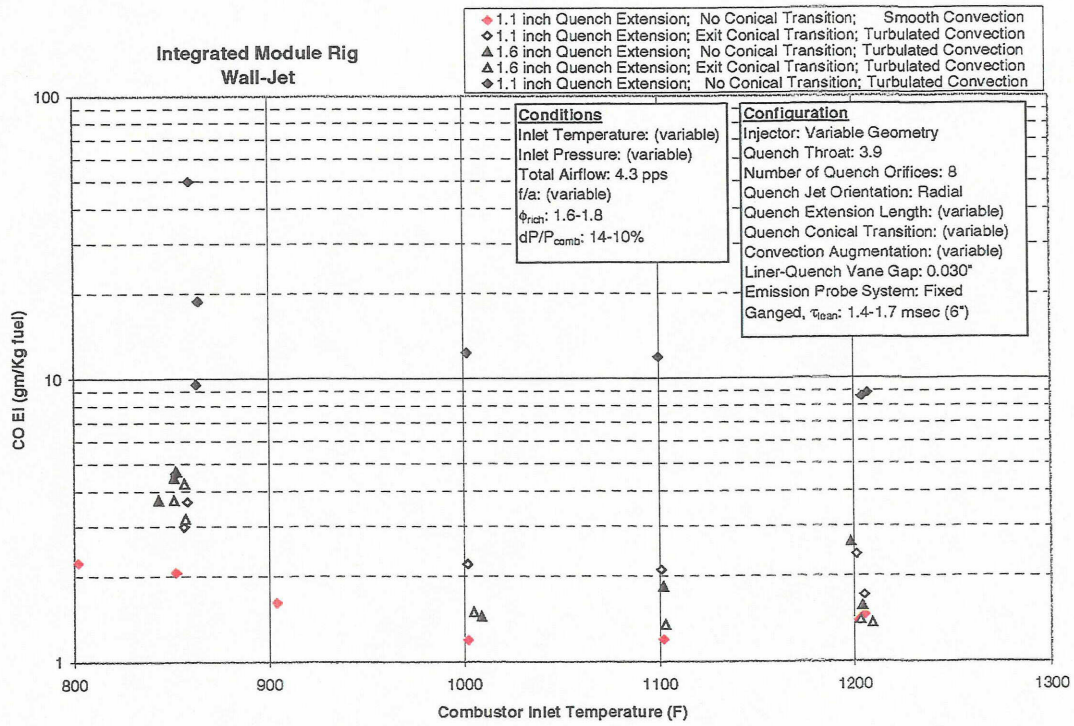

Figure VI - 112 CO Emissions as a Function of Inlet Temperature

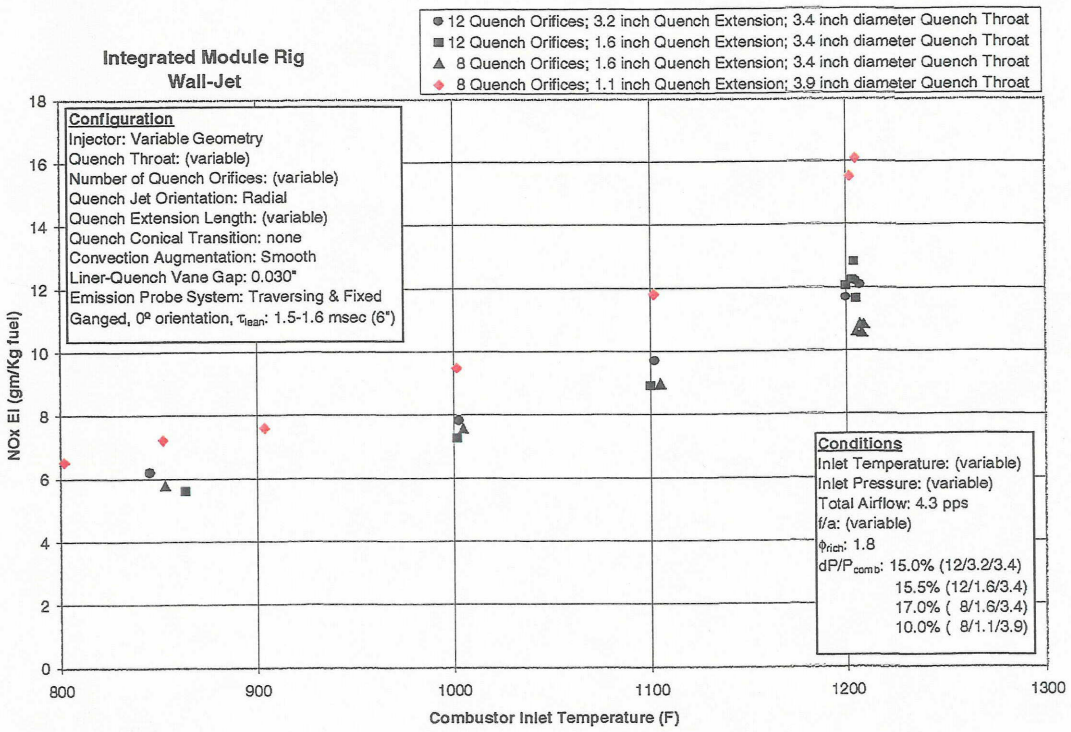

Figure VI - 113 NOx Emissions as a Function of Inlet Temperature

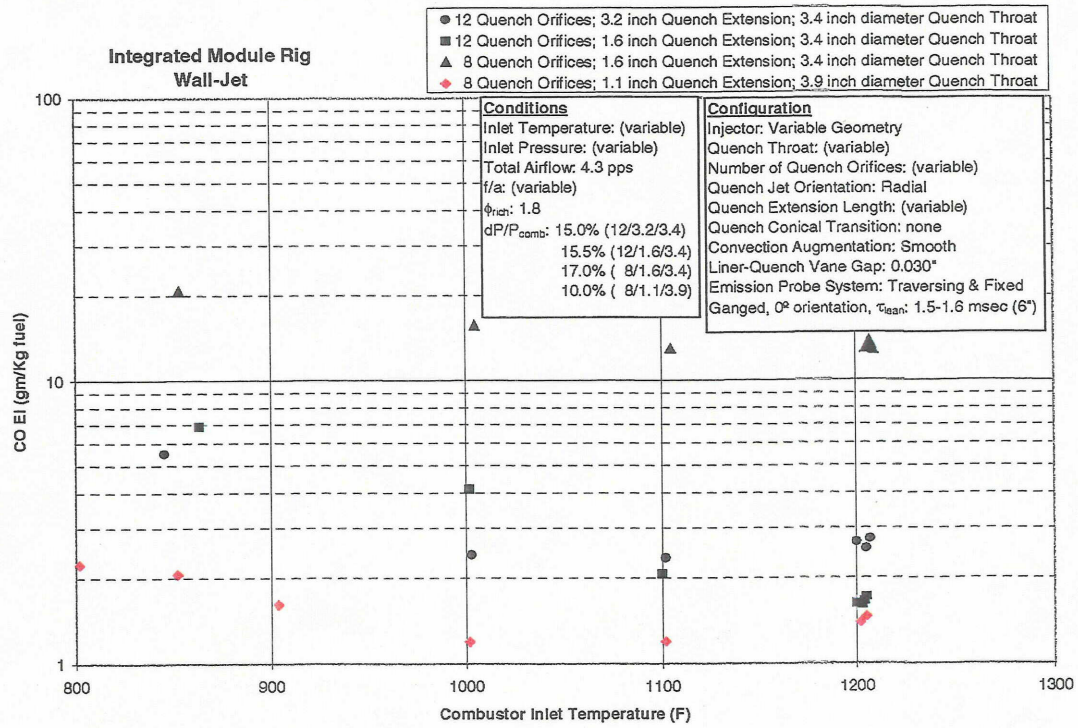

Figure VI - 114 CO Emissions as a Function of Inlet Temperature

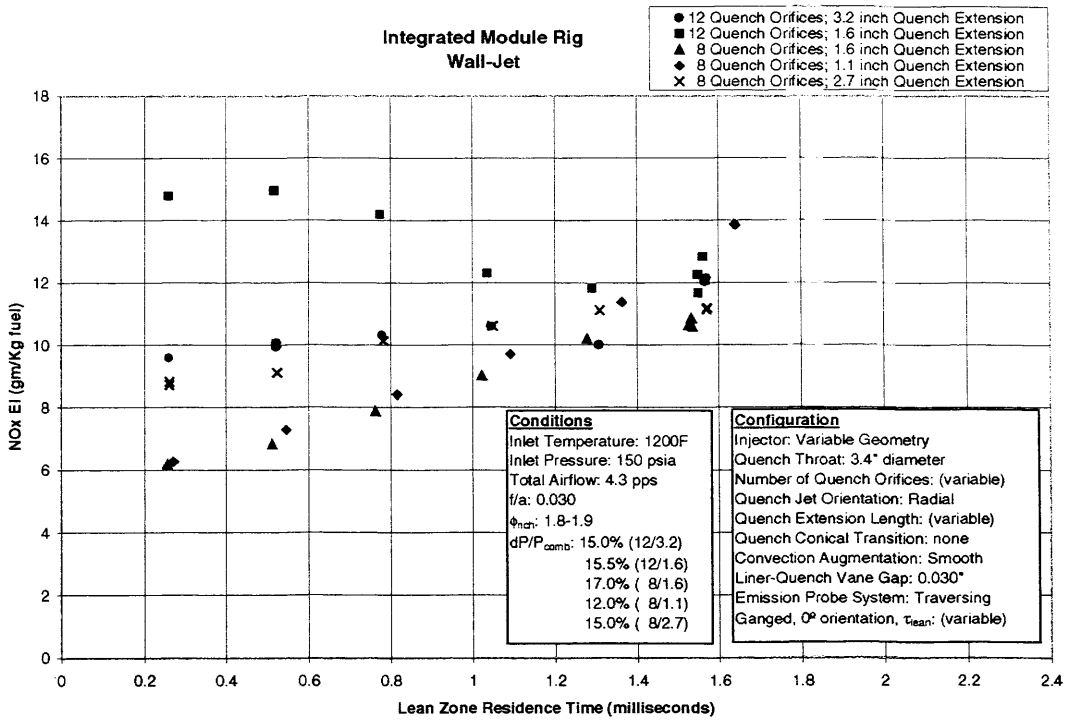

Figure VI - 115 NOx Emissions as a Function of Lean Zone Residence Time

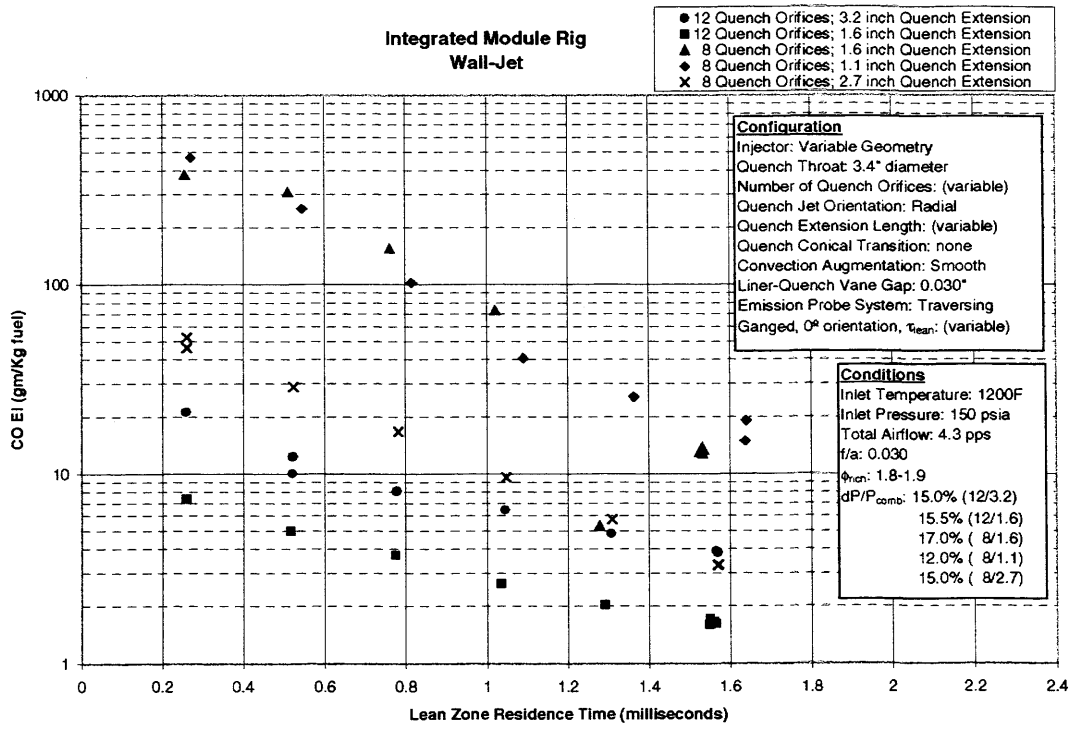

Figure VI - 116 CO Emissions as a Function of Lean Zone Residence Time

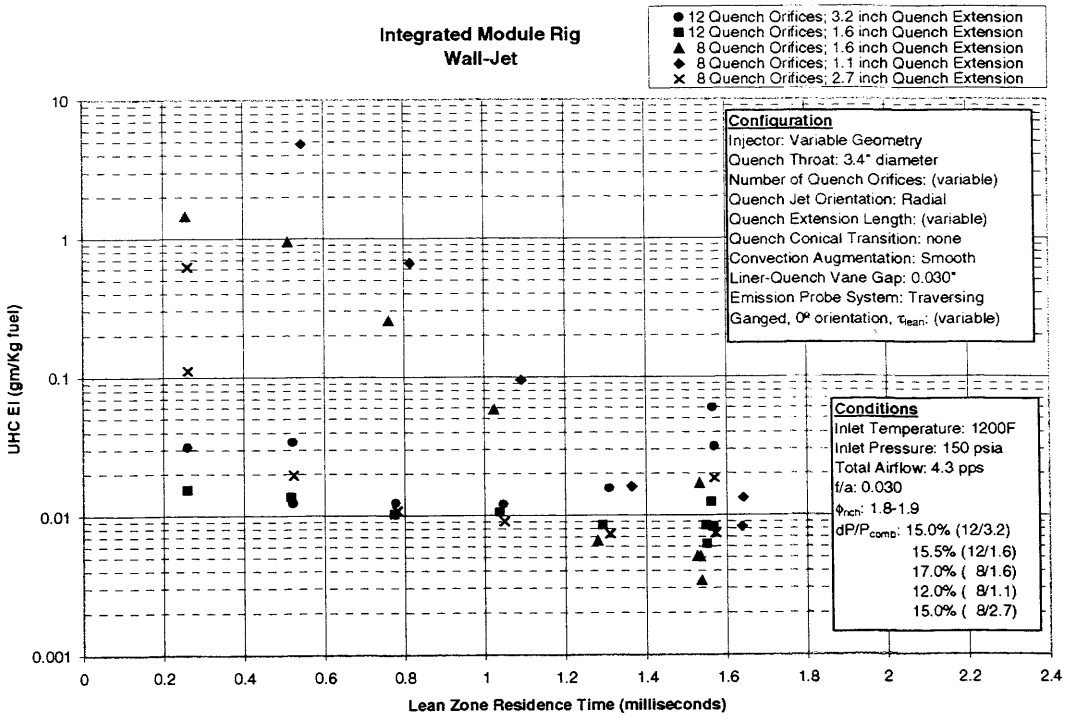

Figure VI - 117 UHC Emissions as a Function of Lean Zone Residence Time

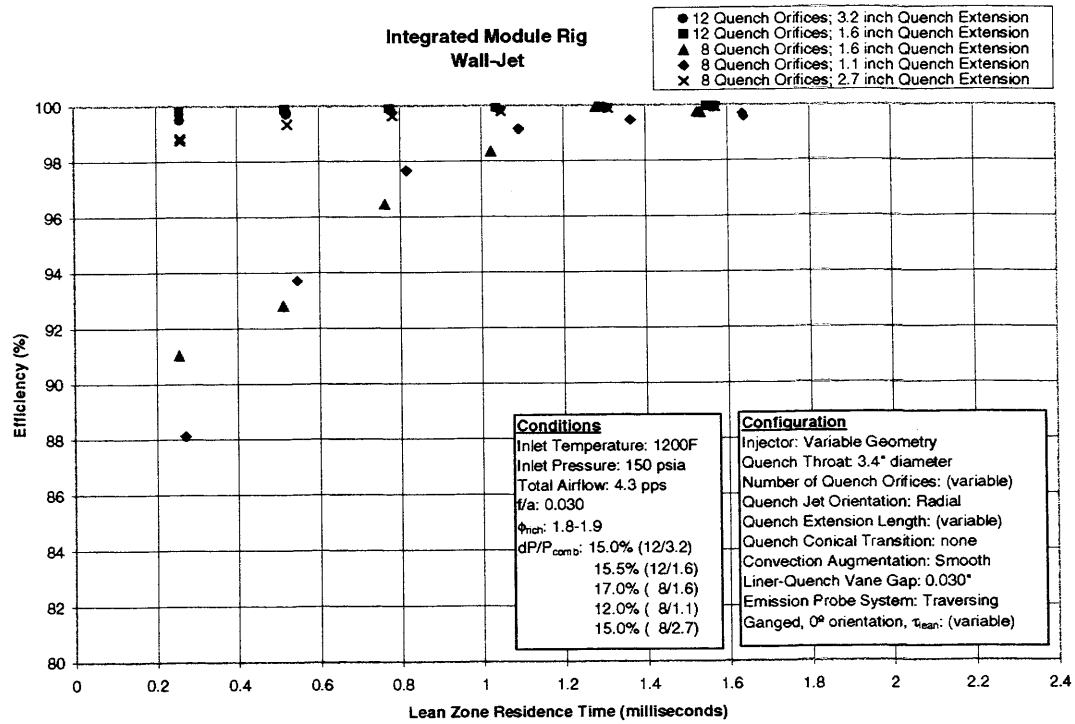

Figure VI - 118 Efficiency as a Function of Lean Zone Residence Time

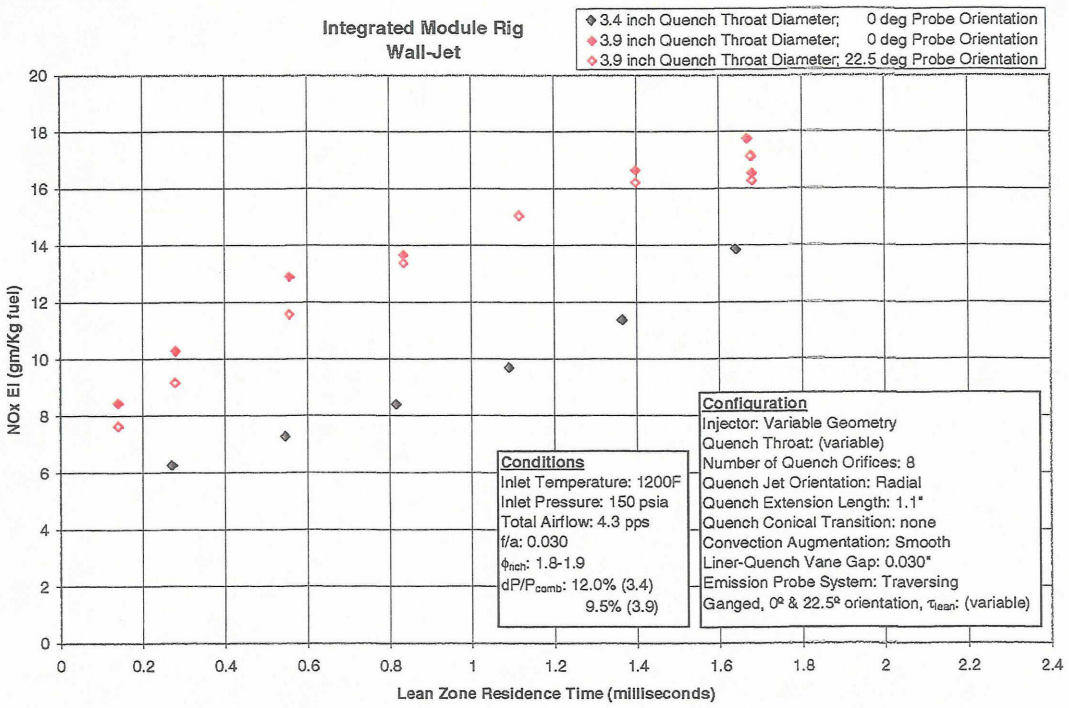

Figure VI - 119 NOx Emissions as a Function of Lean Zone Residence Time

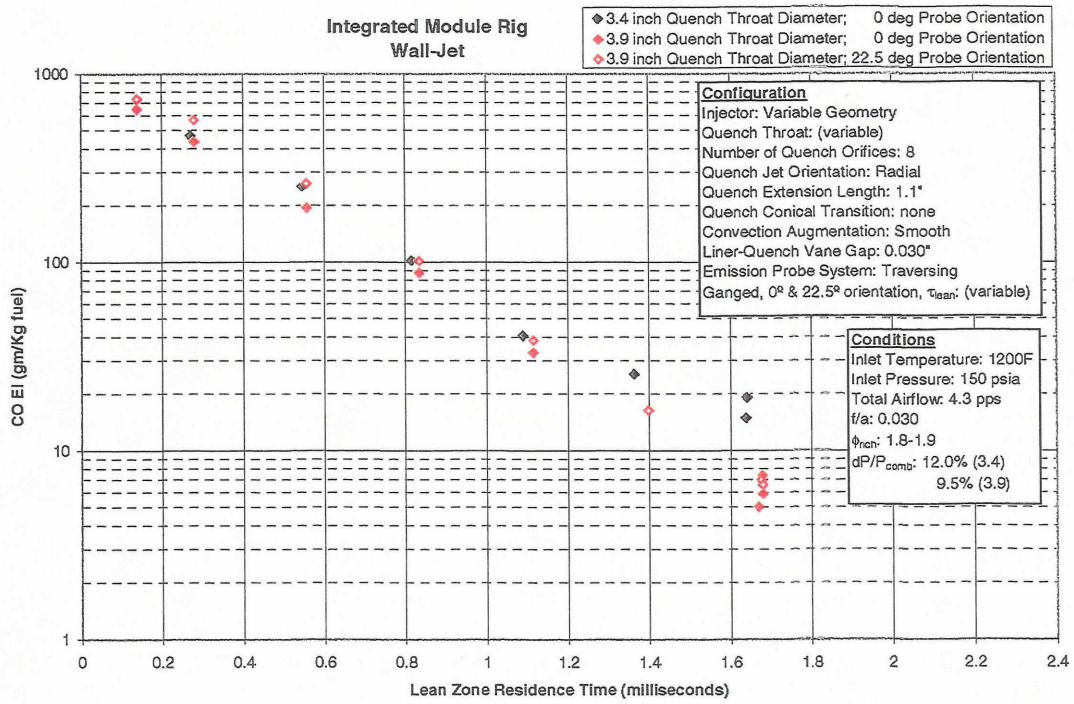

Figure VI - 120 CO Emissions as a Function of Lean Zone Residence Time

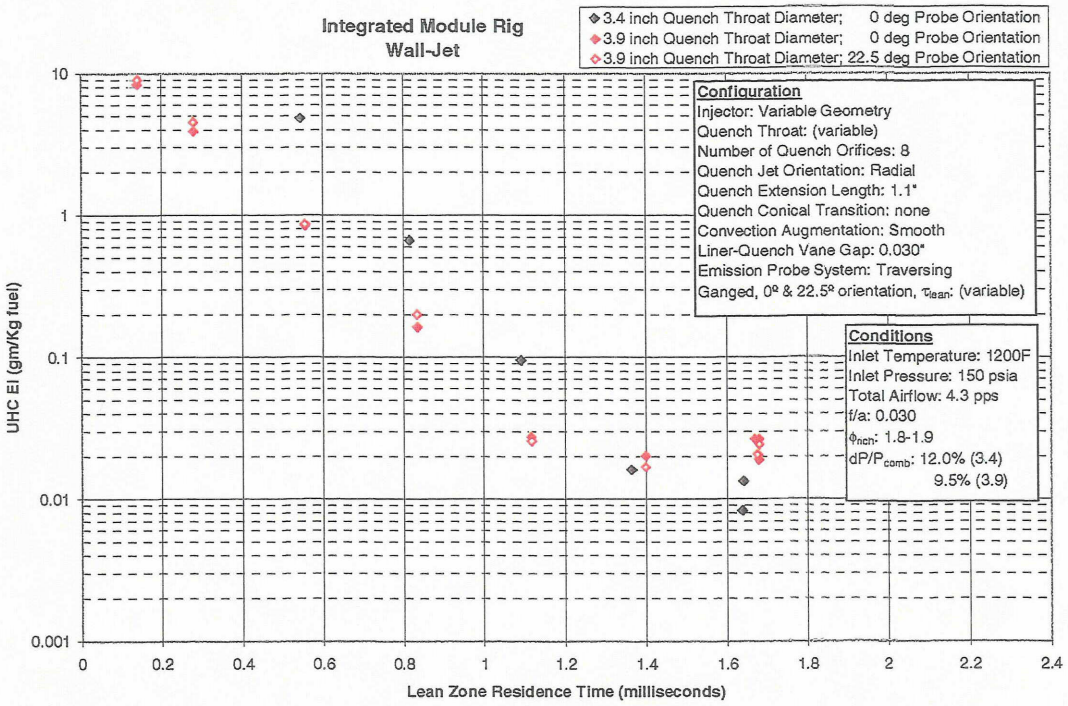

Figure VI - 121 UHC Emissions as a Function of Lean Zone Residence Time

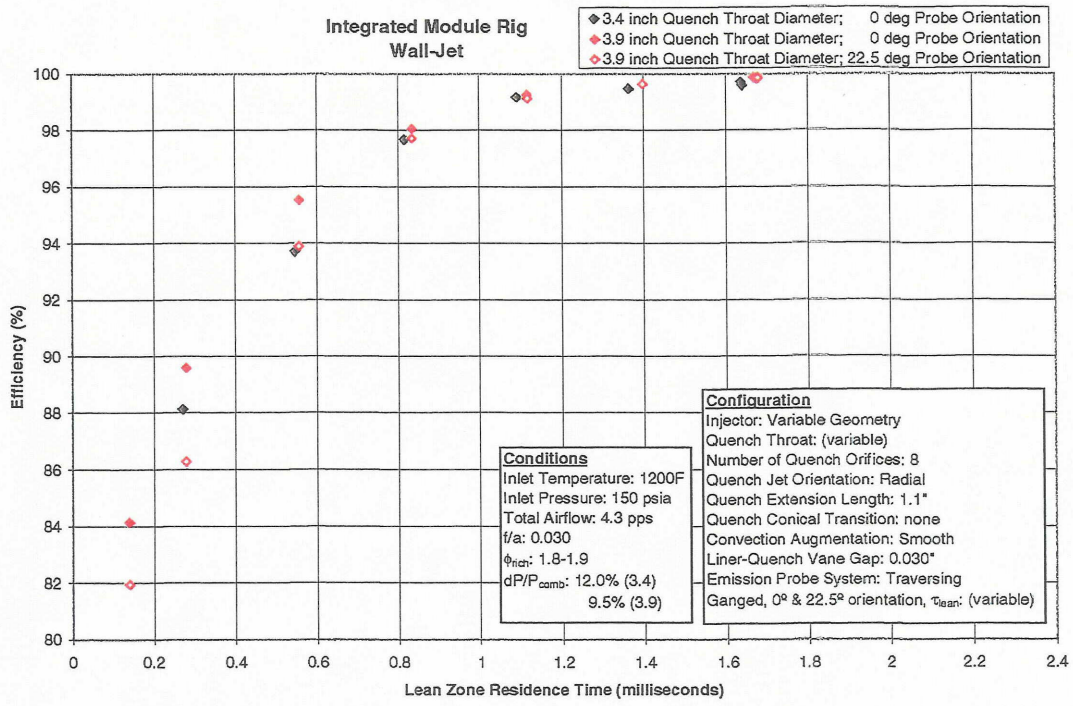

Figure VI - 122 Efficiency as a Function of Lean Zone Residence Time

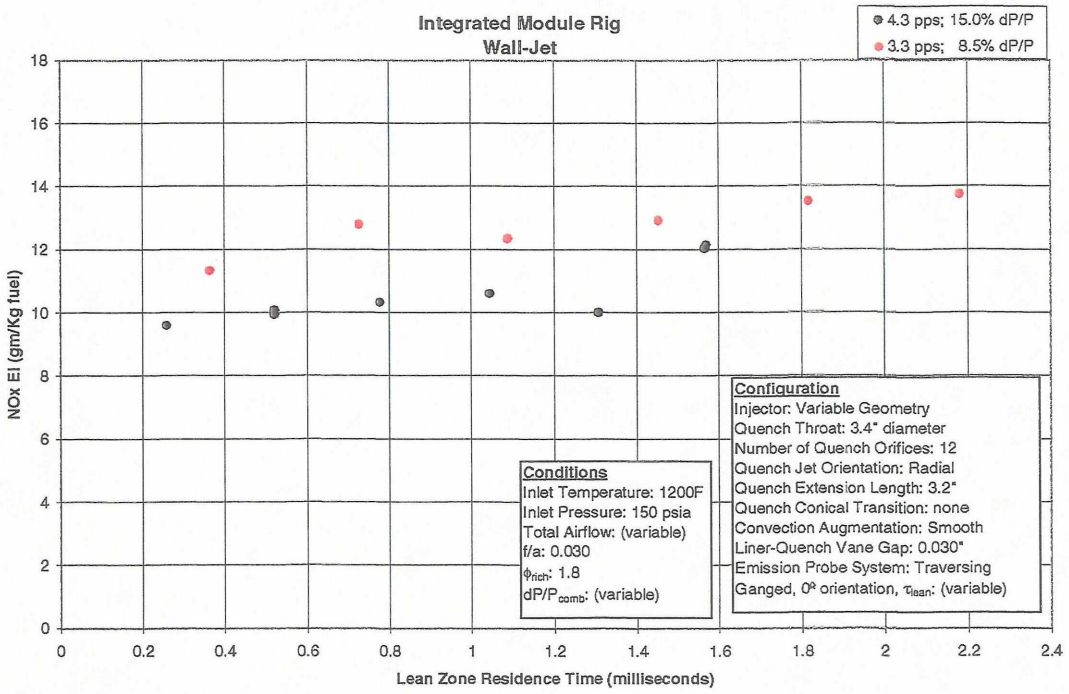

Figure VI - 123 NOx Emissions as a Function of Lean Zone Residence Time

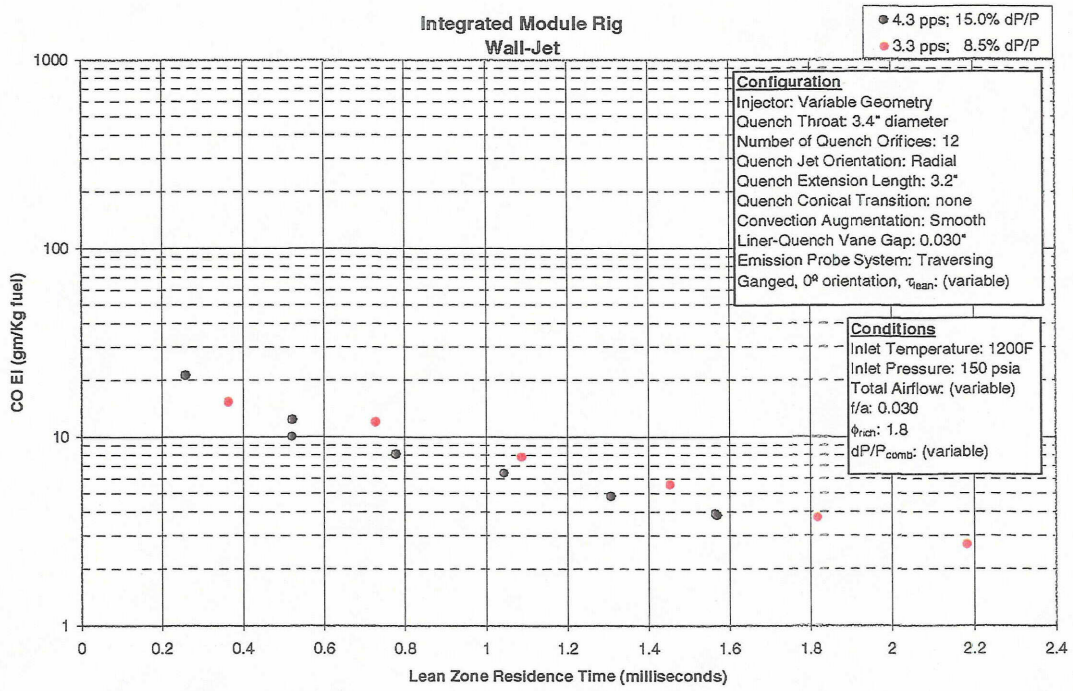

Figure VI - 124 CO Emissions as a Function of Lean Zone Residence Time

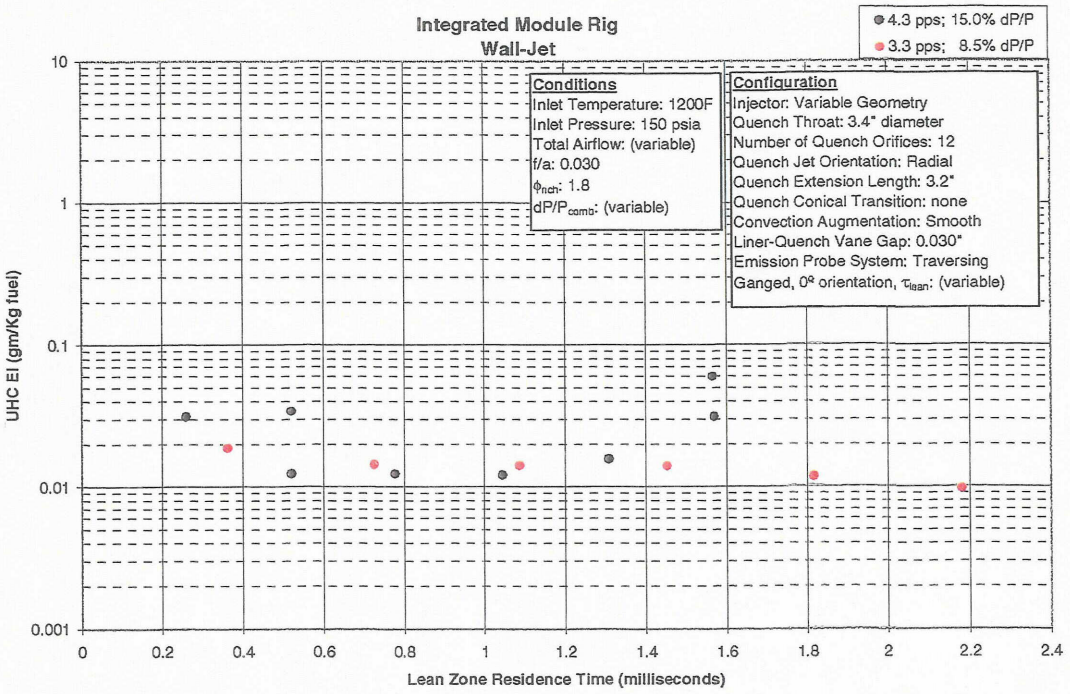

Figure VI - 125 UHC Emissions as a Function of Lean Zone Residence Time

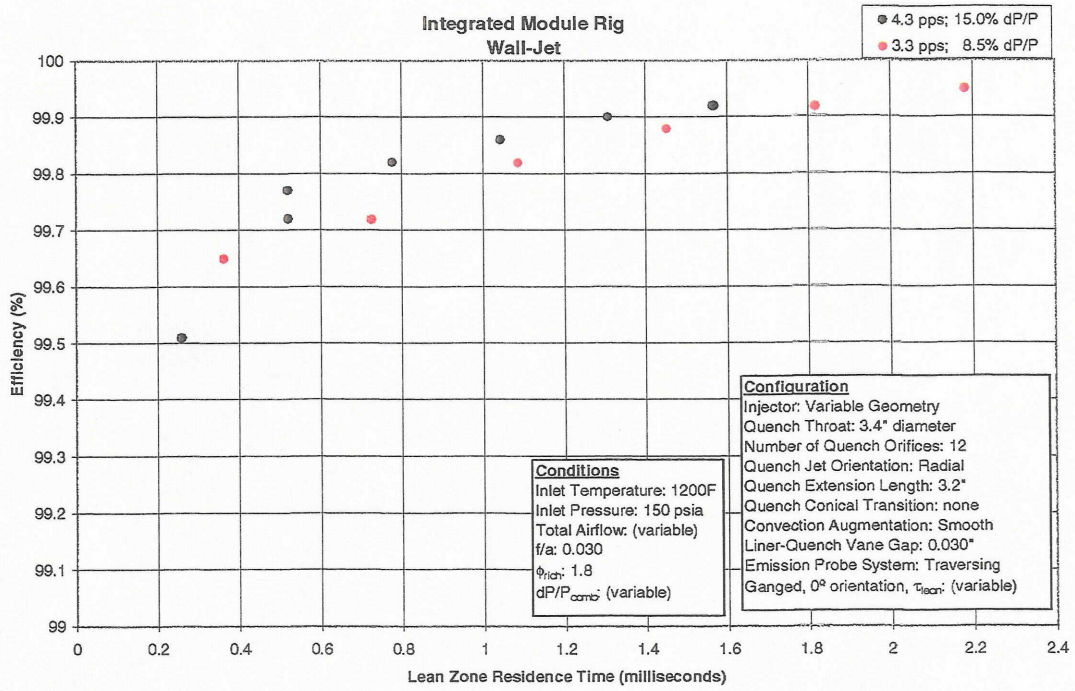

Figure VI - 126 Efficiency as a Function of Lean Zone Residence Time

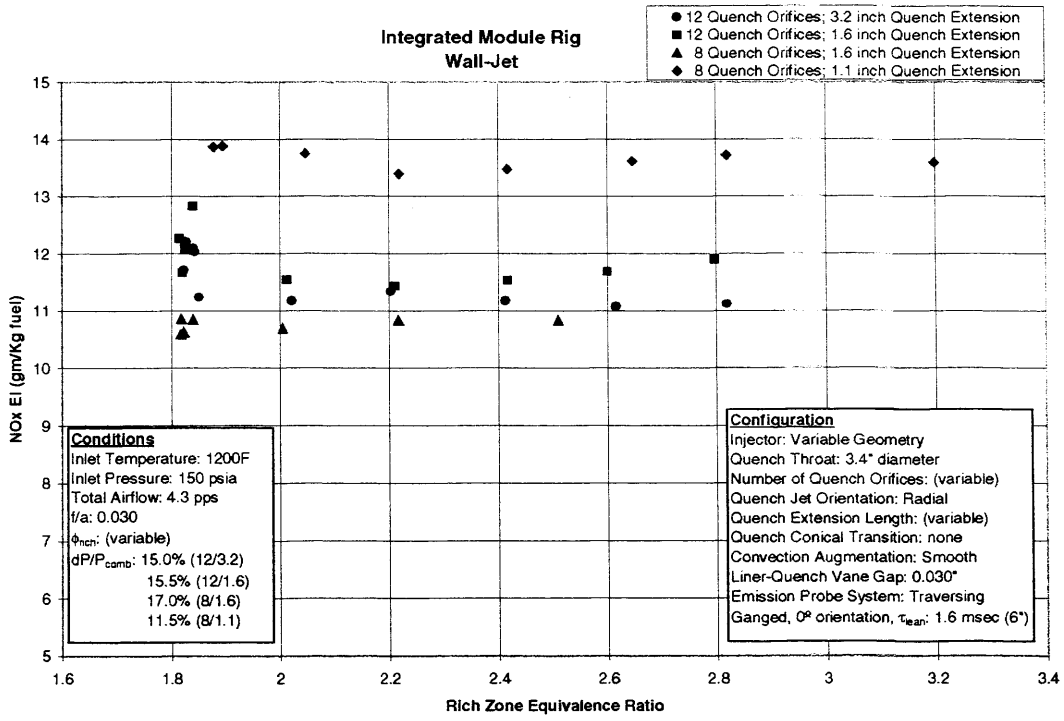

Figure VI - 127 NOx Emissions as a Function of Rich Zone Equivalence Ratio

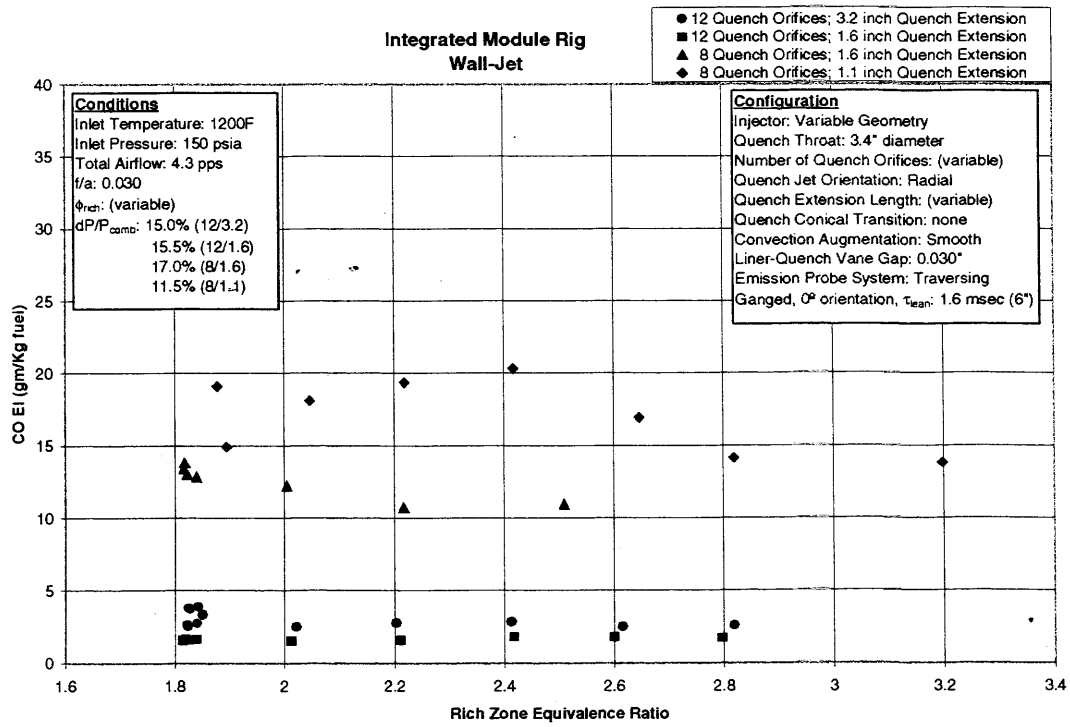

Figure VI - 128 CO Emissions as a Function of Rich Zone Equivalence Ratio

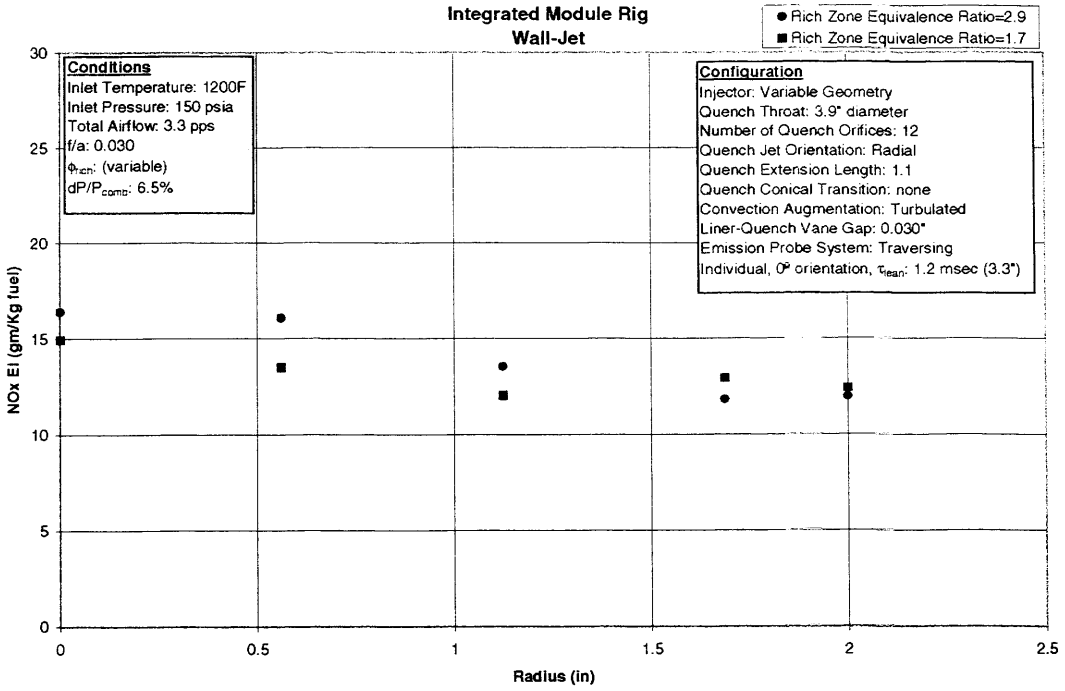

Figure VI - 129 NOx Emissions as a Function of Radial Location

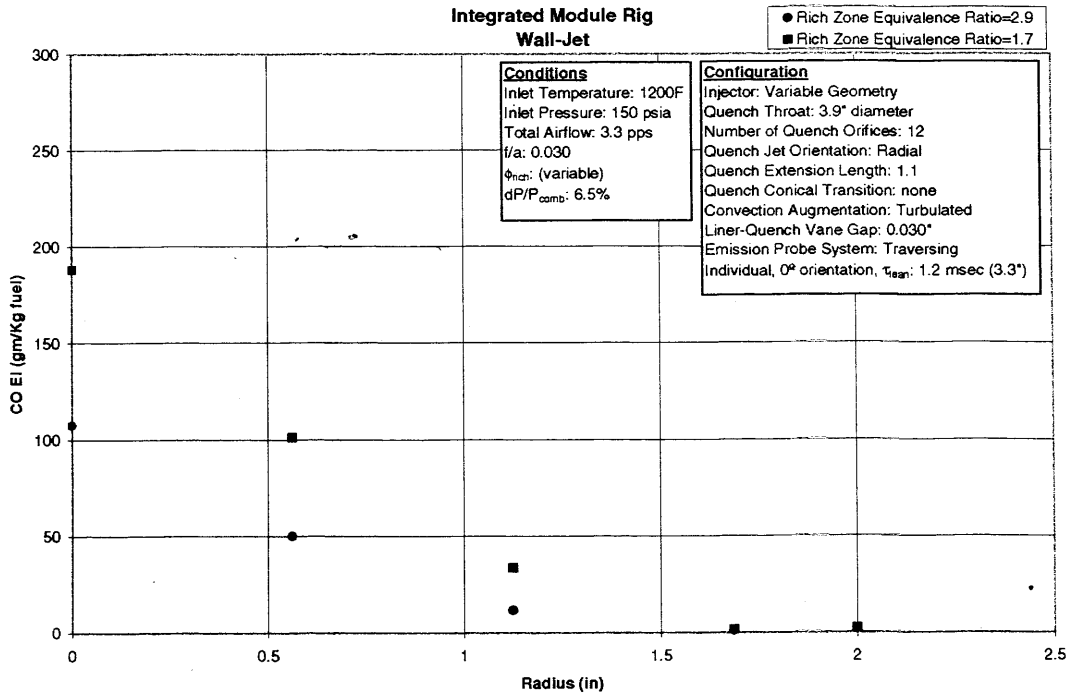

Figure VI - 130 CO Emissions as a Function of Radial Location

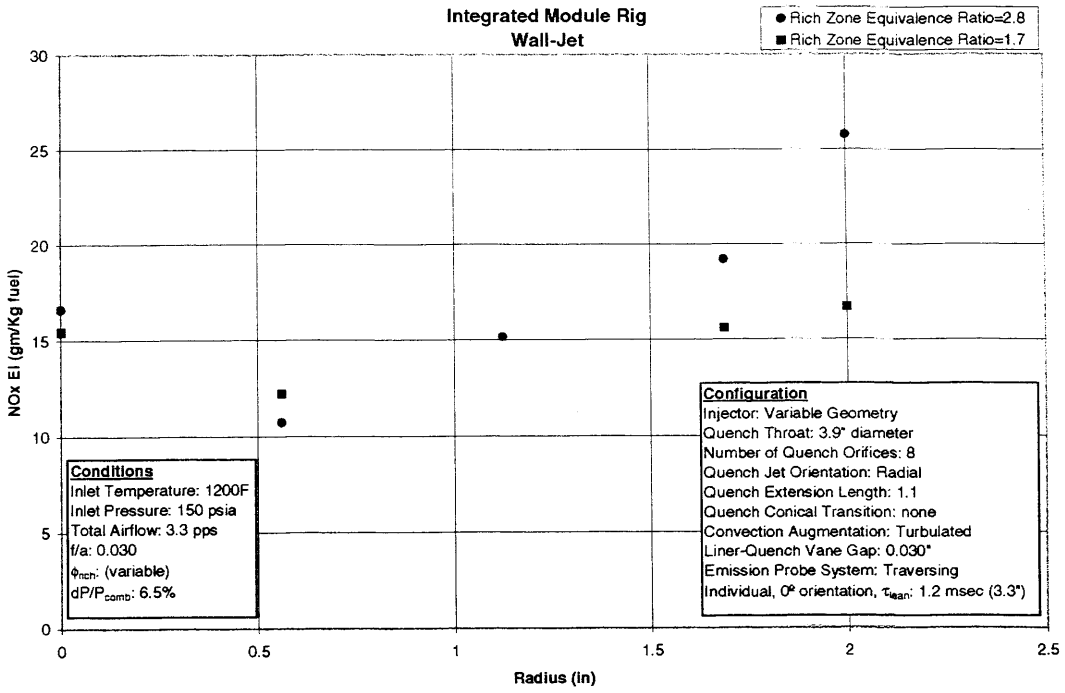

Figure VI - 131 NOx Emissions as a Function of Radial Location

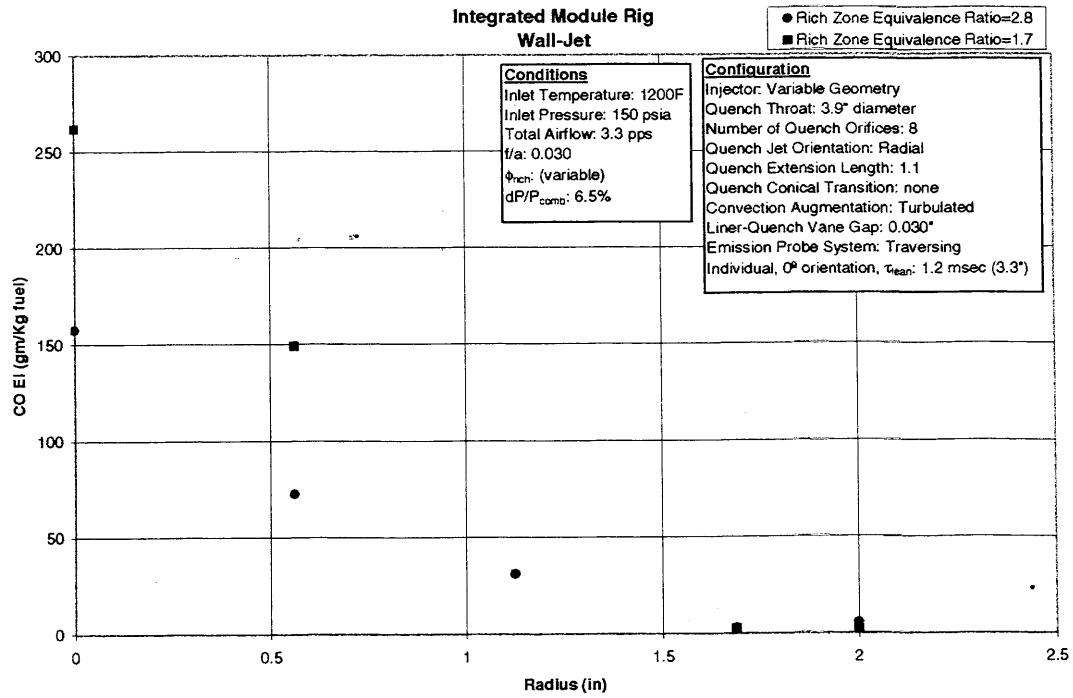

Figure VI - 132 CO Emissions as a Function of Radial Location

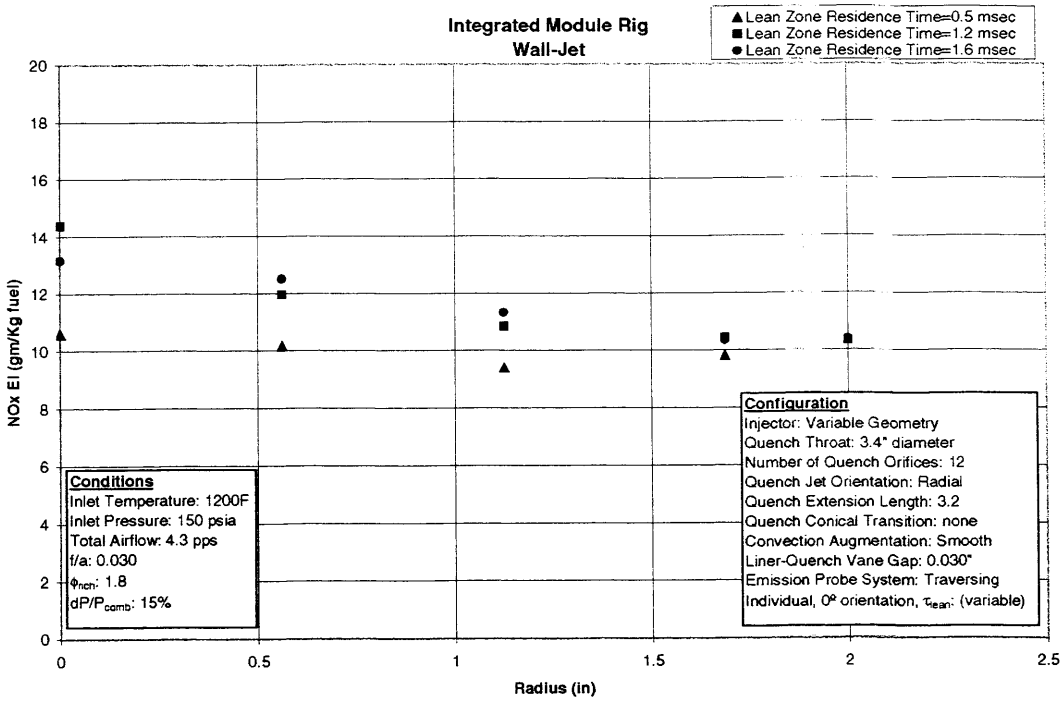

Figure VI - 133 NOx Emissions as a Function of Radial Location

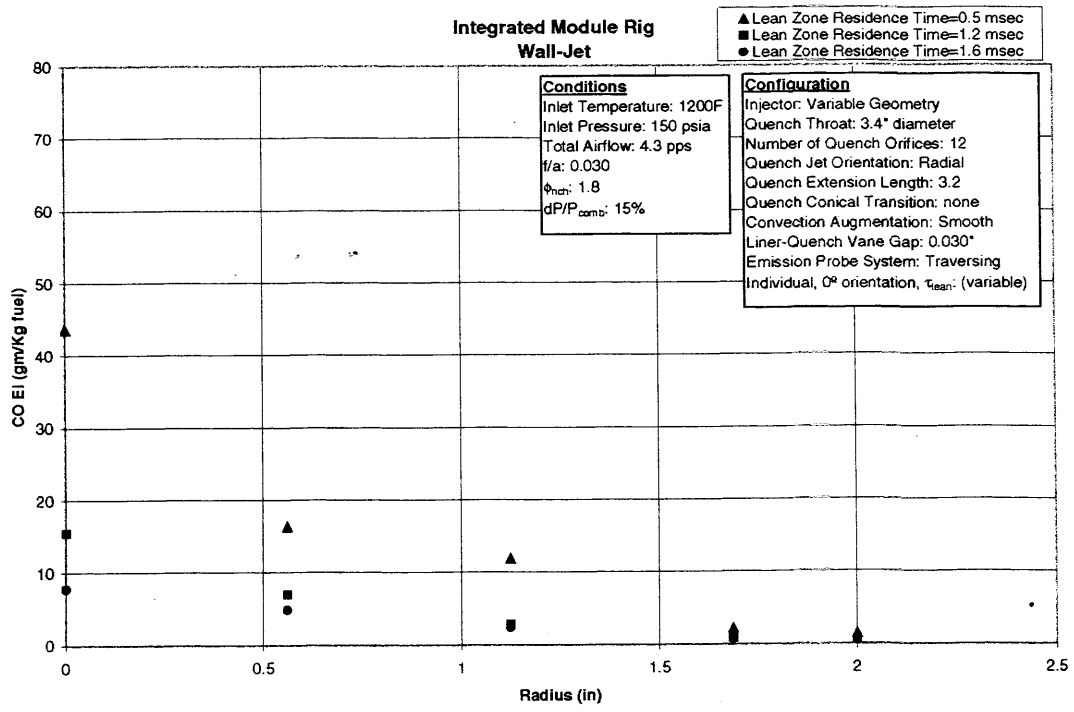

Figure VI - 134 CO Emissions as a Function of Radial Location

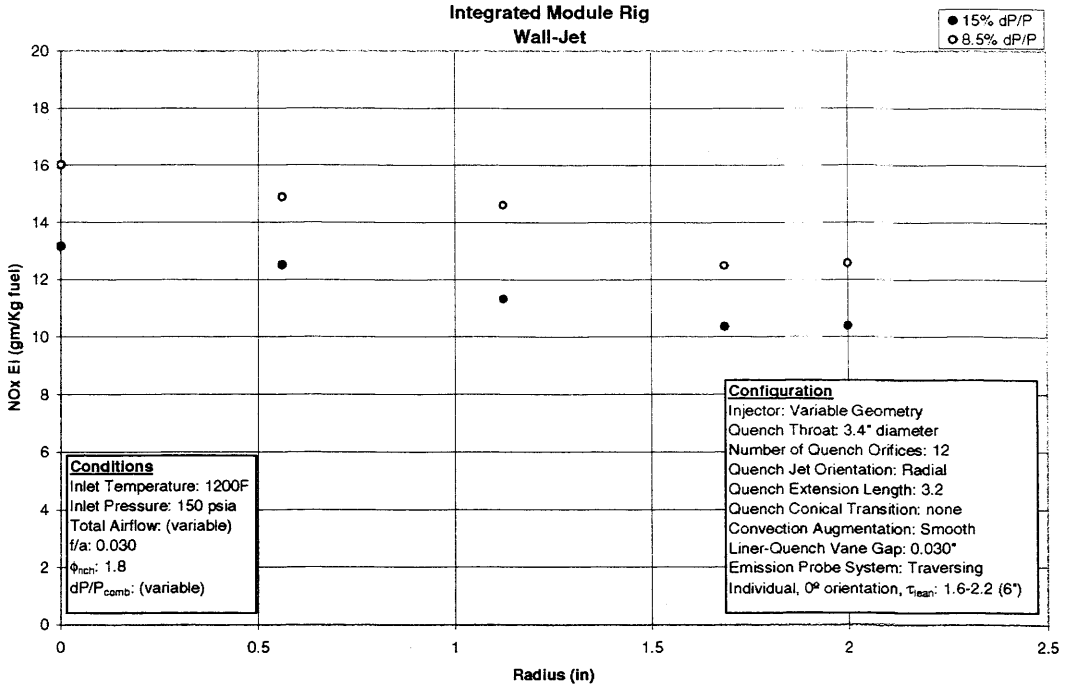

Figure VI - 135 NOx Emissions as a Function of Radial Location

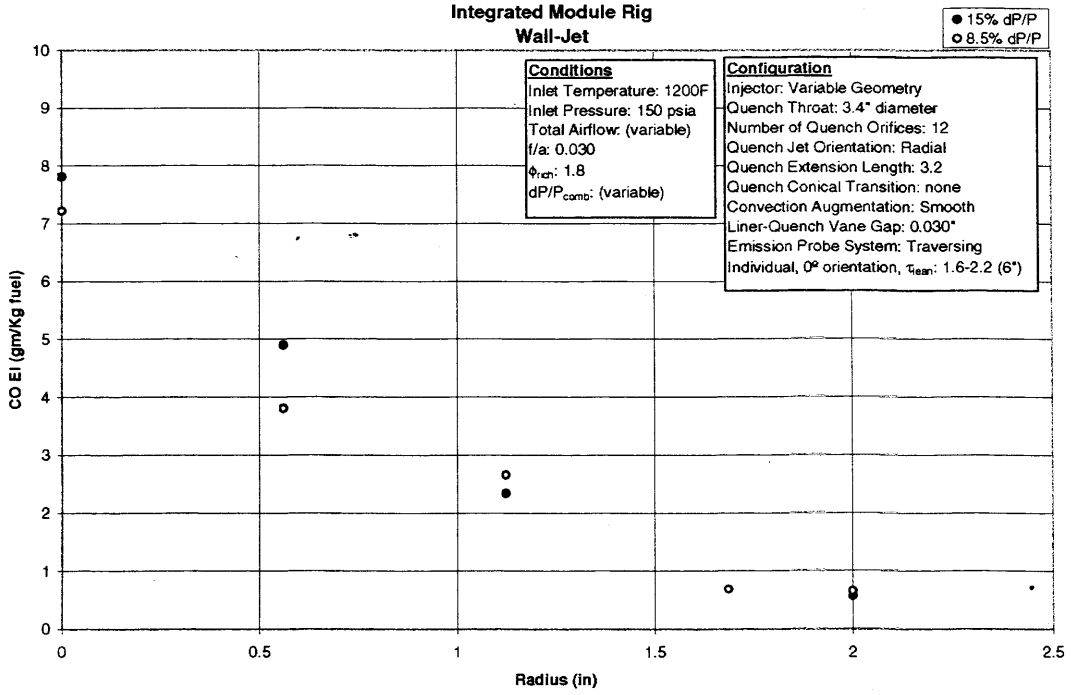

Figure VI - 136 CO Emissions as a Function of Radial Location

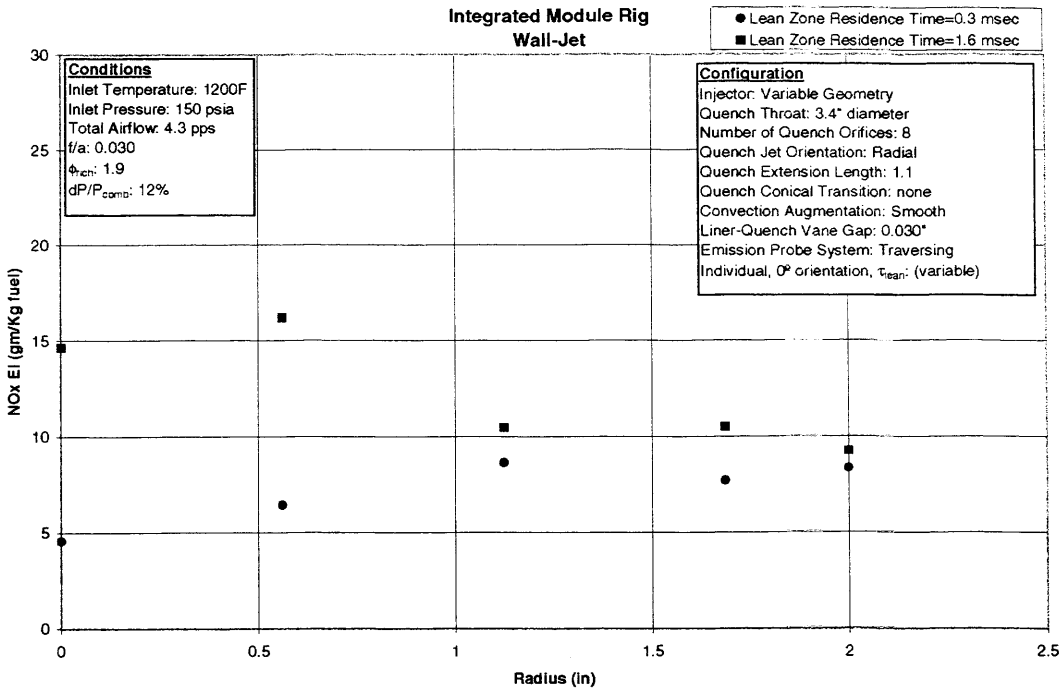

Figure VI - 137 NOx Emissions as a Function of Radial Location

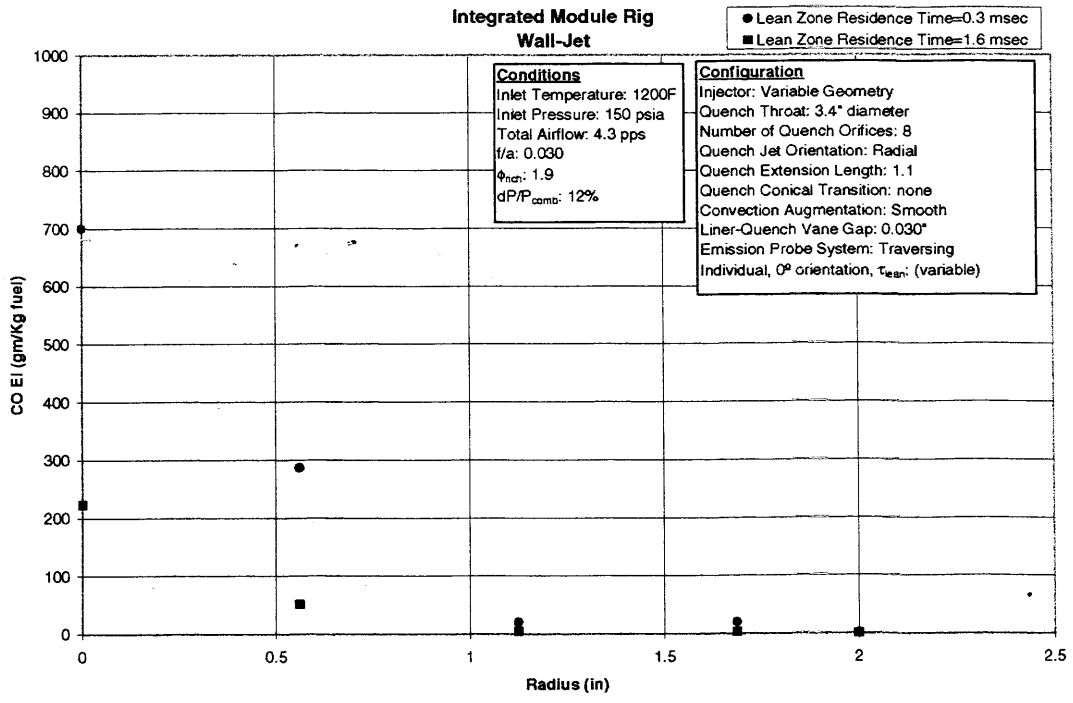

Figure VI - 138 CO Emissions as a Function of Radial Location

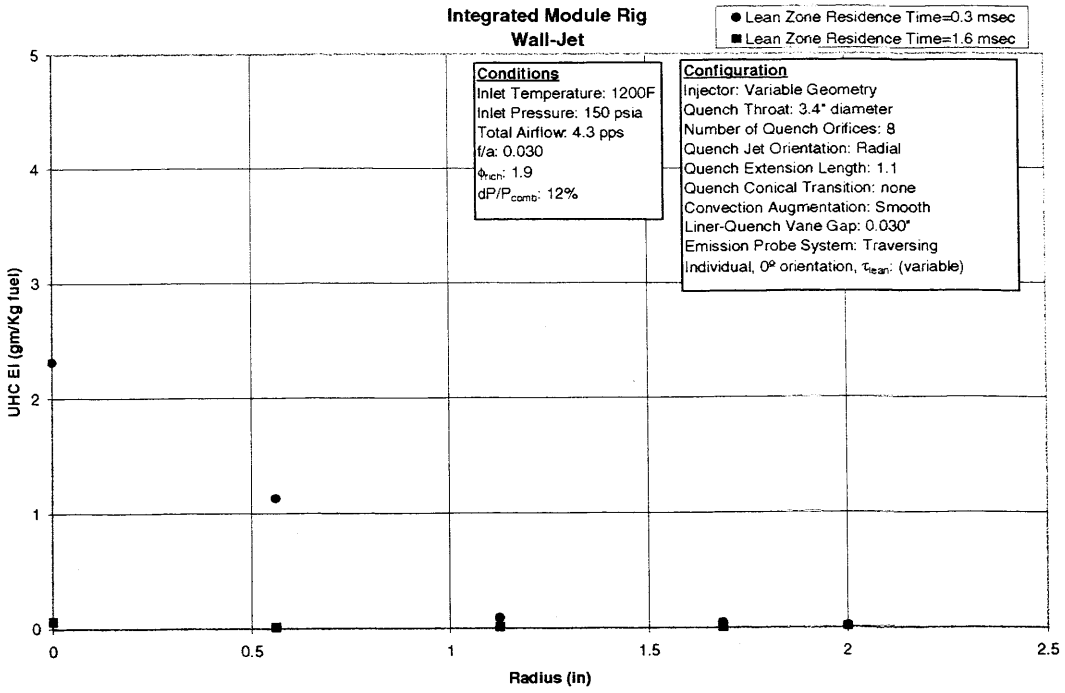

Figure VI - 139 UHC Emissions as a Function of Radial Location

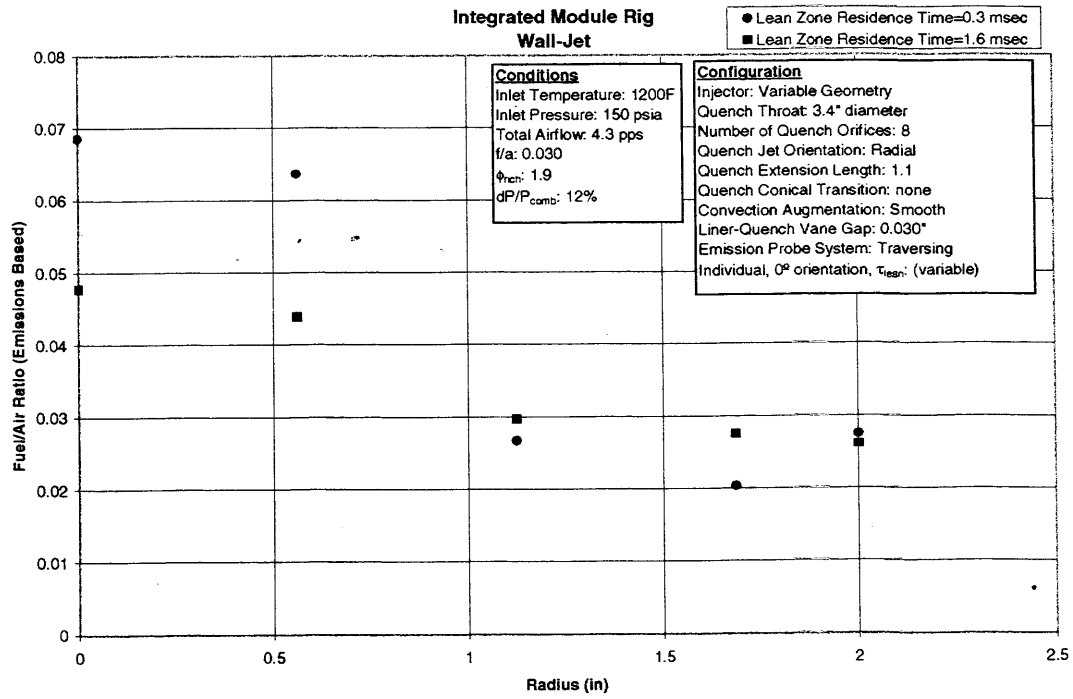

Figure VI - 140 Emissions Fuel/Air Ratio as a Function of Radial Location

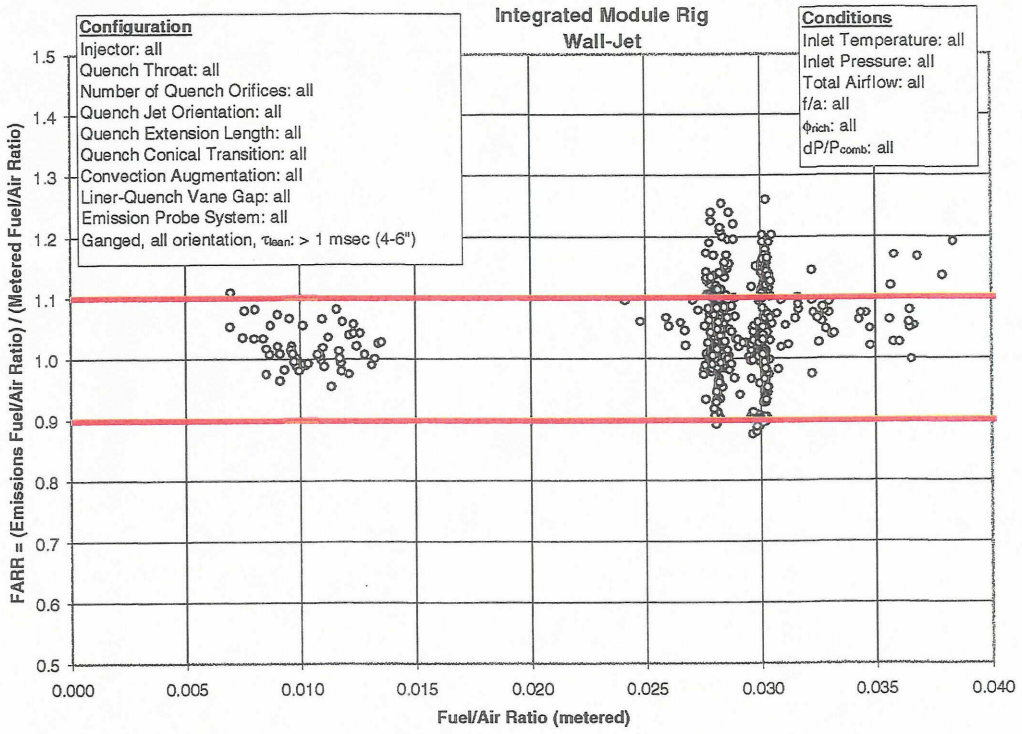

Figure VI - 141 FARR for all Integrated Module Rig Wall-Jet Configurations; Ganged, > 1 msec, (> 4")

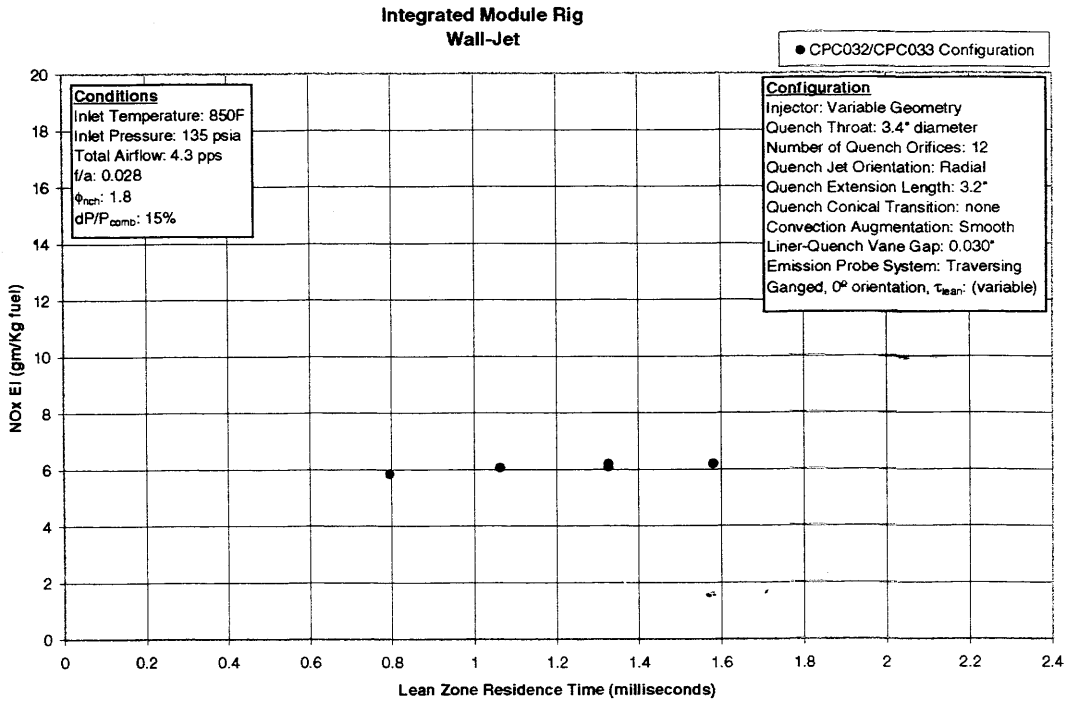

Figure VI - 142 NOx Emissions as a Function of Lean Zone Residence Time for Wall-Jet Configuration CPC032-CPC033

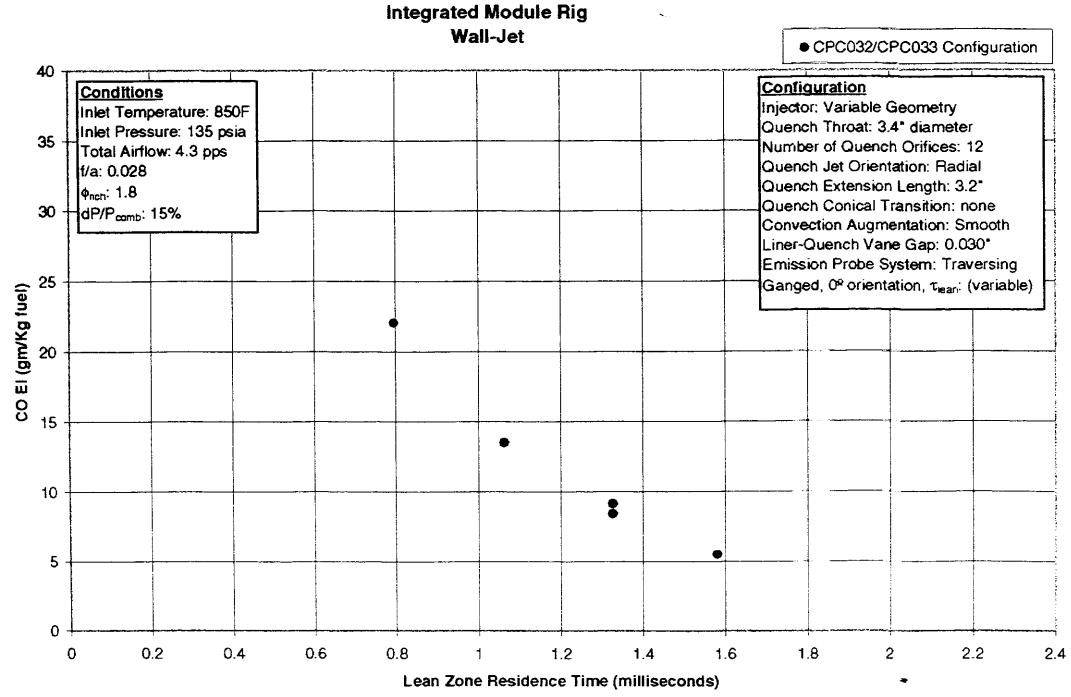

Figure VI - 143 CO Emissions as a Function of Lean Zone Residence Time for Wall-Jet Configuration CPC032-CPC033

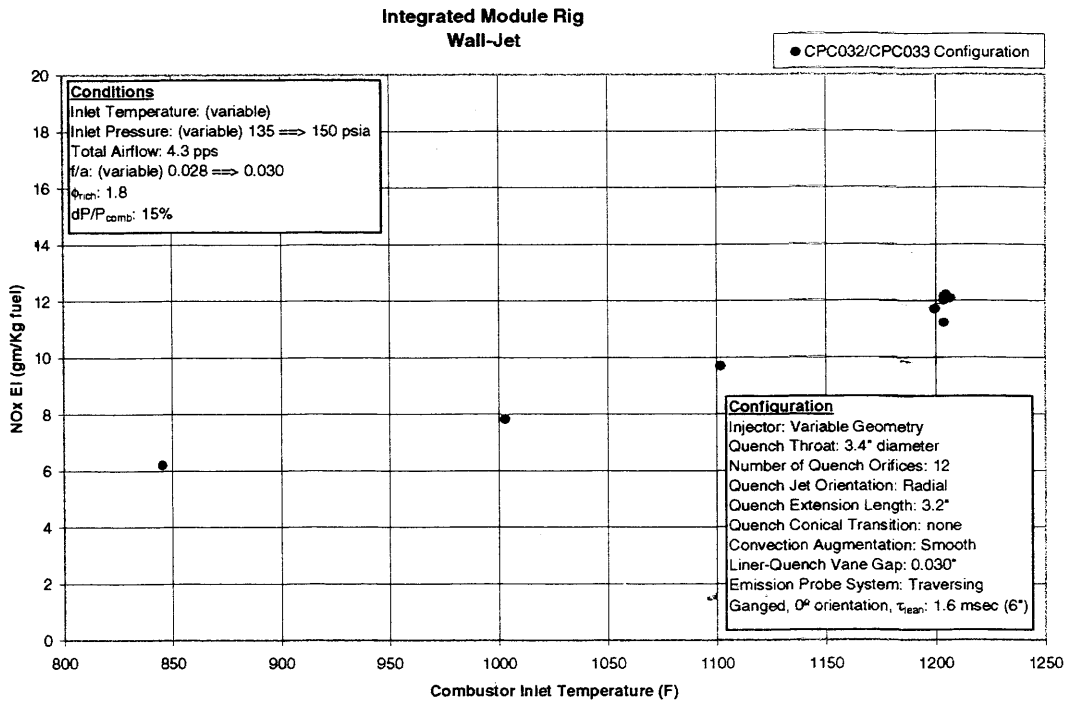

Figure VI - 144 NOx Emissions as a Function of Inlet Temperature for Wall-Jet Configuration CPC032-CPC033

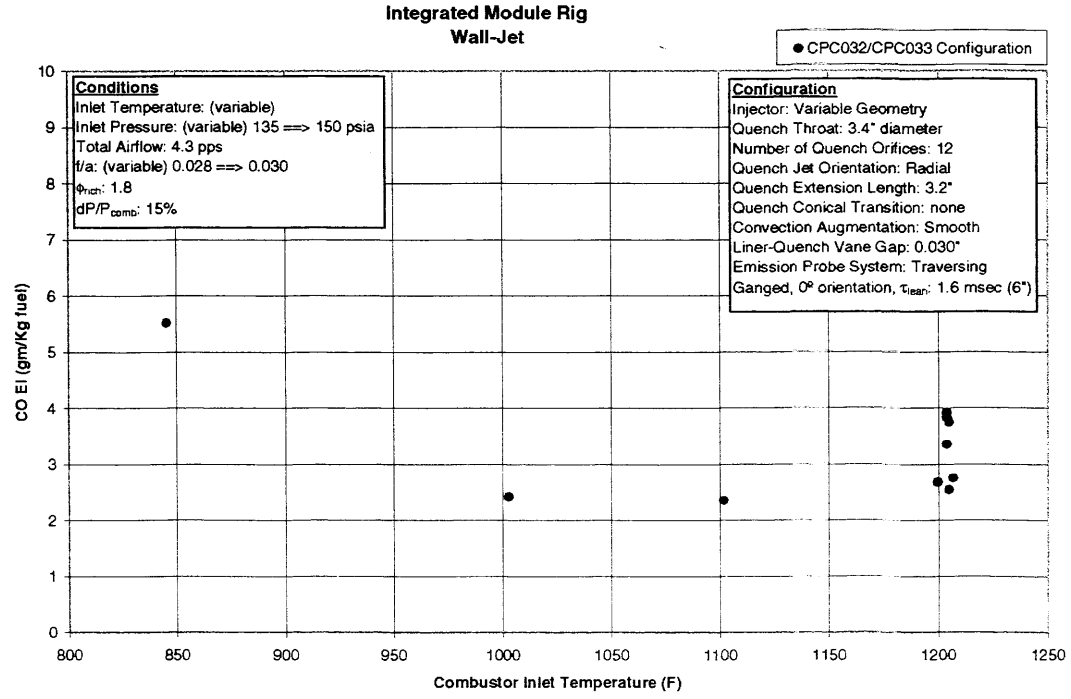

Figure VI - 145 CO Emissions as a Function of Inlet Temperature for Wall-Jet Configuration CPC032-CPC033

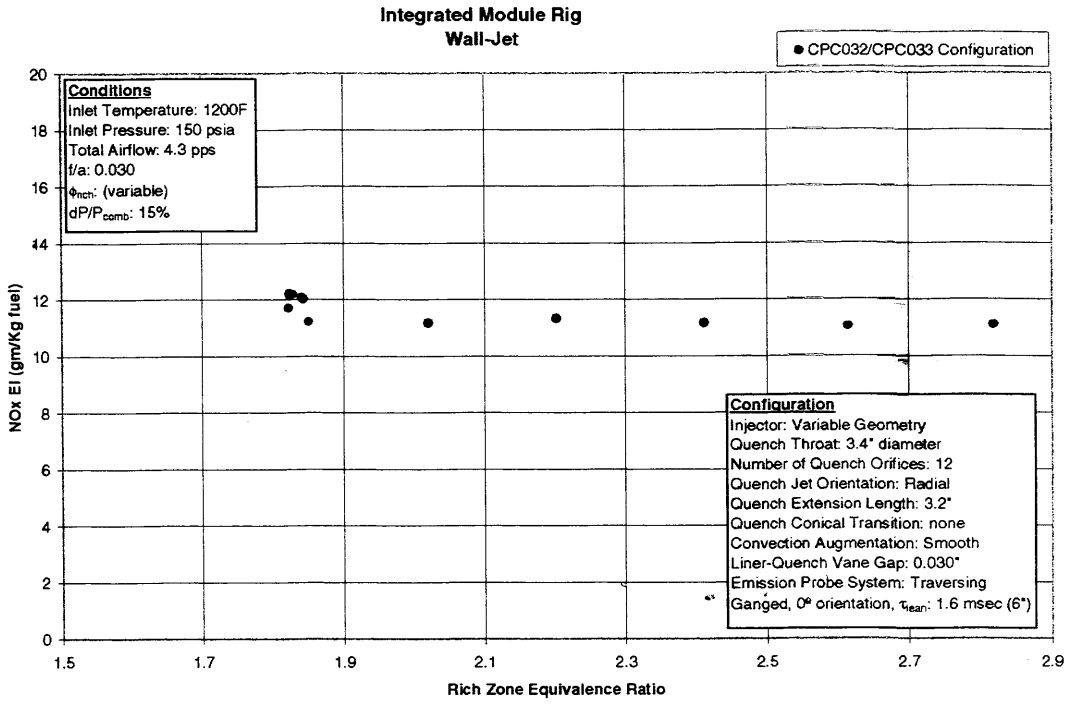

Figure VI - 146 NOx Emissions as a Function of Rich Zone Equivalence Ratio for Wall-Jet Configuration CPC032-CPC033

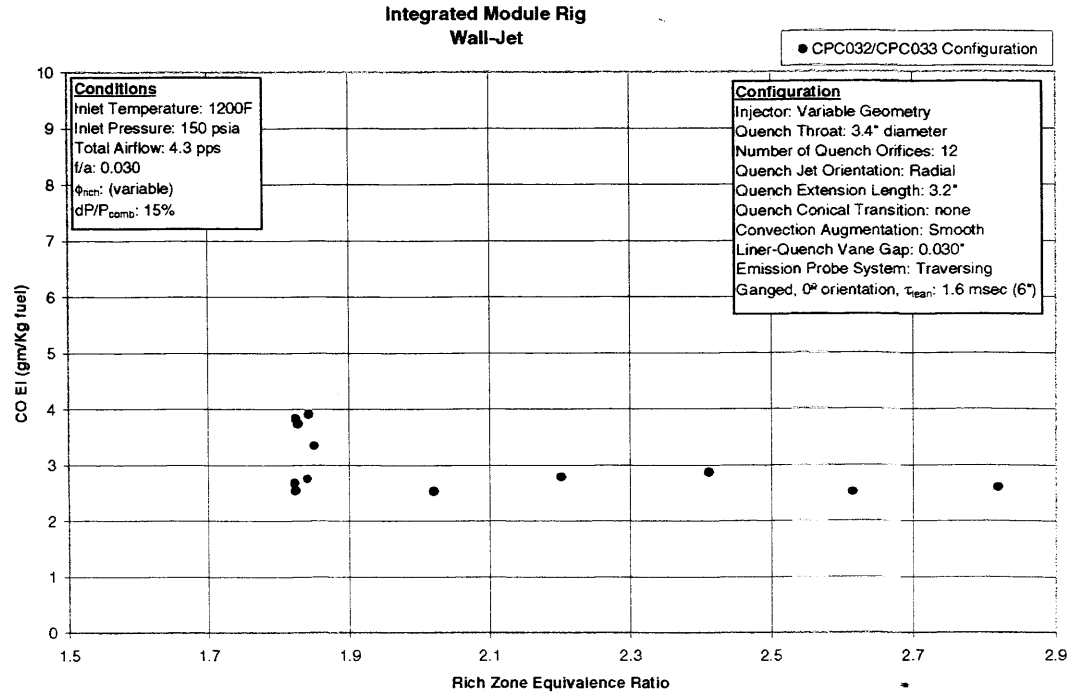

Figure VI - 147 CO Emissions as a Function of Rich Zone Equivalence Ratio for Wall-Jet Configuration CPC032-CPC033

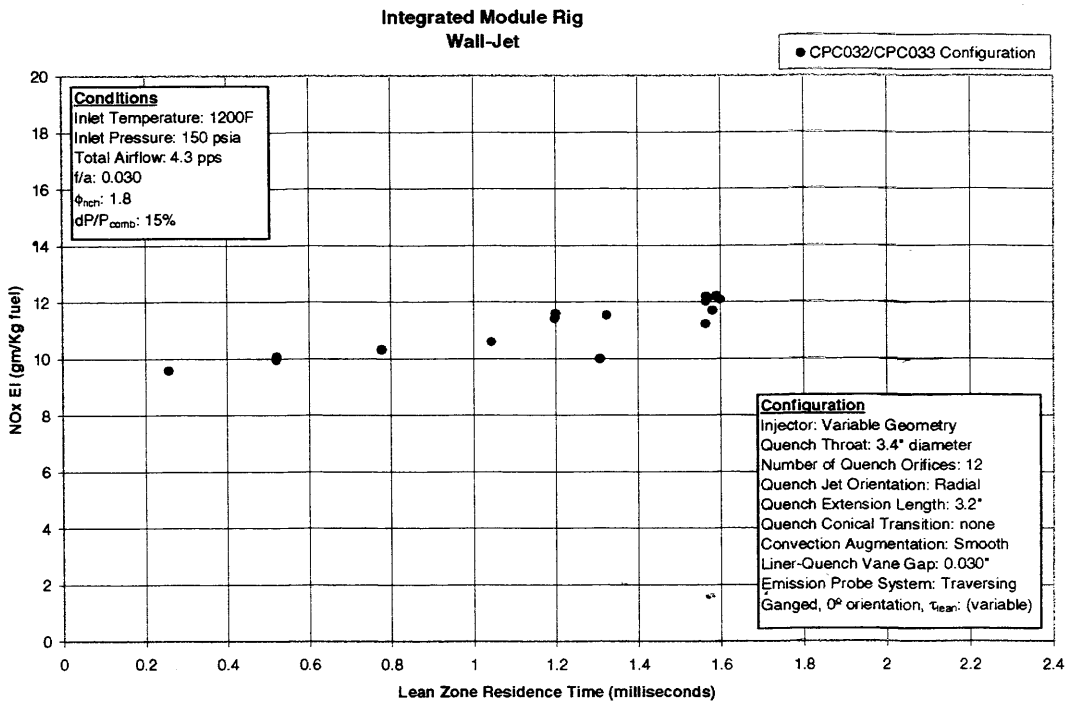

Figure VI - 148 NOx Emissions as a Function of Lean Zone Residence Time for Wall-Jet Configuration CPC032-CPC033

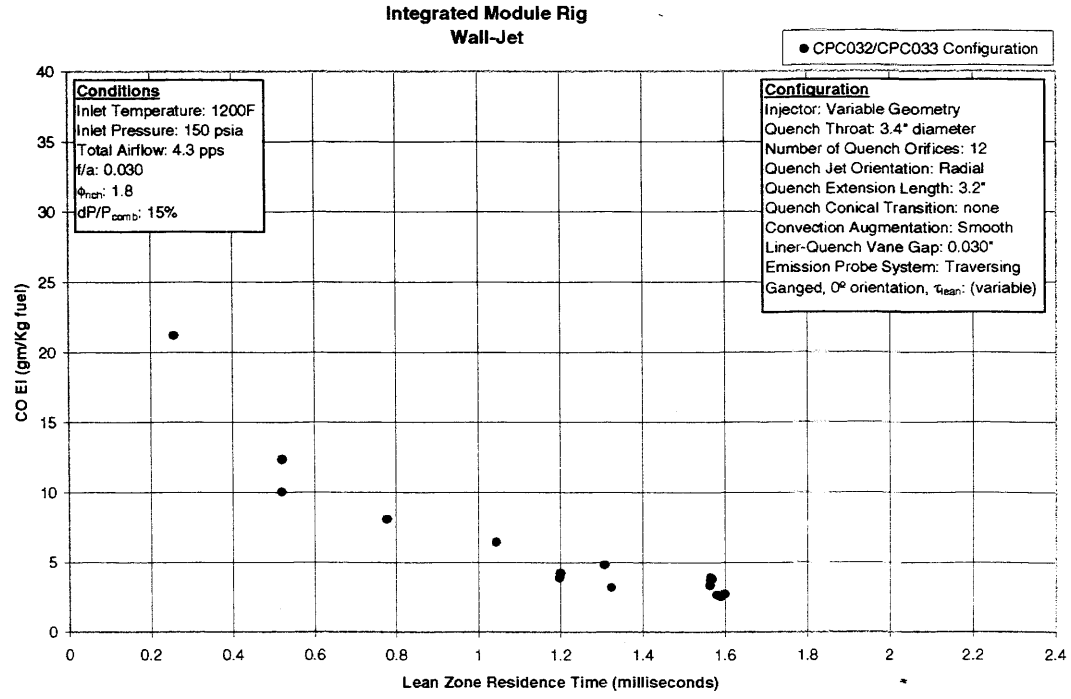

Figure VI - 149 CO Emissions as a Function of Lean Zone Residence Time for Wall-Jet Configuration CPC032-CPC033

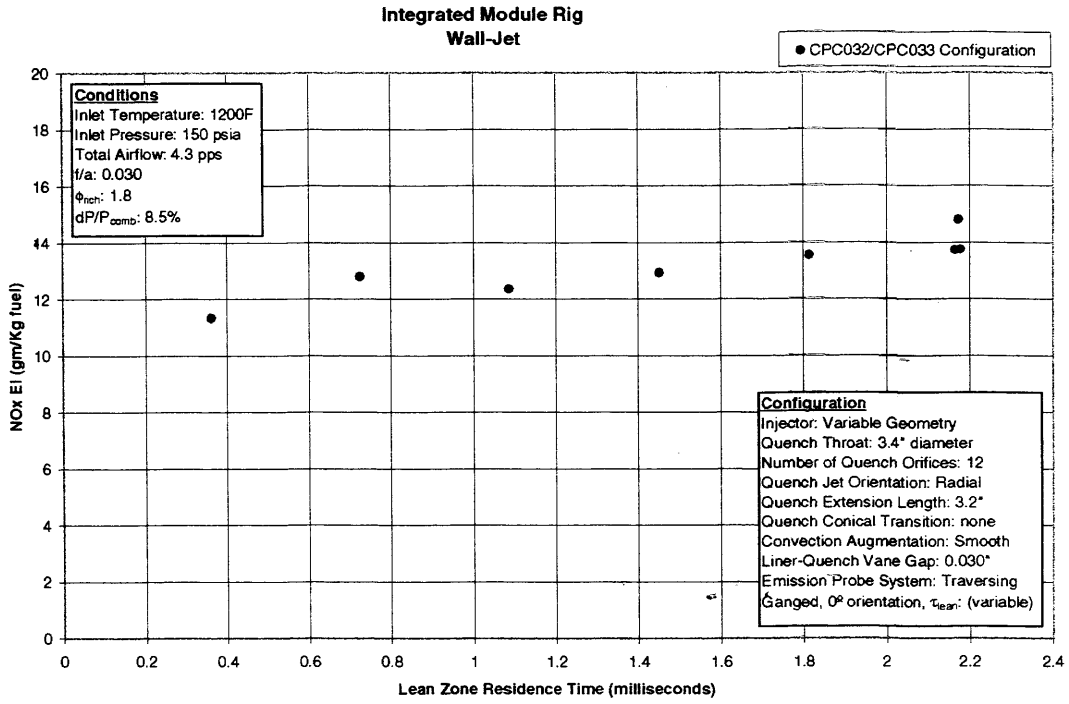

Figure VI - 150 NOx Emissions as a Function of Lean Zone Residence Time for Wall-Jet Configuration CPC032-CPC033

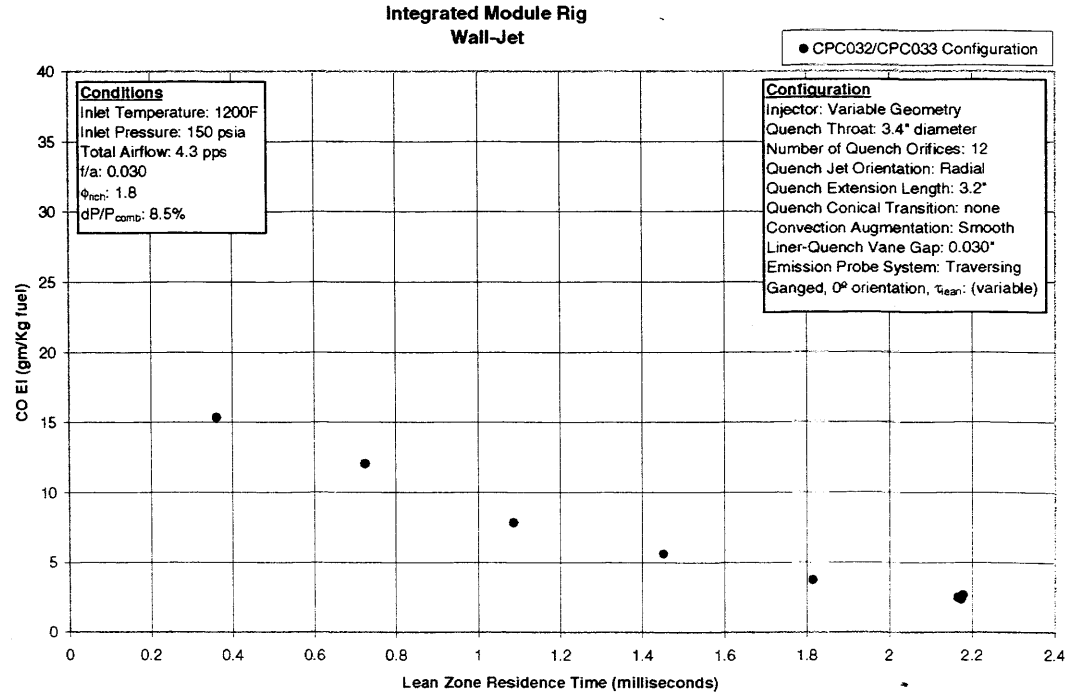

Figure VI - 151 CO Emissions as a Function of Lean Zone Residence Time for Wall-Jet Configuration CPC032-CPC033

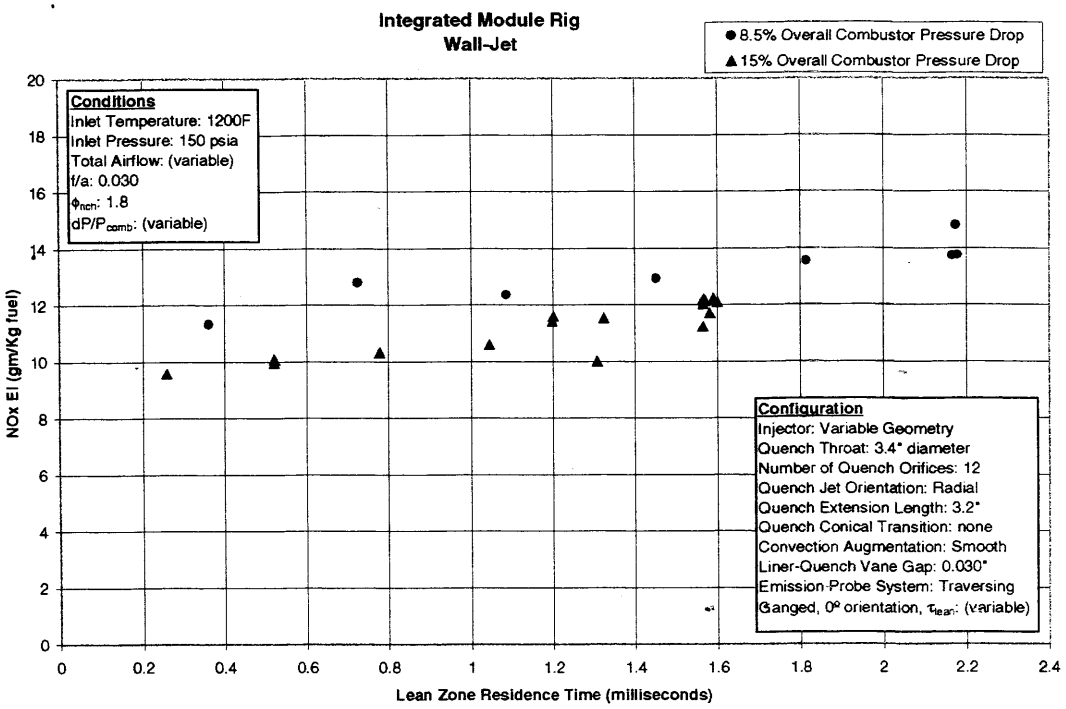

Figure VI - 152 NOx Emissions as a Function of Lean Zone Residence Time for Wall-Jet Configuration CPC032-CPC033

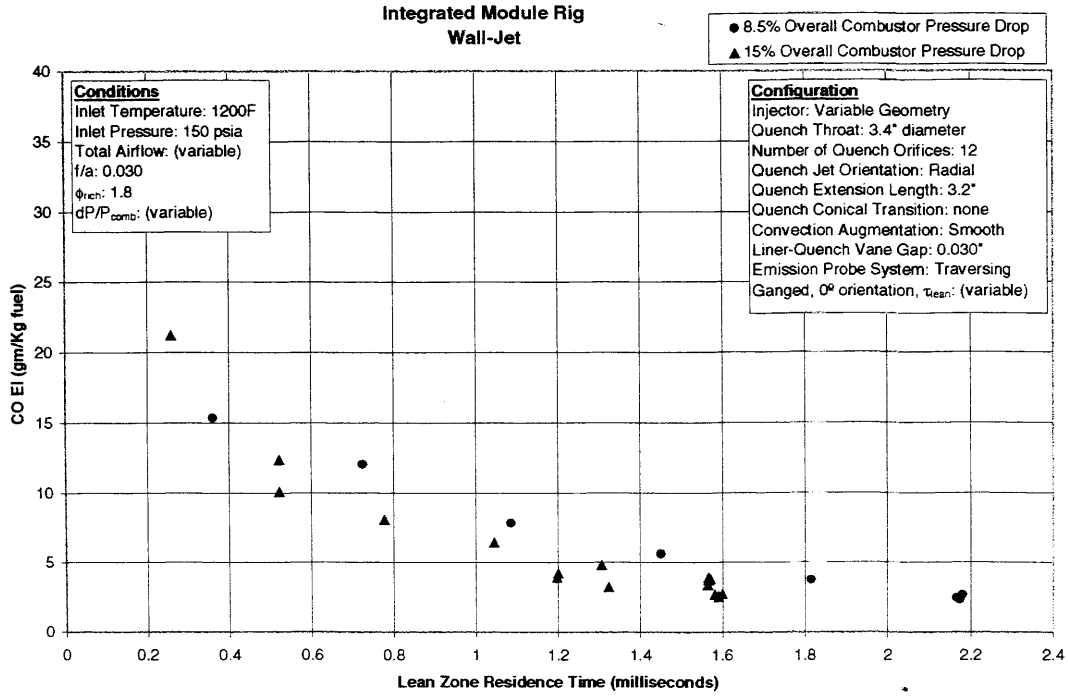

Figure VI - 153 CO Emissions as a Function of Lean Zone Residence Time for Wall-Jet Configuration CPC032-CPC033

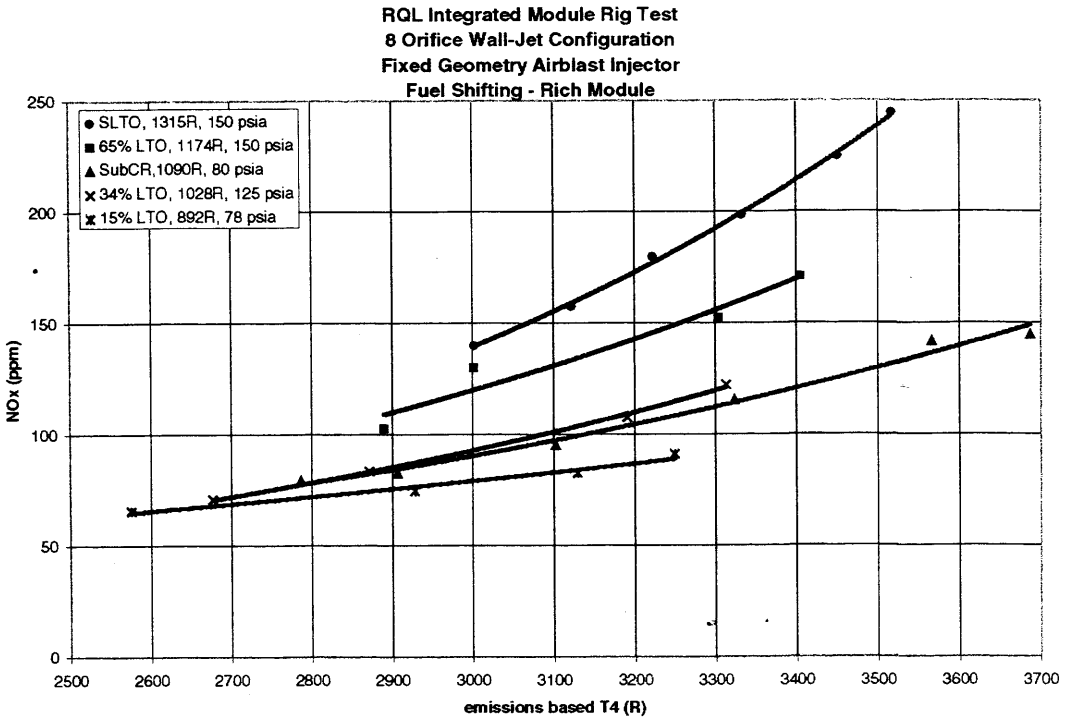

Figure VI - 154 NOx Emissions of a Rich Module for Fuel Shifting Assessment

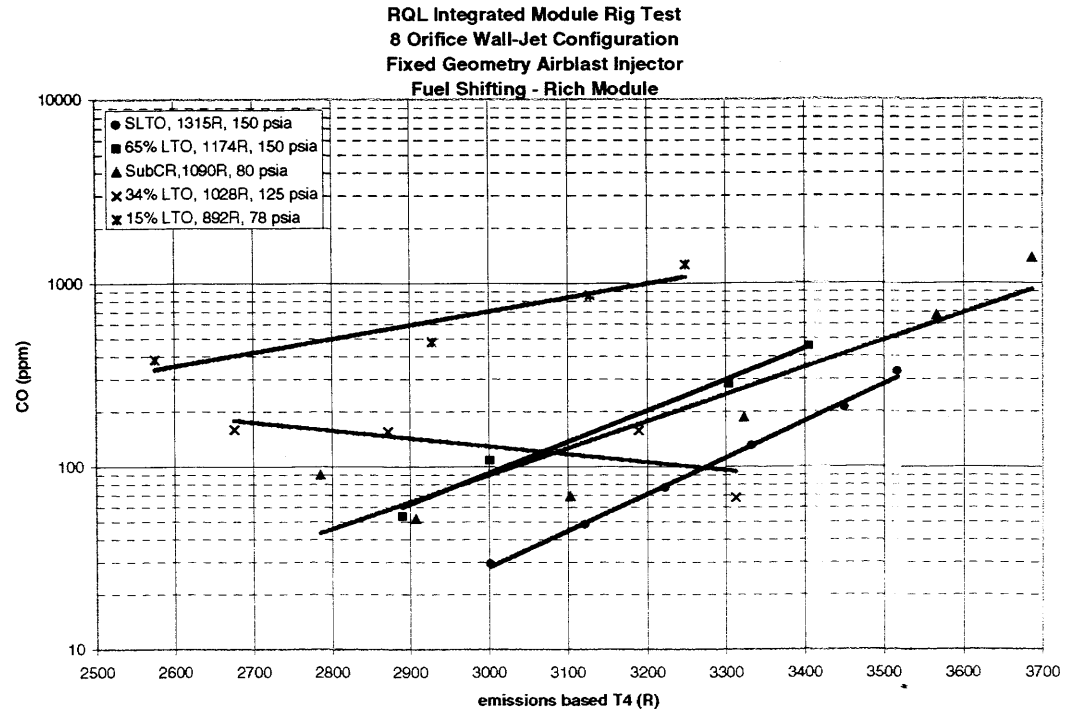

Figure VI - 155 CO Emissions of a Rich Module for Fuel Shifting Assessment

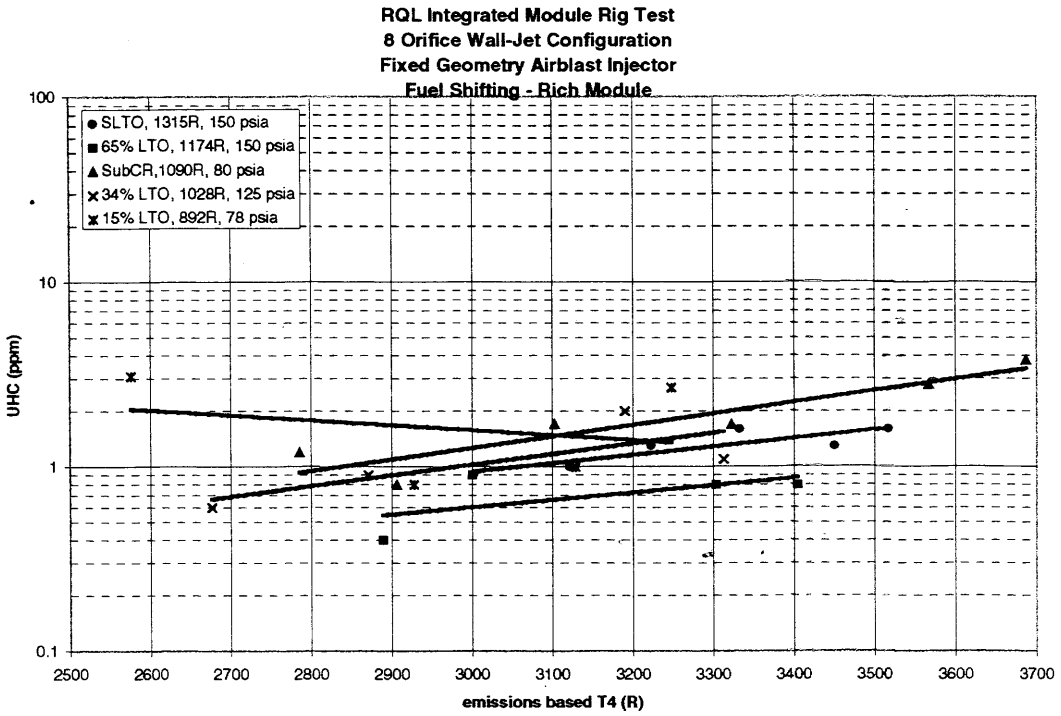

Figure VI - 156 UHC Emissions of a Rich Module for Fuel Shifting Assessment

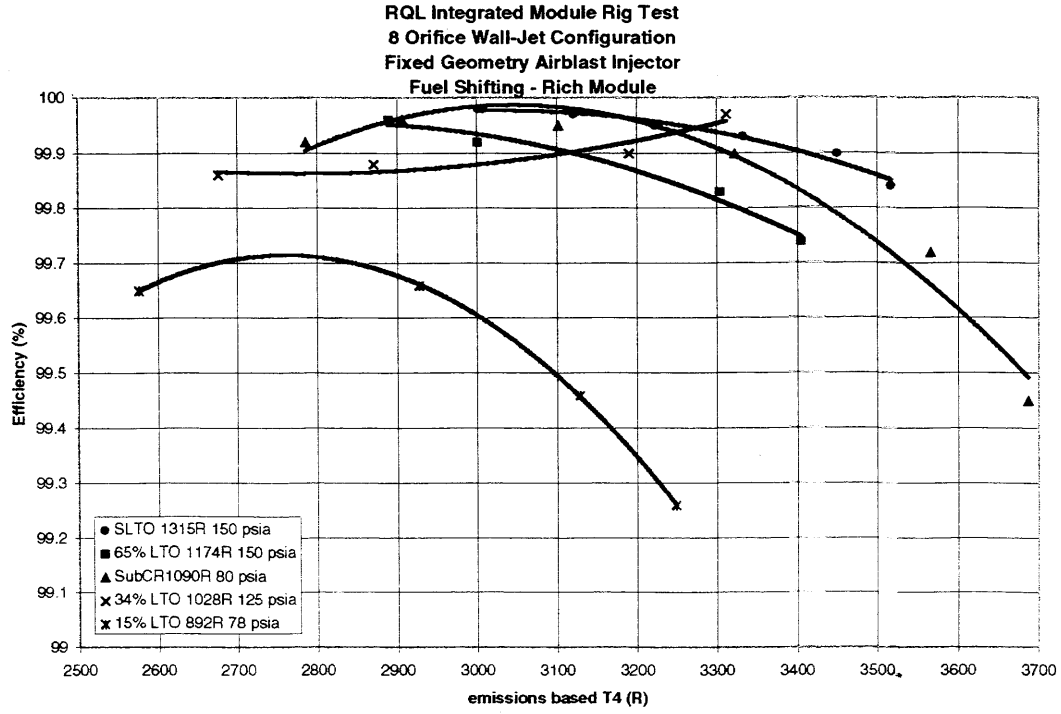

Figure VI - 157 Efficiency of a Rich Module for Fuel Shifting Assessment

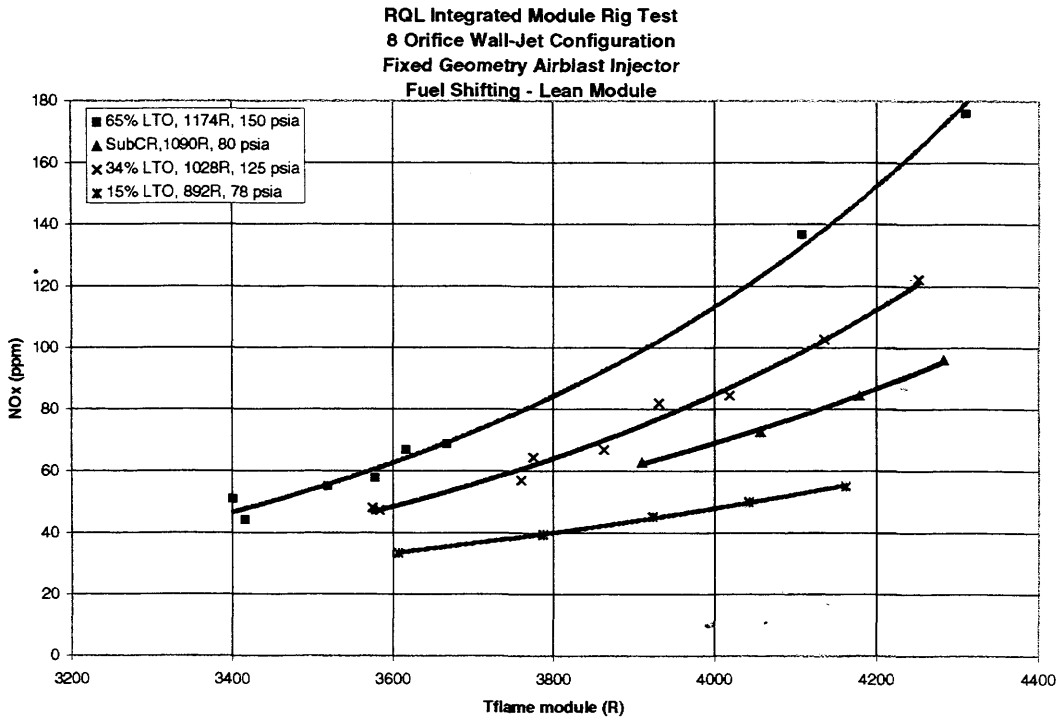

Figure VI - 158 NOx Emissions of a Lean Module for Fuel Shifting Assessment

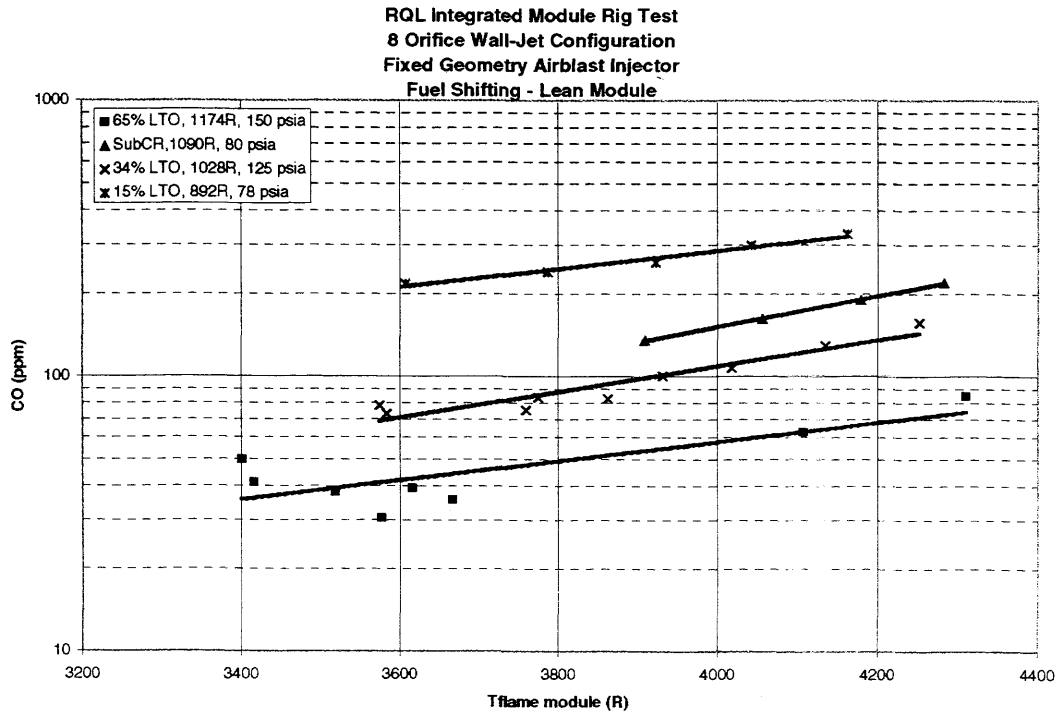

Figure VI - 159 CO Emissions of a Lean Module for Fuel Shifting Assessment

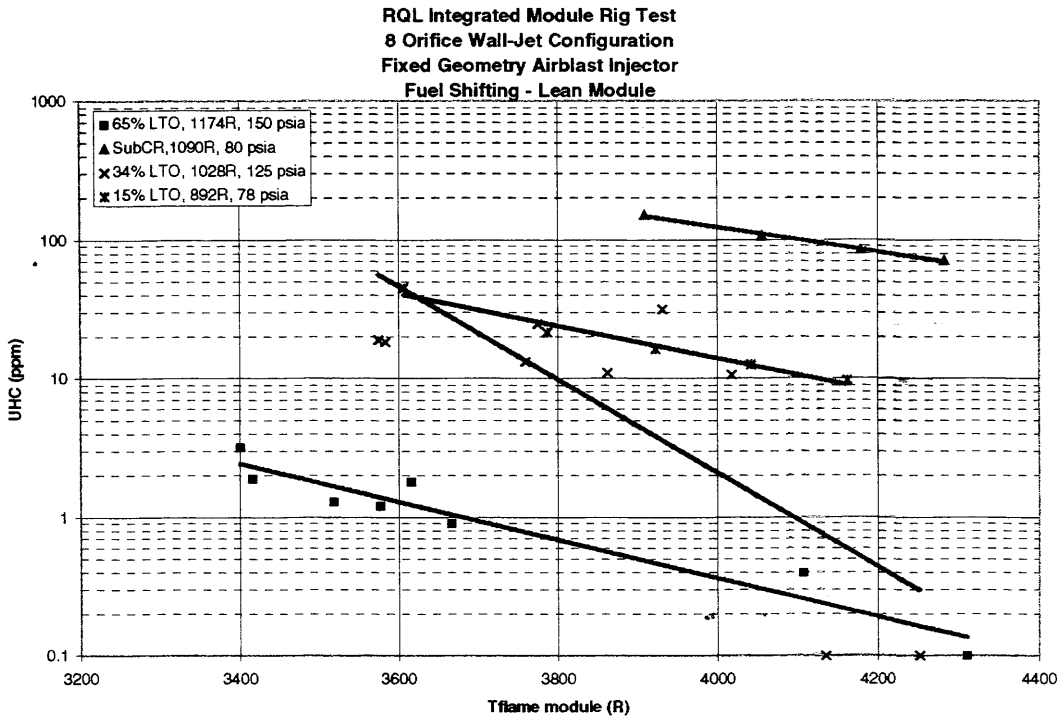

Figure VI - 160 UHC Emissions of a Lean Module for Fuel Shifting Assessment

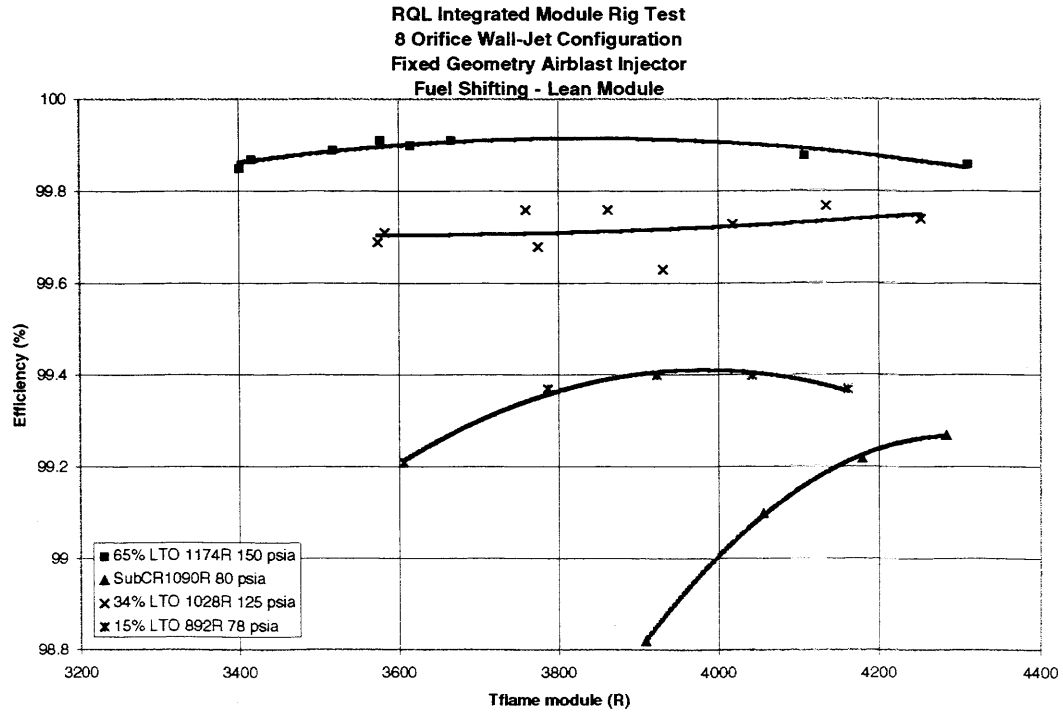

Figure VI - 161 Efficiency of a Lean Module for Fuel Shifting Assessment

Emissions Formulation for Fuel Shifted Wall Jet RQL

Thrust Settings And Time-In-Mode For Landing / Takeoff Cycle (Supersonic)

Index Number	Operating Condition	NOx EI	CO EI	UHC EI
1	Idle	4.8	20.50	1.35
2	Descent	3.8	13.56	2.95
3	Approach	4.4	7.00	1.92
4	Climb	6.4	0.98	0.01
5	Take-off	11.2	1.69	0.01
Integrated LTO		5.2	7.9	0.7
Goal		< 5.0	< 7.8	< 1.0

Figure VI - 162 Airport Vicinity Emissions Assessment for a Fuel-Shifted Wall-Jet RQL Combustor

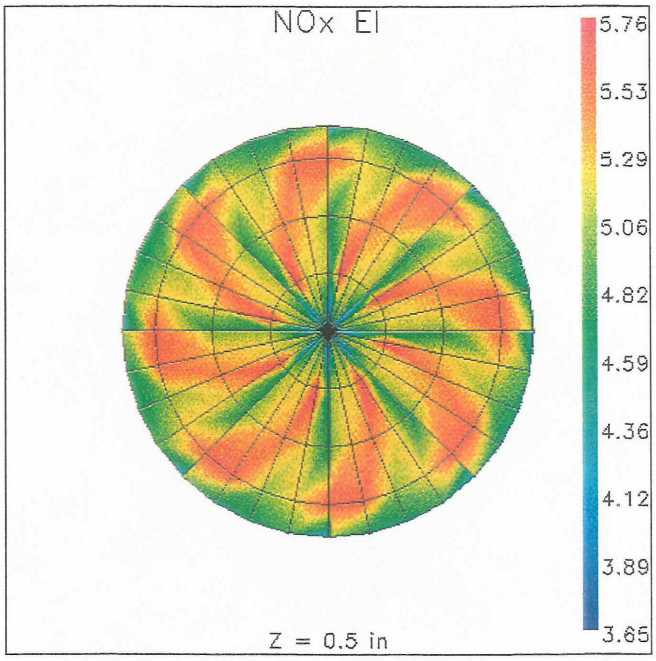

Figure VI - 163 NOx Emissions from Detailed Sampling over 45 degree Region (graphic replicated for 360 degree representation) at 0.5" Downstream from Lean Zone Inlet

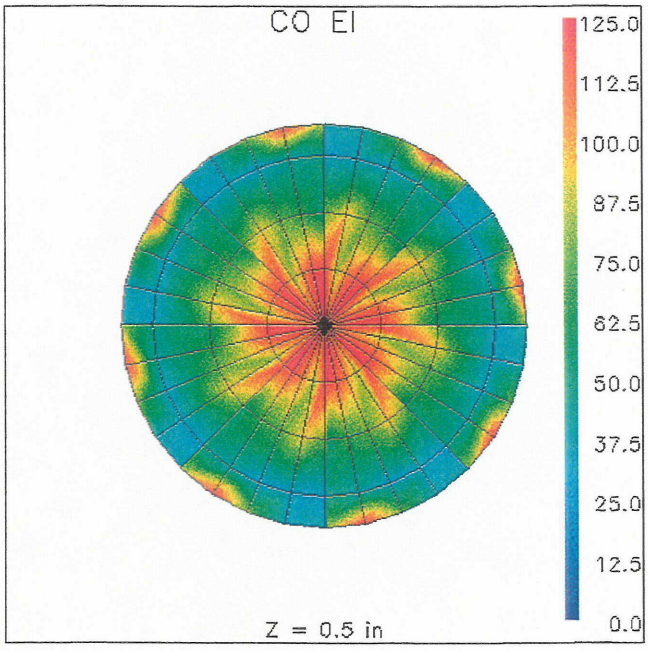

Figure VI - 164 CO Emissions from Detailed Sampling over 45 degree Region (graphic replicated for 360 degree representation) at 0.5" Downstream from Lean Zone Inlet

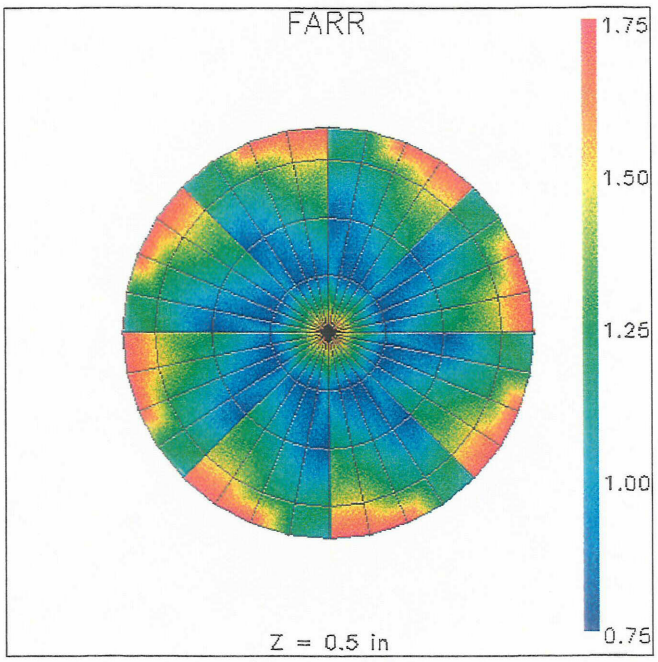

Figure VI - 165 Fuel-Air Uniformity [FARR = (emissions fuel/air) / (metered fuel/air)] from Detailed Sampling over 45 degree Region (graphic replicated for 360 degree representation) at 0.5" Downstream from Lean Zone Inlet

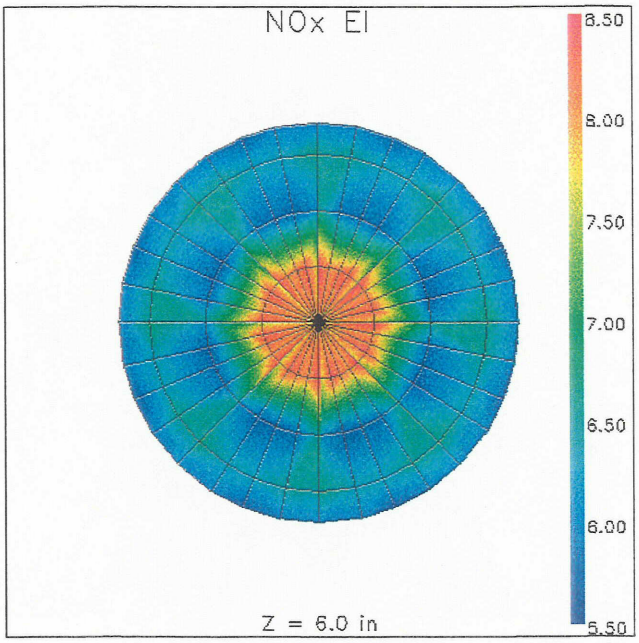

Figure VI - 166 NOx Emissions from Detailed Sampling over 45 degree Region (graphic replicated for 360 degree representation) at 6" Downstream from Lean Zone Inlet

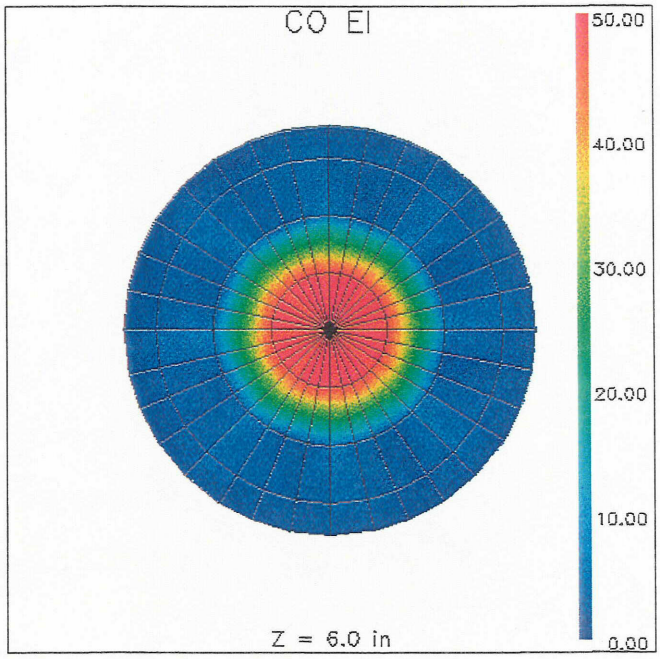

Figure VI - 167 CO Emissions from Detailed Sampling over 45 degree Region (graphic replicated for 360 degree representation) at 6" Downstream from Lean Zone Inlet

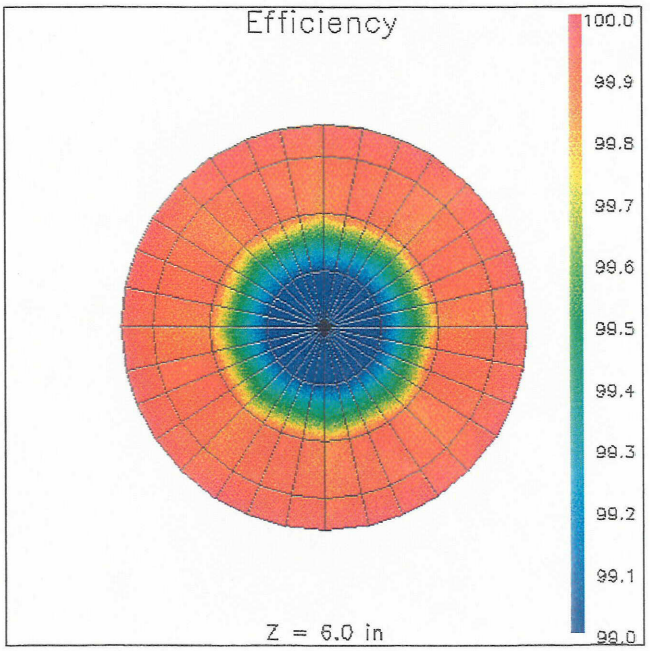

Figure VI - 168 Efficiency from Detailed Sampling over 45 degree Region (graphic replicated for 360 degree representation) at 6" Downstream from Lean Zone Inlet

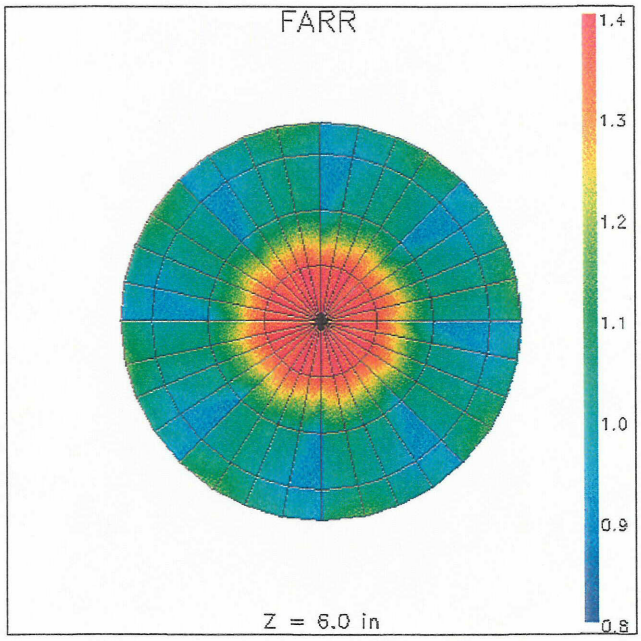

Figure VI - 169Fuel-Air Uniformity [FARR = (emissions fuel/air) / (metered fuel/air)] from Detailed Sampling over 45 degree Region (graphic replicated for 360 degree representation) at 6" Downstream from Lean Zone Inlet

Figure VI - 170 Thermal Paint Contours from Heat Transfer Evaluation

Section VII Figures

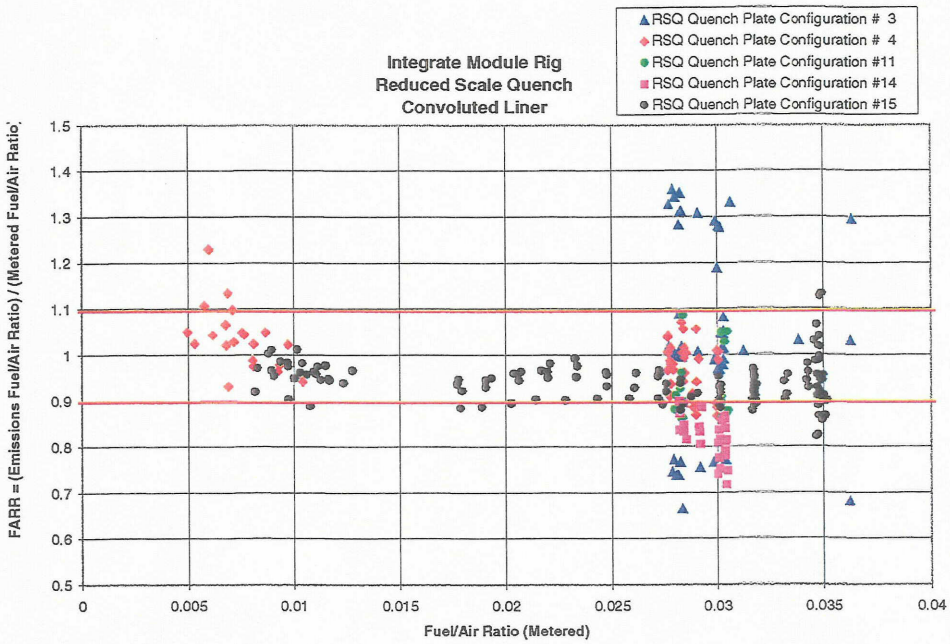

Figure VII - 1 FARR (Emissions Fuel/Air Ratio relative to Metered Fuel/Air Ratio) as a Function of Metered Fuel/Air Ratio

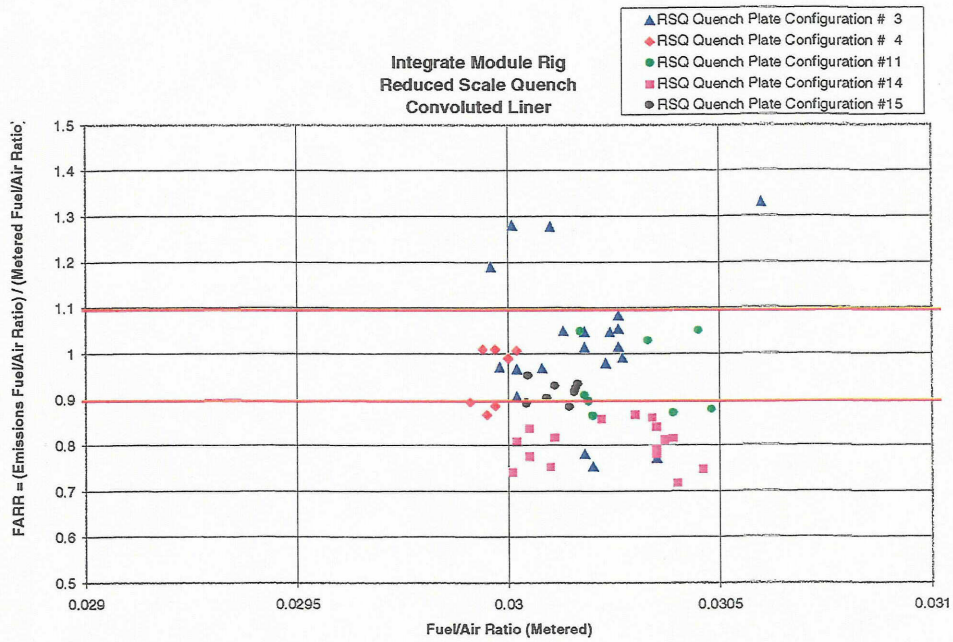

Figure VII - 2 FARR (Emissions Fuel/Air Ratio relative to Metered Fuel/Air Ratio) as a Function of Metered Fuel/Air Ratio

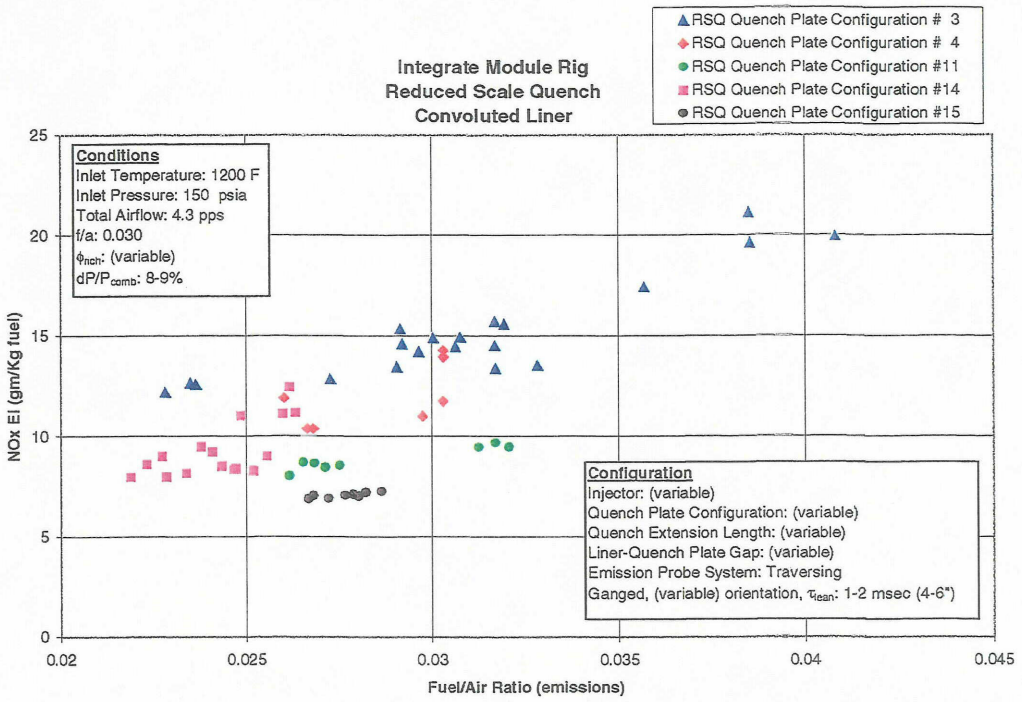

Figure VII - 3 NOx Emissions as a Function of Emissions Fuel/Air Ratio for all Reduced Scale Quench Configurations

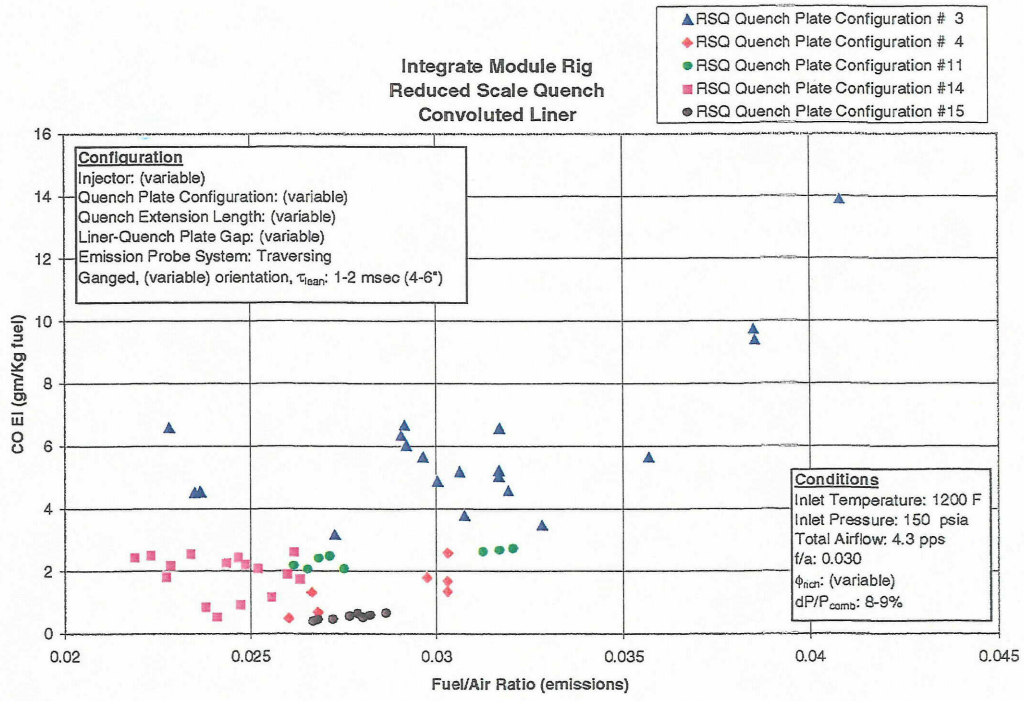

Figure VII - 4 CO Emissions as a Function of Emissions Fuel/Air Ratio for all Reduced Scale Quench Configurations

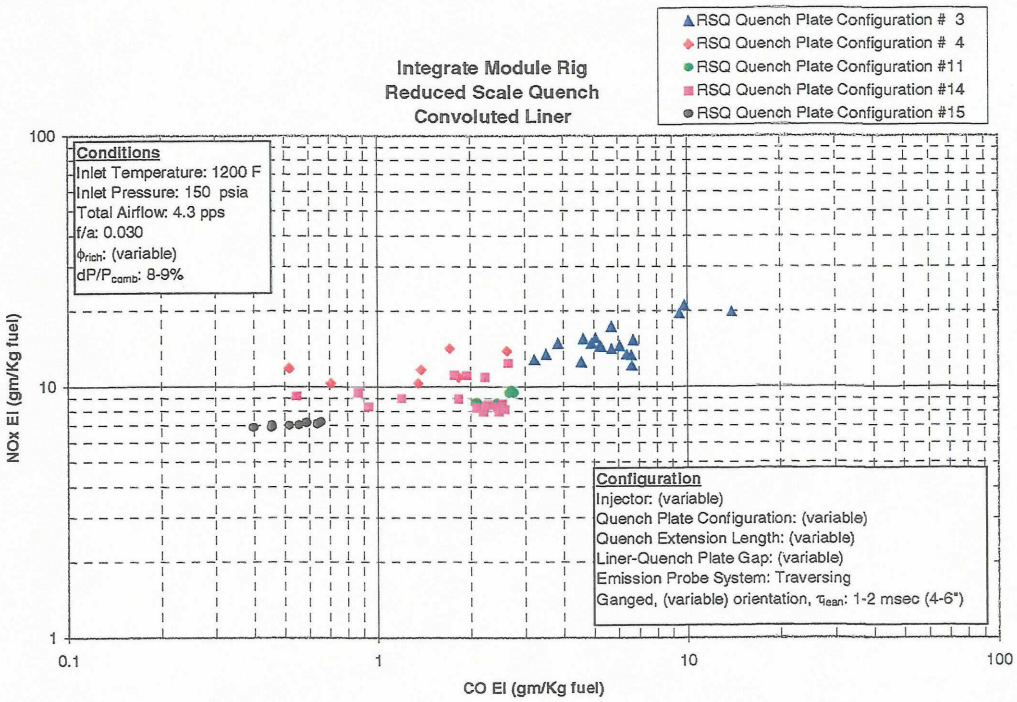

Figure VII - 5 NOx Emissions as a Function of CO Emissions for all Reduced Scale Quench Configurations

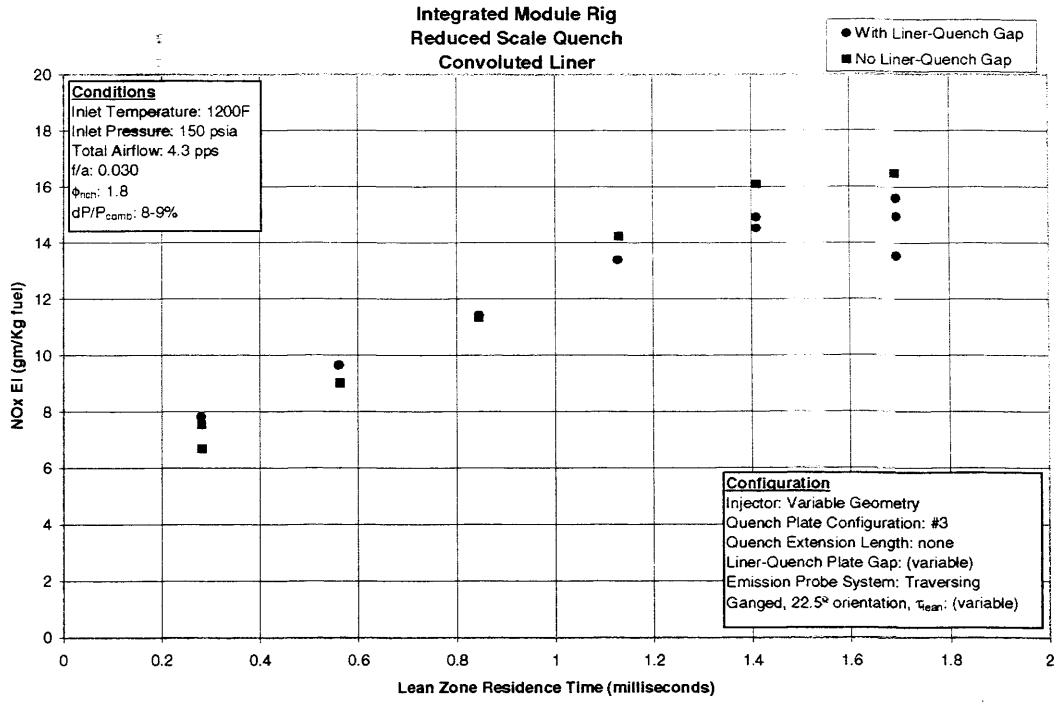

Figure VII - 6 Effect of Gap Between Rich Zone Convoluted Liner and Quench Plate on NOx Emissions as a Function of Lean Zone Residence Time

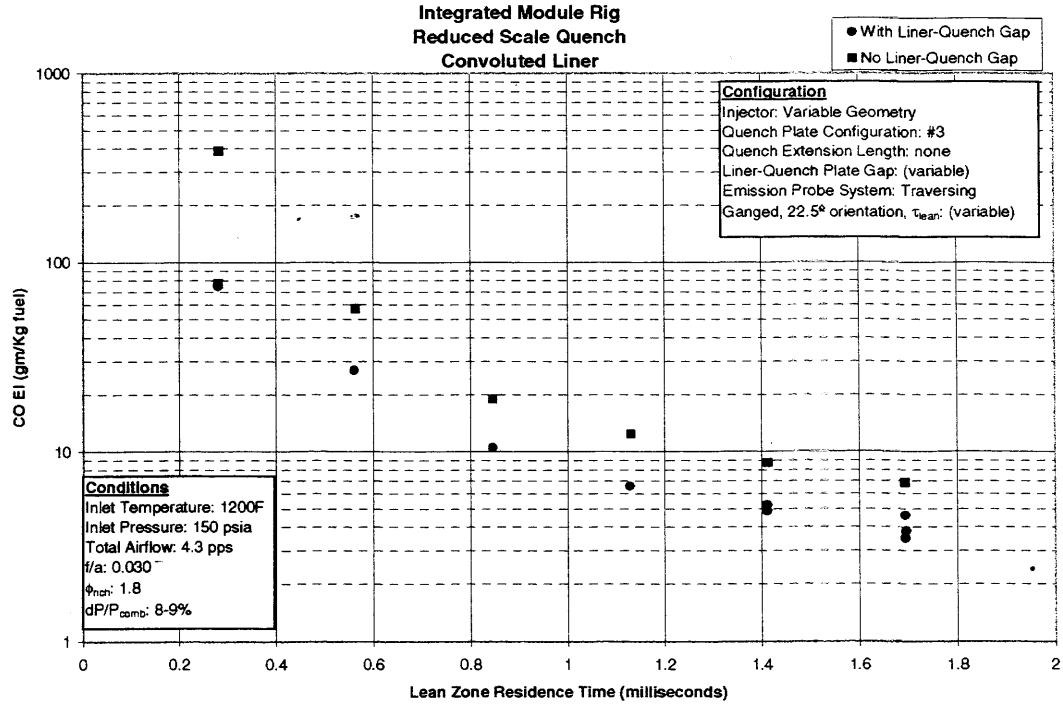

Figure VII - 7 Effect of Gap Between Rich Zone Convoluted Liner and Quench Plate on CO Emissions as a Function of Lean Zone Residence Time

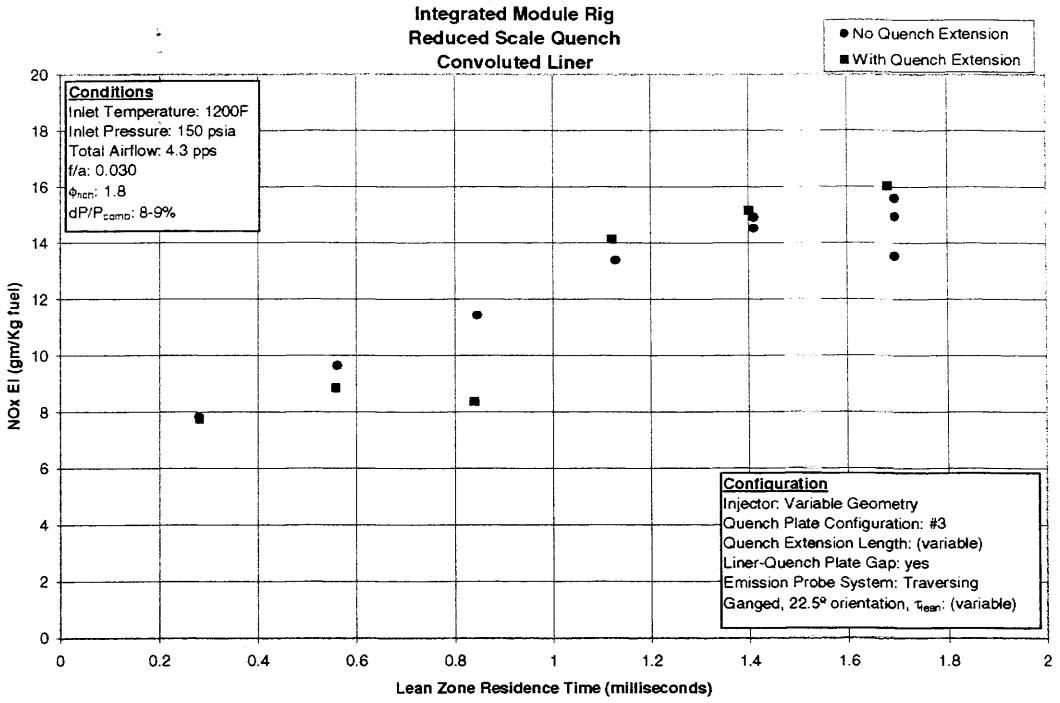

Figure VII - 8 Effect of Quench Extension on NOx Emissions as a Function of Lean Zone Residence Time

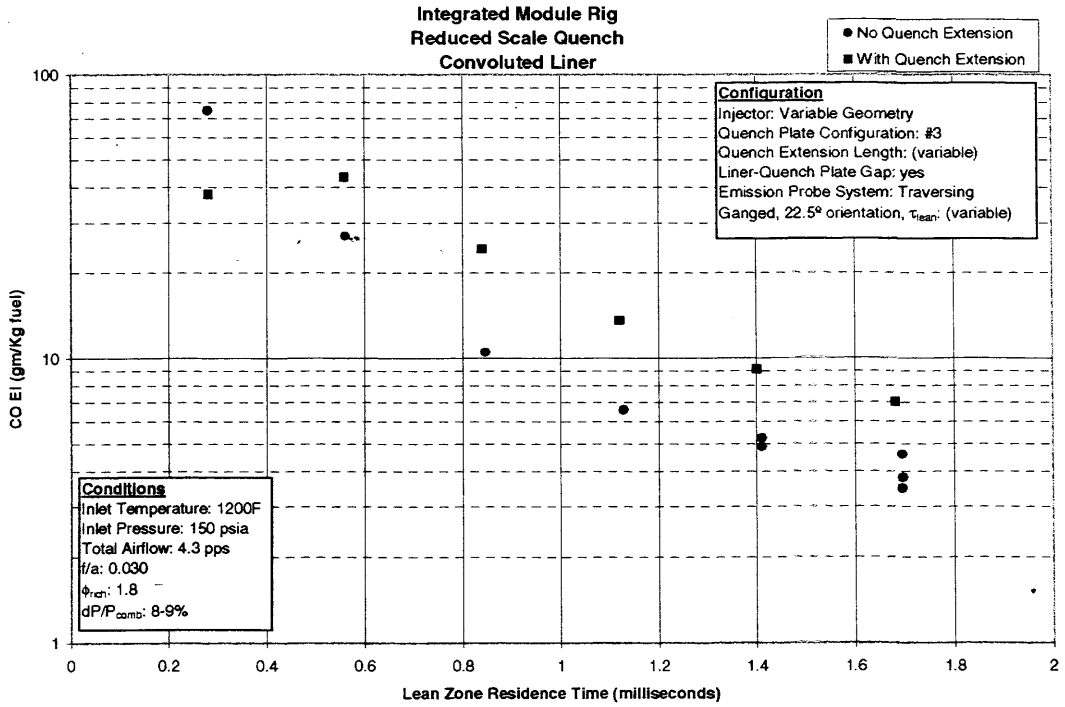

Figure VII - 9 Effect of Quench Extension on CO Emissions as a Function of Lean Zone Residence Time

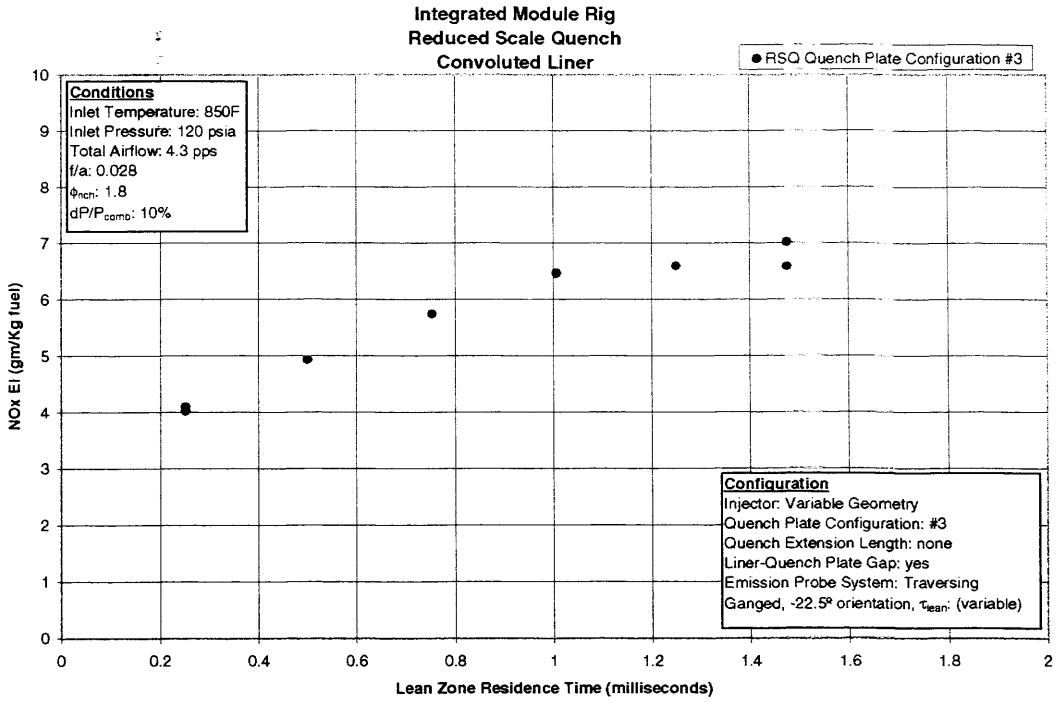

Figure VII - 10 NOx Emissions as a Function of Lean Zone Residence Time for Quench Plate Configuration #3

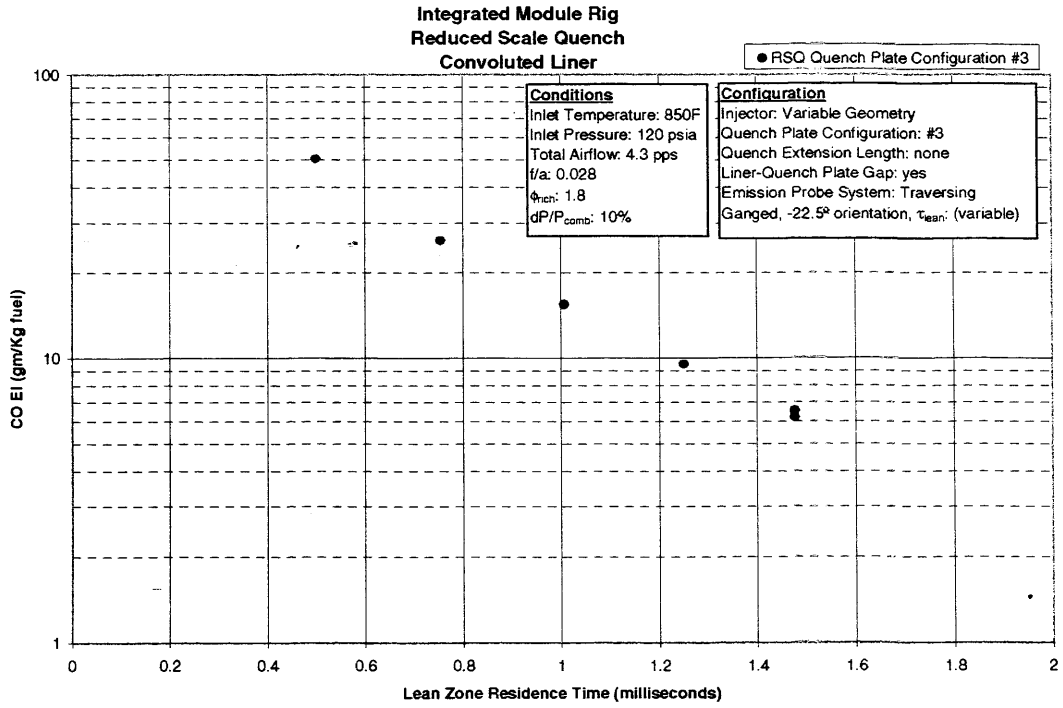

Figure VII - 11 CO Emissions as a Function of Lean Zone Residence Time for Quench Plate Configuration #3

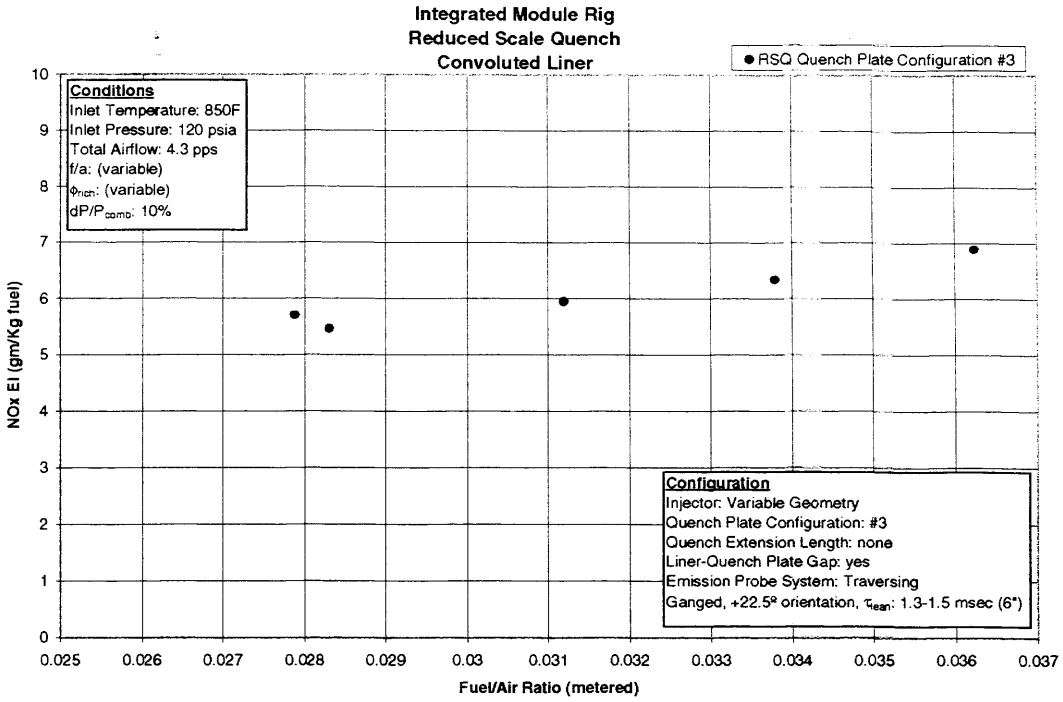

Figure VII - 12 NOx Emissions as a Function of Fuel/Air Ratio for Quench Plate Configuration #3

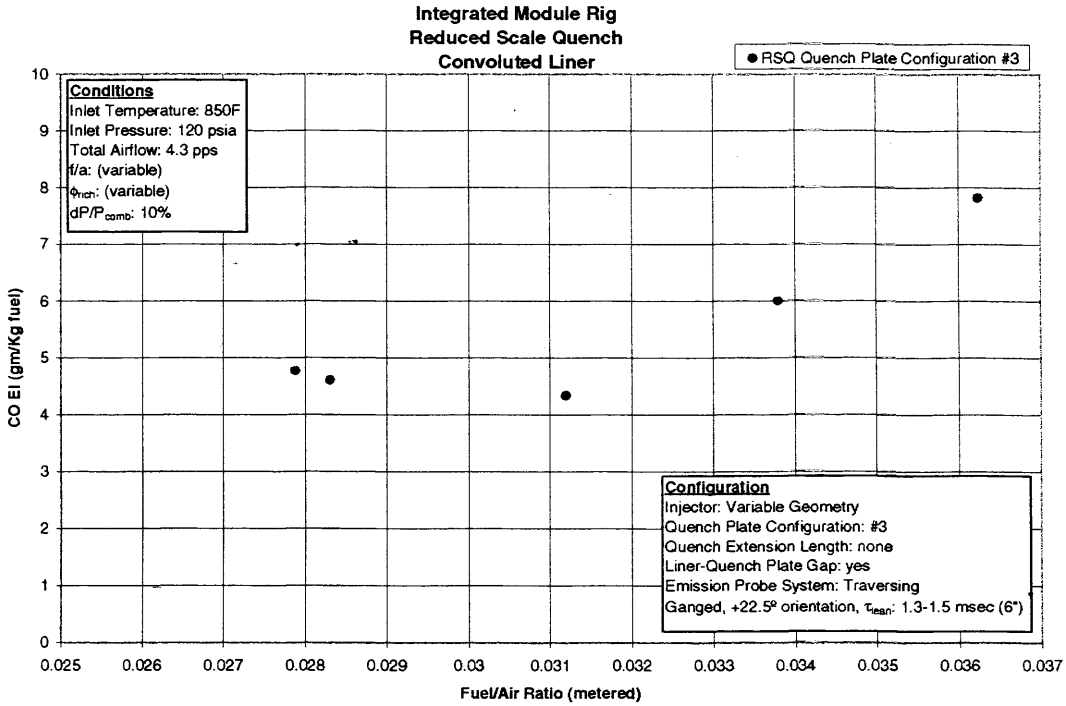

Figure VII - 13 CO Emissions as a Function of Fuel/Air Ratio for Quench Plate Configuration #3

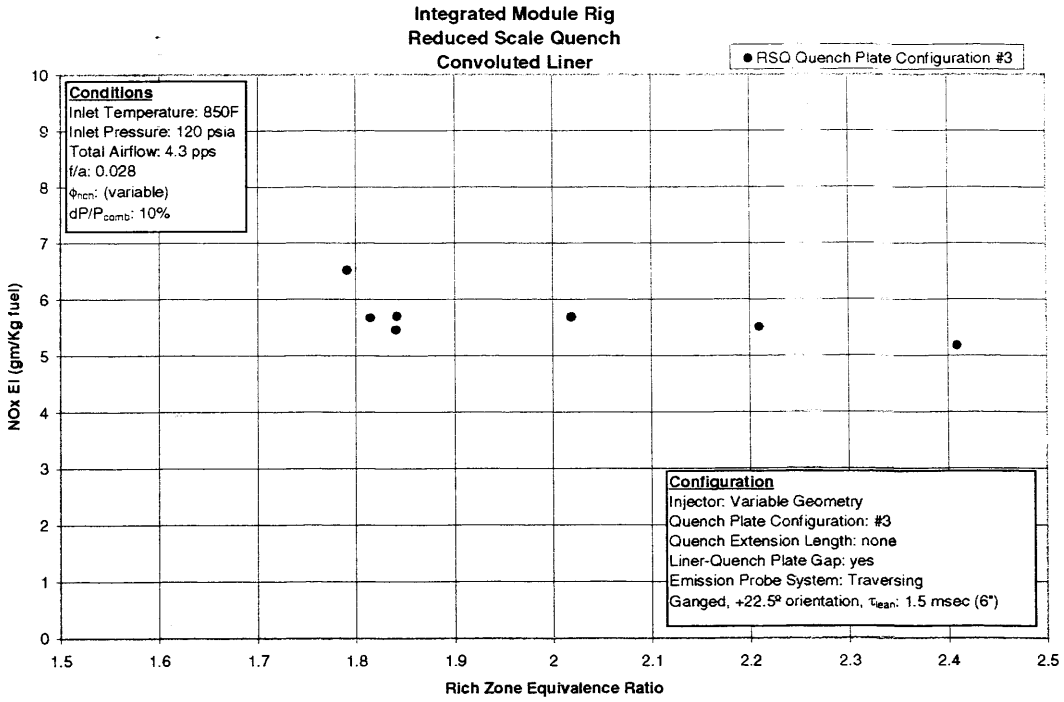

Figure VII - 14 NOx Emissions as a Function of Rich Zone Equivalence Ratio for Quench Plate Configuration #3

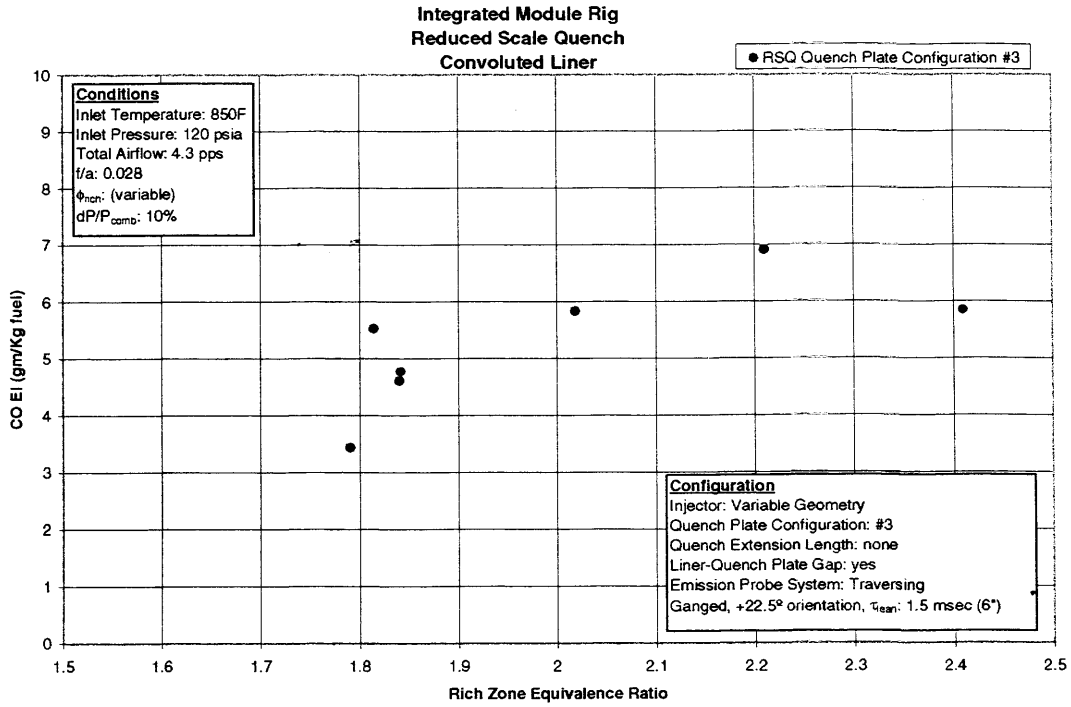

Figure VII - 15 CO Emissions as a Function of Rich Zone Equivalence Ratio for Quench Plate Configuration #3

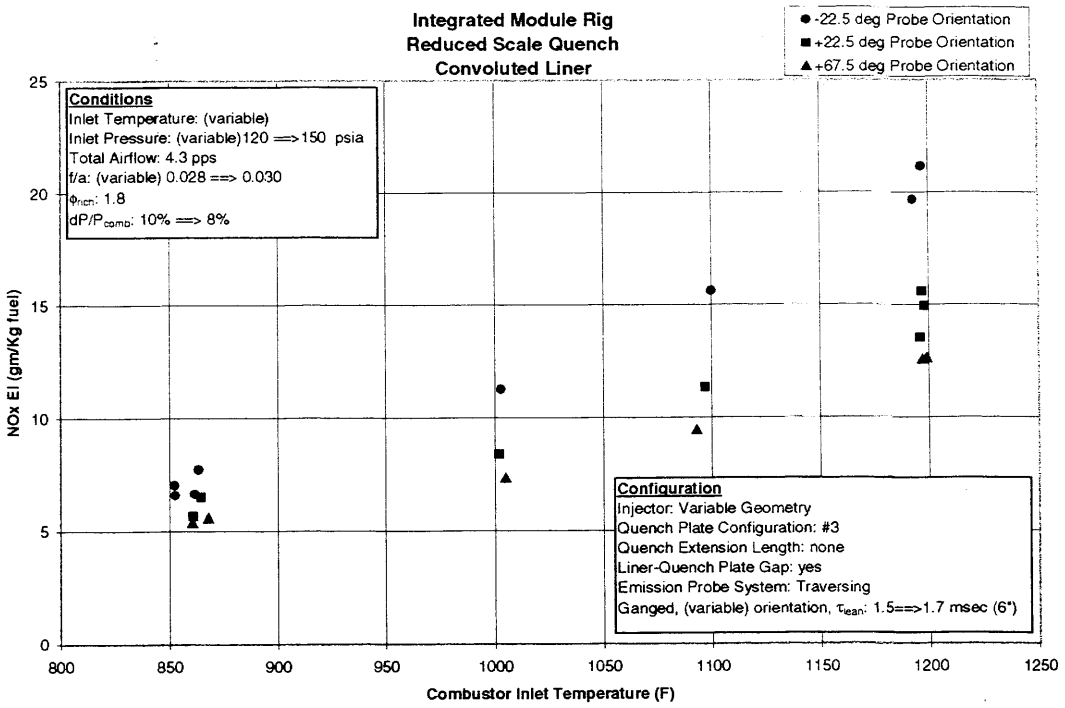

Figure VII - 16 NOx Emissions as a Function of Inlet Temperature for Quench Plate Configuration #3

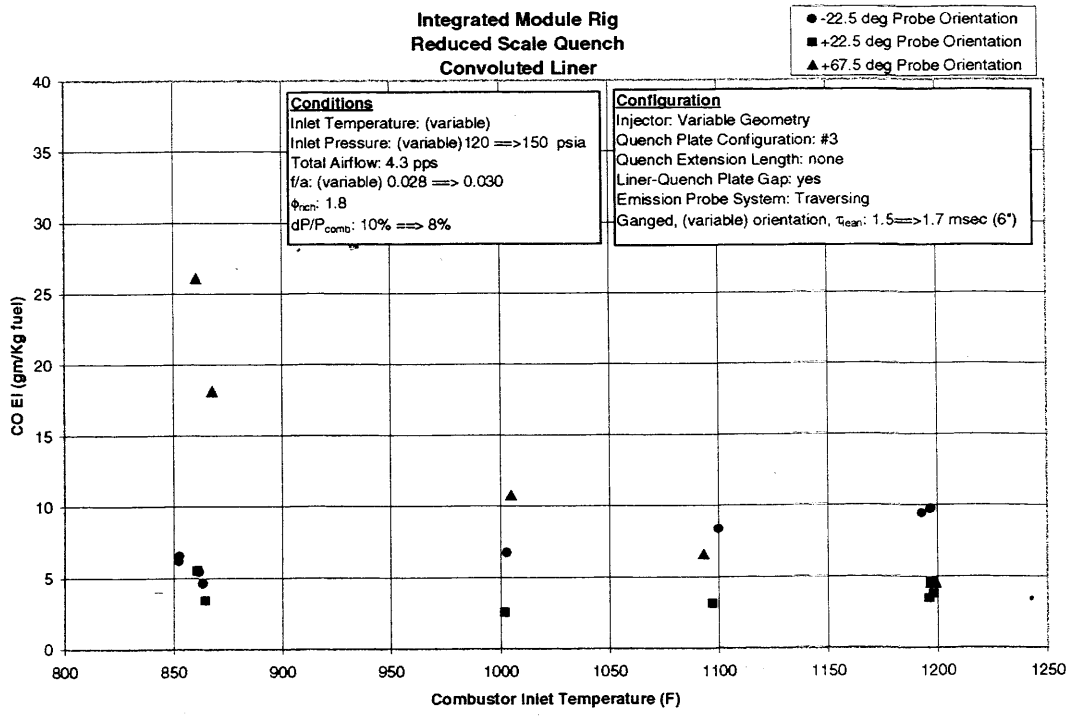

Figure VII - 17 CO Emissions as a Function of Inlet Temperature for Quench Plate Configuration #3

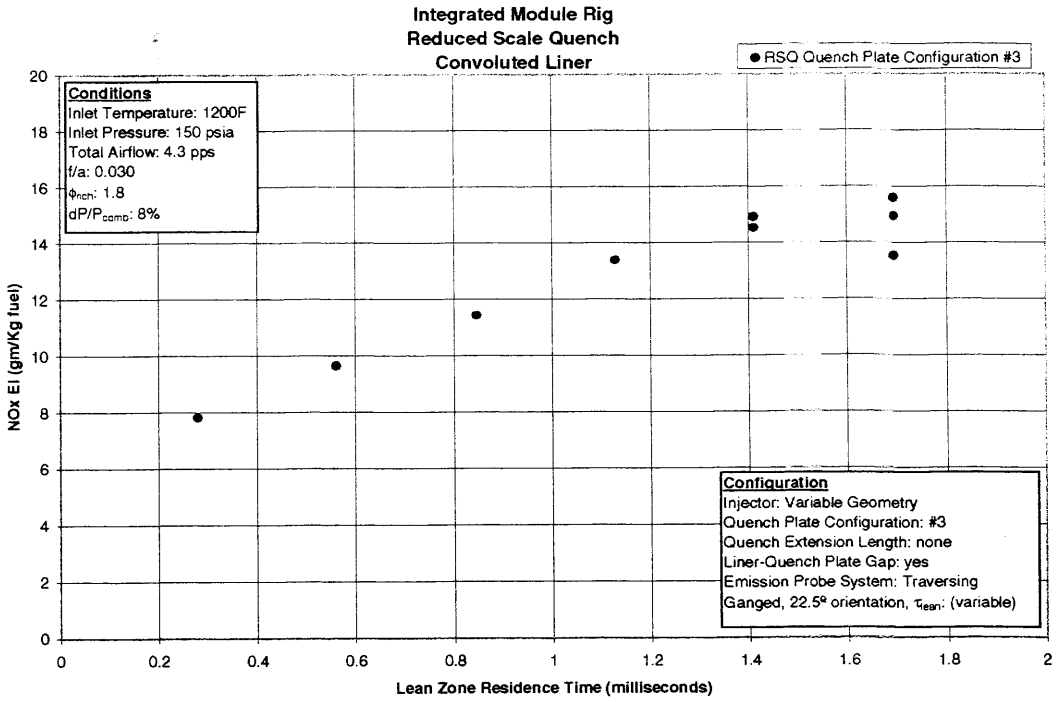

Figure VII - 18 NOx Emissions as a Function of Lean Zone Residence Time for Quench Plate Configuration #3

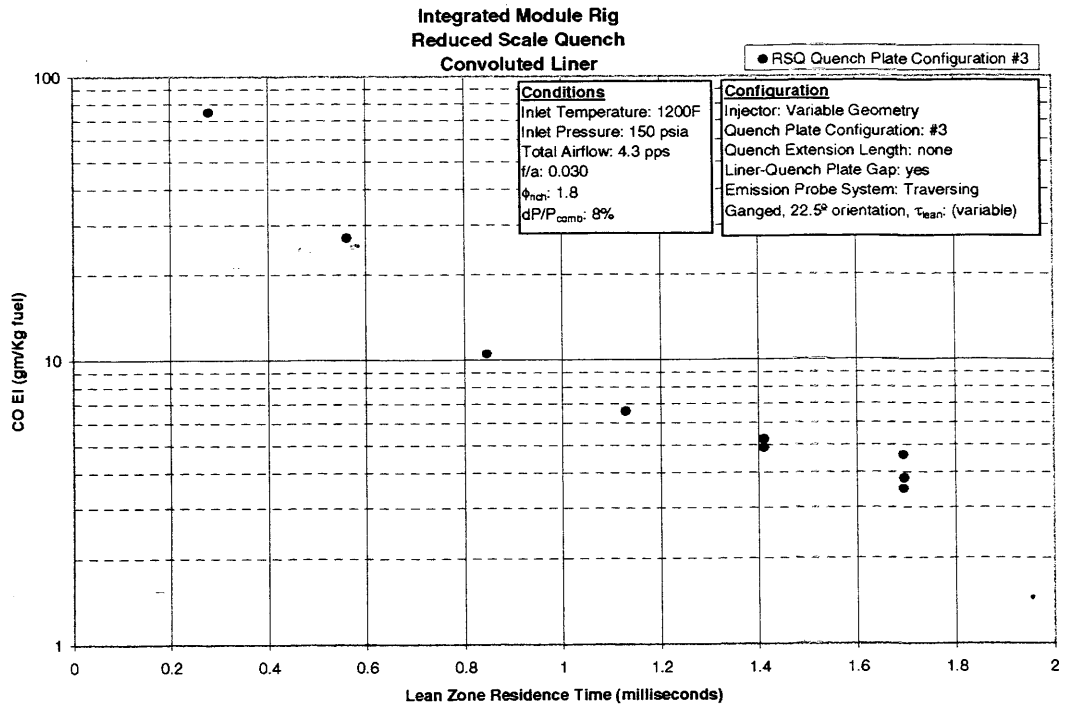

Figure VII - 19 CO Emissions as a Function of Lean Zone Residence Time for Quench Plate Configuration #3

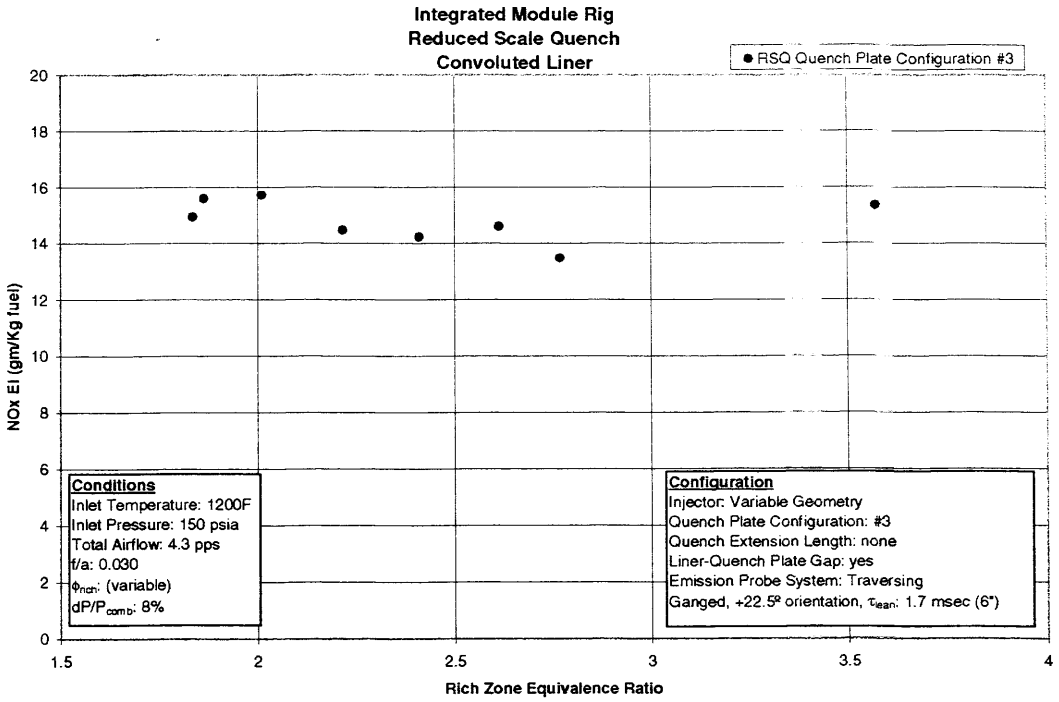

Figure VII - 20 NOx Emissions as a Function of Rich Zone Equivalence Ratio for Quench Plate Configuration #3

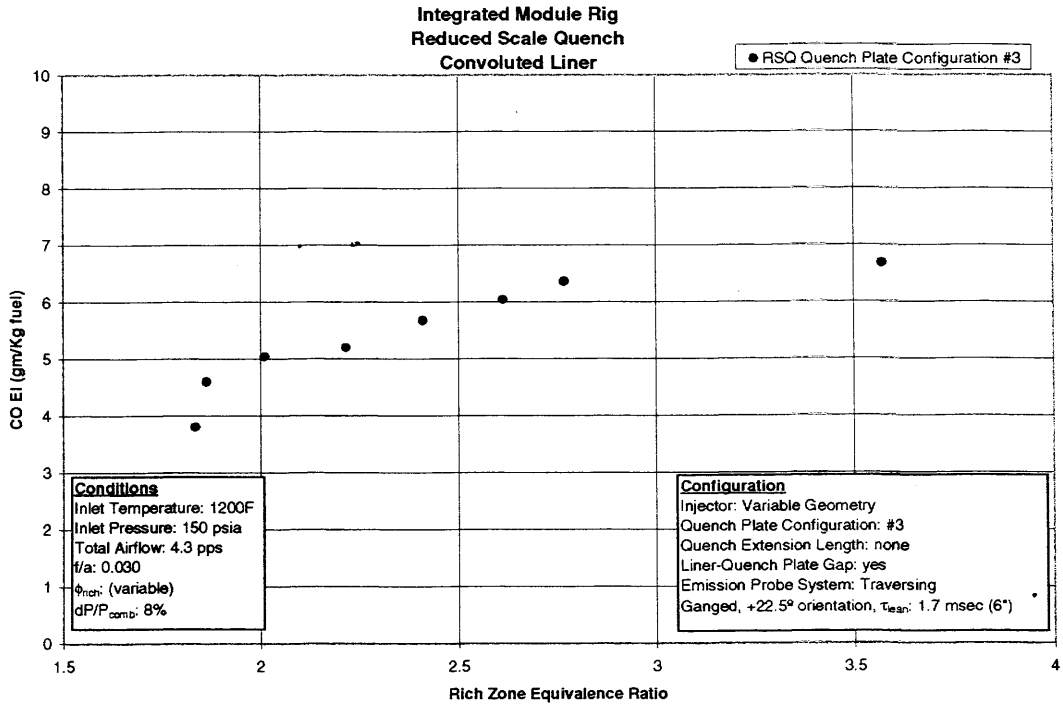

Figure VII - 21 CO Emissions as a Function of Rich Zone Equivalence Ratio for Quench Plate Configuration #3

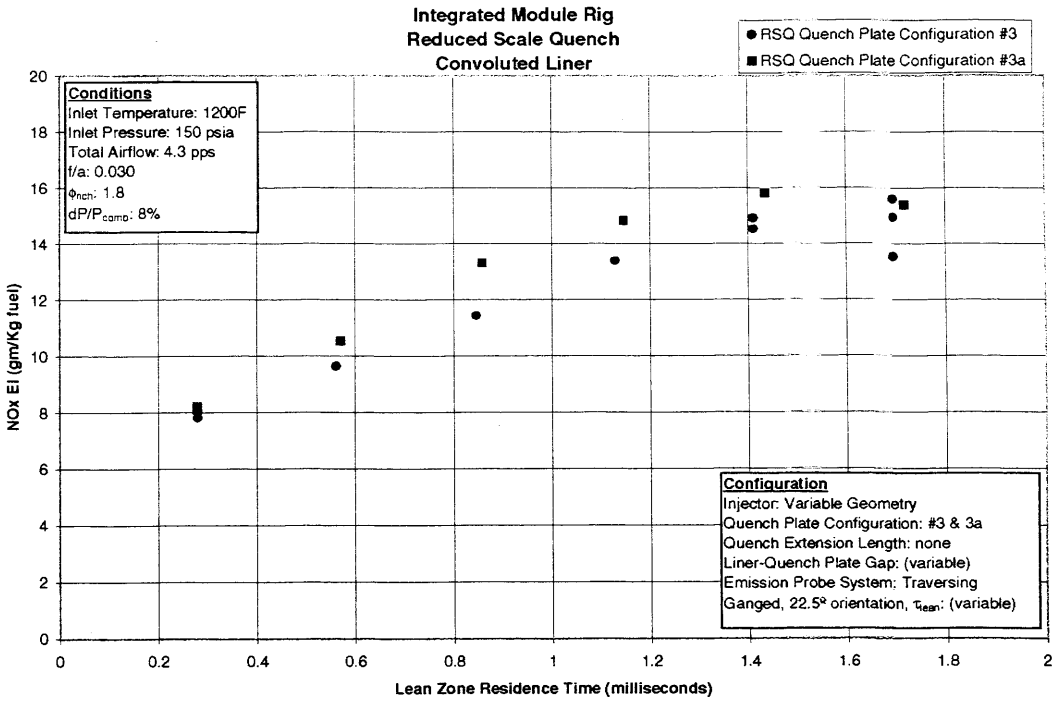

Figure VII - 22 NOx Emissions as a Function of Lean Zone Residence Time for Quench Plate Configuration #3 (gap) and Quench Plate Configuration #3a (no gap)

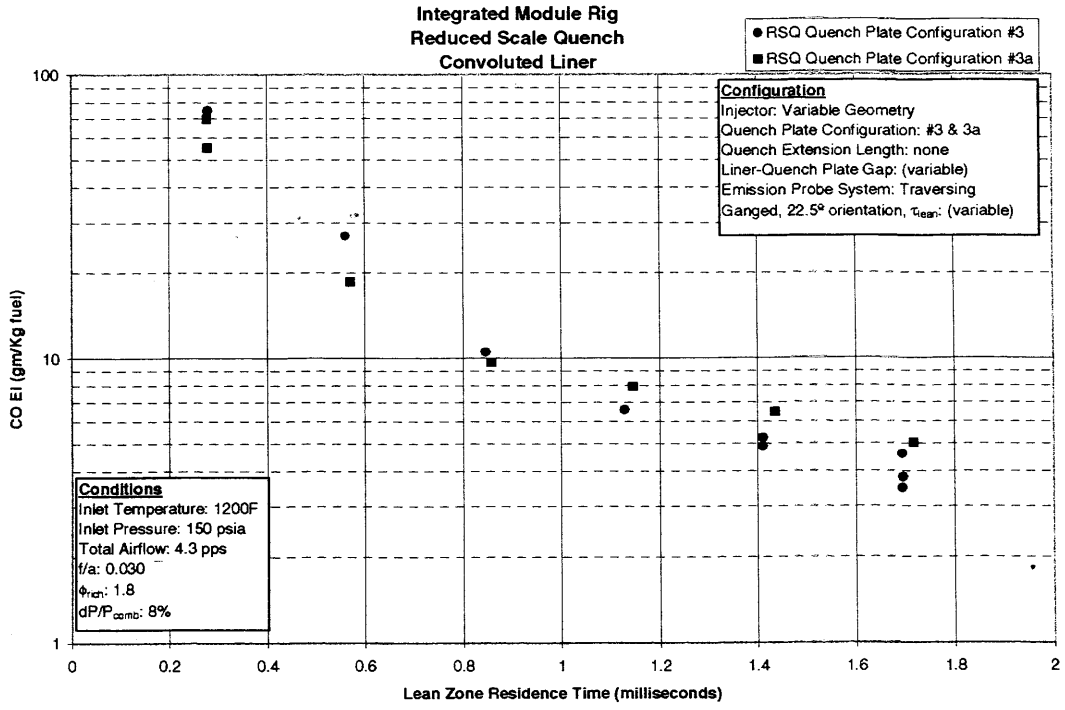

Figure VII - 23 CO Emissions as a Function of Lean Zone Residence Time for Quench Plate Configuration #3 (gap) and Quench Plate Configuration #3a (no gap)

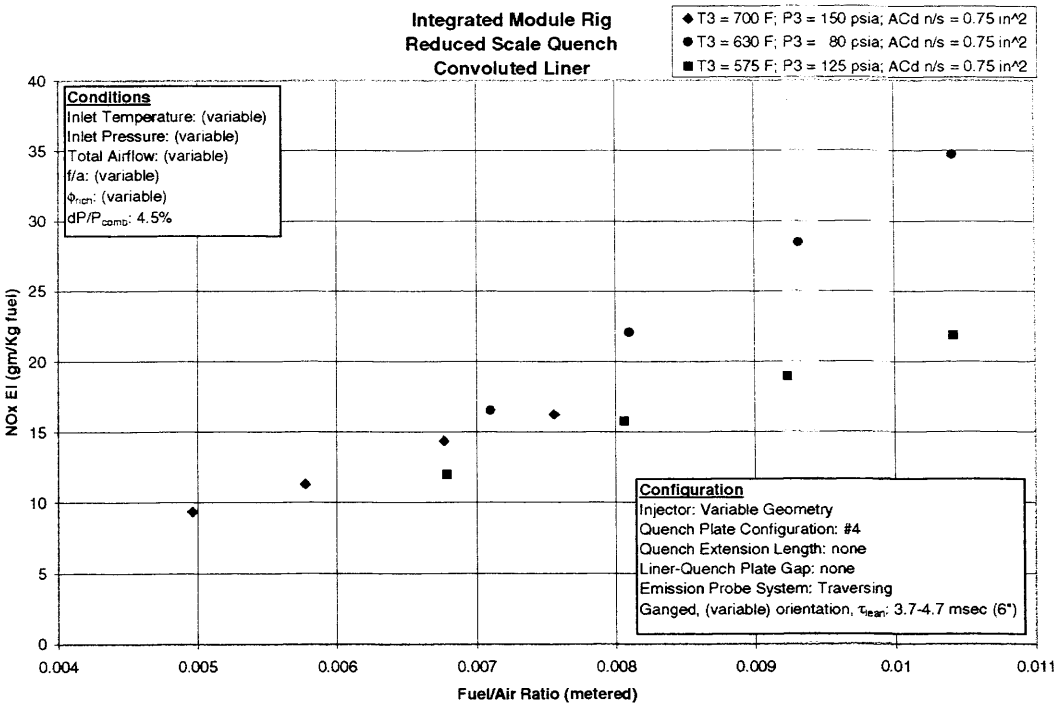

Figure VII - 24 NOx Emissions as a Function of Fuel/Air Ratio for Quench Plate Configuration #4

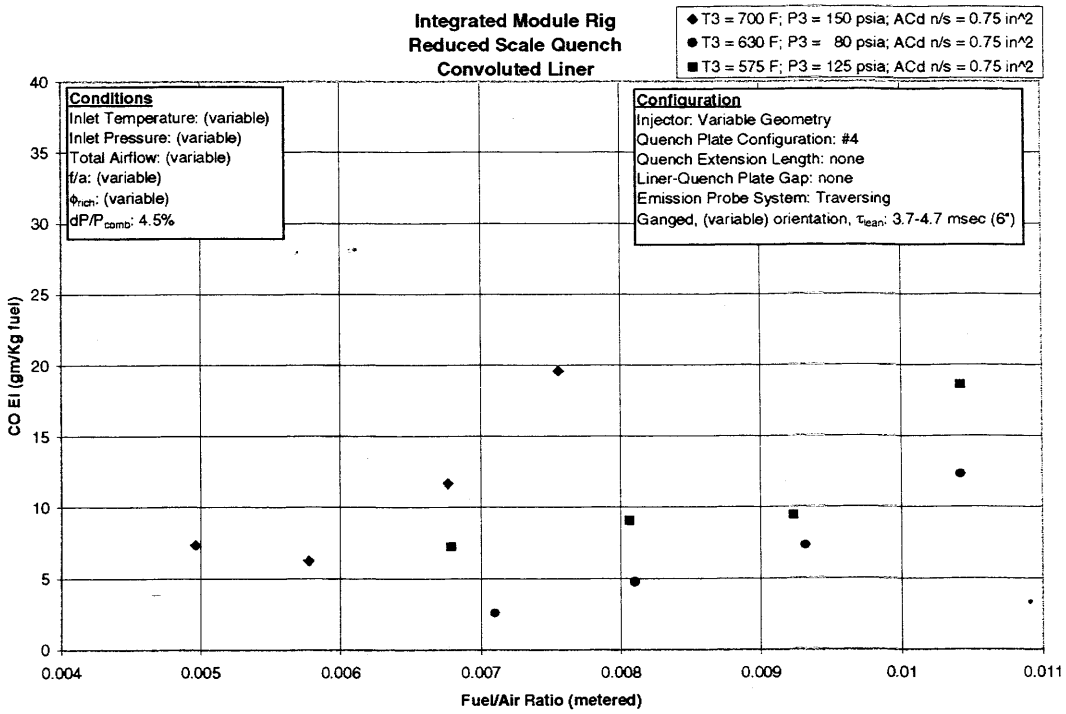

Figure VII - 25 CO Emissions as a Function of Fuel/Air Ratio for Quench Plate Configuration #4

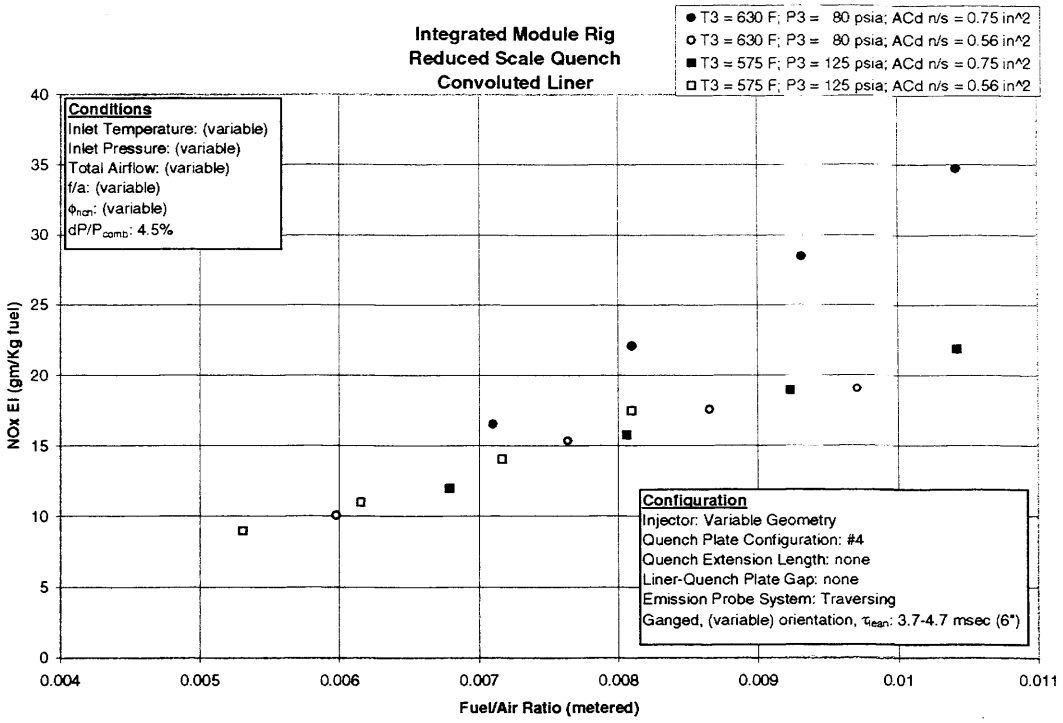

Figure VII - 26 NOx Emissions as a Function of Fuel/Air Ratio for Quench Plate Configuration #4

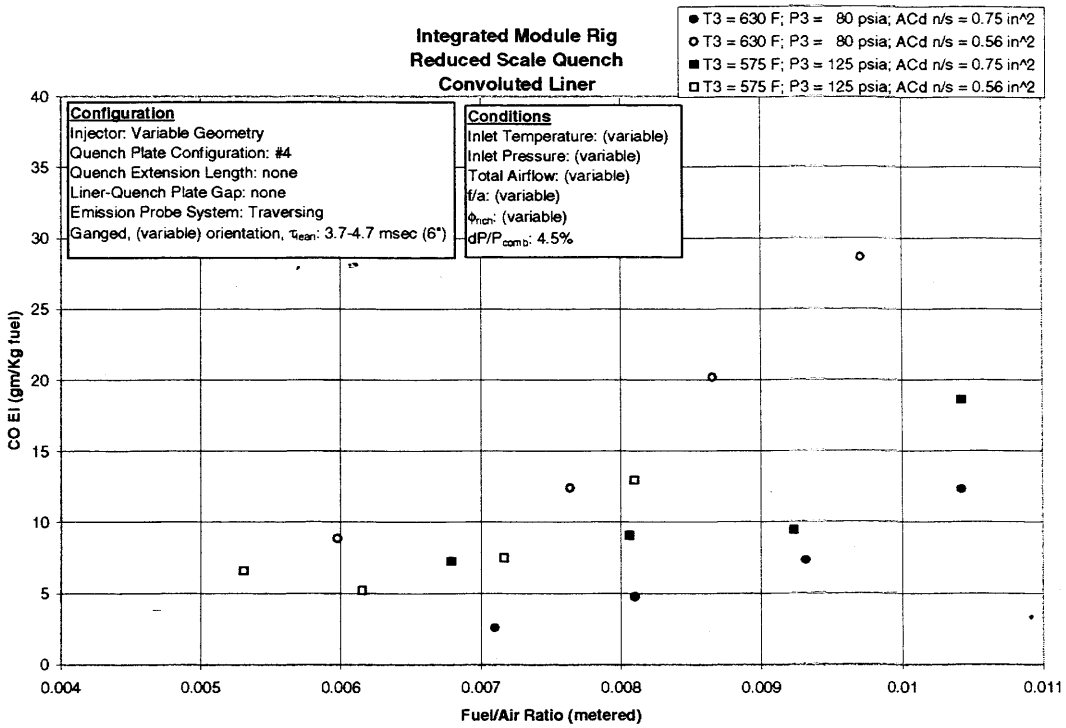

Figure VII - 27 CO Emissions as a Function of Fuel/Air Ratio for Quench Plate Configuration #4

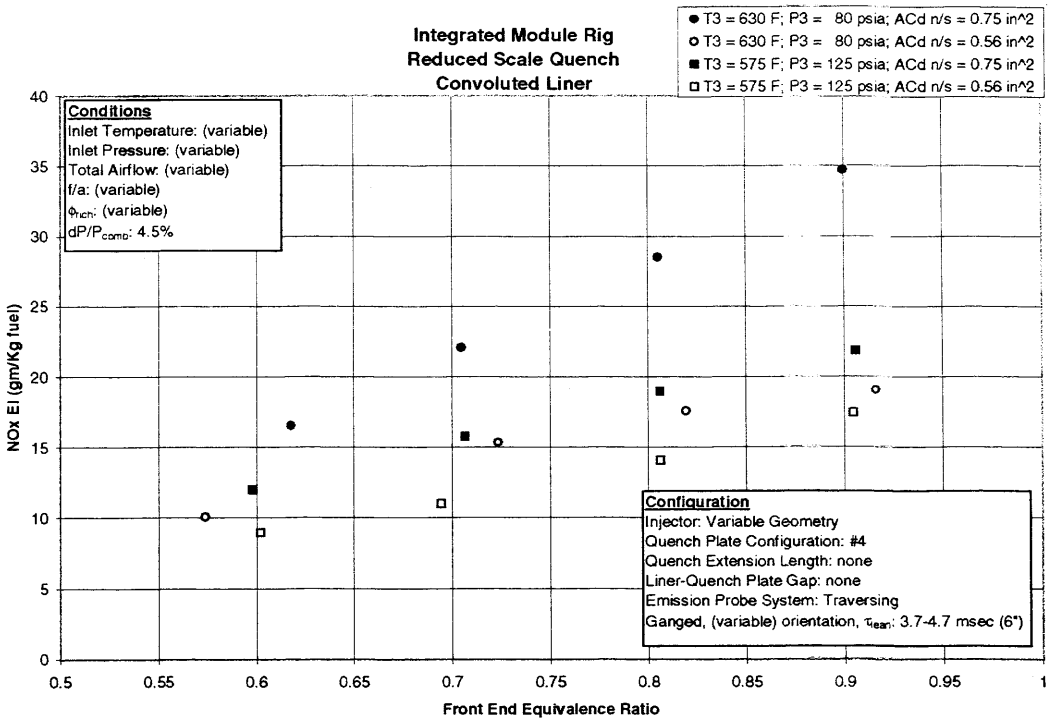

Figure VII - 28 NOx Emissions as a Function of Front End Equivalence Ratio for Quench Plate Configuration #4

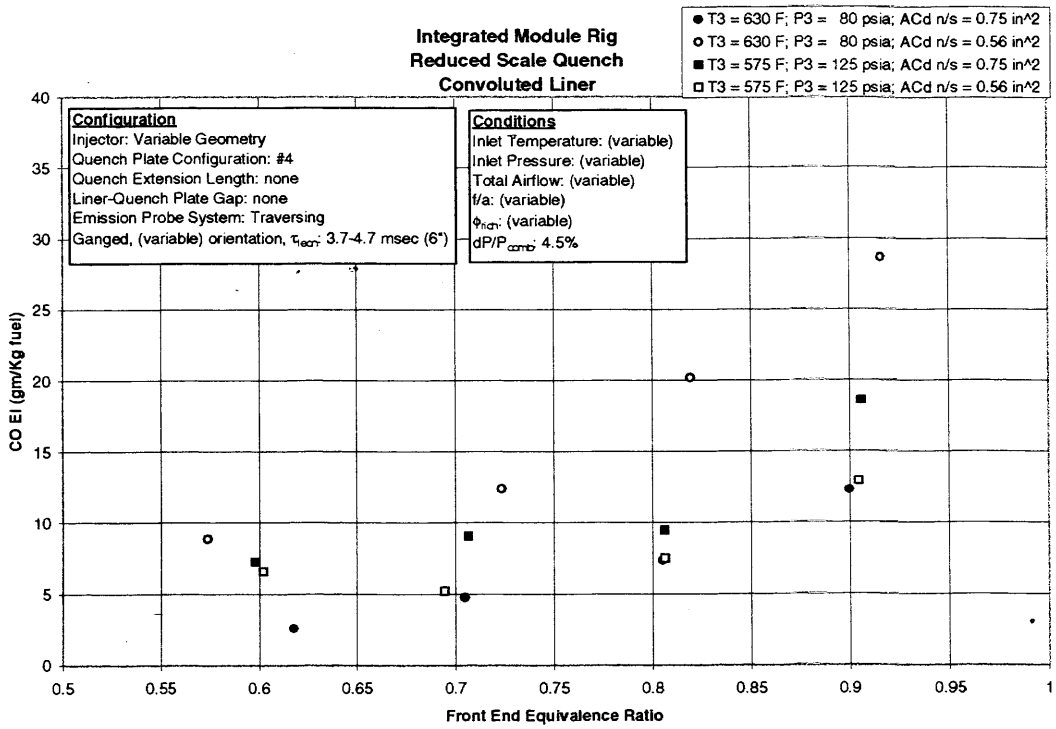

Figure VII - 29 CO Emissions as a Function of Front End Equivalence Ratio for Quench Plate Configuration #4

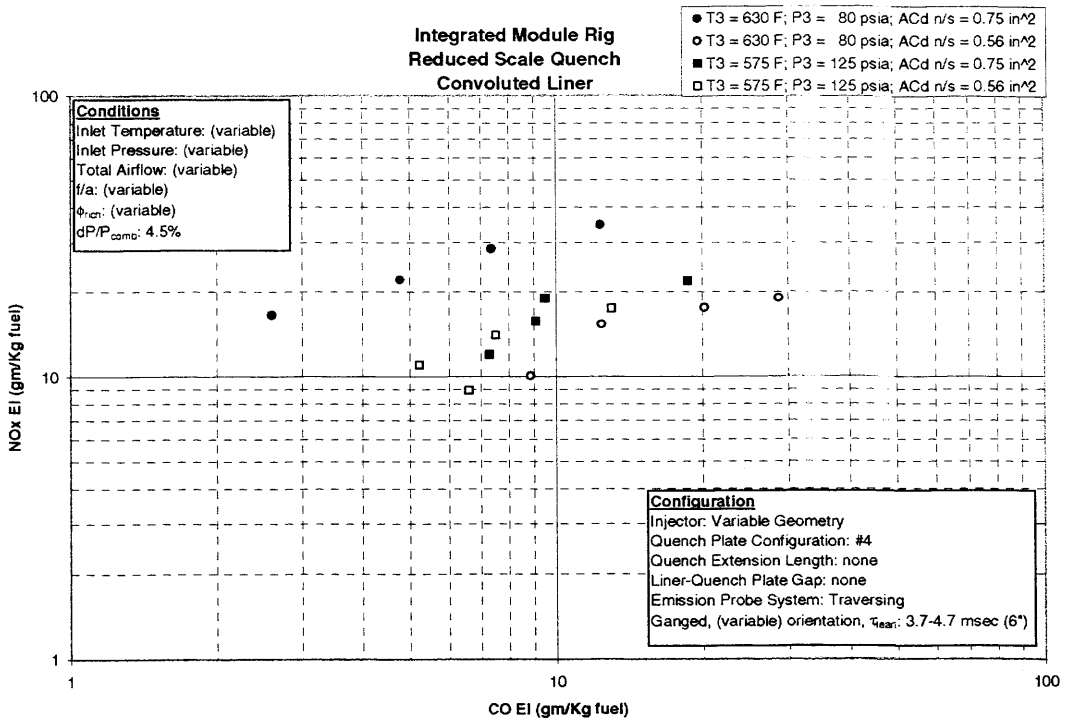

Figure VII - 30 NOx Emissions as a Function of CO Emissions for Quench Plate Configuration #4

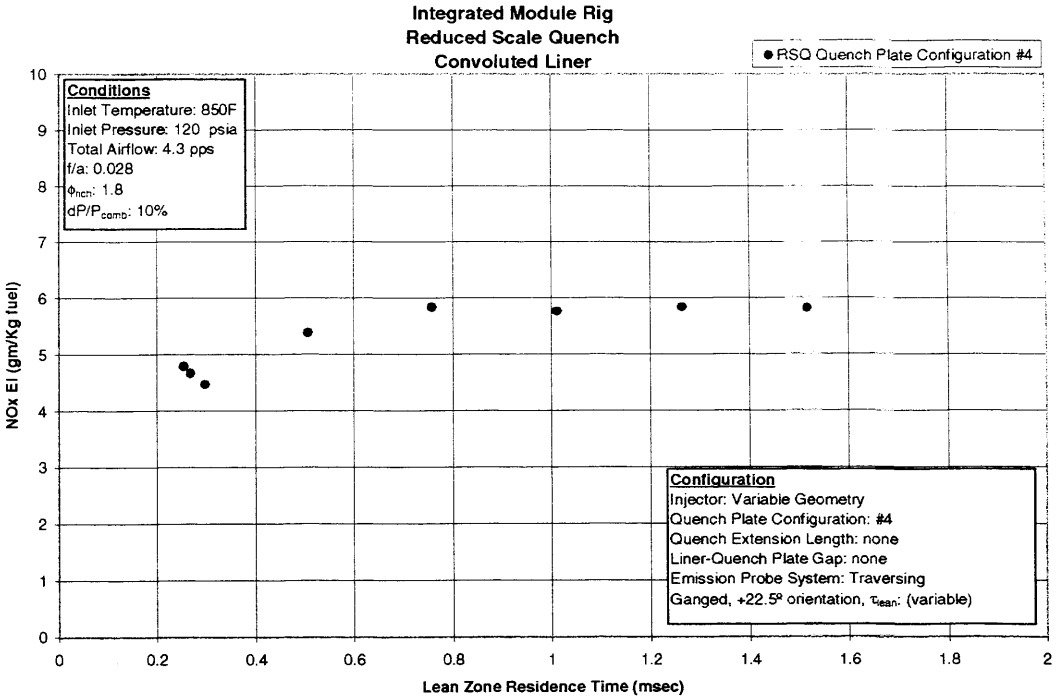

Figure VII - 31 NOx Emissions as a Function of Lean Zone Residence Time for Quench Plate Configuration #4

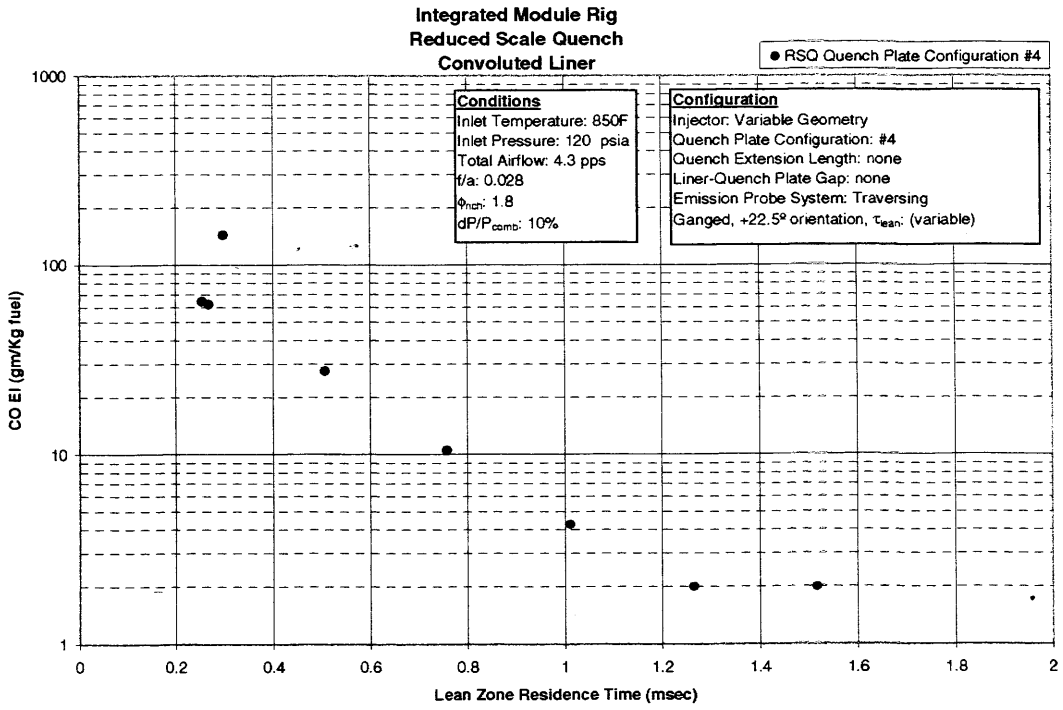

Figure VII - 32 CO Emissions as a Function of Lean Zone Residence Time for Quench Plate Configuration #4

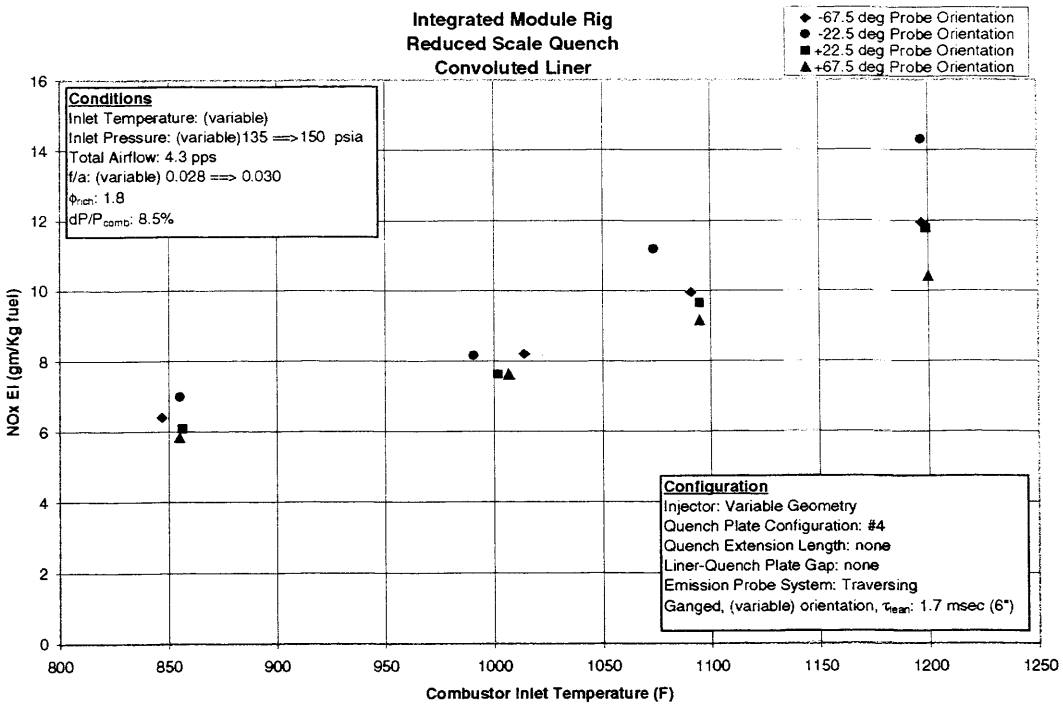

Figure VII - 33 NOx Emissions as a Function of Inlet Temperature for Quench Plate Configuration #4

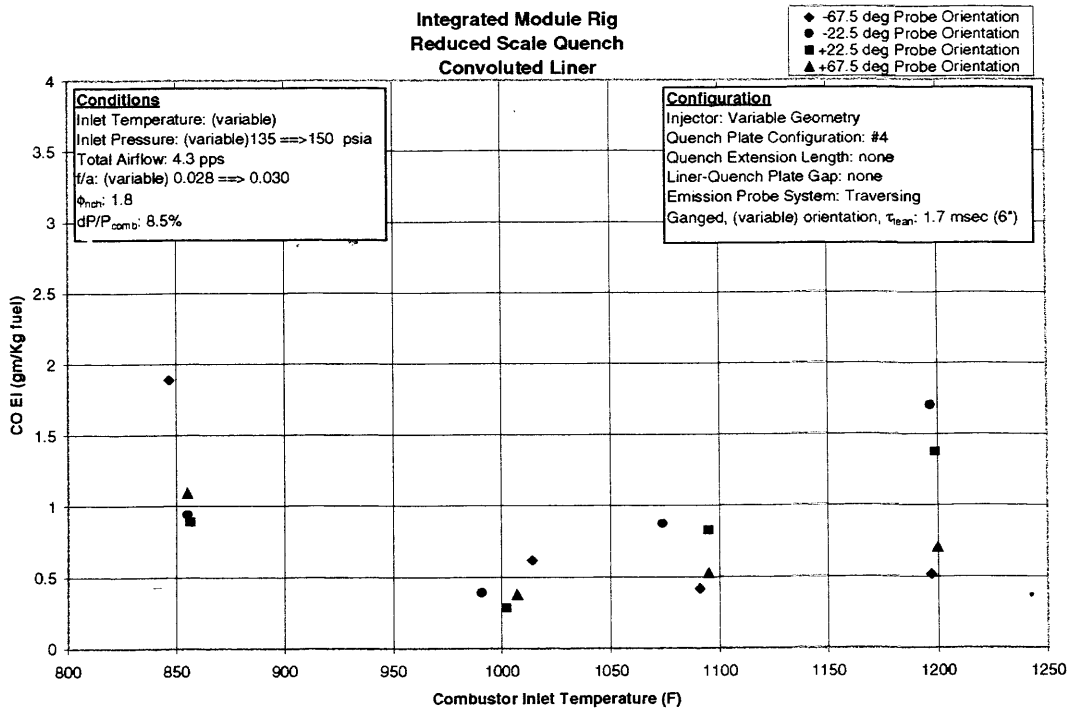

Figure VII - 34 CO Emissions as a Function of Inlet Temperature for Quench Plate Configuration #4

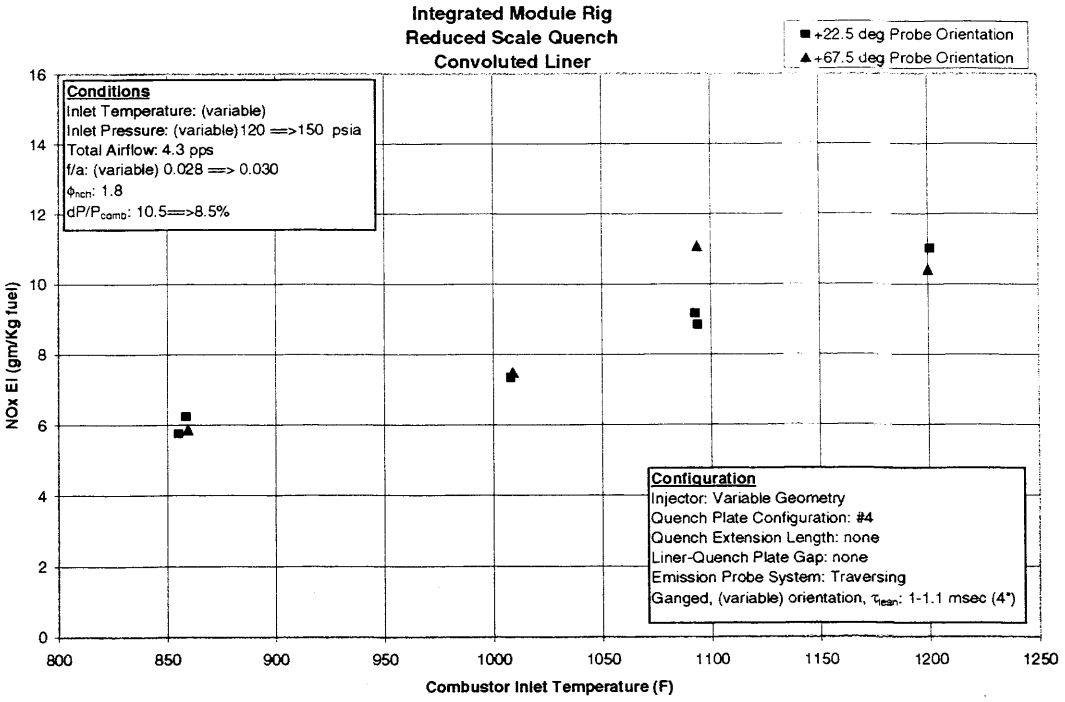

Figure VII - 35 NOx Emissions as a Function of Inlet Temperature for Quench Plate Configuration #4

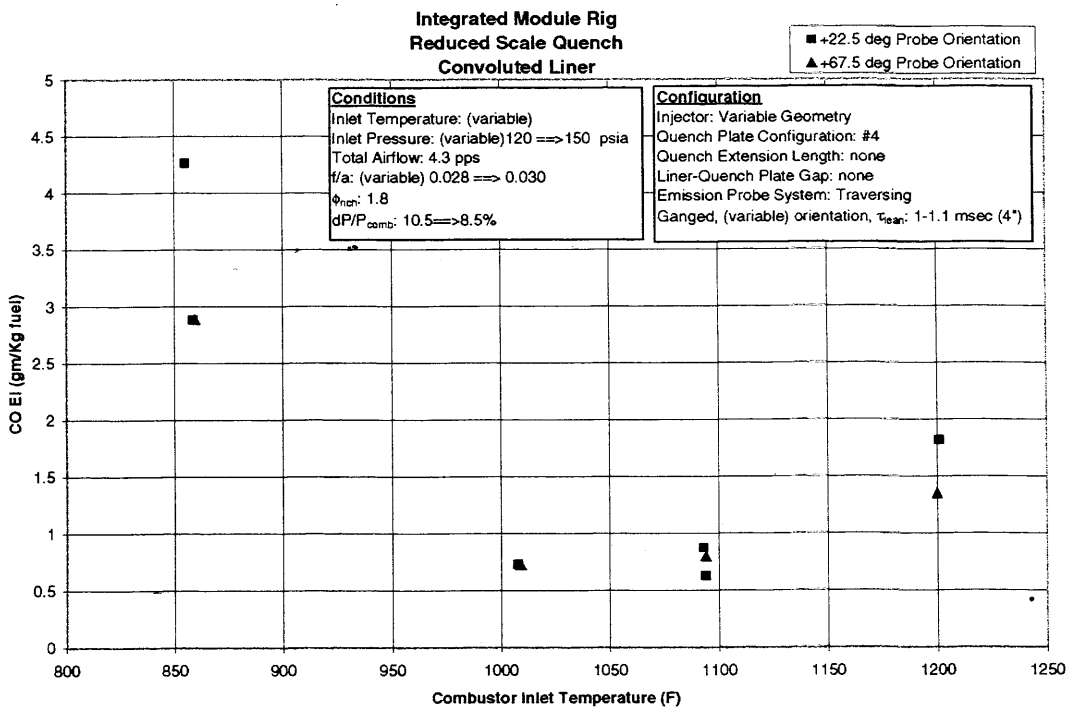

Figure VII - 36 CO Emissions as a Function of Inlet Temperature for Quench Plate Configuration #4

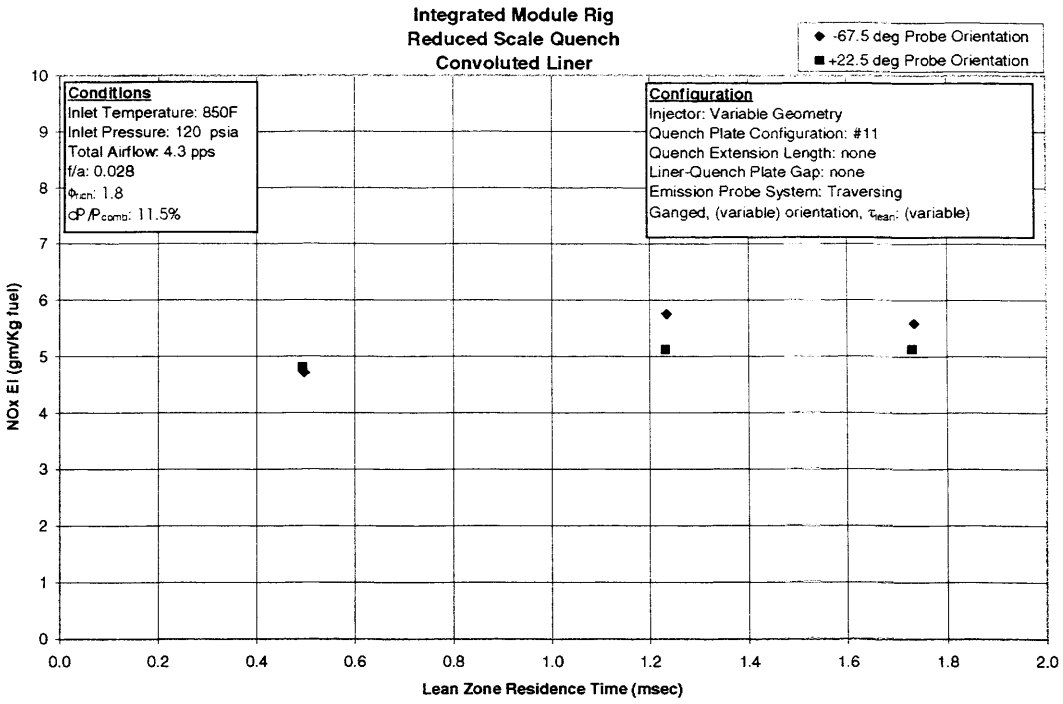

Figure VII - 37 NOx Emissions as a Function of Lean Zone Residence Time for Quench Plate Configuration #11

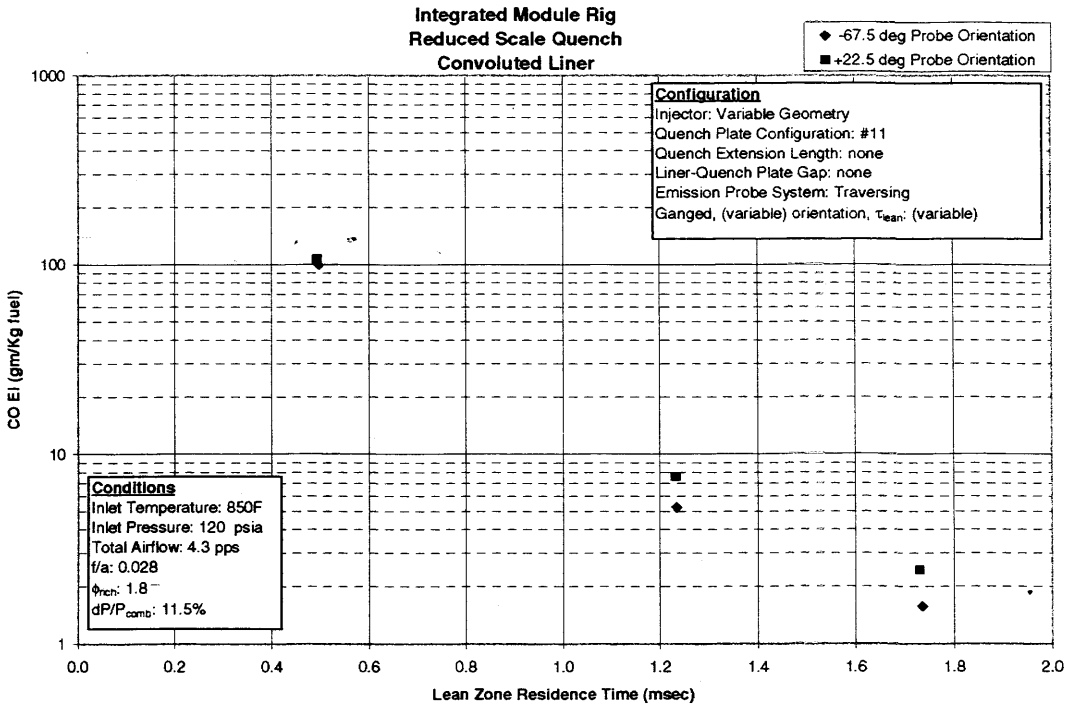

Figure VII - 38 CO Emissions as a Function of Lean Zone Residence Time for Quench Plate Configuration #11

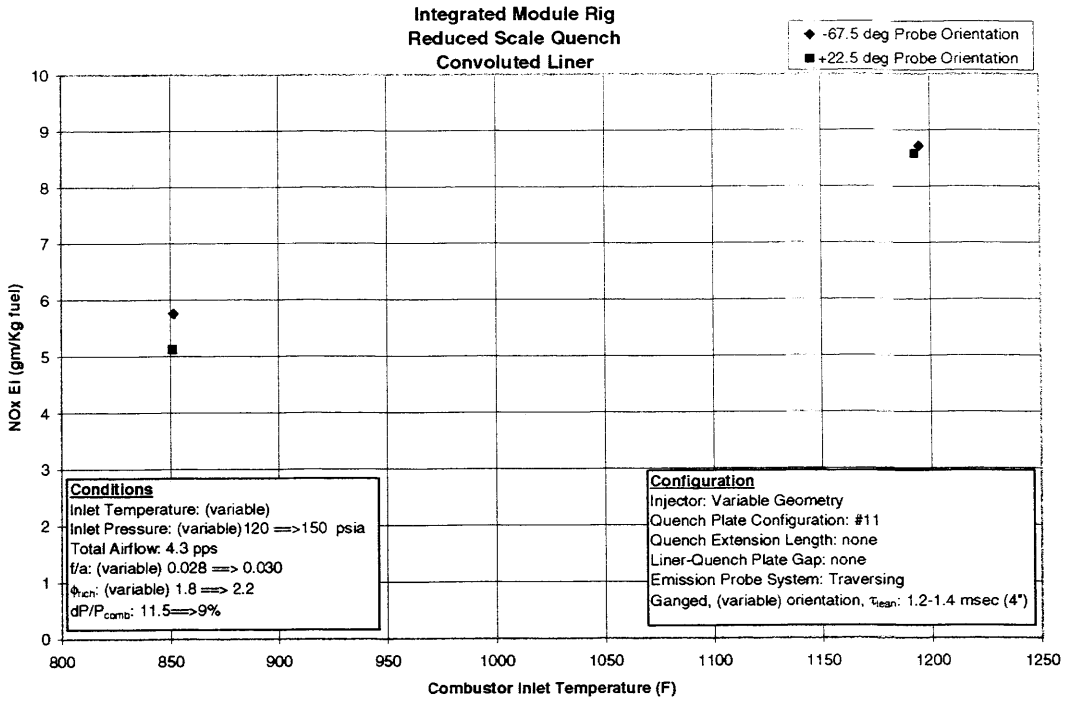

Figure VII - 39 NOx Emissions as a Function of Inlet Temperature for Quench Plate Configuration #11

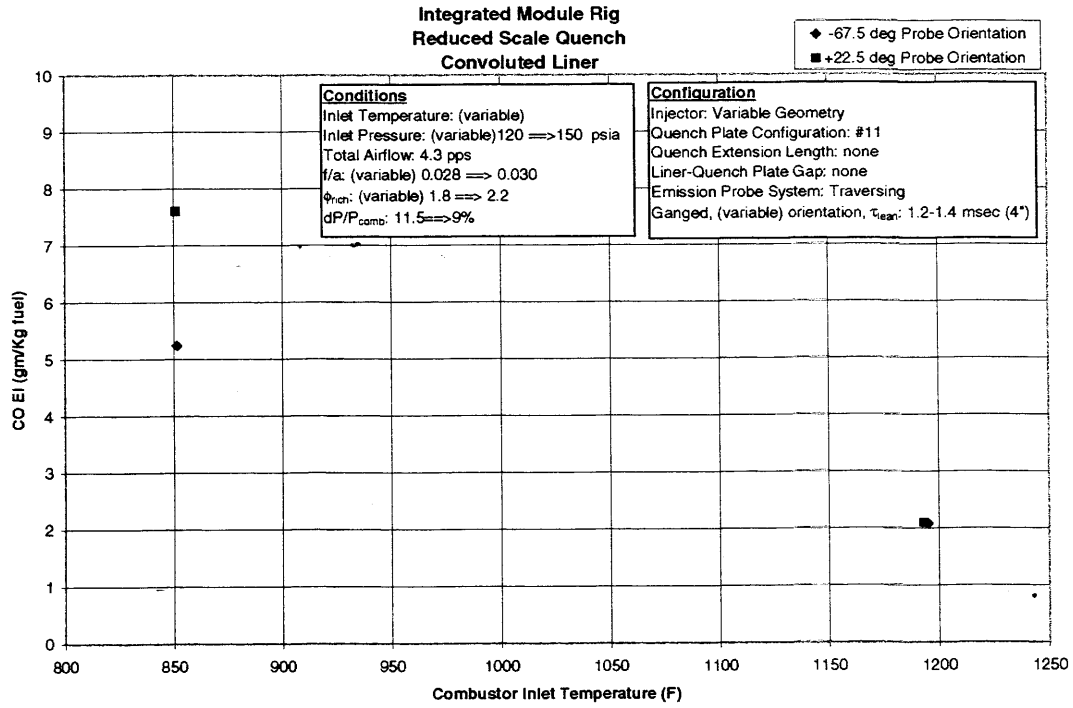

Figure VII - 40 CO Emissions as a Function of Inlet Temperature for Quench Plate Configuration #11

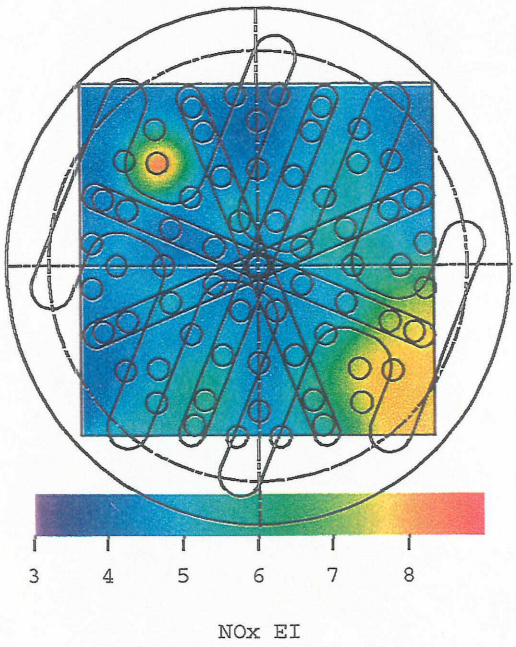

Figure VII - 41 NOx Emissions Contours for Quench Plate Configuration #11 (850F, 120 psia, 0.028 f/a, 1" Downstream from Lean Zone Inlet)

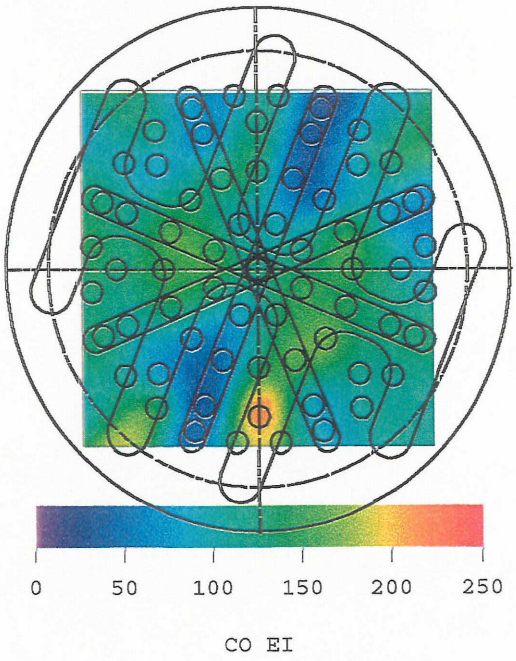

Figure VII - 42 CO Emissions Contours for Quench Plate Configuration #11 (850F, 120 psia, 0.028 f/a, 1" Downstream from Lean Zone Inlet)

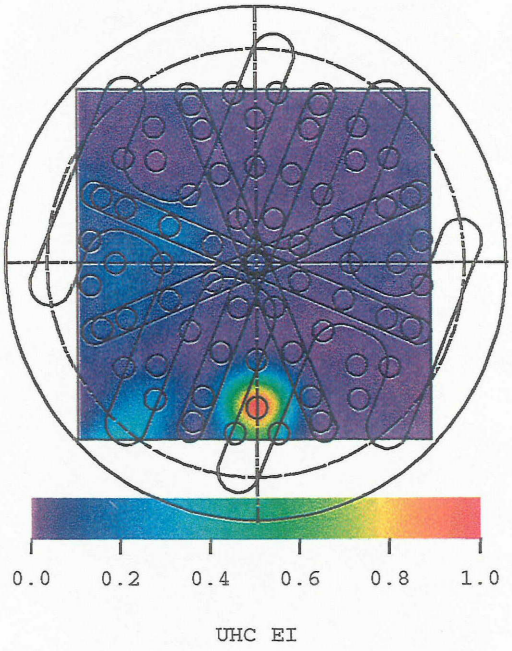

Figure VII - 43 UHC Emissions Contours for Quench Plate Configuration #11 (850F, 120 psia, 0.028 f/a, 1" Downstream from Lean Zone Inlet)

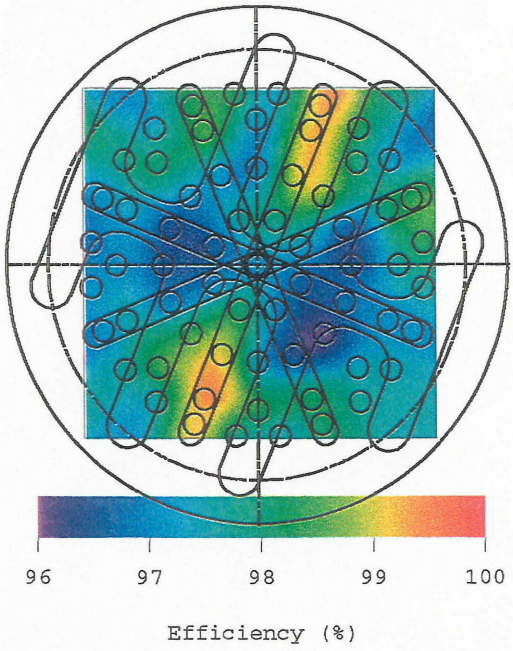

Figure VII - 44 Efficiency Contours for Quench Plate Configuration #11 (850F, 120 psia, 0.028 f/a, 1" Downstream from Lean Zone Inlet)

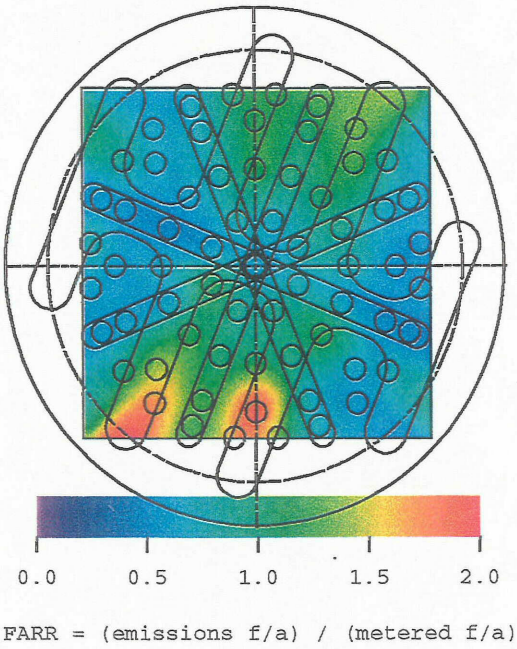

Figure VII - 45 FARR Contours for Quench Plate Configuration #11 (850F, 120 psia, 0.028 f/a, 1" Downstream from Lean Zone Inlet)

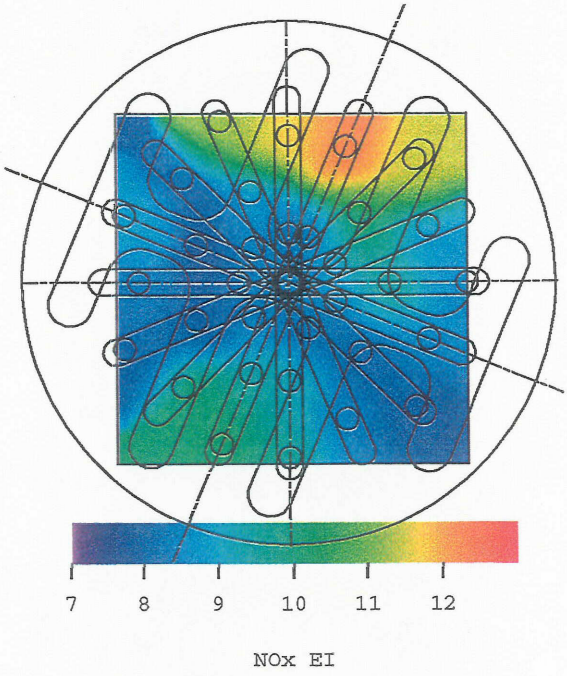

Figure VII - 46 NOx Emissions Contours for Quench Plate Configuration #11 (1200F, 150 psia, 0.030 f/a, 4" Downstream from Lean Zone Inlet)

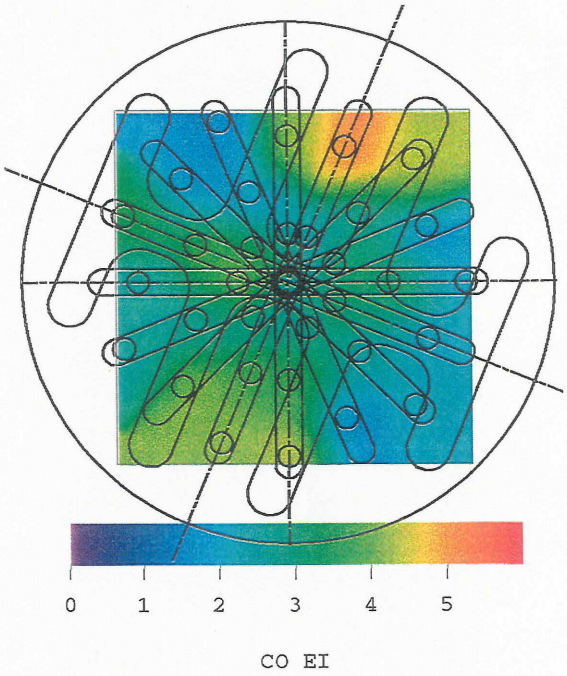

Figure VII - 47 CO Emissions Contours for Quench Plate Configuration #11 (1200F, 150 psia, 0.030 f/a, 4" Downstream from Lean Zone Inlet)

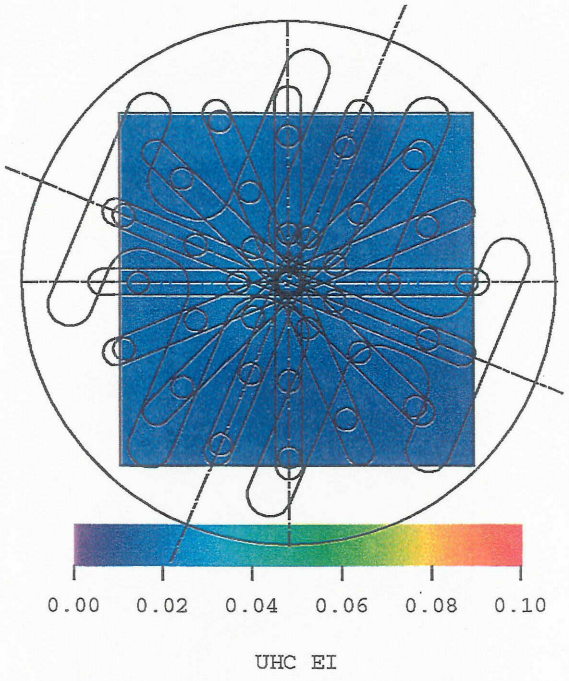

Figure VII - 48 UHC Emissions Contours for Quench Plate Configuration #11 (1200F, 150 psia, 0.030 f/a, 4" Downstream from Lean Zone Inlet)

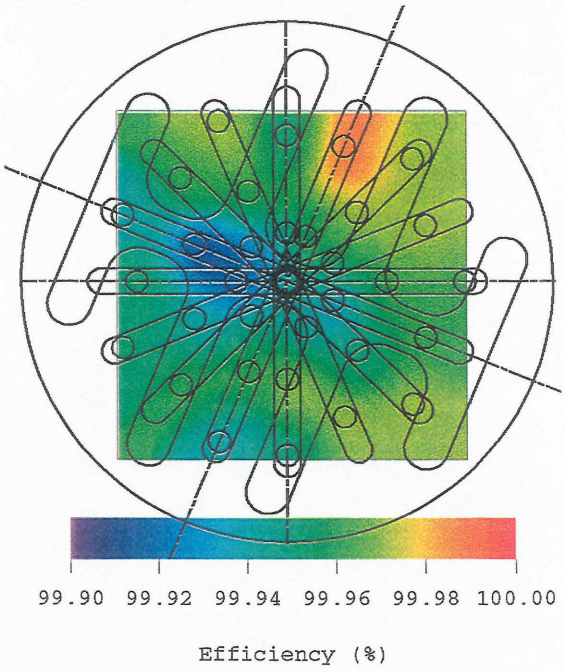

Figure VII - 49 Efficiency Contours for Quench Plate Configuration #11 (1200F, 150 psia, 0.030 f/a, 4" Downstream from Lean Zone Inlet)

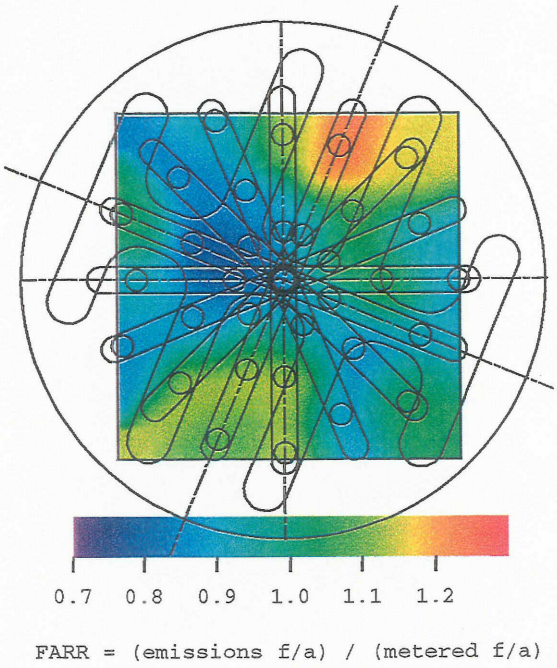

Figure VII - 50 FARR Contours for Quench Plate Configuration #11 (1200F, 150 psia, 0.030 f/a, 4" Downstream from Lean Zone Inlet)

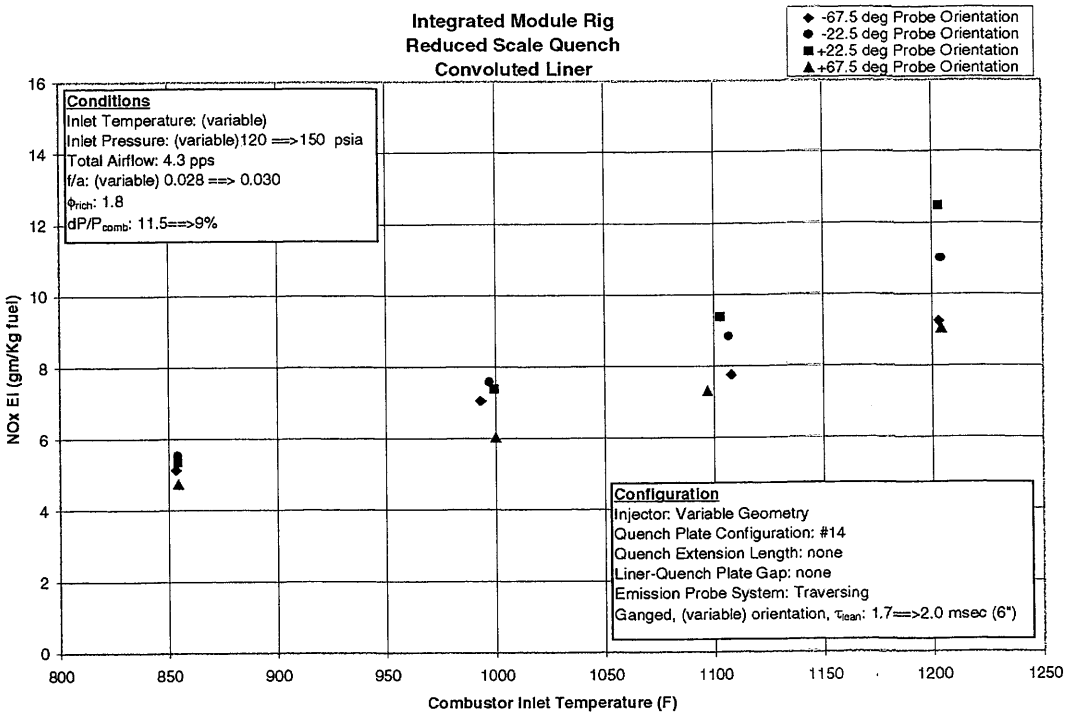

Figure VII - 51 NOx Emissions as a Function of Inlet Temperature for Quench Plate Configuration #14

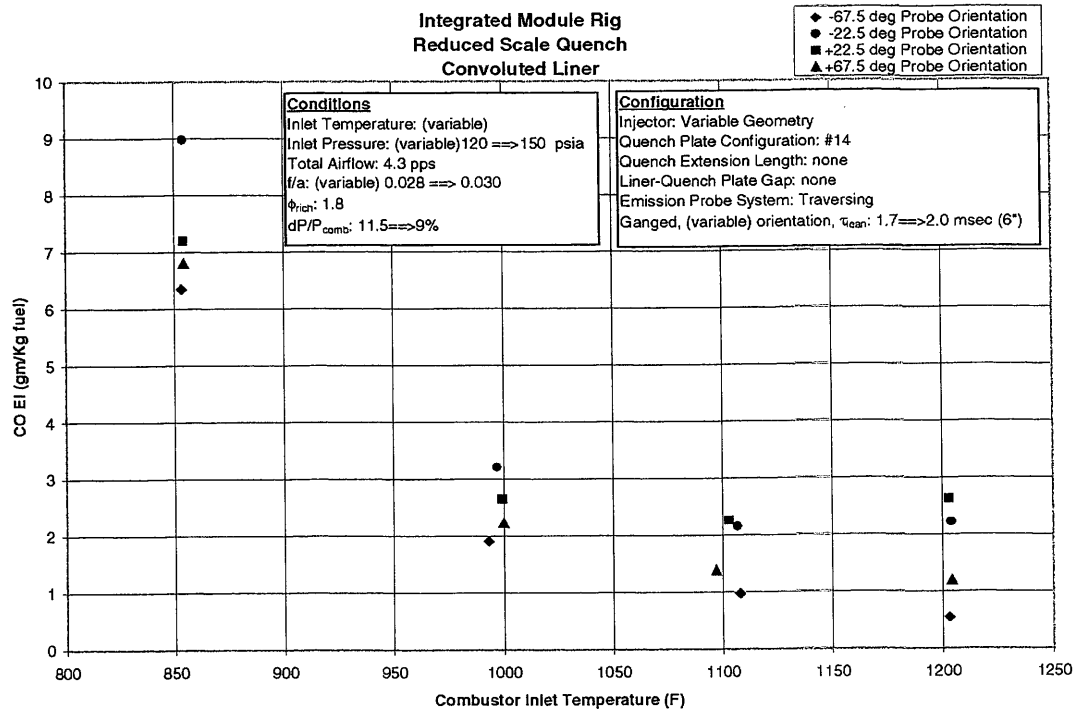

Figure VII - 52 CO Emissions as a Function of Inlet Temperature for Quench Plate Configuration #14

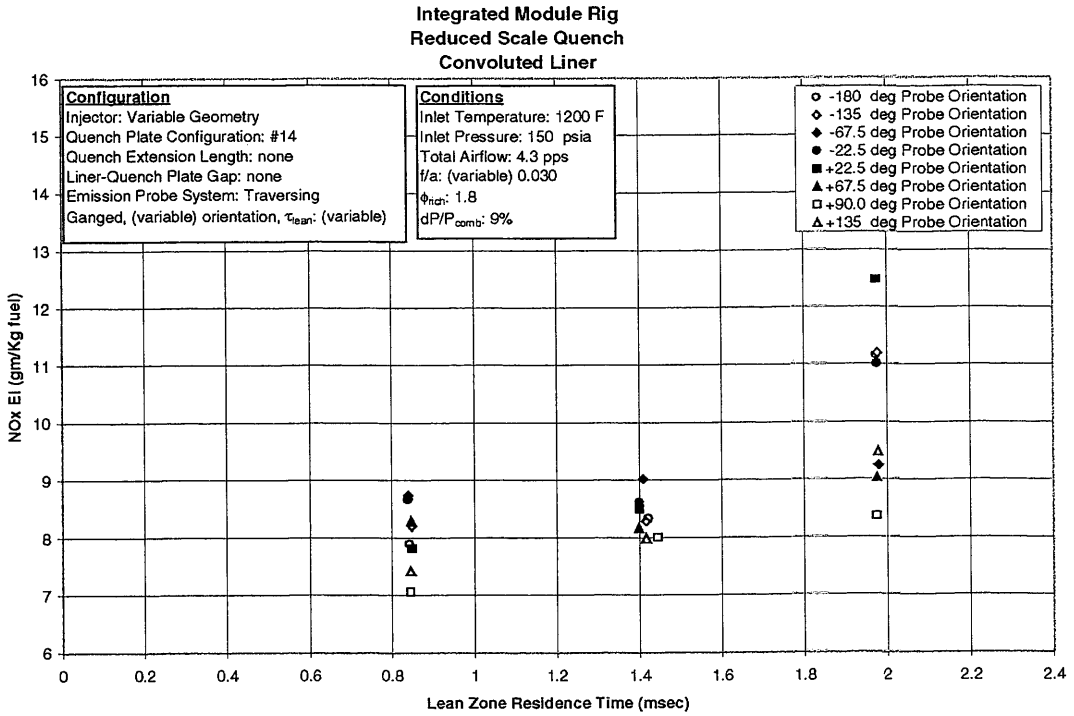

Figure VII - 53 NOx Emissions as a Function of Lean Zone Residence time for Quench Plate Configuration #14

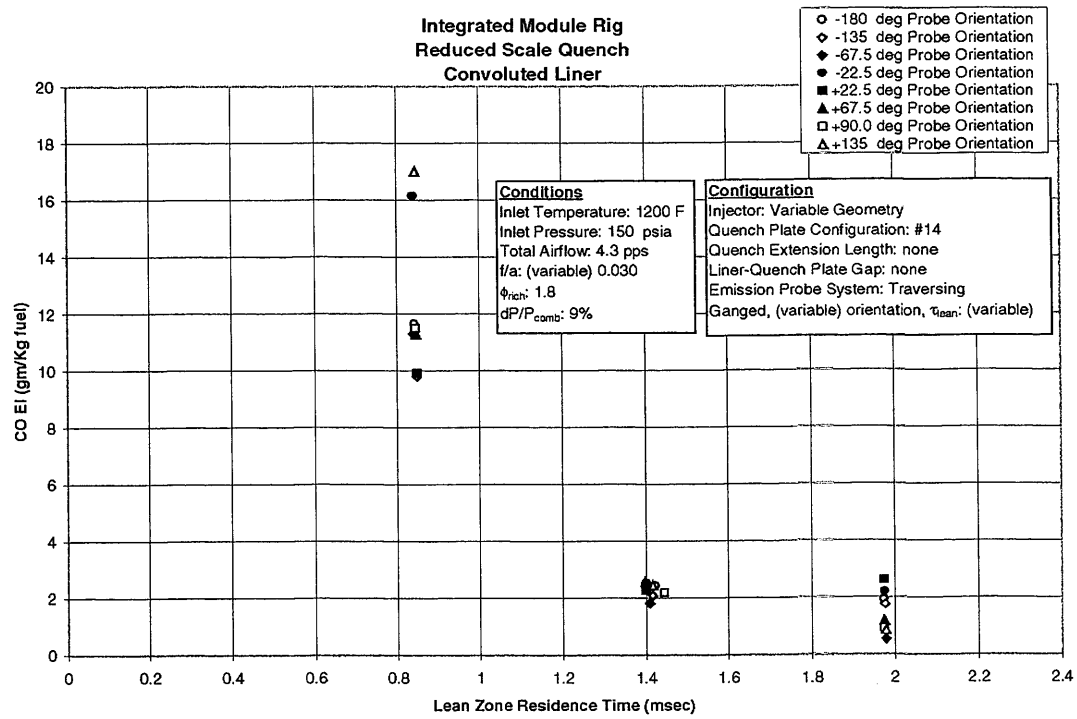

Figure VII - 54 CO Emissions as a Function of Lean Zone Residence time for Quench Plate Configuration #14

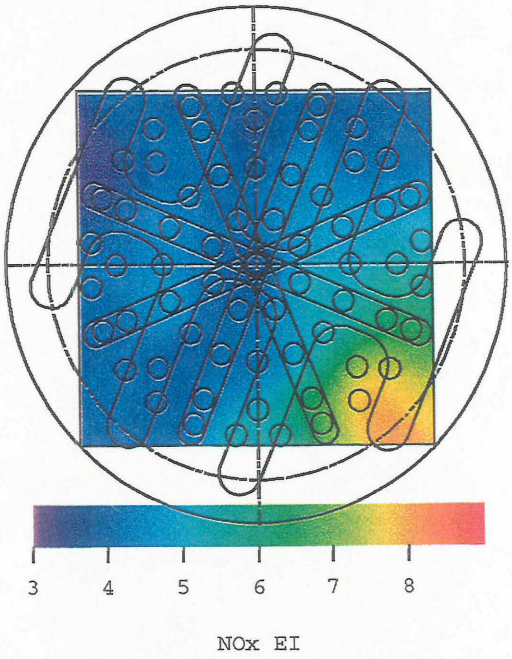

Figure VII - 55 NOx Emissions Contours for Quench Plate Configuration #14 (850F, 120 psia, 0.028 f/a, 1" Downstream from Lean Zone Inlet)

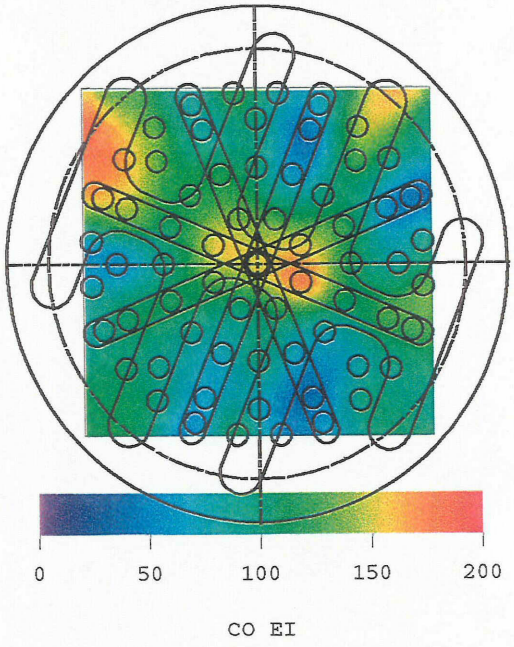

Figure VII - 56 CO Emissions Contours for Quench Plate Configuration #14 (850F, 120 psia, 0.028 f/a, 1" Downstream from Lean Zone Inlet)

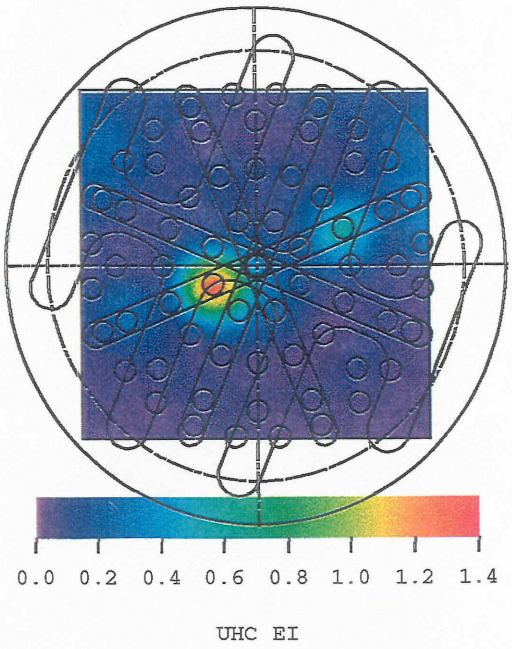

Figure VII - 57 UHC Emissions Contours for Quench Plate Configuration #14 (850F, 120 psia, 0.028 f/a, 1" Downstream from Lean Zone Inlet)

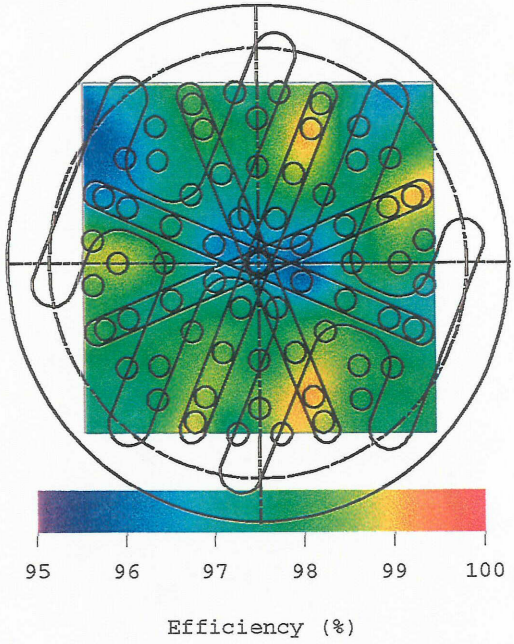

Figure VII - 58 Efficiency Contours for Quench Plate Configuration #14 (850F, 120 psia, 0.028 f/a, 1" Downstream from Lean Zone Inlet)

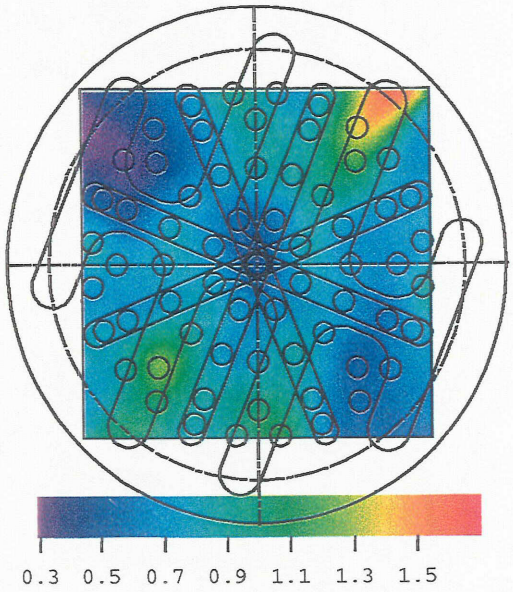

Figure VII - 59 FARR Contours for Quench Plate Configuration #14 (850F, 120 psia, 0.028 f/a, 1" Downstream from Lean Zone Inlet)

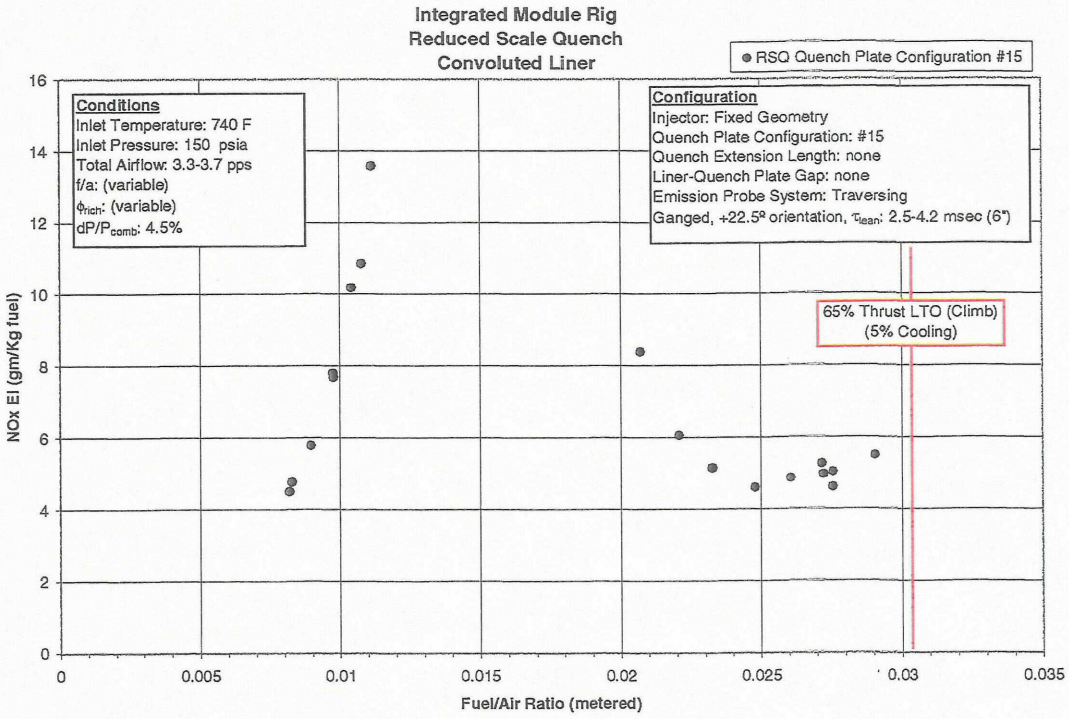

Figure VII - 60 NOx Emissions at 65% Thrust LTO (Climb) for Quench Plate Configuration #15

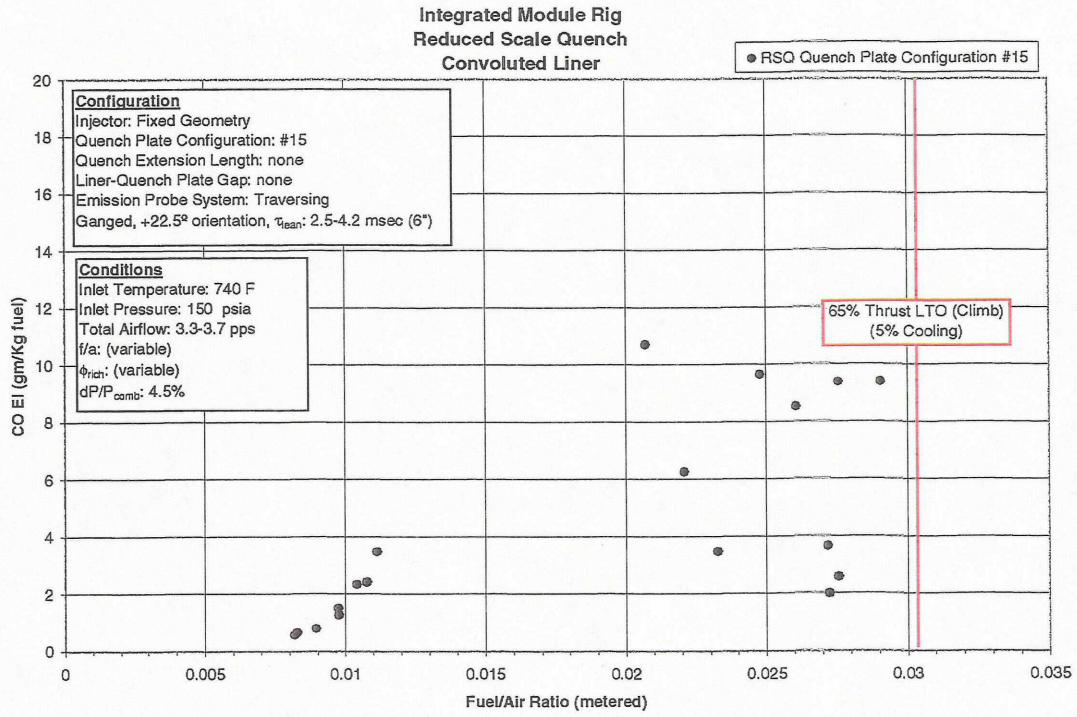

Figure VII - 61 CO Emissions at 65% Thrust LTO (Climb) for Quench Plate Configuration #15

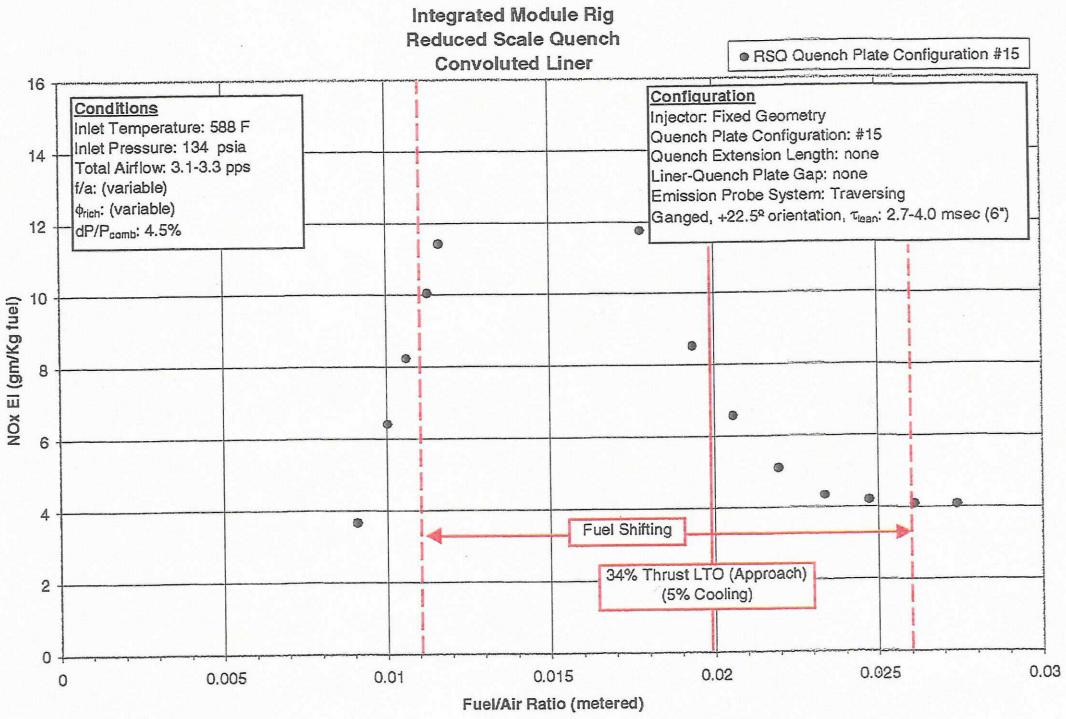

Figure VII - 62 NOx Emissions at 34% Thrust LTO (Approach) for Quench Plate Configuration #15

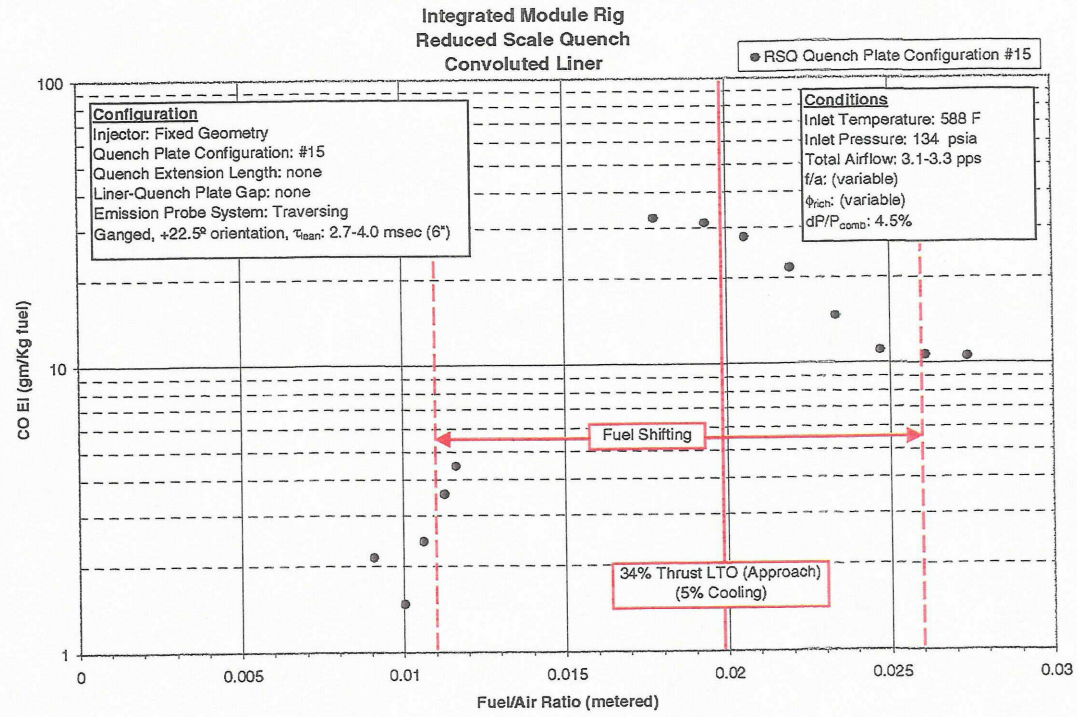

Figure VII - 63 CO Emissions at 34% Thrust LTO (Approach) for Quench Plate Configuration #15

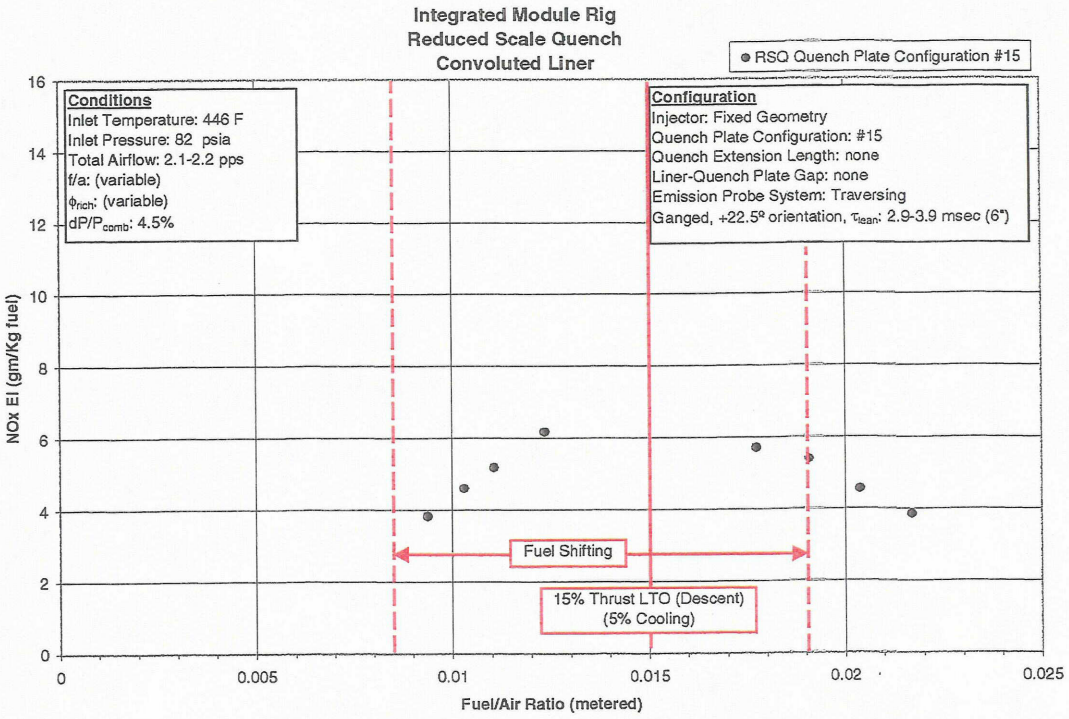

Figure VII - 64 NOx Emissions at 15% Thrust LTO (Descent) for Quench Plate Configuration #15

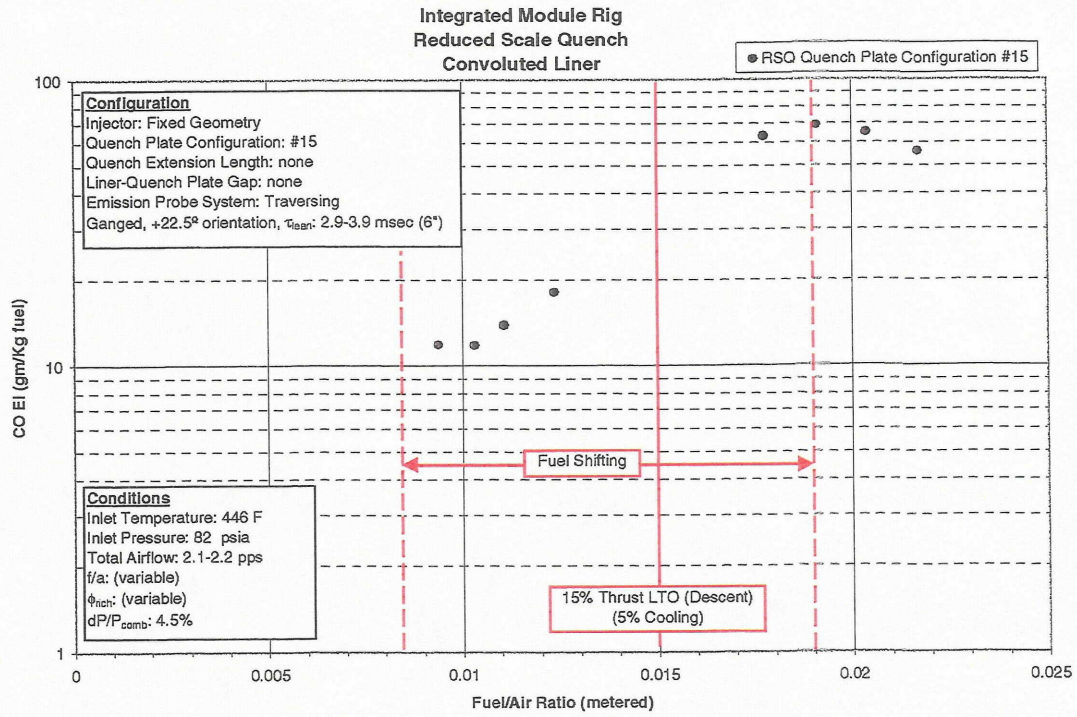

Figure VII - 65 CO Emissions at 15% Thrust LTO (Descent) for Quench Plate Configuration #15

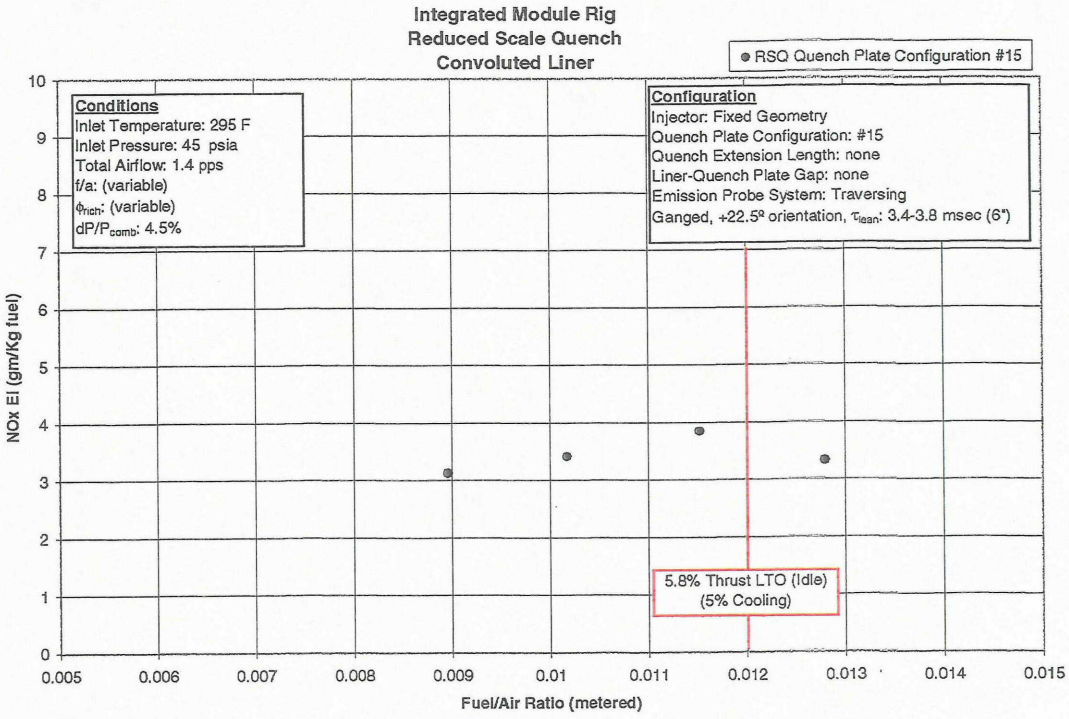

Figure VII - 66 NOx Emissions at 5.8% Thrust LTO (Idle) for Quench Plate Configuration #15

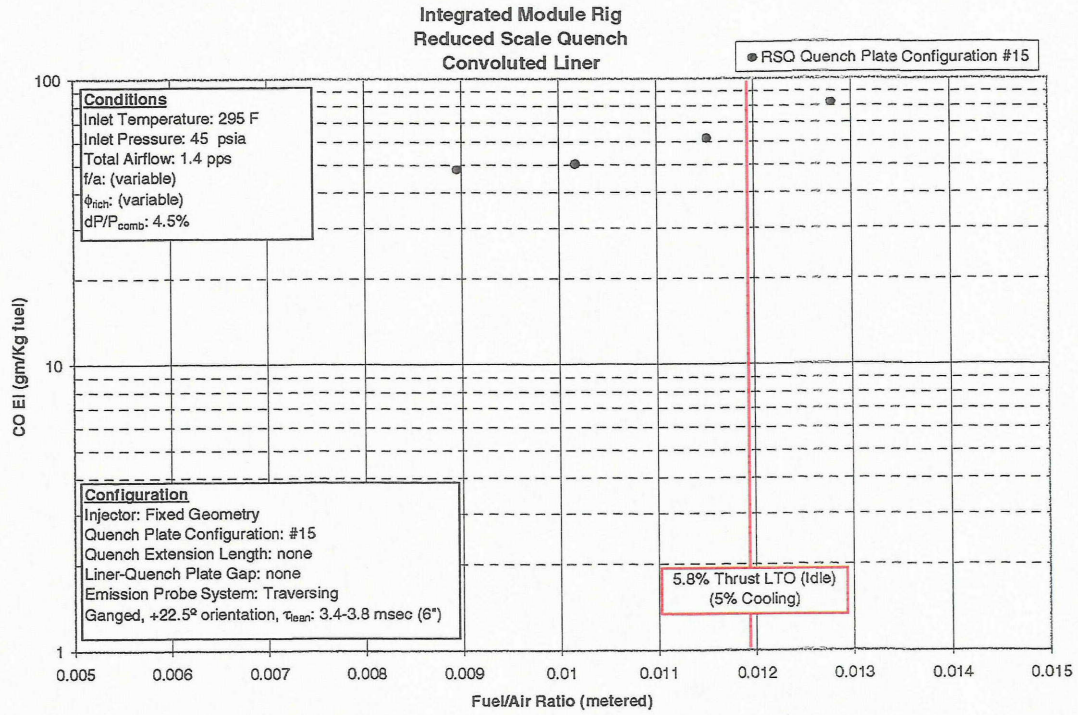

Figure VII - 67 CO Emissions at 5.8% Thrust LTO (Idle) for Quench Plate Configuration #15

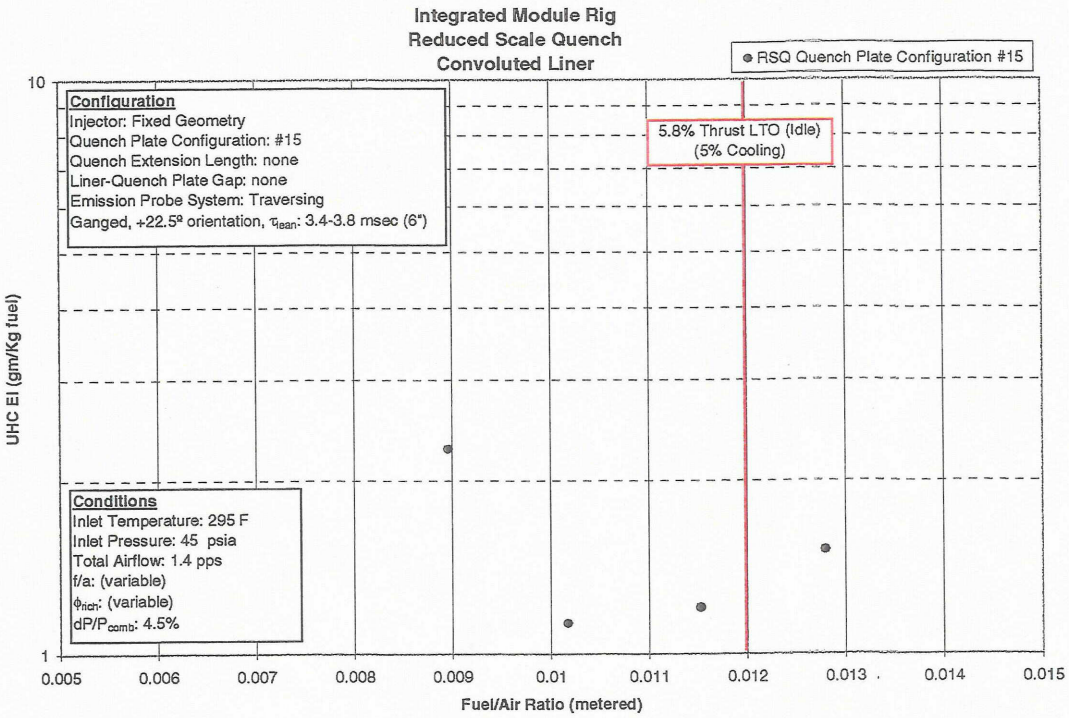

Figure VII - 68 UHC Emissions at 5.8% Thrust LTO (Idle) for Quench Plate Configuration #15

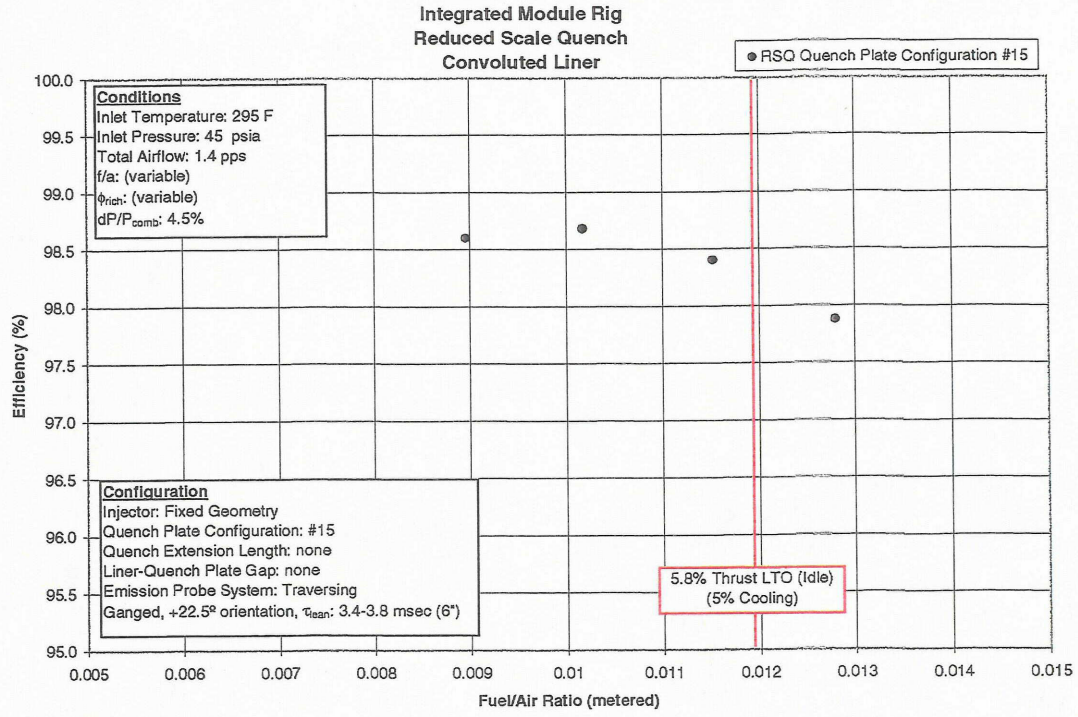

Figure VII - 69 Efficiency at 5.8% Thrust LTO (Idle) for Quench Plate Configuration #15

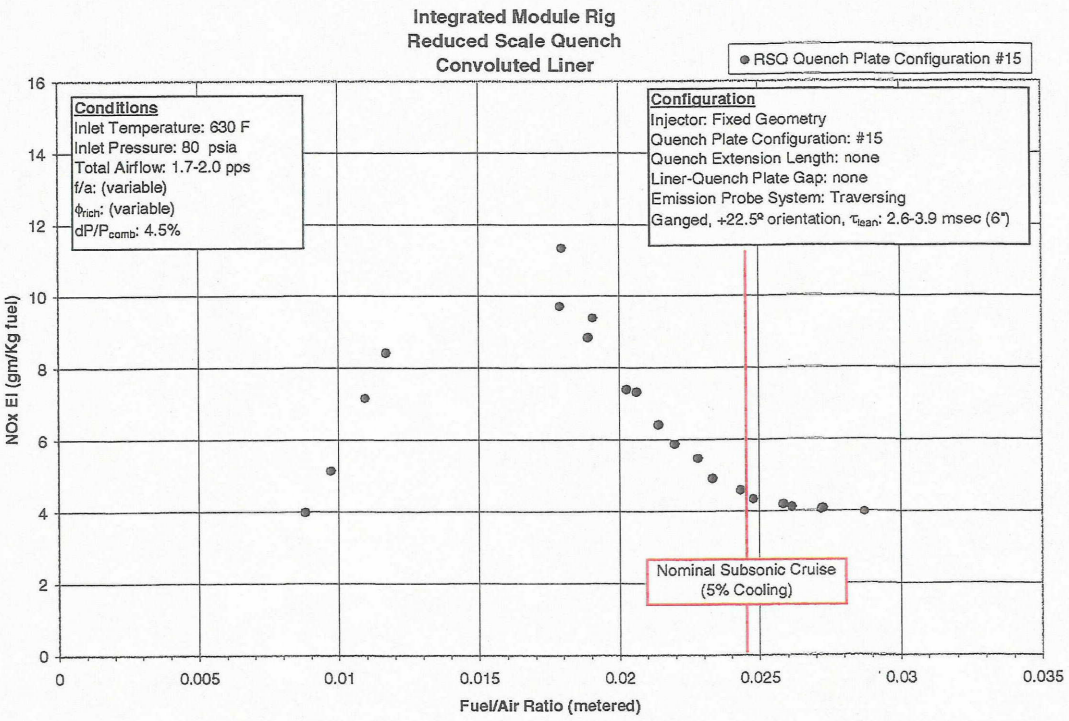

Figure VII - 70 NOx Emissions at Nominal Subsonic Cruise for Quench Plate Configuration #15

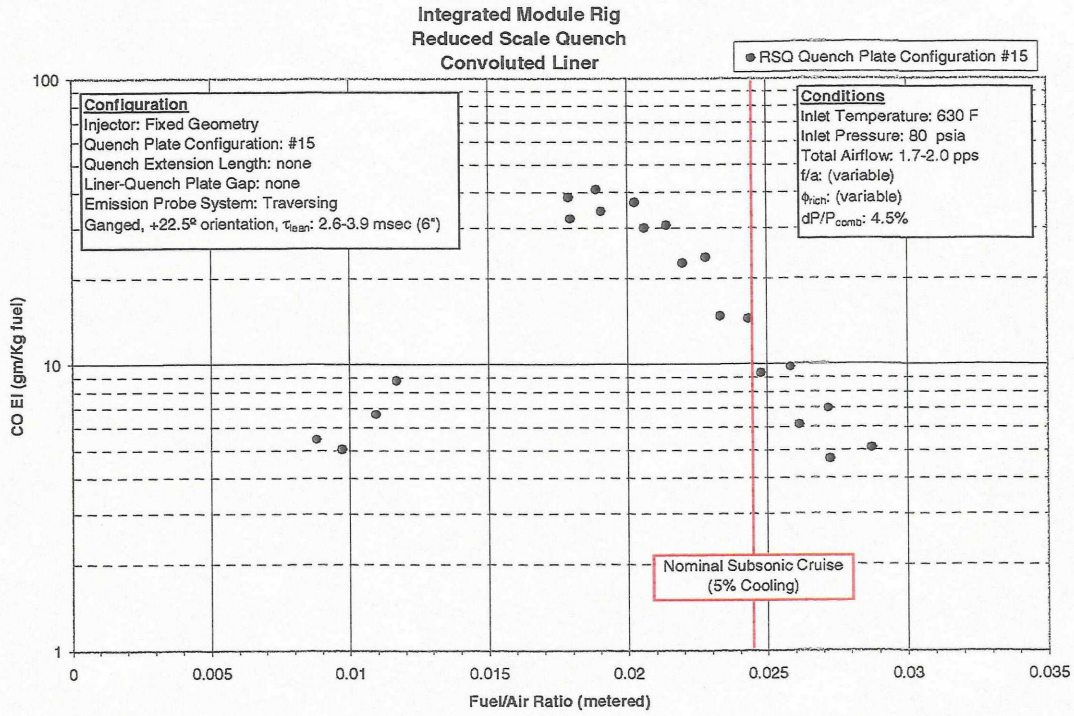

Figure VII - 71 CO Emissions at Nominal Subsonic Cruise for Quench Plate Configuration #15

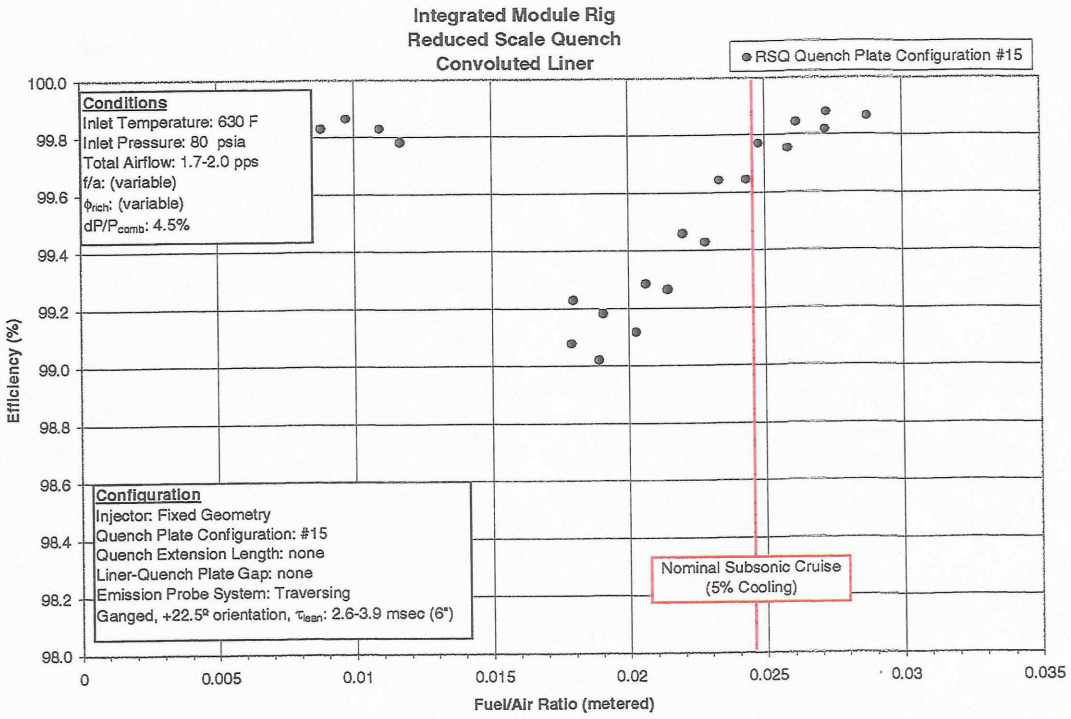

Figure VII - 72 Efficiency at Nominal Subsonic Cruise for Quench Plate Configuration #15

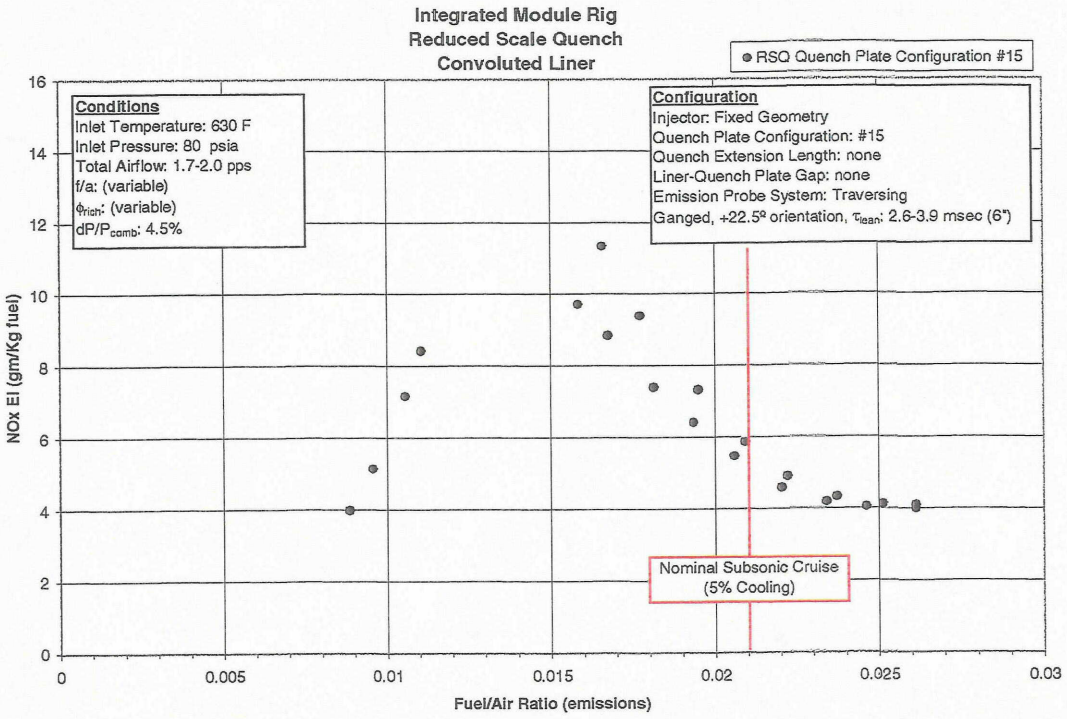

Figure VII - 73 NOx Emissions at Nominal Subsonic Cruise (as a Function of Emissions Fuel/Air Ratio) for Quench Plate Configuration #15

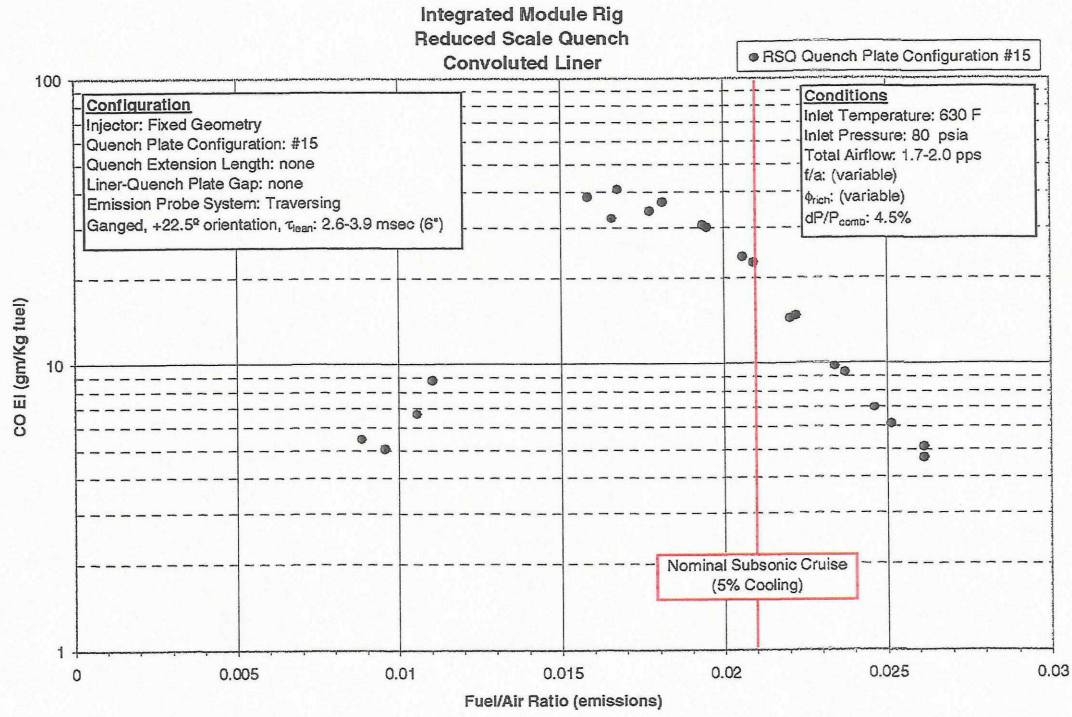

Figure VII - 74 CO Emissions at Nominal Subsonic Cruise (as a Function of Emissions Fuel/Air Ratio) for Quench Plate Configuration #15

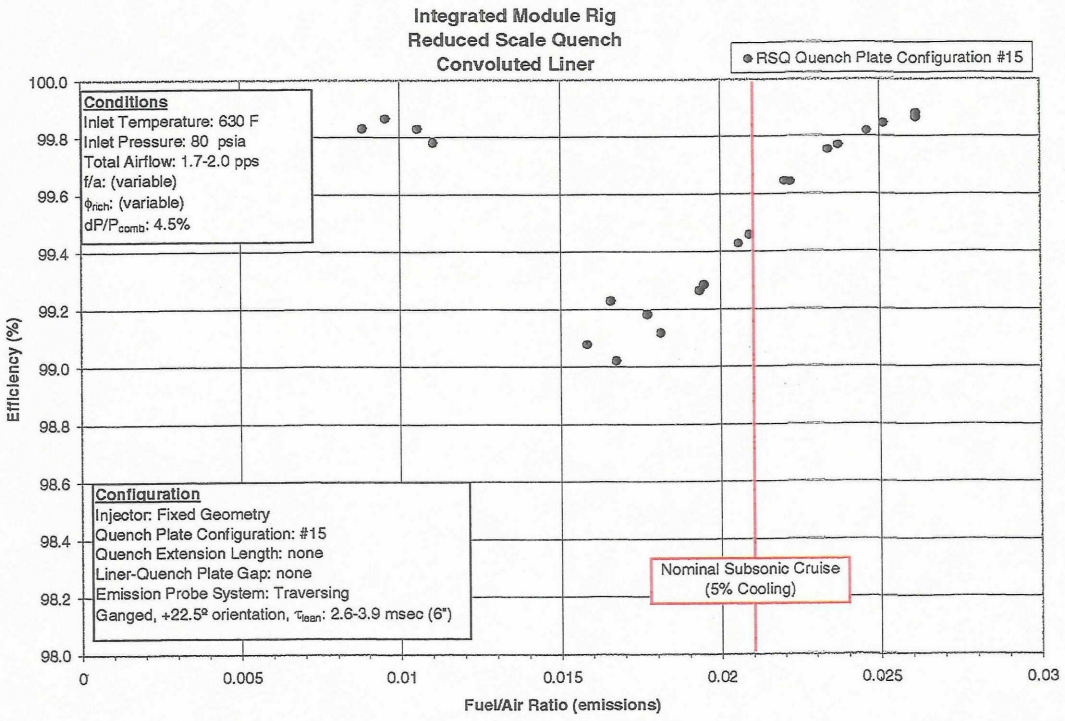

Figure VII - 75 Efficiency at Nominal Subsonic Cruise (as a Function of Emissions Fuel/Air Ratio) for Quench Plate Configuration #15

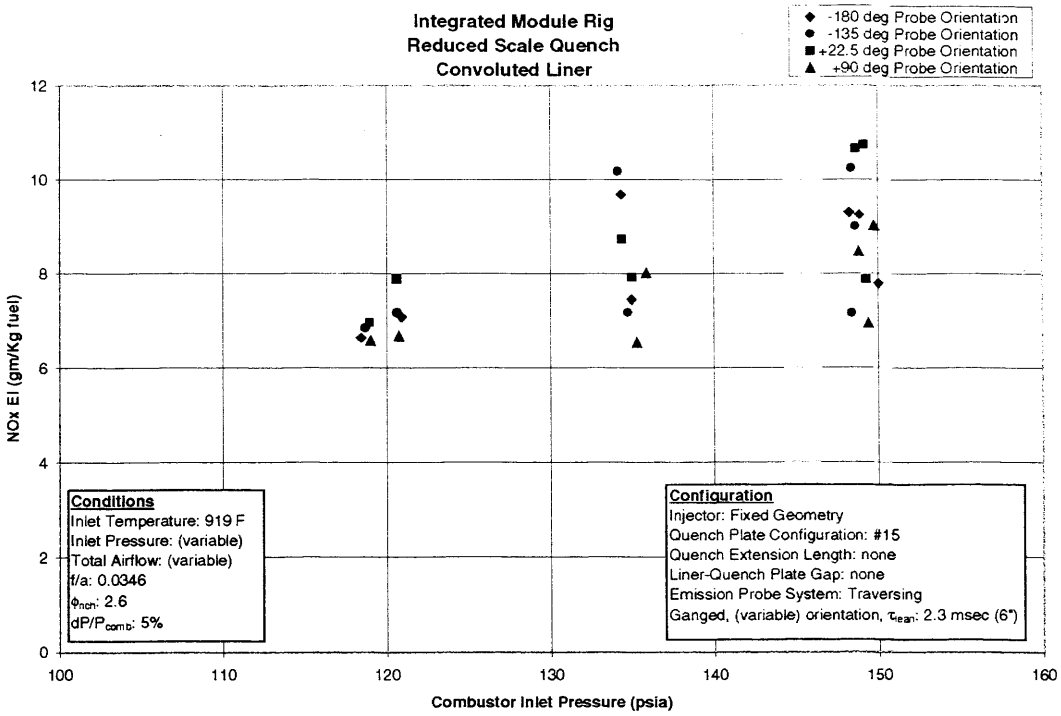

Figure VII - 76 NOx Emissions as a Function of Inlet Pressure for Quench Plate Configuration #15

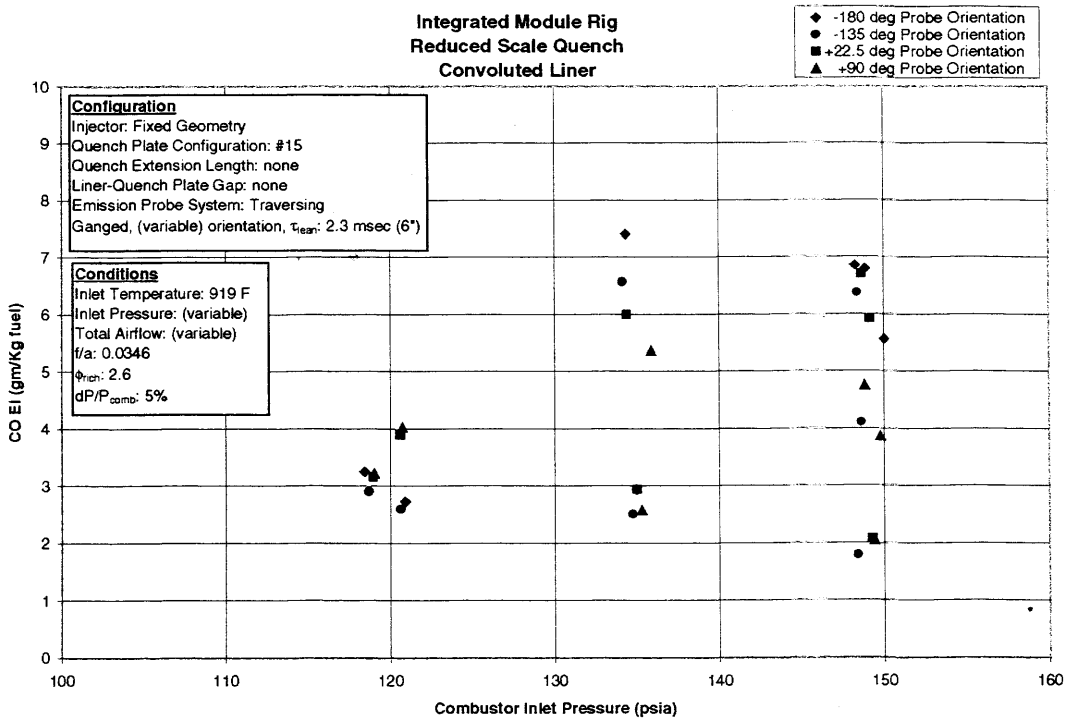

Figure VII - 77 CO Emissions as a Function of Inlet Pressure for Quench Plate Configuration #15

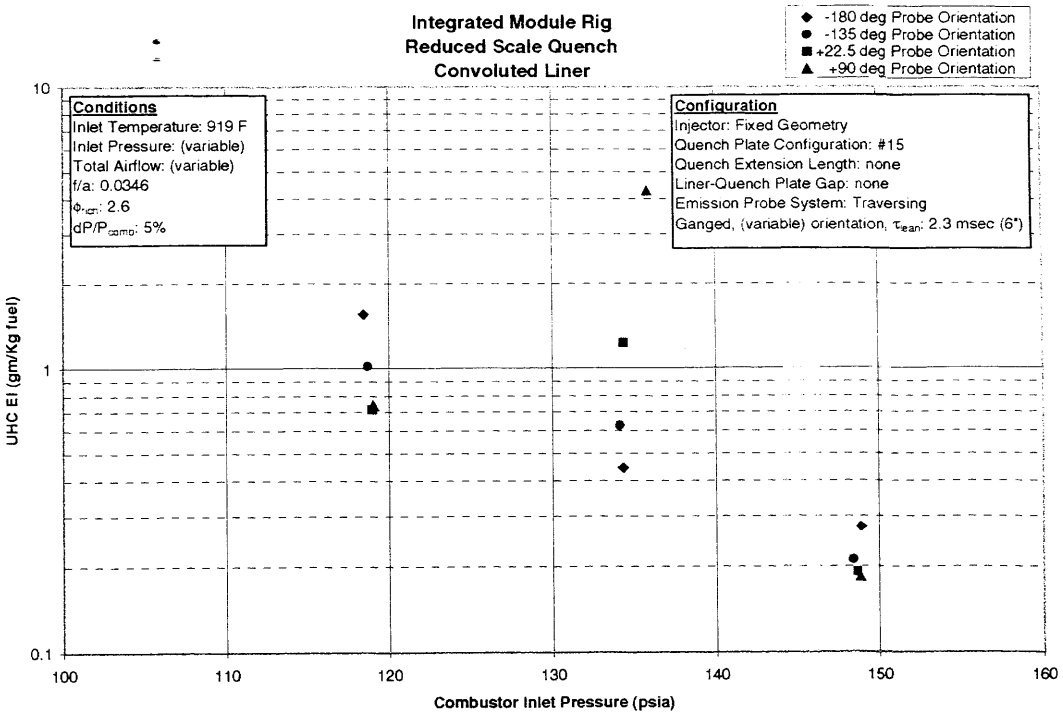

Figure VII - 78 UHC Emissions as a Function of Inlet Pressure for Quench Plate Configuration #15

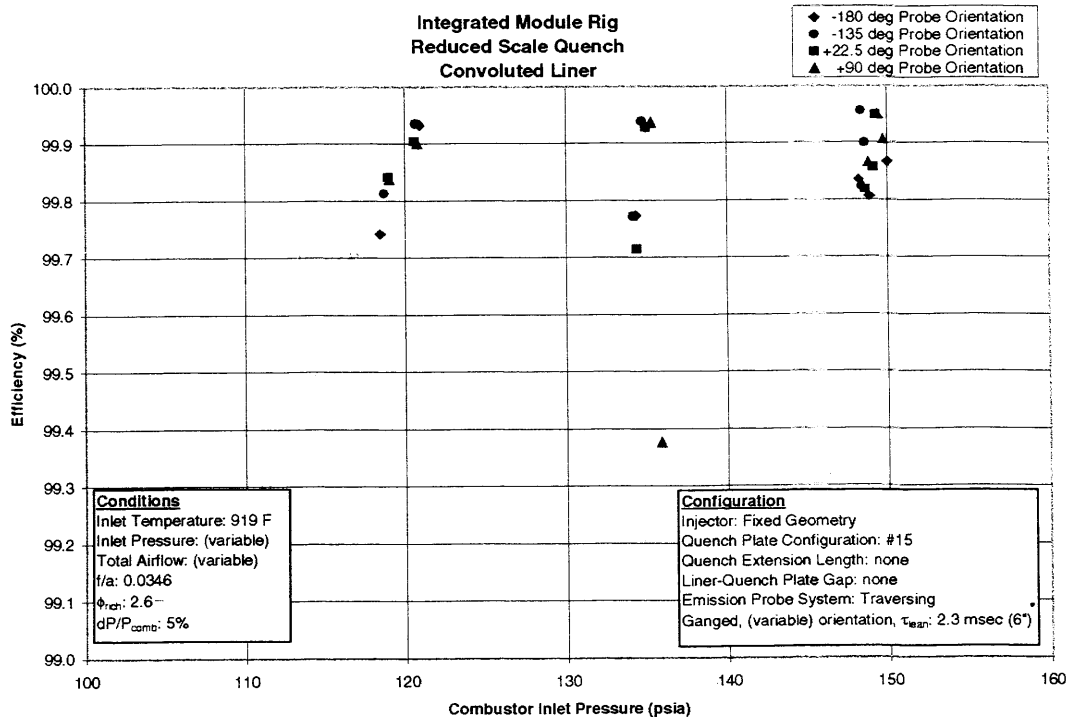

Figure VII - 79 Efficiency as a Function of Inlet Pressure for Quench Plate Configuration #15

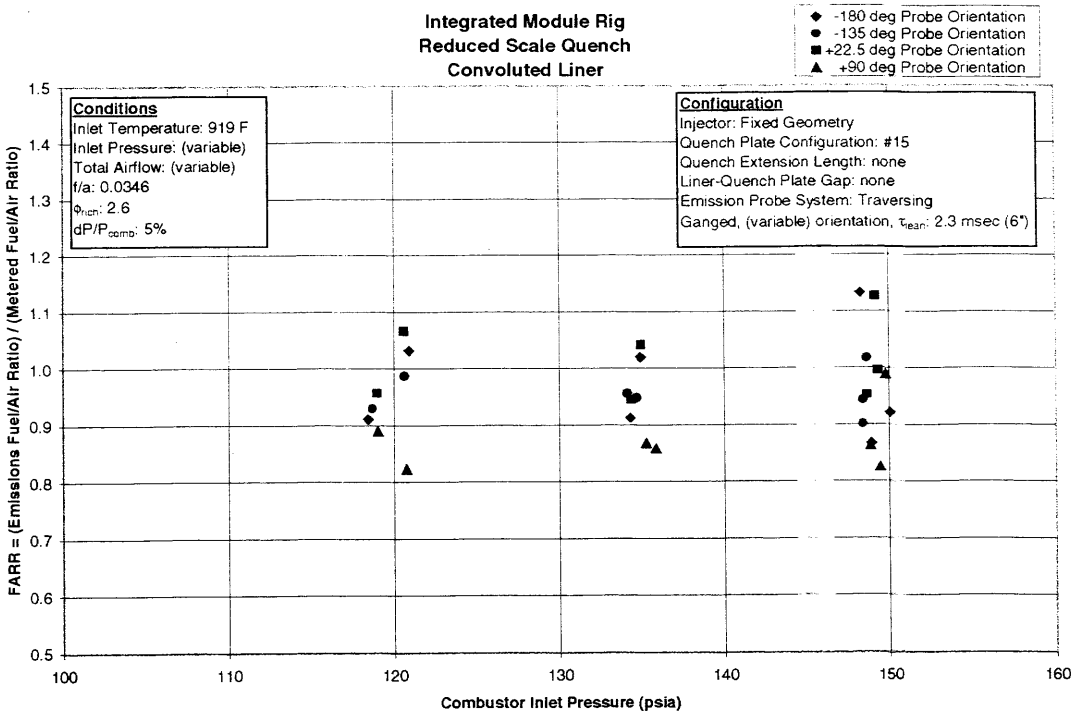

Figure VII - 80 FARR (Emission Fuel/Air Ratio relative to Metered Fuel/Air Ratio) as a Function of Inlet Pressure for Quench Plate Configuration #15

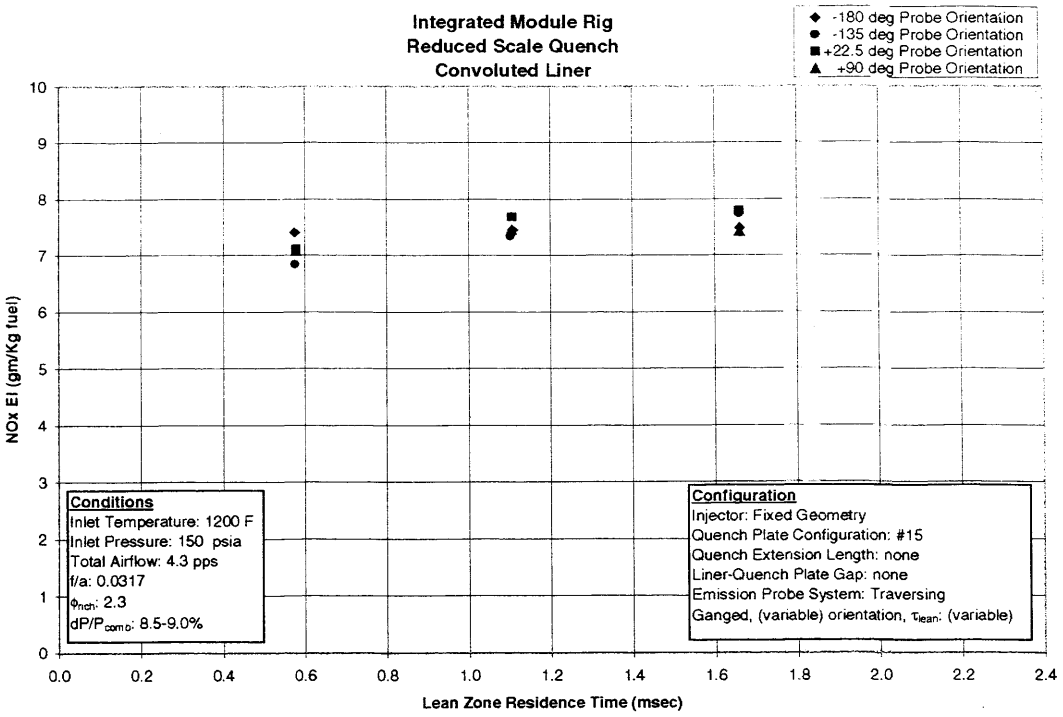

Figure VII - 81 NOx Emissions as a Function of Lean Zone Residence Time for Quench Plate Configuration #15

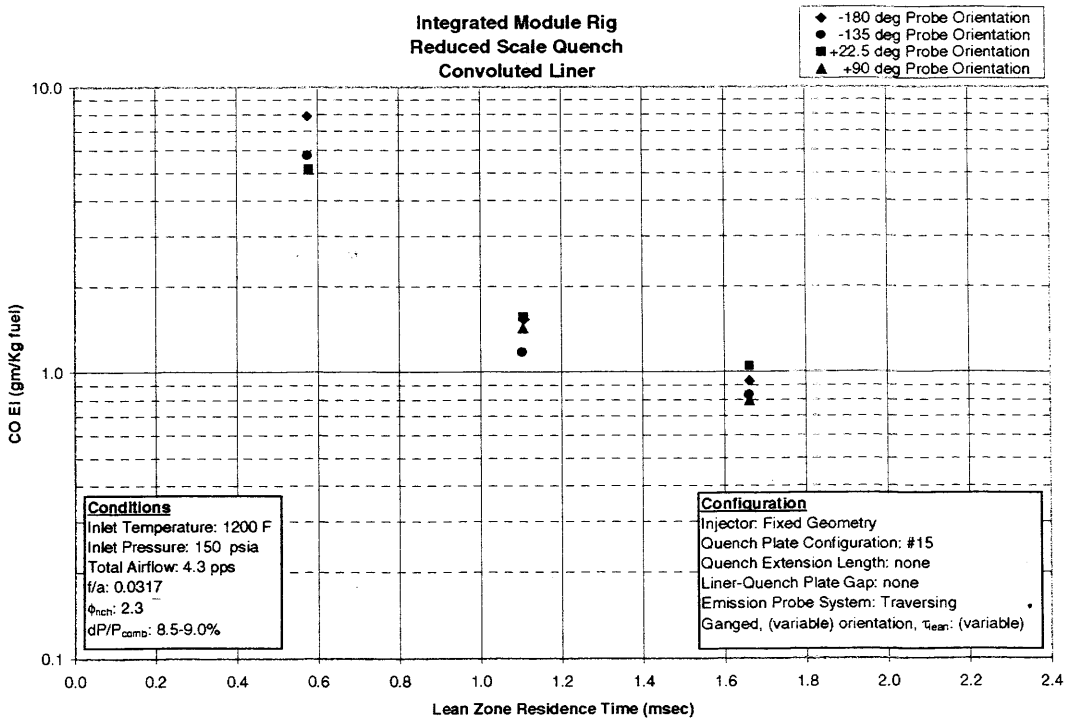

Figure VII - 82 CO Emissions as a Function of Lean Zone Residence Time for Quench Plate Configuration #15

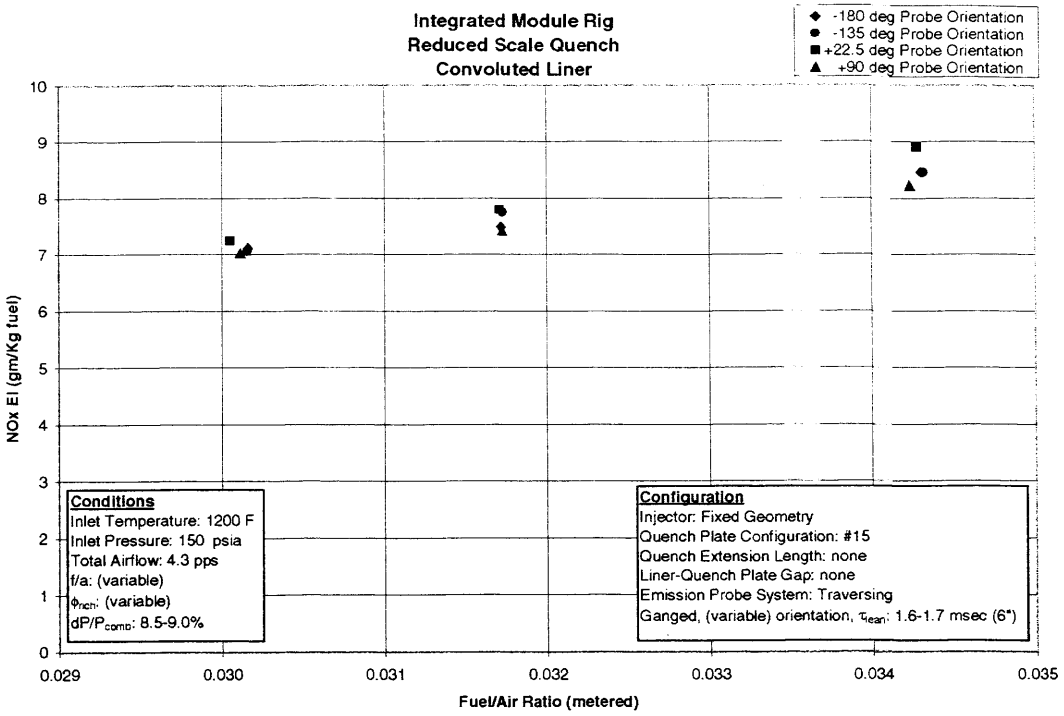

Figure VII - 83 NOx Emissions as a Function of Fuel/Air Ratio for Quench Plate Configuration #15

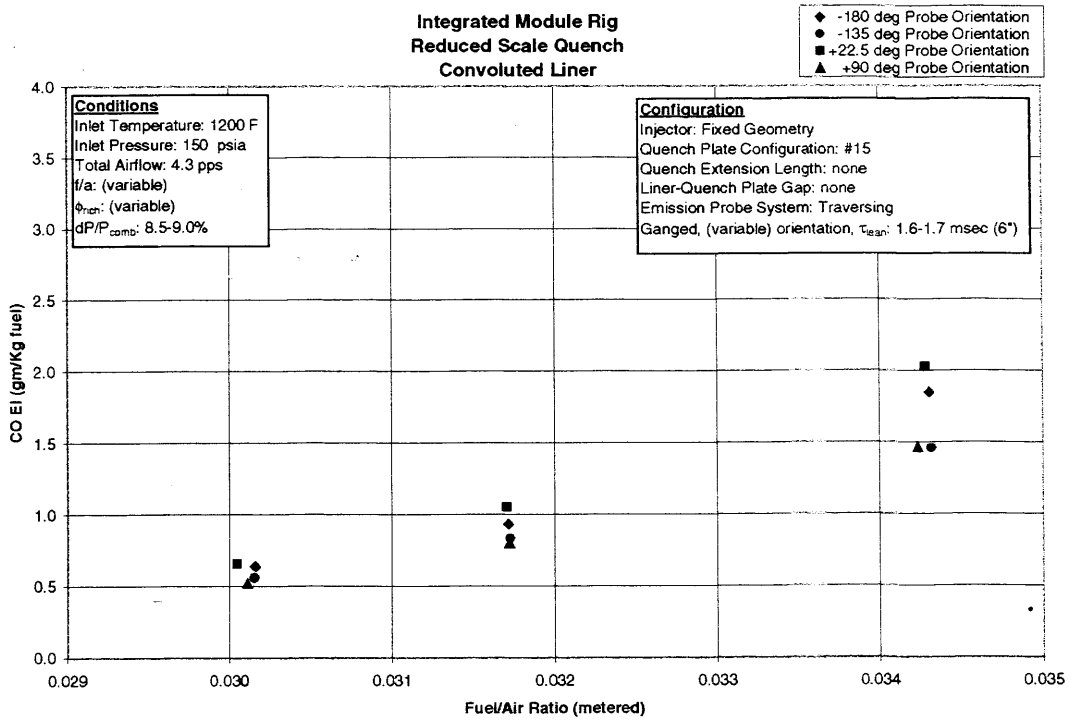

Figure VII - 84 CO Emissions as a Function of Fuel/Air Ratio for Quench Plate Configuration #15

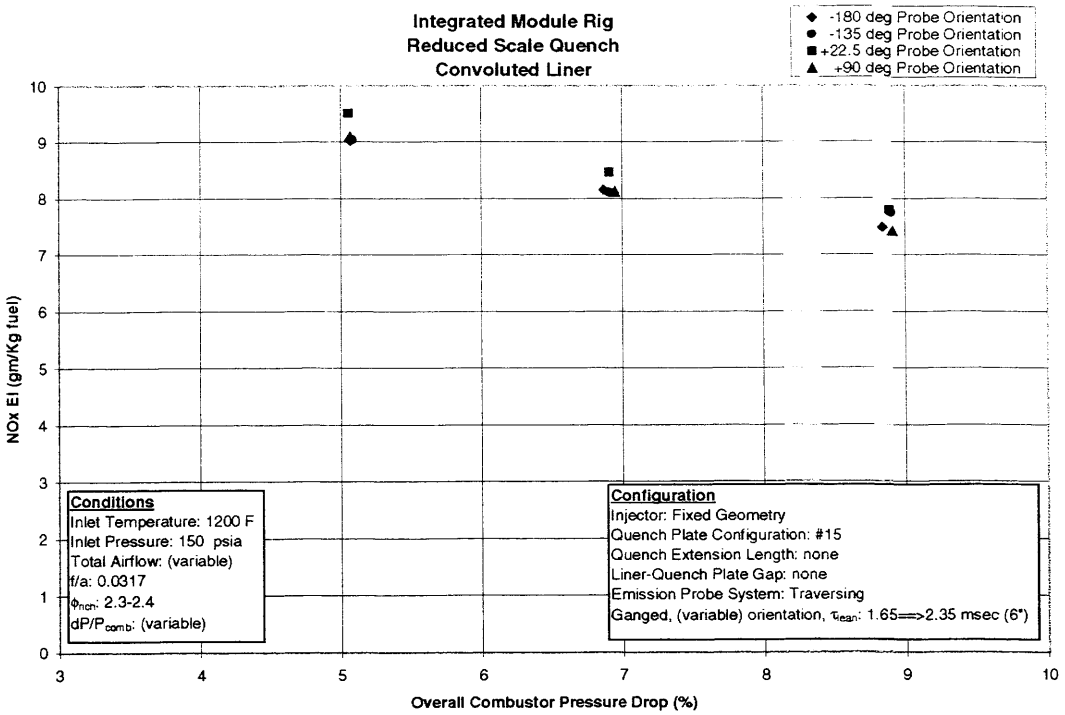

Figure VII - 85 NOx Emissions as a Function of Combustor Pressure Drop for Quench Plate Configuration #15

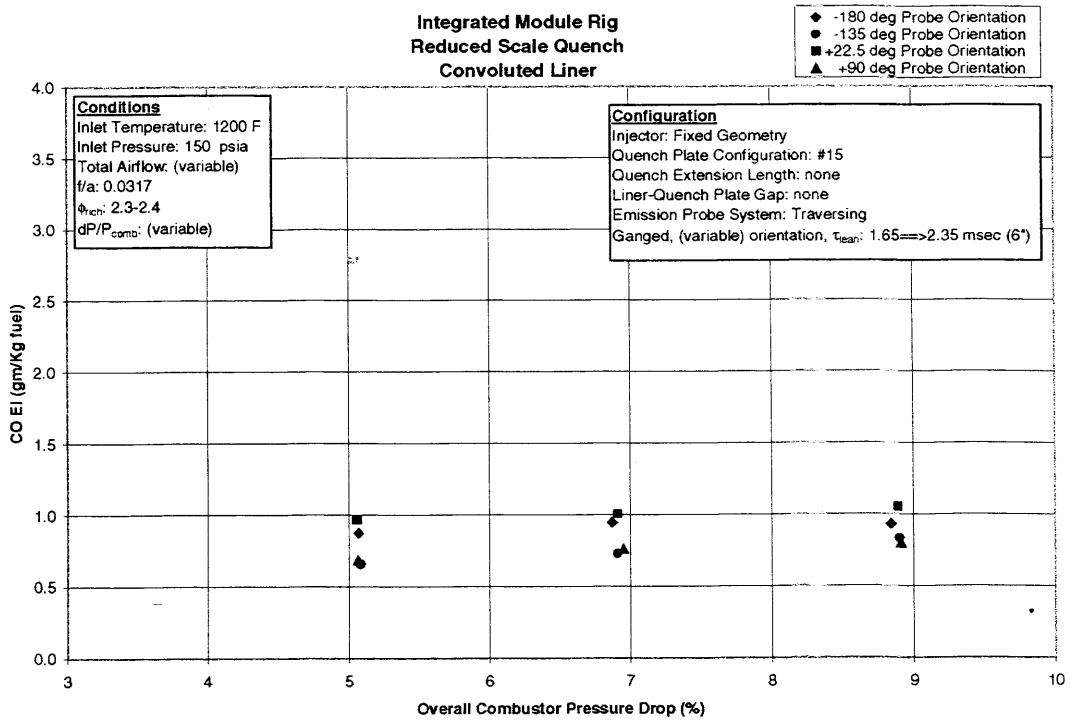

Figure VII - 86 CO Emissions as a Function of Combustor Pressure Drop for Quench Plate Configuration #15

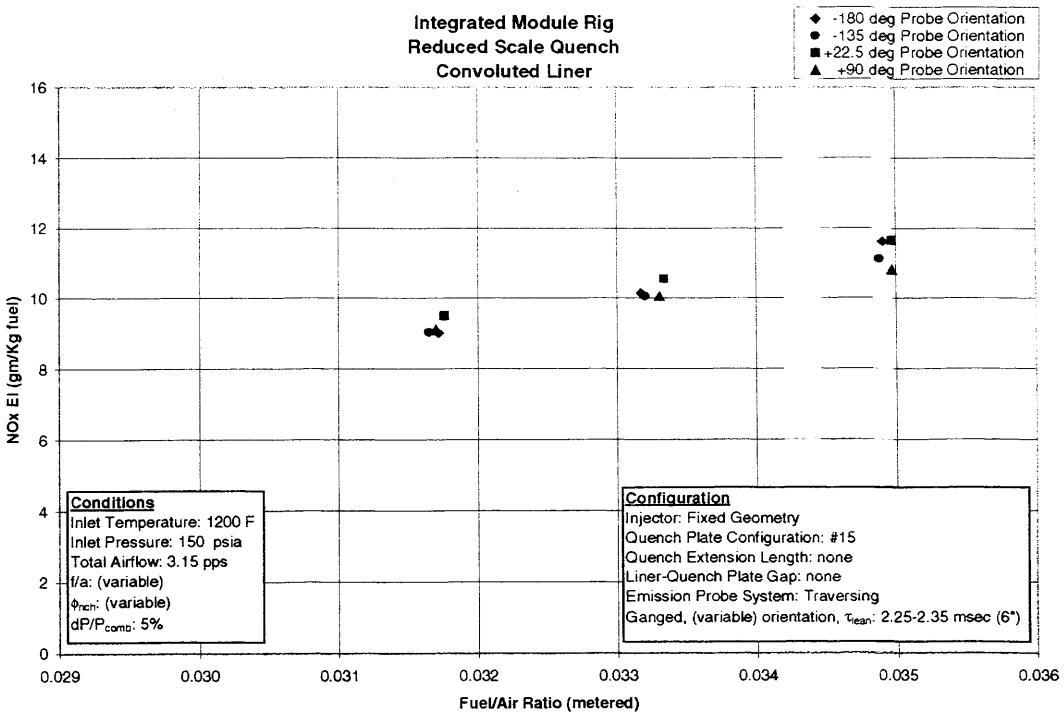

Figure VII - 87 NOx Emissions as a Function of Fuel/Air Ratio for Quench Plate Configuration #15

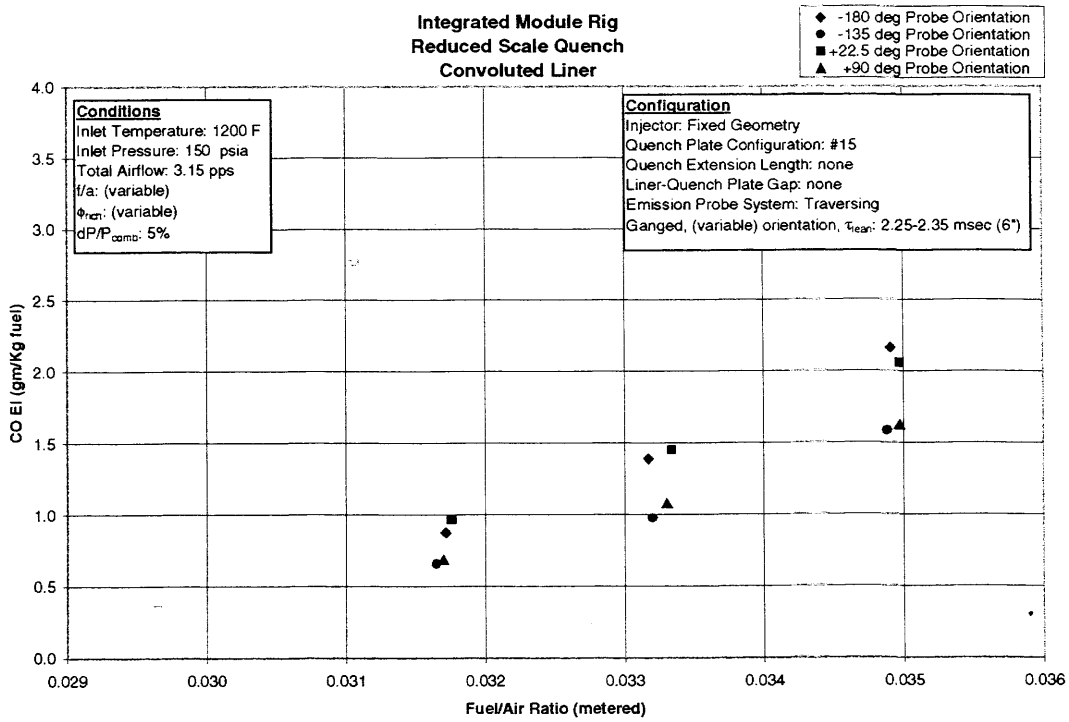

Figure VII - 88 CO Emissions as a Function of Fuel/Air Ratio for Quench Plate Configuration #15

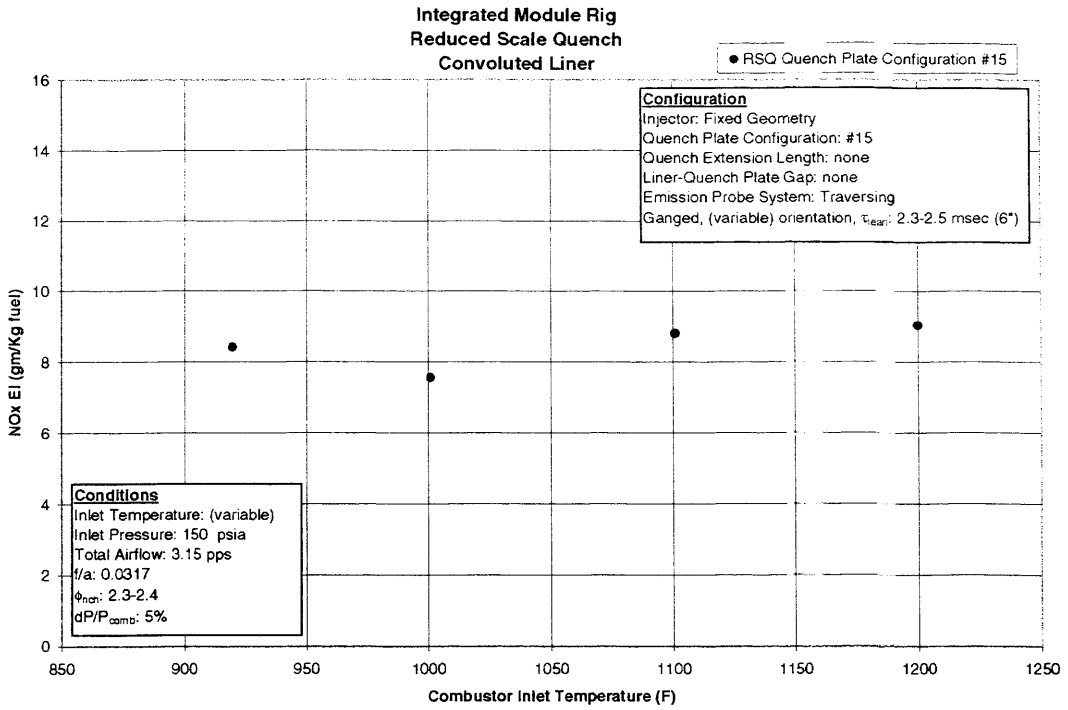

Figure VII - 89 NOx Emissions as a Function of Inlet Temperature for Quench Plate Configuration #15

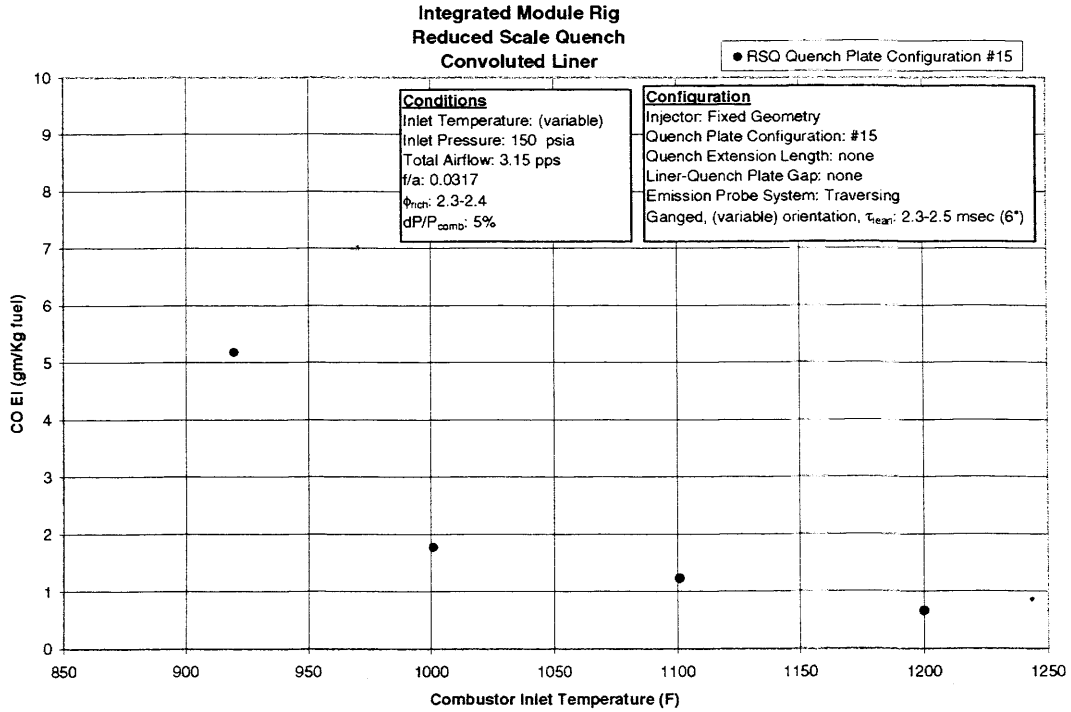

Figure VII - 90 CO Emissions as a Function of Inlet Temperature for Quench Plate Configuration #15

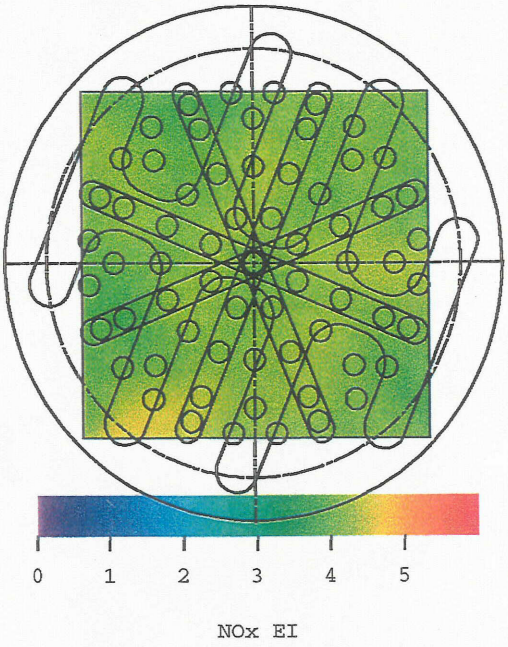

Figure VII - 91 NOx Emissions Contours for Quench Plate Configuration #15 (920F, 120 psia, 0.028 f/a, 1" Downstream from Lean Zone Inlet)

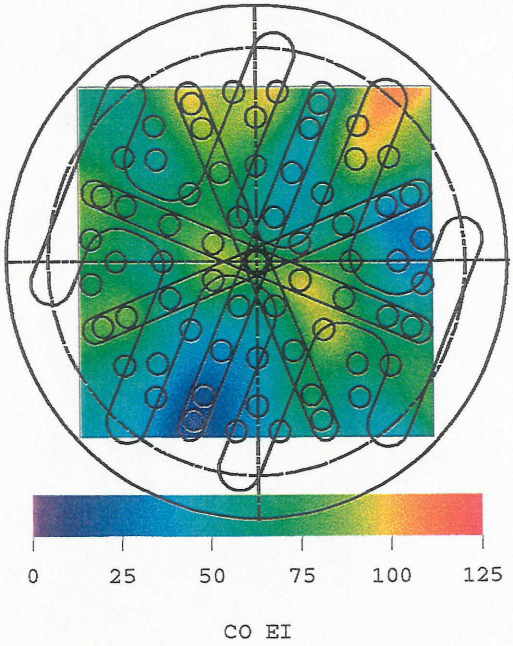

Figure VII - 92 CO Emissions Contours for Quench Plate Configuration #15 (920F, 120 psia, 0.028 f/a, 1" Downstream from Lean Zone Inlet)

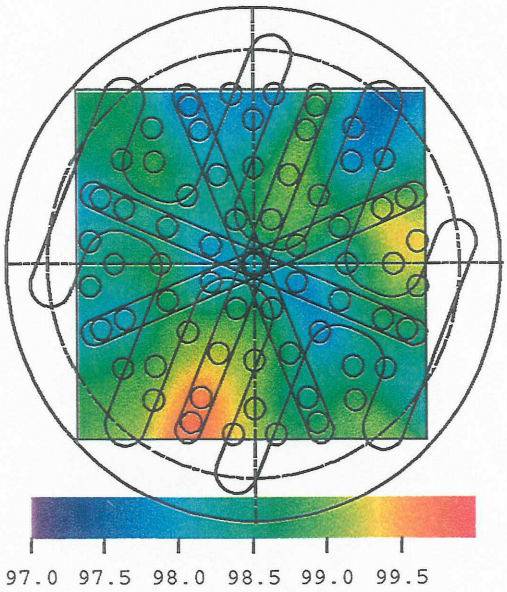

Figure VII - 93 Efficiency Contours for Quench Plate Configuration #15 (920F, 120 psia, 0.028 f/a, 1" Downstream from Lean Zone Inlet)

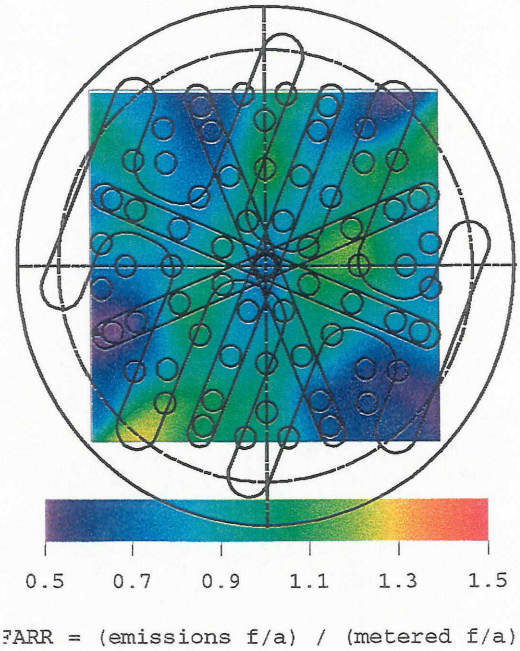

Figure VII - 94 FARR Contours for Quench Plate Configuration #15 (920F, 120 psia, 0.028 f/a, 1" Downstream from Lean Zone Inlet)

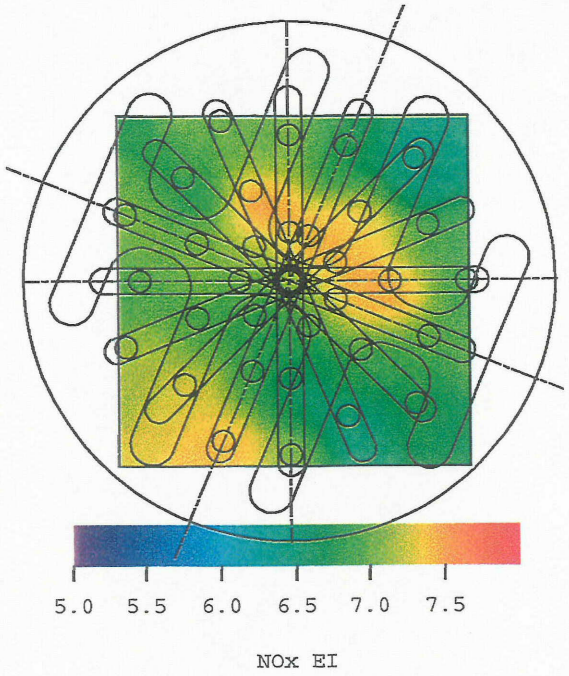

Figure VII - 95 NOx Emissions Contours for Quench Plate Configuration #15 (1200F, 150 psia, 0.030 f/a, 6" Downstream from Lean Zone Inlet)

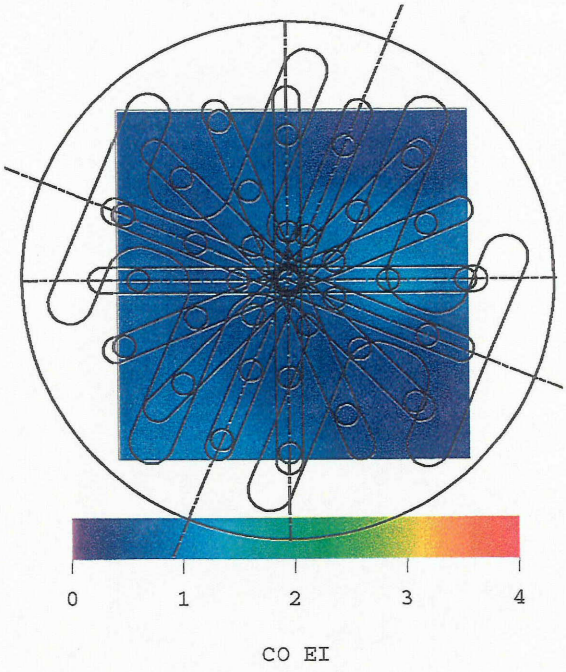

Figure VII - 96 CO Emissions Contours for Quench Plate Configuration #15 (1200F, 150 psia, 0.030 f/a, 6" Downstream from Lean Zone Inlet)

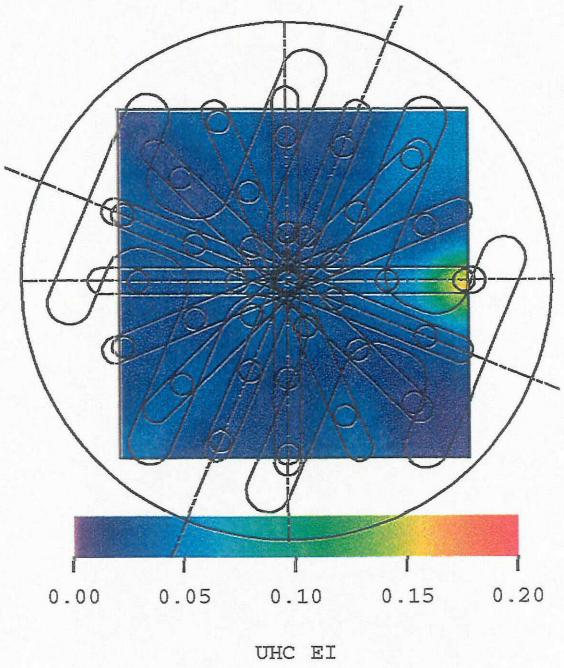

Figure VII - 97 UHC Emissions Contours for Quench Plate Configuration #15 (1200F, 150 psia, 0.030 f/a, 6" Downstream from Lean Zone Inlet)

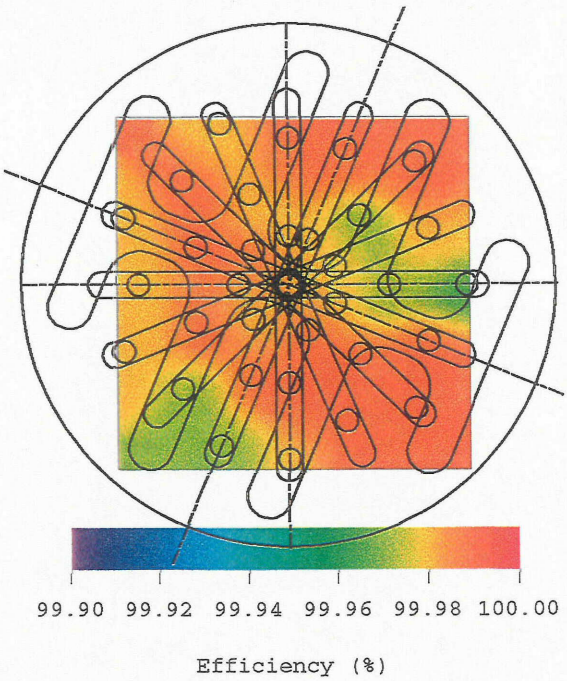

Figure VII - 98 Efficiency Contours for Quench Plate Configuration #15 (1200F, 150 psia, 0.030 f/a, 6" Downstream from Lean Zone Inlet)

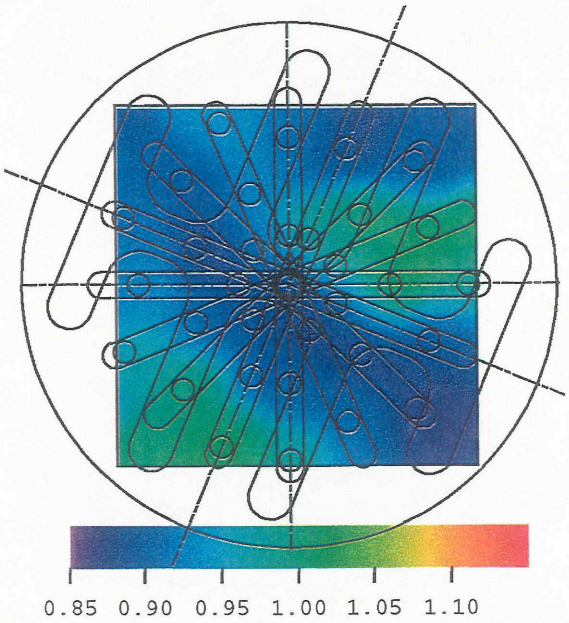

Figure VII - 99 FARR Contours for Quench Plate Configuration #15 (1200F, 150 psia, 0.030 f/a, 6" Downstream from Lean Zone Inlet)

REPORT DOCUMENTATION PAGE

Form Approved
OMB No. 0704-0188

1. AGENCY USE ONLY (*Leave blank*)	2. REPORT DATE	3. REPORT TYPE AND DATES COVERED
	February 2004	Final Contractor Report

4. TITLE AND SUBTITLE

RQL Integrated Module Rig Test

5. FUNDING NUMBERS

WBS–22–714–01–39
NAS3–27235

6. AUTHOR(S)

Frederick S. Koopman, John T. Ols, Frederick C. Padget IV, and
Kenneth S. Siskind

7. PERFORMING ORGANIZATION NAME(S) AND ADDRESS(ES)

Pratt & Whitney
P.O. Box 109600
West Palm Beach, Florida 33410

8. PERFORMING ORGANIZATION REPORT NUMBER

E–14295

9. SPONSORING/MONITORING AGENCY NAME(S) AND ADDRESS(ES)

National Aeronautics and Space Administration
Washington, DC 20546–0001

10. SPONSORING/MONITORING AGENCY REPORT NUMBER

NASA CR—2004-212881
MTD211A5

11. SUPPLEMENTARY NOTES

Project Manager, James D. Holdeman, Turbomachinery and Propulsion Systems Division, NASA Glenn Research Center, organization code 5830, 216–433–5846.

12a. DISTRIBUTION/AVAILABILITY STATEMENT

Unclassified - Unlimited
Subject Category: 07 Distribution: Nonstandard

Available electronically at http://gltrs.grc.nasa.gov

This publication is available from the NASA Center for AeroSpace Information, 301–621–0390.

12b. DISTRIBUTION CODE

13. ABSTRACT ***(Maximum 200 words)***

This report documents the activities conducted under Work Breakdown Structure (WBS) 1.0.2.7 of the NASA Critical Components (CPC) Program under Contract NAS3-27235 to evaluate the low emissions potential of a Rich-Quench-Lean combustor capable of achieving the program goal of emissions of nitrogen oxides (NO_xEI) less than 5 gm/Kg fuel at the supersonic light condition while maintaining combustion efficiencies in excess of 99.9 percent. The chosen combustor module would then be tested in the subscale annular rig test prior to testing in the subscale core engine demonstrator, if the RQL concept were to be chosen at the Combustor Downselect.

14. SUBJECT TERMS

Combustor; Gas turbine; Rich burn; RQL

15. NUMBER OF PAGES
218

16. PRICE CODE

17. SECURITY CLASSIFICATION OF REPORT	18. SECURITY CLASSIFICATION OF THIS PAGE	19. SECURITY CLASSIFICATION OF ABSTRACT	20. LIMITATION OF ABSTRACT
Unclassified	Unclassified	Unclassified	